

# Upper bounds on eigenvalue multiplicities for spheres and plane domains revisited

(berard-helffer-2024-HoMiNa-1206.tex, December 9, 2024)

Pierre Bérard

Bernard Helffer

(pierrehberard@gmail.com) PIERRE BÉRARD, INSTITUT FOURIER, UNIVERSITÉ  
GRENOBLE ALPES AND CNRS, CS 40700, 38058 GRENOBLE CEDEX 9, FRANCE

(Bernard.Helffer@univ-nantes.fr) BERNARD HELFFER, LABORATOIRE DE MATH-  
ÉMATIQUES JEAN LERAY, NANTES UNIVERSITÉ AND CNRS, F44000 NANTES  
CEDEX, FRANCE

*Dedicated to Steve Zelditch*

2020 *Mathematics Subject Classification.* 58C40, 35P99.

*Key words and phrases.* Spectral theory, Laplacian, Schrödinger operator, Eigenvalue, Multiplicity.

ABSTRACT.

We revisit two papers which appeared in 1999:

[1] *M. Hoffmann-Ostenhof, T. Hoffmann-Ostenhof, and N. Nadirashvili. On the multiplicity of eigenvalues of the Laplacian on surfaces. Ann. Global Anal. Geom. 17 (1999) 43–48.*

[2] *T. Hoffmann-Ostenhof, P. Michor, and N. Nadirashvili. Bounds on the multiplicity of eigenvalues for fixed membranes. Geom. Funct. Anal. 9 (1999) 1169–1188.*

The main result of these papers is that the multiplicity  $\text{mult}(\lambda_k(M))$  of the  $k$ th eigenvalue of the Riemannian surface  $M$  is bounded from above by  $(2k - 3)$  provided that  $k \geq 3$ . In [1],  $M$  is homeomorphic to a sphere. In [2],  $M$  is a plane domain with Dirichlet boundary condition. In both cases, the starting label of eigenvalues is 1. The proofs given in [1,2] are not very detailed, and often rely on figures or special configurations of nodal sets.

The purpose of this monograph is to provide detailed general proofs for the above upper bounds and to extend the results to Robin boundary conditions. We also provide a survey of previous results (Chapter 1) as well as the proofs of some prerequisite theorems (Chapter 2).

When  $M$  is homeomorphic to a sphere, we provide a complete proof of the upper bound,  $\text{mult}(\lambda_k) \leq (2k - 3)$  for any  $k \geq 3$ , by introducing and carefully studying the *combinatorial type* and a *labeling of the nodal domains* of some particular eigenfunctions (Chapter 3). When  $M$  is a plane domain, we consider the three boundary conditions, Dirichlet, Neumann, Robin, and we also study the *combinatorial types* and a *labeling of the nodal domains* of some particular eigenfunctions. More precisely, we prove the inequality  $\text{mult}(\lambda_k) \leq (2k - 2)$  for general  $C^\infty$  bounded domains and all  $k \geq 3$  (Chapter 4). We prove the inequality  $\text{mult}(\lambda_k) \leq (2k - 3)$  for  $k \geq 3$  under the additional assumption that the domain is *simply connected* (Chapter 5). Chapter 3 serves as a warm-up for Chapters 4 and 5 which form the core of this monograph. These three chapters rely on Euler's inequality applied to the nodal graph of eigenfunctions (see Chapter 2), and a careful analysis of some eigenfunctions which optimize Euler's inequality. Chapter 6 contains related results (nodal line conjecture; Courant-sharp eigenvalues).

## Contents

Chapter 1. Introduction and Survey of Previous Results	5
1.1. Introduction	5
1.2. Survey of previous results	7
Chapter 2. Prerequisites on Eigenvalue Problems	11
2.1. Eigenvalue Problems	11
2.2. Euler Type Formulas for Nodal Sets	20
2.3. Proof of the Local Structure Theorem at an Interior Point	24
2.4. Proof of the Local Structure Theorem at a Boundary Point	27
Chapter 3. Eigenvalue Bounds for Riemannian Spheres with Potential	43
3.1. Revisiting the Multiplicity Bounds for Riemannian Spheres	43
3.2. Spheres: Labeling Nodal Loops and Nodal Domains	50
Chapter 4. Plane Domains: the Estimate $\text{mult}(\lambda_k) \leq (2k - 2)$ for $k \geq 3$	57
4.1. Bounding $\text{mult}(\lambda_k)$ from Above	57
4.2. $\Omega$ Simply Connected: the Estimate $\text{mult}(\lambda_k) \leq (2k - 2)$ for $k \geq 3$	59
4.3. General Case: the Estimate $\text{mult}(\lambda_k) \leq (2k - 2)$ for $k \geq 3$	70
Chapter 5. Simply Connected Plane Domains: the Estimate $\text{mult}(\lambda_k) \leq (2k - 3)$ for $k \geq 3$	81
5.1. Introduction	81
5.2. Properties of $\lambda_k$ -Eigenfunctions under Assumptions 5.2	82
5.3. Nodal Sets of $\lambda_k$ -Eigenfunctions under Assumptions 5.2	109
5.4. Behavior of $\lambda_k$ -Eigenfunctions near $\Gamma$ under Assumptions 5.2	116
5.5. Labeling Nodal Domains	133
5.6. Eigenfunctions with Two Prescribed Boundary Singular Points: proof of Lemma 5.8 and further results	146
5.7. Conclusion	163
5.8. Simpler proof of Lemma 5.16	164
Chapter 6. Further Results	167
6.1. Upper Bounds on the Multiplicities and the Nodal Line Conjecture	167
6.2. Upper Bounds for Multiplicities vs Courant-sharp Eigenvalues	171
Bibliography	175
Alphabetical Index	181



## CHAPTER 1

# Introduction and Survey of Previous Results

### 1.1. Introduction

In this monograph, we are concerned with upper bounds for the multiplicities of the eigenvalues  $\{\lambda_k, k \geq 1\}$  of a Schrödinger operator  $-\Delta + V$  on a compact, smooth (ie.  $C^\infty$ ), connected Riemannian surface. When the boundary  $\partial M$  is not empty, we consider the Dirichlet, Neumann or Robin boundary conditions. We *do not* consider the Steklov eigenvalue problem for which we refer to the papers of Karpukhin, Kokarev and Polterovich [KaKP2014], Fraser and Schoen [FrSc2016], Jammes [Jam2016], Colbois, Girouard, Gordon and Sher [CoGGS2024], and their reference lists.

Our main purpose is to revisit the papers [HoHN1999] (Riemannian surfaces homeomorphic to a sphere<sup>1</sup>) and [HoMN1999] (planar domains with smooth boundary) whose proofs are not very detailed and often rely on figures and special configurations of nodal sets. We introduce and carefully study the *combinatorial type* (defined in Subsection 3.1.2) of some particular eigenfunctions, as well as a *labeling* of their nodal domains (see Sections 3.2 and 5.5). For domains in  $\mathbb{R}^2$ , we provide a unified treatment for the three boundary conditions (Dirichlet, Neumann, Robin). We also illustrate our proofs with many figures.

In the sequel  $\Delta$  is the Laplace-Beltrami operator on the surface  $M$  for some smooth Riemannian metric  $g$  (our convention is that  $\Delta$  is a nonpositive operator), and  $V$  is a smooth real valued function. We list the eigenvalues in nondecreasing order, multiplicities accounted for. Our convention is that, in all cases, we label the eigenvalues *starting from the label 1*,

$$\lambda_1 < \lambda_2 \leq \lambda_3 \leq \dots,$$

and we denote the multiplicity of  $\lambda_k$  by  $\text{mult}(\lambda_k)$ . We refer to Chapter 2 for more definitions and notation.

In Section 1.2 we provide a survey of the main results on the multiplicity problem, and the ideas behind their proofs.

Chapter 2 is devoted to definitions, notation and prerequisites on eigenvalues and eigenfunctions of Schrödinger operators on compact surfaces. In Section 2.2, we state Euler type formulas for nodal graphs. They will be applied extensively in the sequel. In Sections 2.3 and 2.4, we give detailed proofs of the local structure theorem for an eigenfunction near a singular point. They will also be used extensively in the following chapters.

---

<sup>1</sup>In [HoHN1999], the authors refer to “compact surfaces without boundary and genus 0”, and implicitly assume that the surface is orientable. In this monograph, we have chosen a shorter terminology. We will refer to Riemannian spheres  $(M, g)$  with potential  $V$ , where  $M$  is a  $C^\infty$  surface homeomorphic to the sphere, equipped with a  $C^\infty$  Riemannian metric  $g$ , and with a  $C^\infty$  real valued potential  $V$ . See Chapter 3.

In Chapter 3, we revisit [HoHN1999]. Introducing the *combinatorial type* of some particular nodal sets (Definition 3.4) and a *labeling* of their nodal domains (Section 5.5), we provide a complete proof of the inequality  $\text{mult}(\lambda_k) \leq (2k - 3)$  for all  $k \geq 3$ , for Riemannian spheres with potential, see Theorem 3.1. This chapter is meant as a warm-up for the remaining chapters.

In the next two chapters, we revisit [HoMN1999] and prove the following theorem.

**THEOREM 1.1.** *Consider the eigenvalue problem for the operator  $-\Delta + V$  in a  $C^\infty$  bounded domain  $\Omega$ , with the Dirichlet, Neumann or  $h$ -Robin boundary condition.*

- (i) *Without any further assumption on  $\Omega$ , for any  $k \geq 3$ ,  $\text{mult}(\lambda_k) \leq (2k - 2)$ .*
- (ii) *Assuming that  $\Omega$  is simply connected, for any  $k \geq 3$ ,  $\text{mult}(\lambda_k) \leq (2k - 3)$ .*

The proof of Assertion (i) is given in Chapter 4; the proof of Assertion (ii) in Chapter 5.

**REMARKS 1.2.**

- (1) In [HoMN1999, Theorem B, p. 1172], the authors state that the bound,  $\text{mult}(\lambda_k) \leq (2k - 3)$  for all  $k \geq 3$ , holds for all smooth bounded domains  $\Omega \subset \mathbb{R}^2$ . In [Berd2018, Section 4], Berdnikov points out a gap in the proof when  $\Omega$  is not simply connected. This is why we restrict ourselves to simply connected domains in Assertion (ii).
- (2) Theorem 1.1 covers both Dirichlet and Robin boundary conditions, whereas [HoMN1999] only deals with the Dirichlet boundary condition. As a matter of fact, the proofs in both cases, Dirichlet and Robin, are very similar, except for a specific energy argument in the Robin case (Lemma 5.17).

In Chapter 6 we relate the problem of bounding multiplicities from above to the question of *Courant-sharp eigenvalues* (eigenvalues one of whose eigenfunctions maximizes the number of nodal domains, see Remark 4.4), and the particular case of the multiplicity of the second eigenvalue,  $\text{mult}(\lambda_2)$ , to the *Nodal Line Conjecture*.

In comparison with the first and second versions of [arXiv:2202.06587](#) posted in 2022, the text has been completely revised and reorganized as a monograph. The gaps in the proofs which remained in the second version (September 2022) were filled in. Comments and suggestions will be much appreciated.

*Acknowledgements.* During the preparation of this monograph, we consulted several colleagues: A. Berdnikov, L. Friedlander, T. Hoffmann-Ostenhof, P. Jammes, M. Karpukhin, J. Kennedy, F. Laudenbach, Z. Liqun, N. Nadirashvili, I. Polterovich, S. Zelditch. We thank them all for their comments. Since the publication of the first version of this work in February 2022, we had several fruitful discussions with N. Nadirashvili, which led us to explore new approaches to fill in the gaps in the proofs provided in [HoMN1999]. We also acknowledge the comments and further references recently provided by V. Bobkov.

Finally, we thank Steve Zelditch for his comments, a few months before his death in September 2022, and we express our deep appreciation of his contributions to spectral geometry.

## 1.2. Survey of previous results

In the case of closed surfaces, the first upper bounds on multiplicities were obtained by Cheng [Chen1976], Besson [Bess1980], and Nadirashvili [Nadi1987]. We denote their respective upper bounds on  $\text{mult}(\lambda_k)$  by  $m_k^*$ , with  $*$   $\in \{B, C, N\}$ , where  $B$  stands for “Besson”,  $C$  for “Cheng”, and  $N$  for “Nadirashvili”, and provide a summary of their results in Table 1.1 (with our convention that the labeling of eigenvalues begins with 1, not 0).

The upper bounds for the multiplicity of the second eigenvalue (i.e., the least positive eigenvalue of a closed surface) given in the fourth column are sharp. For the sphere the bound is achieved for the canonical (round) metric, [Chen1976]; for the projective space the bound is achieved for the metric induced by the canonical metric of the sphere, [Bess1980]; for the torus the bound is achieved for the equilateral torus  $\mathbb{T}_e$  with metric induced from  $\mathbb{R}^2$ , [Bess1980]; for the Klein bottle, the bound is achieved for a nontrivial pair  $(g, V)$  constructed in [Nadi1987, §2], and for smooth metrics constructed in [ColV1987, Théorème 4.2]. An interesting feature of  $\mathbb{S}^2, \mathbb{RP}^2$  and  $\mathbb{T}^2$  is that the bounds for  $\text{mult}(\lambda_2)$  are also achieved for metrics different from the ones mentioned above, see [Bess1980].

In [ColV1987, Théorème 1.5], Colin de Verdière shows that for a closed surface  $M$ ,

$$\sup \{ \text{mult}(\lambda_2(M, -\Delta_g + V)) \mid (g, V) \} \geq C(M) - 1,$$

where the supremum is taken over the Riemannian metrics and potentials on  $M$ , and where  $C(M)$  is the *chromatic number* of  $M$  (the maximal number  $N$  such that the complete graph on  $N$  vertices  $K_N$  can be embedded into  $M$ ). Table 1.1 shows that equality holds for  $\mathbb{S}^2, \mathbb{RP}^2, \mathbb{T}^2$  and  $\mathbb{K}^2$ ; it also holds for surfaces with  $\chi(M) \geq -3$ , [Seve2002], where  $\chi(M)$  is the Euler characteristic of  $M$ . It was conjectured that equality holds for all closed surfaces. See Fortier Bourque et alii [FoGPP2023] for two counter-examples.

Cheng and Besson, express their upper bounds in terms of the genus. When the surface  $M$  is orientable,  $\chi(M) = 2 - 2\gamma(M)$ , where  $\gamma(M)$  is the genus of  $M$ , and the surface is homeomorphic to a 2-sphere with  $\gamma(M)$  handles attached. When the surface  $M$  is not orientable,  $\chi(M) = 1 - \gamma(\tilde{M})$ , where  $\gamma(\tilde{M})$  is the genus of the orientable cover  $\tilde{M}$  of  $M$ , and the surface is the connected sum of  $(\gamma(\tilde{M}) + 1)$  copies of the projective plane.

Better upper bounds were later obtained by M. and T. Hoffmann-Ostenhof and Nadirashvili [HoHN1999] (Riemannian spheres with potential, see Chapter 3), Sévenec [Seve2002], Fortier Bourque and Petri [FoBP2024] (improved bounds on the multiplicity of  $\lambda_2$  when  $\chi(M) < 0$ ), Berdnikov, Nadirashvili and Penskoi [BeNP2016] (improved bounds for the multiplicities on the projective plane), Fortier Bourque and Petri [FoBP2024] (Klein quartic).

In [Nadi1987, Theorem 2], Nadirashvili also considers smooth bounded domains  $\Omega \subset \mathbb{R}^2$  and proves that the multiplicity of the  $k$ th eigenvalue  $\lambda_k$  of an operator  $-\Delta + V$  with Dirichlet or Neumann boundary condition is at most  $(2k - 1)$ .

In the paper [HoMN1999], Hoffmann-Ostenhof, Michor and Nadirashvili, improve Nadirashvili’s bound for bounded plane domains with  $C^\infty$  boundary and Dirichlet boundary condition. More precisely, they state that the multiplicity of  $\lambda_k$  is at most

$M$	$\chi(M)$	orientability	$\text{mult}(\lambda_2) \leq$	for $k \geq 1$ , $\text{mult}(\lambda_k) \leq$
$\mathbb{S}^2$	2	orientable	3	$\begin{cases} m_k^C = \frac{1}{2}k(k+1) \\ m_k^B = 2k-1 \\ m_k^N = 2k-1 \end{cases}$
$\mathbb{RP}^2$	1	non-orientable	5	$\begin{cases} m_k^C = \text{not considered} \\ m_k^B = 4k-1 \\ m_k^N = 2k+1 \end{cases}$
$\mathbb{T}^2$	0	orientable	6	$\begin{cases} m_k^C = \frac{1}{2}(k+2)(k+3) \\ m_k^B = 2k+3 \\ m_k^N = 2k+2 \end{cases}$
$\mathbb{K}^2$	0	non-orientable	5	$\begin{cases} m_k^C = \text{not considered} \\ m_k^B = \text{not considered} \\ m_k^N = 2k+1 \end{cases}$
$M^2$	$\chi(M) < 0$	orientable	–	$\begin{cases} m_k^C = \frac{1}{2}(k - \chi(M) + 2)(k - \chi(M) + 3) \\ m_k^B = 2k - 2\chi(M) + 3 \\ m_k^N = 2k - 2\chi(M) + 1 \end{cases}$
$M^2$	$\chi(M) < 0$	non-orientable	–	$\begin{cases} m_k^C = \text{not considered} \\ m_k^B = 4k - 4\chi(M) + 3 \\ m_k^N = 2k - 2\chi(M) + 1 \end{cases}$

TABLE 1.1. Closed surfaces: multiplicity upper bounds obtained by Cheng, Besson, and Nadirashvili (labeling starting from 1)

$(2k-3)$ . Berdnikov [Berd2018] considers the case of compact surfaces with boundary, under the assumption that  $\chi(M) + b_0(\partial M)$  is negative (where  $b_0$  denotes the number of connected components). He points out some problem in the proof of Theorem B in [HoMN1999] when the domain is not simply connected. Unfortunately, we also detected another unclear argument in the proof.

The general strategy to prove upper bounds for the eigenvalue multiplicities is a combination of the following ingredients:

- (i) Courant's nodal domain theorem, Theorem 2.4.
- (ii) Local structure theorems for eigenfunctions near a singular point, Theorem 2.8.
- (iii) Existence of eigenfunctions with prescribed singular points, provided the dimension of the eigenspace is large enough, Subsection 2.1.3.
- (iv) Euler's formula for the graph associated with the nodal set of an eigenfunction, Section 2.2.
- (v) The *rotating function argument*, which first appeared in [Bess1980], § 3.1.2.3.
- (vi) Energy arguments, Lemma 5.17, and eigenvalue monotonicity.

In one form or another, these arguments go back to Cheng [Chen1976], Besson [Bess1980], and Nadirashvili [Nadi1987].

Two other papers, respectively [HeHO1999] by Helffer, M. and T. Hoffmann-Ostenhof and Owen, and [HeHN2002] by Helffer, M. and T. Hoffmann-Ostenhof and Nadirashvili, have used the same techniques for related purposes (for example the Aharonov-Bohm operators). Similar techniques are used in the analysis of the properties of minimal partitions [HeHT2009, BoHe2017].



We refer to the papers of Burger, Colbois and/or Colin de Verdière [[BuCo1985](#), [Colb1985](#), [ColV1986](#), [ColV1987](#), [CoCo1988](#)] and to the paper of Letrouit and Machado [[LeMa2024](#)] for results of a different flavor.



## CHAPTER 2

### Prerequisites on Eigenvalue Problems

#### 2.1. Eigenvalue Problems

**2.1.1. Definitions, notation and preliminary results.** In this chapter,  $M$  denotes a closed surface (compact, no boundary), or a compact surface with boundary. The boundary is denoted by  $\partial M$ , and the interior  $M \setminus \partial M$  is denoted by  $\text{int}(M)$ . Unless otherwise stated, the surface is assumed to be smooth and connected. We equip  $M$  with a smooth Riemannian metric  $g$ , and we consider a (non-magnetic) Schrödinger operator of the form  $-\Delta_g + V$ , where  $\Delta_g$  is the Laplace-Beltrami operator for the metric  $g$  and  $V$  is a smooth real valued function on  $M$ .

The notation is as follows. The Riemannian measure is denoted by  $v_g$ . When  $\partial M \neq \emptyset$ ,  $\sigma_g$  is the Riemannian measure of  $\partial M$  for the metric induced by  $g$ , and  $\nu$  is the unit normal to  $\partial M$  pointing inward.

When  $M$  is closed ( $\partial M = \emptyset$ ), we consider the closed (no boundary condition) eigenvalue problem

$$(2.1) \quad -\Delta u + Vu = \lambda u \quad \text{in } M,$$

associated with the quadratic form

$$(2.2) \quad \int_M (|du|_g^2 + Vu^2) dv_g, \quad \text{with domain } H^1(M).$$

When  $\partial M \neq \emptyset$ , we consider the boundary eigenvalue problem

$$(2.3) \quad \begin{cases} -\Delta u + Vu = \lambda u & \text{in } \text{int}(M), \\ B(u) = 0 & \text{on } \partial M, \end{cases}$$

where  $B(u)$  is one the following boundary conditions:

$$(2.4) \quad B(u) = \begin{cases} u & \text{(Dirichlet),} \\ \frac{\partial u}{\partial \nu} & \text{(Neumann),} \\ \frac{\partial u}{\partial \nu} - h u & \text{(}h\text{-Robin).} \end{cases}$$

In the Robin case,  $h$  is a given  $C^\infty$  function on  $\partial M$ .

The associated quadratic forms are

$$(2.5) \quad \int_M (|du|_g^2 + Vu^2) dv_g, \quad \text{with domain } H_0^1(M).$$

for the Dirichlet problem, and

$$(2.6) \quad \int_M (|du|_g^2 + Vu^2) dv_g + \int_{\partial M} h (u_{\partial M})^2 d\sigma_g, \quad \text{with domain } H^1(M),$$

for the Neumann problem (in this case  $h = 0$ ) and for the  $h$ -Robin problem.

For the closed, Dirichlet, Neumann or  $h$ -Robin eigenvalue problems, the spectrum of  $-\Delta + V$  is discrete, and consists of a sequence of non-negative eigenvalues with finite multiplicities,

$$(2.7) \quad \lambda_1 < \lambda_2 \leq \lambda_3 \leq \cdots \nearrow \infty,$$

which we list in nondecreasing order, multiplicities accounted for, starting from the label 1. In the sequel, we only consider *real valued* eigenfunctions.

NOTATION 2.1. The *eigenspace* associated with the eigenvalue  $\lambda_k$  will be denoted by  $U(\lambda_k)$ . Its dimension, the *multiplicity* of  $\lambda_k$ , will be denoted by  $\text{mult}(\lambda_k)$  or  $\dim U(\lambda_k)$ .

REMARK 2.2. Whenever necessary, we shall indicate the dependence on  $M, g, V, h$  and the boundary condition, for example,  $\lambda_k(M, g, V, \mathfrak{d})$  for the Dirichlet eigenvalues of  $-\Delta + V$  on  $(M, g)$  with the Dirichlet boundary condition on  $\partial M$ .

DEFINITIONS 2.3 (Terminology).

- (i) The *nodal set* of a nontrivial eigenfunction  $u$  is denoted by  $\mathcal{Z}(u)$ , and defined by

$$(2.8) \quad \mathcal{Z}(u) = \overline{\{x \in \text{int}(M) \mid u(x) = 0\}}.$$

When  $\partial M \neq \emptyset$ ,  $\mathcal{Z}(u)$  is the closure in  $M$  of the set of interior zeros of  $u$ .

- (ii) In dimension 2, the nodal set  $\mathcal{Z}(u)$  of an eigenfunction  $u$  is also called the *nodal line* of  $u$ .
- (iii) The *nodal domains* of the eigenfunction  $u$  are the connected components<sup>1</sup> of  $\text{int}(M) \setminus \mathcal{Z}(u)$ . We denote the number of nodal domains of  $u$  by  $\kappa(u)$ .

A key ingredient in the forthcoming proofs is the following.

THEOREM 2.4 (Courant's nodal domain theorem, [Cour1923]). *With the previous definitions, a  $\lambda_k$ -eigenfunction has at most  $k$  nodal domains.*

For modern proofs we refer to [BeMe1982], [Ales1998] or [SoZe2011].

Eigenfunctions associated with  $\lambda_1$  are characterized by the fact that they have precisely one nodal domain. An eigenfunction associated with  $\lambda_k, k \geq 2$ , has at least two nodal domains. An eigenfunction associated with  $\lambda_2$  has precisely two nodal domains.

REMARK 2.5. For any  $k \geq 2$  and any  $\lambda_k$ -eigenfunction  $u$ ,  $\kappa(u) \geq 2$ , a consequence of the fact that  $u$  is  $L^2$ -orthogonal to a first eigenfunction. It turns out that this lower bound can in general not be improved, see [Ster1925, Lewy1977], [BeBo1982], [BeHe2015s, BeHe2015r], and the recent papers [JuZe2022] and [CiJLS2022].

REMARK 2.6. As a matter of fact, for  $k$  large enough (depending on  $M, g, V$ ),  $\sup \{\kappa(u) \mid 0 \neq u \in U(\lambda_k)\} < k$ , see Pleijel's paper [Plej1956] and Section 6.2 for more details and references.

<sup>1</sup>In the sequel, unless otherwise stated, we shall use the word *component* for the expression *connected component*.

### 2.1.2. Local structure of eigenfunctions near a zero.

DEFINITIONS 2.7 (Terminology). We say that a function  $u$  *vanishes at order*  $n \geq 1$  at a point  $x$ , and we write  $\text{ord}(u, x) = n$ , if (in a local coordinate system) the function and all its derivatives of order less than or equal to  $(n - 1)$  vanish at  $x$ , and at least one derivative of order  $n$  does not vanish at  $x$ . A *critical zero* of  $u$  is a point at which  $u$  vanishes at order at least 2 (i.e.,  $u(x) = 0$  and  $\nabla_x u = 0$ ). A critical zero  $x$  of  $u$  is called an *interior critical zero* if  $x \in \text{int}(M)$ , and a *boundary critical zero* if  $x \in \partial M$ .

THEOREM 2.8 (Local structure theorem). *Let  $u$  be a nontrivial eigenfunction of the Schrödinger operator  $-\Delta + V$  on a smooth compact Riemannian surface  $M$  (with or without boundary), where  $V$  is a smooth real valued potential. Then,  $u \in C^\infty(M)$ , and does not vanish at infinite order at any point of  $M$ . Furthermore, depending on the boundary condition on  $\partial M$ ,  $u$  has the following properties.*

- (i) *For  $x_0 \in M$  an interior point, if  $u$  has a zero of order  $\ell$  at  $x_0$ , then there exist local polar coordinates  $(r, \omega)$  centered at  $x_0$  such that*

$$(2.9) \quad u(x) = r^\ell (a \sin(\ell\omega) + b \cos(\ell\omega)) + \mathcal{O}(r^{\ell+1}),$$

*where  $a, b \in \mathbb{R}$ ,  $a^2 + b^2 \neq 0$ .*

- (ii) *For  $x_0 \in \partial M$ , if a Dirichlet eigenfunction  $u$  has a zero of order  $\ell$  at  $x_0$ , then there exist local polar coordinates  $(r, \omega)$  centered at  $x_0$ , such that*

$$(2.10) \quad u(x) = a r^\ell \sin(\ell\omega) + \mathcal{O}(r^{\ell+1})$$

*for some  $a \in \mathbb{R}$ ,  $a \neq 0$ . The angle  $\omega$  is chosen so that the tangent to the boundary at  $x_0$  is given by the equation  $\omega = 0$ .*

- (iii) *For  $x_0 \in \partial M$ , if a Robin eigenfunction  $u$  has a zero of order  $\ell$  at  $x_0$ , then there exist local polar coordinates  $(r, \omega)$  centered at  $x_0$ , such that*

$$(2.11) \quad u(x) = b r^\ell \cos(\ell\omega) + \mathcal{O}(r^{\ell+1})$$

*for some  $b \in \mathbb{R}$ ,  $b \neq 0$ . The angle  $\omega$  is chosen so that the tangent to the boundary at  $x_0$  is given by the equation  $\omega = 0$ .*

We provide detailed proofs adapted to our purposes in Sections 2.3 and 2.4. The starting point is to use the unique continuation theorem, see [Aron1957] when  $x_0$  is an interior point, and [DoFe1990a] when  $x_0$  is a boundary point.

Classical references for the first assertion are [Bers1955, HaWi1953]. For a proof of the local structure theorem under weaker regularity assumptions on the boundary, and for references to the literature, we refer to [GiHe2019, Appendix A].

From a local point of view, we have the following corollary.

COROLLARY 2.9.

- (i) *Let  $x_0 \in \text{int}(M)$ . If  $u$  has a zero of order  $\ell$  at  $x_0$ , then exactly  $\ell$  nodal arcs pass through  $x_0$ . More precisely, in a neighborhood of  $x_0 \in \text{int}(M)$ , the nodal set  $\mathcal{Z}(u)$  consists of  $2\ell$  semi-arcs emanating from  $x_0$  tangentially to the rays  $\{\omega = \omega_j\}$  where  $\omega_j := j\frac{\pi}{\ell}$ ,  $0 \leq j < 2\ell$ . The semi-tangents to these semi-arcs dissect the full unit circle in the tangent plane at  $x_0$  into  $2\ell$  equal parts.*
- (ii) *Let  $x_0 \in \partial M$ . Let  $u$  be a Dirichlet eigenfunction. If  $u$  has a zero of order  $\ell \geq 2$  at  $x_0$ , then exactly  $(\ell - 1)$  semi-arcs hit  $\partial M$  at  $x_0$ , their semi-tangents at  $x_0$*

dissect the half unit circle in the tangent plane at  $x_0$  into  $\ell$  sectors given by the equation  $\sin(\ell\omega) = 0$ .

- (iii) Let  $x_0 \in \partial M$ . Let  $u$  be a Robin eigenfunction. If  $u$  has a zero of order  $\ell \geq 1$  at  $x_0$ , then exactly  $\ell$  semi-arcs hit  $\partial M$  at  $x_0$ , their semi-tangents at  $x_0$  dissect the half unit circle in the tangent plane at  $x_0$  into  $\ell$  sectors given by the equation  $\cos(\ell\omega) = 0$ .

Assertion (i) is proved in Section 2.3. For Assertions (ii) and (iii), see Section 2.4, or the references in [GiHe2019, Appendix].

Points at which nodal arcs meet in the interior  $\text{int}(M)$ , and points at which the nodal set hits the boundary  $\partial M$  play an important role in the global understanding of nodal sets. The terminology in the following definition comes from the framework of partitions.

DEFINITION 2.10 (Terminology). Define the *singular points* of an eigenfunction  $u$  as follows.

- (i) A point  $x_0 \in \text{int}(M)$  is an *interior singular point* of  $u$  if and only if it is an interior critical zero; the set of interior singular points of  $u$  is denoted by  $\mathcal{S}_i(u)$ . The *index*  $\nu(u, x_0)$  of the interior singular point  $x_0$  is defined as the number of nodal semi-arcs emanating from  $x_0$ ,  $\nu(u, x_0) = 2 \text{ord}(u, x_0)$ .
- (ii) A point  $x_0 \in \partial M$  is a *boundary singular point* of  $u$  if and only if the nodal set  $\mathcal{Z}(u)$  hits the boundary  $\partial M$  at  $x_0$ ; the set of boundary singular points of  $u$  is denoted by  $\mathcal{S}_b(u)$ . The *index*  $\rho(u, x_0)$  of the boundary singular point  $x_0$  is defined as the number of nodal semi-arcs hitting  $\partial M$  at  $x_0$ . If  $u$  is a Dirichlet eigenfunction,  $\rho(u, x_0) = (\text{ord}(u, x_0) - 1)$ ; if  $u$  is a Robin eigenfunction,  $\rho(u, x_0) = \text{ord}(u, x_0)$ .

The set  $\mathcal{S}(u)$  of singular points of  $u$  is the set  $\mathcal{S}(u) = \mathcal{S}_i(u) \cup \mathcal{S}_b(u)$ .

REMARK 2.11. The order of vanishing is *semi-continuous* in the following sense. Let  $\{v_n\}$  be a sequence of functions which converges to some  $v$  uniformly in  $C^k$  for some  $k \geq 1$ . Let  $\{x_n\}$  be a sequence of points which converges to some  $x$  in  $M$ . Assume that  $\text{ord}(v_n, x_n) \geq k$  for all  $n$ . Then,  $\text{ord}(v, x) \geq k$ . Since they are defined in terms of order of vanishing, the indices  $\nu$  and  $\rho$  inherit this property.

From the global point of view, the set  $\mathcal{S}(u)$  is finite, and the components of  $\mathcal{Z}(u) \setminus \mathcal{S}(u)$  are smooth 1-dimensional submanifolds homeomorphic to either circles or open intervals whose boundaries consist of singular points.

DEFINITIONS 2.12 (Terminology).

- (i) We call a circle-like component of  $\mathcal{Z}(u) \setminus \mathcal{S}(u)$  a *nodal circle*; we call an interval-like component, a *nodal interval*.
- (ii) Let  $I_{x,y}$  be a nodal interval with boundary  $\{x, y\} \subset \mathcal{S}(u)$ . In this case, the closed nodal interval  $\bar{I}_{x,y} := I_{x,y} \cup \{x, y\}$  can be parametrized by arc-length, from  $x$  to  $y$ , by  $\gamma_{x,y} : [0, L_{x,y}] \rightarrow M$ , with  $\gamma_{x,y}(0) = x$  and  $\gamma_{x,y}(L_{x,y}) = y$  or, from  $y$  to  $x$ , by  $\gamma_{y,x}$  given by  $\gamma_{y,x}(t) = \gamma_{x,y}(L_{x,y} - t)$ . The semi-tangents to  $\bar{I}_{x,y}$  at  $x$  and  $y$  are given by the local structure theorem. The point  $x$  (resp.  $y$ ) might be an interior singular point, or a boundary singular point. If  $x = y$ , we say that the component  $\bar{I}_{x,x}$  is a *nodal loop* at  $x$ . In this case the loop is not a smooth circle, but a continuous, piecewise  $C^1$  circle.

From a global point of view, we have the following corollary of the structure theorem.

COROLLARY 2.13.

- (1) *The nodal set of  $u$  is the union of the finitely many singular points, the nodal circles in the interior of  $M$ , and the nodal intervals some of which may hit  $\partial M$ .*
- (2) *Each component of  $\partial M$  is hit by an even number of nodal intervals: if  $\Gamma$  is a component of  $\partial M$ , then*

$$\sum_{z \in \mathcal{S}_b(u) \cap \Gamma} \rho(u, z) \in 2\mathbb{N}.$$

*Proof.* The first assertion is well-known. We give the proof of the second assertion for completeness.

◇ *Dirichlet case.* The component  $\Gamma$  is topologically a circle which meets  $\mathcal{S}_b(u)$  at finitely many points  $z_j$ ,  $1 \leq j \leq k$ , which are precisely the zeros of the normal derivative  $\partial_\nu u(z)$ . Choosing a parametrization  $z$  of  $\Gamma$  and taking the local structure of  $u$  at each  $z_j$  into account, we see that each time  $z$  passes some  $z_j$ , the sign of  $\partial_\nu u$  is multiplied by  $(-1)^{\rho(z_j)}$ . Running through  $\Gamma$  once, we must have

$$\prod_j (-1)^{\rho(z_j)} = (-1)^{\sum_j \rho(u, z_j)} = 1.$$

◇ *Robin case.* The proof is similar, actually simpler. □

**2.1.3. Eigenfunctions with prescribed singular points.** In order to bound multiplicities, we will use eigenfunctions with prescribed singular points of sufficiently high index. Their existence is given by the following lemmas. These lemmas appear in one form or another in the previous papers on eigenvalue multiplicity bounds, [Chen1976, Theorem 3.4], [Bess1980, Theorem 2.1], [Nadi1987, Lemma 4], [HoHN1999, Proposition 2], [HoMN1999, Lemma 2.9].

The first lemma prescribes an interior singular point.

LEMMA 2.14. *Let  $M$  be a compact surface (with or without boundary), and  $x$  an interior point. Let  $U$  be a linear subspace of an eigenspace of  $-\Delta + V$ , see (2.1) or (2.3), with  $\dim U = m \geq 2$ .*

- (i) *There exists a function  $0 \neq u \in U$  such that  $x$  is a singular point of  $u$  with index  $\nu(u, x) \geq 2 \lfloor \frac{m}{2} \rfloor$  (the integer part of  $\frac{m}{2}$ ), equivalently with  $\text{ord}(u, x) \geq \lfloor \frac{m}{2} \rfloor$ .*
- (ii) *Furthermore, if  $m$  is odd, there exist at least two linearly independent such functions.*

*Proof.* We use induction on  $m$ . Recall that  $\nu(u, x) = 2 \text{ord}(u, x)$ . The assertion is clear when  $m = 2$ . Assume  $m = 3$ , and let  $\{u_1, u_2, u_3\}$  be a basis of  $U$ . Then, we can find  $0 \neq v_1 \in \text{span}\{u_1, u_2\}$  such that  $\text{ord}(v_1, x) \geq 1$ . The subspace  $V_1$  of  $U$  orthogonal<sup>2</sup> to  $v_1$  has dimension 2, and hence there exists  $0 \neq v_2 \in V_1$  such that  $\text{ord}(v_2, x) \geq 1$ . Then  $v_1$  and  $v_2$  are two linearly independent functions in  $U$  vanishing at order at least 1 at  $x$ .

Assume that the lemma holds for  $2p$  and  $(2p + 1)$  for some  $p \geq 1$ .

<sup>2</sup>Orthogonality is meant with respect to the inner product induced by the  $L^2$ -inner product of eigenfunctions.

Let  $U$  be linear subspace of an eigenspace with dimension  $(2p + 2)$ , and basis

$$\{u_1, \dots, u_{2p+2}\}.$$

By the induction hypothesis, in the subspace  $V_1 := \text{span}\{u_1, \dots, u_{2p+1}\}$ , we can find two linearly independent functions  $v_1, v_2$  such that  $\text{ord}(v_i, x) \geq p$ . If one of them vanishes at order at least  $(p + 1)$ , the assertion for  $U$  is satisfied. If not, according to Theorem 2.8 (i), there exist  $(a_i, b_i)$ ,  $i = 1, 2$ , with  $a_i^2 + b_i^2 \neq 0$ , such that

$$v_i = r^p \left( a_i \sin(p\omega) + b_i \cos(p\omega) \right) + \mathcal{O}(r^{p+1}).$$

The subspace  $V_2$  of  $U$  orthogonal to  $v_1$  and  $v_2$  has dimension  $2p$  and hence, there exists  $0 \neq v_3 \in V_2$  such that  $\text{ord}(v_3, x) \geq p$ . If  $v_3$  vanishes at order at least  $(p + 1)$  at  $x$ , we are done. Otherwise, there exist  $(a_3, b_3)$ , with  $a_3^2 + b_3^2 \neq 0$  such that

$$v_3 = r^p \left( a_3 \sin(p\omega) + b_3 \cos(p\omega) \right) + \mathcal{O}(r^{p+1}).$$

The functions  $r^p \left( a \sin(p\omega) + b \cos(p\omega) \right)$  are the homogeneous harmonic polynomials of degree  $p$  in  $\mathbb{R}^2$ , a vector space of dimension 2. The three polynomials  $r^p \left( a_i \sin(p\omega) + b_i \cos(p\omega) \right)$ ,  $i \in \{1, 2, 3\}$  must be linearly dependent, and hence there exists a nontrivial linear combination of  $v_1, v_2, v_3$  which vanishes at order at least  $(p + 1)$  at  $x$ .

Let  $U$  be an eigenspace with dimension  $(2p + 3)$ , with basis  $\{u_1, \dots, u_{2p+3}\}$ . By the previous proof, in the subspace  $V_1 := \text{span}\{u_1, \dots, u_{2p+2}\}$ , there exists  $0 \neq v_1$  such that  $\text{ord}(v_1, x) \geq (p + 1)$ . For the same reason, in the subspace  $V_2$  orthogonal to  $v_1$ , there exists  $0 \neq v_2$  such that  $\text{ord}(v_2, x) \geq (p + 1)$ . The functions  $v_1, v_2$  are two linearly independent functions in  $U$  vanishing at order at least  $(p + 1)$  at  $x$ .

The proof of Lemma 2.14 is complete.  $\square$

The next lemmas prescribe respectively one or two boundary singular points.

**LEMMA 2.15.** *Let  $M$  be a compact surface with boundary, and  $x \in \partial M$ . Let  $U$  be a linear subspace of an eigenspace of  $-\Delta + V$ , see (2.3), with  $\dim U = m \geq 2$ . Then, there exists a function  $0 \neq u \in U$  such that  $x$  is a boundary singular point of  $u$  with index  $\rho(u, x) \geq (m - 1)$ .*

*Proof.* We use induction on  $m$ . Recall that  $\rho(u, x) = (\text{ord}(u, x) - 1)$  for Dirichlet eigenfunctions, resp.  $\rho(u, x) = \text{ord}(u, x)$  for Robin eigenfunctions.

$\diamond$  *Dirichlet boundary condition.* When  $m = 2$ , the assertion is clear. Assume it is true for some  $m \geq 2$ . Let  $U$  be a linear subspace of an eigenspace with dimension  $(m + 1)$ , and basis  $\{u_1, \dots, u_{m+1}\}$ . Consider the subspace  $V_1 = \text{span}\{u_1, \dots, u_m\}$ . By the induction hypothesis, there exists  $0 \neq v_1 \in V_1$  such that  $\text{ord}(v_1, x) \geq m$ . If  $v_1$  vanishes at order at least  $(m + 1)$ , we are done. Otherwise, by Theorem 2.8, Equation (2.10), there exists  $a_1 \neq 0$  such that, in local polar coordinates at  $x$ ,

$$v_1(z) = a_1 r^m \sin(m\omega) + \mathcal{O}(r^{m+1}).$$

The subspace  $V_2 = \{u \in U \mid u \perp v_1\}$  orthogonal to  $v_1$  has dimension  $m$ , and hence there exists  $0 \neq v_2 \in V_2$  such that  $\text{ord}(v_2, x) \geq m$ . If  $v_2$  vanishes at order at least  $(m + 1)$ , we are done. Otherwise, as above we can write

$$v_2(z) = a_2 r^m \sin(m\omega) + \mathcal{O}(r^{m+1})$$

for some  $a_2 \neq 0$ , and hence the linear combination  $v = a_2 v_1 - a_1 v_2$  vanishes at order at least  $(m + 1)$ .  $\checkmark$



◇ *Robin boundary condition.* When  $m = 2$ , the assertion is clear. Assume it is true for some  $m \geq 2$ . Let  $U$  be a linear subspace of an eigenspace with dimension  $(m + 1)$ , with basis  $\{u_1, \dots, u_{m+1}\}$ . Consider the subspace  $U_1 = \text{span}\{u_1, \dots, u_m\}$ . By the induction hypothesis, there exists  $0 \neq v_1 \in U_1$  such that

$$\text{ord}(v_1, x) \geq (m - 1).$$

If  $v_1$  vanishes at order at least  $m$ , we are done. Otherwise, by Theorem 2.8, Equation (2.11), there exists  $b_1 \neq 0$  such that, in local polar coordinates at  $x$ ,

$$v_1(z) = b_1 r^m \cos((m - 1)\omega) + \mathcal{O}(r^{m+1}).$$

We can then consider the subspace  $U_2$  orthogonal to  $v_1$  in  $U$ , and conclude by arguing as above. ✓

The proof of Lemma 2.15 is complete. □

LEMMA 2.16. *Let  $M$  be a compact surface with boundary, and  $x, y \in \partial M$ , with  $x \neq y$ . Let  $U$  be a linear subspace of an eigenspace of  $-\Delta + V$ , see (2.3), with  $\dim U = m \geq 3$ . Then, there exists a function  $0 \neq u \in U$  such that  $x$  and  $y$  are boundary singular points of  $u$  with indices  $\rho(u, x) \geq (m - 2)$  and  $\rho(u, y) \geq 1$ .*

*Proof.*

◇ *Dirichlet boundary condition.* Choose  $\{u_1, \dots, u_m\}$  a basis of  $U$ . Looking at a general element  $u = \sum \alpha_j \phi_j$  in  $U$ , the condition at  $y$  reads

$$\sum_{j=1}^m \alpha_j (\partial_\nu \phi_j)(y) = 0.$$

There are two cases.

- ◇ If  $\partial_\nu \phi_j(y) = 0$  for all  $j$ , the condition at  $y$  is satisfied for any  $u \in U$ ;
- ◇ If  $\partial_\nu \phi_j(y) \neq 0$  for some  $j$ , then there exists a subspace  $U' \subset U$  of dimension  $(m - 1) \geq 2$  such that the condition at  $y$  is satisfied for any  $u \in U'$ .

We can then apply Lemma 2.15 with  $U$  in the first case and with  $U'$  in the second case. ✓

◇ *Robin boundary condition.* The condition  $\rho(u, y) \geq 1$  holds if and only if  $u$  vanishes at  $y$ . Since  $m \geq 3$  there exists a linear subspace  $U' \subset U$ , with  $\dim U' \geq (m - 1) \geq 2$  such that any  $u \in U'$  satisfies  $u(y) = 0$ . Then, Lemma 2.15 implies that there exists  $0 \neq u \in U'$  such that  $\rho(u, x) \geq (m - 2)$ . ✓

The proof of Lemma 2.16 is complete. □

LEMMA 2.17. *Let  $M$  be a compact surface. Let  $U$  be a linear subspace of an eigenspace of  $-\Delta + V$ , see (2.1) or (2.3).*

- (i) *Let  $x \in \text{int}(M)$ , and let  $u_1, u_2, u_3$  be three linearly independent functions in  $U$ , such that  $\nu(u_1, x) = \nu(u_2, x) = \nu(u_3, x) \geq 2$ . Then, there exists  $0 \neq u \in \text{span}\{u_1, u_2, u_3\}$  such that  $\nu(u, x) \geq \nu(u_1, x) + 2$ .*
- (ii) *Let  $x \in \partial M$ , and let  $u_1, u_2$  be two linearly independent functions in  $U$ , such that  $\rho(u_1, x) = \rho(u_2, x) \geq 1$ . Then, there exists  $0 \neq u \in \text{span}\{u_1, u_2\}$  such that  $\rho(u, x) \geq \rho(u_1, x) + 1$ .*

*Proof.* Since the index of a singular point can be expressed in terms of the vanishing order, the lemma follows from Theorem 2.8. Indeed, under the assumption of Assertion (i), we can write

$$u_i(z) = p_i(z - x) + \mathcal{O}(|z - x|^{k+1}),$$

in local coordinates centered at  $x$ , where  $p_i$  is a nonzero harmonic homogeneous polynomial of degree  $k = \frac{\nu(u_1, x)}{2}$  in two variables. Since the vector space of such polynomials has dimension 2, there exist real numbers  $\alpha_1, \alpha_2$  and  $\alpha_3$ , not all of them equal to zero, such that  $\alpha_1 p_1 + \alpha_2 p_2 + \alpha_3 p_3 = 0$ . It follows that  $\alpha_1 u_1 + \alpha_2 u_2 + \alpha_3 u_3$  vanishes at order at least  $(k + 1)$  at  $x$ . This proves Assertion (i).

The proof of Assertion (ii) is similar, using the local forms (2.10) or (2.11) depending on the boundary condition, Dirichlet or Robin.  $\square$

For later purposes, we introduce the following notation.

NOTATION 2.18. Let  $u$  be an eigenfunction of  $-\Delta + V$ , see (2.3), in the compact surface with boundary  $M$ . Define the function  $\check{u}$  on  $\partial M$  by

$$(2.12) \quad \check{u} = \begin{cases} u|_{\partial M} & \text{in the Robin case,} \\ \partial_\nu u & \text{in the Dirichlet case.} \end{cases}$$

Then, for any  $y \in \partial M$ ,  $\rho(u, y) \geq 1$  if and only if  $\check{u}(y) = 0$ .

The following lemma will also be useful.

LEMMA 2.19. *Let  $u$  be an eigenfunction of  $-\Delta + V$ , see (2.3).*

- (i) *If  $u$  is a Dirichlet eigenfunction, and  $y \in \partial M$ , then  $u$  vanishes at order  $k$  at  $y$  if and only if the function  $\partial_\nu u$  vanishes at order  $(k - 1)$  at  $y$  along  $\partial M$ .*
- (ii) *If  $u$  is a Robin eigenfunction, and  $y \in \partial M$ , then  $u$  vanishes at order  $k$  at  $y$  if and only if the function  $u|_{\partial M}$  vanishes at order  $k$  at  $y$  along  $\partial M$ .*

*Therefore, the order of vanishing of the function  $\check{u}$  at some boundary point  $y$  is precisely the number  $\rho(u, y)$  of nodal arcs hitting  $\partial M$  at  $y$ .*

*Proof.* The proof is by induction on  $k$ . The equation  $\Delta u = (V - \lambda)u$  implies relations between the derivatives of  $u$  of degree  $k$ , evaluated at  $y$ , assuming that the derivatives of order less than or equal to  $(k - 1)$  vanish at  $y$ .

More precisely, according to [YaZh2021, Section 2], fixing some  $y \in \partial M$ , we can choose local boundary isothermal coordinates at  $y$  such that the equation  $(-\Delta + V)u = \lambda u$  in a neighborhood of  $y$  is transformed into the equation

$$(e) \quad \Delta v = Av$$

in some half-ball  $\{(\xi_1, \xi_2) \in \mathbb{R}^2 \mid \xi_1^2 + \xi_2^2 < a^2, \xi_2 > 0\}$ , where 0 is the image of  $y$ . Here,  $\Delta$  is the ordinary Laplacian in the variables  $(\xi_1, \xi_2)$ ,  $a$  is some given positive number,  $A$  and  $v$  are  $C^\infty$  up to the boundary, and correspond to  $(V - \lambda)$  and  $u$  respectively.

In the proof, we use the following conventions.

- $\diamond$  The symbol  $\stackrel{t}{\equiv}$  indicates a trivial identity.
- $\diamond$  The symbol  $\stackrel{e}{\equiv}$  indicates an identity which follows from the above identity (e).
- $\diamond$  The symbol  $\stackrel{(m)}{\equiv}$  indicates an identity which holds up to a linear combination of derivatives of  $v$  of order less than or equal to  $m$ .
- $\diamond$  The symbol  $\partial^{(p,q)}$  stands for  $\frac{\partial^{p+q}}{\partial \xi_1^p \partial \xi_2^q}$ .

For  $k \geq 2$ , we have

$$\begin{aligned} \partial^{(k-2q, 2q)} v &\stackrel{t}{\equiv} \partial^{(k-2q, 2q-2)} \partial^{(0, 2)} v \\ &\stackrel{e}{\equiv} \partial^{(k-2q, 2q-2)} \left( -\partial^{(2, 0)} v + Av \right) \\ &\stackrel{(k-2)}{\equiv} -\partial^{(k-2q+2, 2q-2)} v. \end{aligned}$$

Assuming that  $u$  vanishes at order larger than or equal to  $(k-1)$  at  $(0, 0)$ , we obtain that

$$(a) \quad \partial^{(k-2q, 2q)} u(0, 0) = (-1)^q \partial^{(k, 0)} u(0, 0), \text{ for } q \in \left\{ 0, 1, \dots, \left\lfloor \frac{k}{2} \right\rfloor \right\}.$$

Similarly,

$$\begin{aligned} \partial^{(k-2q-1, 2q+1)} v &\stackrel{t}{\equiv} \partial^{(k-2q-1, 2q-1)} \partial^{(0, 2)} v \\ &\stackrel{e}{\equiv} \partial^{(k-2q-1, 2q-1)} \left( -\partial^{(2, 0)} v + Av \right) \\ &\stackrel{(k-2)}{\equiv} -\partial^{(k-2q+1, 2q-1)} v. \end{aligned}$$

Assuming that  $u$  vanishes at order larger than or equal to  $(k-1)$  at  $(0, 0)$ , we obtain that

$$(b) \quad \partial^{(k-2q-1, 2q+1)} u(0, 0) = (-1)^q \partial^{(k-1, 1)} u(0, 0), \text{ for } q \in \left\{ 0, 1, \dots, \left\lfloor \frac{k-1}{2} \right\rfloor \right\}.$$

◇ *Dirichlet case.* In this case,  $\check{v}(\xi_1) := \partial^{(0, 1)} v(\xi_1, 0)$ . Since  $v(\xi_1, 0) \equiv 0$ , Equation (a) implies that  $\partial^{(k-2q, 2q)} v(0, 0) = 0$  for all  $q \in \left\{ 0, \dots, \left\lfloor \frac{k}{2} \right\rfloor \right\}$ . If  $v$  vanishes at order greater than or equal to  $(k-1)$ , Equation (b) implies that  $\partial^{(k-2q-1, 2q+1)} v(0, 0) = (-1)^q \partial^{(k-1)} \check{v}(0)$  for all  $q \in \left\{ 0, \dots, \left\lfloor \frac{k-1}{2} \right\rfloor \right\}$ . It follows that if  $v$  vanishes at order greater than or equal to  $(k-1)$ , then  $v$  vanishes at order greater than or equal to  $k$  if and only if  $\partial^{(k-1)} \check{v}(0) = 0$ .

◇ *Robin case.* In this case,  $\check{v}(\xi_1) := v(\xi_1, 0)$ . Assuming that  $v$  vanishes at order at least  $(k-1)$ , Equation (a) implies that  $\partial^{(k-2q, 2q)} v(0, 0) = (-1)^q \partial^k \check{v}(0)$ . Since  $\partial^{(0, 1)} v(\xi_1, 0) \equiv B(\xi_1)u(\xi_1, 0)$  (Robin condition), Equation (b) implies that  $\partial^{(k-2q-1, 2q+1)} u(0, 0) = 0$ . Therefore, if  $v$  vanishes at order at least  $(k-1)$  at  $(0, 0)$ , then  $v$  vanishes at order at least  $k$  if and only if  $\partial^k \check{v}(0) = 0$ .

We have proved that  $v$  vanishes at order at least  $k$  (resp. equal to  $k$ ) at  $(0, 0)$  if and only if  $\check{v}$  vanishes at order  $\rho(v, (0, 0))$  at  $(0, 0)$ .  $\square$

#### 2.1.4. A global property of nodal sets.

LEMMA 2.20. *Let  $(M, g)$  be a compact Riemannian surface. Let  $w_n, w : M \rightarrow \mathbb{R}$  be continuous functions with zero sets  $K_n := w_n^{-1}(0)$  and  $K := w^{-1}(0)$ . Assume that  $w_n \rightarrow w$  uniformly.*

- (i) *The limit points of the sequence  $\{K_n\}$  with respect to the Hausdorff distance associated with the Riemannian distance of  $(M, g)$  are compact and contained in  $K$ . They are connected if the sets  $K_n$  are connected.*
- (ii) *If  $K_n, K$  are nodal sets of eigenfunctions of  $-\Delta + V$ , then the sequence  $\{K_n\}$  converges to  $K$  in the Hausdorff distance.*

*Proof.* The properties that the sequence  $\{K_n\}$  has limit points, and that they are compact (and connected if the sets  $K_n$  are connected) are general. Assume that a subsequence  $\{K_{s(n)}\}$  tends to  $K'$  in the Hausdorff distance. Assume that  $K' \not\subset K$ . Then, there exists some  $z' \in K'$  such that  $w(z') \neq 0$ . Let  $\varepsilon_0 > 0$  be such that  $|w(z')| = 3\varepsilon_0$ .

(a) There exists  $\eta_0$  such that  $d(y_1, y_2) < \eta_0$  implies that  $|w(y_1) - w(y_2)| < \varepsilon_0$ .

(b) Since  $\{K_{s(n)}\}$  tends to  $K'$  in the Hausdorff distance, there exists  $N(\eta_0)$  such that for  $n \geq N(\eta_0)$ ,  $K' \subset \mathcal{U}(K_{s(n)}, \eta_0)$ , the  $\eta_0$ -neighborhood of  $K_{s(n)}$ . In particular there exists some point  $z_{s(n)} \in K_{s(n)}$  such that  $d(z', z_{s(n)}) < \eta_0$ .

(c) There exists  $N(\varepsilon_0)$  such that for  $n \geq N(\varepsilon_0)$ ,  $\|w - w_{s(n)}\| < \varepsilon_0$ .

Take  $n \geq \max\{N(\varepsilon_0), N(\eta_0)\}$ . Then,

$$w(z') = w(z') - w(z_{s(n)}) + w(z_{s(n)}) - w_{s(n)}(z_{s(n)})$$

and we conclude that  $|w(z')| < 2\varepsilon_0$ , a contradiction.

The second assertion uses the nodal character: assume that there exists  $z \in K \setminus K'$ . Then  $d(z, K') =: 2\eta > 0$ , and for  $n$  large enough,  $d(z, K_{s(n)}) > \eta$ . Since  $K$  is a nodal set, there exists a small arc through  $z$ , from some  $z_-$  to some  $z_+$  such that  $w(z_-) < 0$  and  $w(z_+) > 0$ . It follows that for  $n$  large enough we also have  $w_{s(n)}(z_-) < 0$  and  $w_{s(n)}(z_+) > 0$ . This shows that  $w_{s(n)}$  must vanish on this small arc, and hence that there exists some  $z'_n \in K_{s(n)}$  close to  $z$  contradicting the fact that  $d(z, K_n) > \eta$ . Since the only possible limit point of  $\{K_n\}$  is  $K$ , the assertion follows.  $\square$

## 2.2. Euler Type Formulas for Nodal Sets

In this section,  $M$  denotes a smooth surface homeomorphic to  $\mathbb{S}^2$ , or a smooth bounded domain  $M \subset \mathbb{R}^2$  with boundary  $\partial M$ .

**2.2.1. Graphs associated with a nodal set.** We are interested in Euler type formulas for the nodal set  $\mathcal{Z}(u)$  of an eigenfunction  $u$  of the operator  $-\Delta + V$  in  $(M, g)$ , where  $g$  is some smooth Riemannian metric on  $M$ , and  $V$  a smooth real valued potential. When  $\partial M \neq \emptyset$ , we assume a Dirichlet, Neumann or  $h$ -Robin boundary condition on  $\partial M$ , see (2.1) or (2.3).

In this framework, the singular set  $\mathcal{S}(u) = \mathcal{S}_i(u) \cup \mathcal{S}_b(u)$  of  $u$  is finite, and the set  $(\mathcal{Z}(u) \cup \partial M) \setminus \mathcal{S}(u)$  consists of finitely many components  $\{C_j\}$  which are diffeomorphic to either circles or open intervals whose extremities are points in  $\mathcal{S}(u)$ .

The pair  $\mathcal{G}_u = (\mathcal{S}(u), \{C_j\})$  is in general not a *multiple graph* in the sense of [Dies2017, Section 1.10]. Indeed, among the components  $\{C_j\}$ , there might be *nodal circles* or components of  $\partial M$  which do not intersect  $\mathcal{Z}(u)$ . It is not a *simple graph*, as some of the  $C_j$ 's might form multiple edges.

NOTATION 2.21. From now on, we use the definition of graph given in [Gib12010] (i.e., “graph = simple graph”). Given a graph  $G$ , we denote by  $\alpha_0(G)$  the number of vertices, by  $\alpha_1(G)$  the number of edges, and by  $c(G)$  the number of components of  $G$ . For a graph  $G$  embedded in a surface  $M$ , we denote by  $r(G, M)$  the number of components of  $M \setminus G$ .

With the pair  $\mathcal{G}_u$  we will associate a graph (not necessarily connected) to which we will apply the (Euler) formula in [Gib12010, Theorem 1.27]. The vertices of the graph should comprise the singular points of  $\mathcal{S}(u)$ , and the edges should comprise

both sub-arcs of  $\mathcal{Z}(u)$  and sub-arcs of  $\partial M$ . Taking into account the fact that  $\mathcal{G}_u$  is in general not a graph, we first define a multigraph  $G_0 := G_0(u, M)$ , as follows.

- ◇ Let  $e := e(u, M)$  be the number of components of  $(\mathcal{Z}(u) \cup \partial M) \setminus \mathcal{S}(u)$  which are homeomorphic to a circle. We first choose one vertex for each such component. Call  $\{v_1, \dots, v_e\}$  these vertices, if any. Define the set  $V_0$  of vertices of  $G_0$  as  $\mathcal{S}(u) \cup \{v_1, \dots, v_e\}$ .
- ◇ Define the set  $E_0$  of edges of  $G_0$  as the set of components of  $(\mathcal{Z}(u) \cup \partial M) \setminus V_0$  (they are all homeomorphic to intervals).

LEMMA 2.22. *The pair  $G_0 = (V_0, E_0)$  is a multigraph. The number of vertices  $\alpha_0(G_0)$ , and the number of edges  $\alpha_1(G_0)$  of  $G_0$  are given by*

$$(2.13) \quad \begin{cases} \alpha_0(G_0) = e + |\mathcal{S}_i(u)| + |\mathcal{S}_b(u)|, \\ \alpha_1(G_0) = e + \frac{1}{2} \left( \sum_{y \in \mathcal{S}_i(u)} \nu(u, y) + \sum_{z \in \mathcal{S}_b(u)} \rho(u, z) \right) + |\mathcal{S}_b(u)|, \end{cases}$$

where  $e$  is defined above, where  $|\mathcal{S}_i(u)|$  (resp  $|\mathcal{S}_b(u)|$ ) denotes the number of interior (resp. boundary) singular points of  $u$ , and where the numbers  $\nu$  and  $\rho$  are as in Definition 2.10. In particular,

$$(2.14) \quad \alpha_1(G_0) - \alpha_0(G_0) = \frac{1}{2} \left( \sum_{y \in \mathcal{S}_i(u)} (\nu(u, y) - 2) + \sum_{z \in \mathcal{S}_b(u)} \rho(u, z) \right).$$

*Proof.* Clearly  $G_0$  is a multigraph in the sense of [Dies2017, Section 1.10]. The formula for  $\alpha_0$  is clear. The first term in the right-hand side for  $\alpha_1$  counts both the number of points  $v_j$  and the number of components of  $(\mathcal{Z}(u) \cup \partial M) \setminus \mathcal{S}(u)$  which are circles. The second term counts the number of edges between two singular points, each one being a simple curve contained in  $\mathcal{Z}(u) \setminus \mathcal{S}(u)$ . The third term counts the number of edges determined by the boundary singular points on the components of  $\partial M$  which intersect  $\mathcal{S}(u)$ .  $\square$

REMARK 2.23. The second relation in (2.13) also follows from the relation

$$(2.15) \quad 2\alpha_1(\Gamma) = \sum_{x \in V(\Gamma)} \deg_{\Gamma}(x)$$

which holds for any multi-graph  $\Gamma$  (here,  $\deg_{\Gamma}(x)$ , the degree of the vertex  $x$ , is the number of edges of  $\Gamma$  one of whose ends is  $x$ ), see [Dies2017, Section 1.2].

Note that the multigraph  $G_0(u, M)$

- (a) might contain loops at some singular point or at one vertex  $v_j$  ;
- (b) might contain pairs of distinct vertices in  $V_0$  linked by more than one edge.

We now transform the multigraph  $G_0(u, M)$  into a graph  $G(u, M)$  (in the sense of [Gib12010, p. 10]), keeping track of the number of vertices and edges. More precisely, if necessary, we introduce additional vertices and edges by performing one of the following vertex-edge additions.

DEFINITION 2.24. We call *vertex-edge additions* the following modifications of the graph  $G_0(u, M)$ .

- (i) If a component  $\Gamma$  of  $(\mathcal{Z}(u) \cup \partial M) \setminus V_0$  is bounded by only one vertex  $v$  (i.e., there is a loop at  $v$ ), we add two extra vertices  $v_1, v_2$  on  $\Gamma$ , and replace the edge  $\Gamma$  by three edges, the components of  $\Gamma \setminus \{v_1, v_2\}$ .

- (ii) If two distinct vertices of  $V_0$  are the endpoints of more than one edge in  $E_0$ , i.e., of more than one component  $\Gamma_j$  of  $(\mathcal{Z}(u) \cup \partial M) \setminus V_0$ , we add one extra vertex  $w_j$  to each  $\Gamma_j$ , and replace  $\Gamma_j$  by two edges, the components of  $\Gamma_j \setminus \{w_j\}$ .

Figure 2.1 illustrates the transformation of  $\mathcal{Z}(u) \cup \partial M$  into a graph. Lines contained in the boundary appear in black and lines contained in  $\mathcal{Z}(u)$  appear in red. Blue dots represent vertices  $v_i$  initially attached to each circle component. Green dots represent vertices added in the vertex-edge additions. Sub-figure (A) illustrates the transformation of circle components of  $\partial M$  or  $\mathcal{Z}(u)$ , and loops in  $\mathcal{Z}(u)$  into graphs. Sub-figure (B) illustrates the transformation of multiple edges into graphs.

The following lemma is clear.

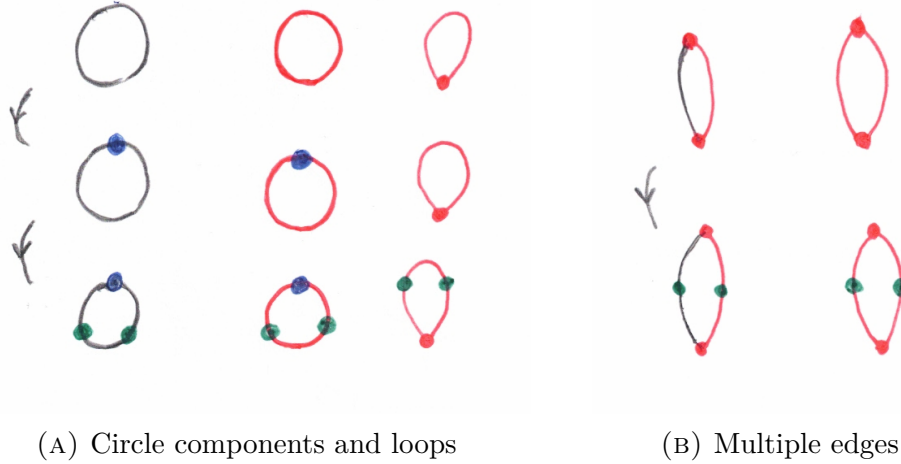


FIGURE 2.1. Vertex-edge additions

LEMMA 2.25. *Performing finitely many vertex-edge additions transforms the multi-graph  $G_0(u, M)$  into a graph  $G(u, M)$ .*

NOTATION 2.26. For an eigenfunction of  $-\Delta + V$  in  $M$ , we introduce the following numbers.

- (a)  $\beta(u)$  is defined as  $\beta(u) = b_0(\mathcal{Z}(u) \cup \partial M) - b_0(\partial M)$ , the difference between the number of components of  $\mathcal{Z}(u) \cup \partial M$ , and the number of components of  $\partial M$ ;
- (b)  $\kappa(u)$  denotes the number of nodal domains of  $u$ ;
- (c)  $\sigma(u) = \sigma_i(u) + \sigma_b(u)$  weighs the singular points of  $u$ ,

$$\begin{cases} \sigma_i(u) = \frac{1}{2} \sum_{x \in \mathcal{S}_i(u)} (\nu(u, x) - 2), \\ \sigma_b(u) = \frac{1}{2} \sum_{x \in \mathcal{S}_b(u)} \rho(u, x). \end{cases}$$

The following lemma follows from the fact that the number  $\alpha_0 - \alpha_1$  remains unchanged if we perform a vertex-edge addition.

LEMMA 2.27. *For the graph  $G := G(u, M)$  obtained from the multigraph  $G_0 := G_0(u, M)$  by performing vertex-edge additions, we have,*

$$\begin{cases} \alpha_1(G) - \alpha_0(G) &= \alpha_1(G_0) - \alpha_0(G_0) &= \sigma(u), \\ c(G) &= c(G_0) &= b_0(\mathcal{Z}(u) \cup \partial M), \\ r(G, M) &= r(G_0, M) &= \kappa(u). \end{cases}$$

**2.2.2. Euler type formulas for nodal sets.** According to [Gib12010, Theorem 1.27] a graph  $\bar{G}$  in  $\mathbb{R}^2$ , divides the plane into  $r(\bar{G})$  regions, with

$$(2.16) \quad r(\bar{G}) = \alpha_1(\bar{G}) - \alpha_0(\bar{G}) + c(\bar{G}) + 1.$$

PROPOSITION 2.28. *Let  $u$  be an eigenfunction of  $-\Delta + V$  on  $M$  (with Dirichlet, Neumann or  $h$ -Robin boundary condition if  $\partial M \neq \emptyset$ ), where  $M$  is topologically a sphere or a domain in  $\mathbb{R}^2$ . The following Euler type formula holds for  $\mathcal{Z}(u)$ .*

$$(2.17) \quad \kappa(u) = 1 + \beta(u) + \sigma(u).$$

*Proof.*

◇ If  $M = \mathbb{S}^2$ , we can view the graph  $G := G(u, M)$  as a graph in  $\mathbb{R}^2$ . Applying (2.16), we obtain

$$r(G, \mathbb{R}^2) = \alpha_1(G) - \alpha_0(G) + c(G) + 1,$$

and it suffices to apply Lemma 2.27 with  $\partial M = \emptyset$ .

◇ If  $M \subset \mathbb{R}^2$ , we can view  $G = G(u, M)$  as a graph in  $\mathbb{R}^2$  for which

$$r(G, \mathbb{R}^2) = r(G, M) + b_0(\partial M)$$

and to apply Lemma 2.27. □

PROPOSITION 2.29. *Let  $u$  be an eigenfunction of  $-\Delta + V$  in  $M$ . For any component  $\Gamma$  of  $\partial M$ , we have*

$$(2.18) \quad \sum_{z \in \mathcal{S}_b(u) \cap \Gamma} \rho(z) \in 2\mathbb{N}.$$

*Furthermore,*

$$(2.19) \quad b_0(\mathcal{Z}(u) \cup \partial M) - b_0(\partial M) + \frac{1}{2} \sum_{y \in \mathcal{S}_b(u)} \rho(y) \geq 1.$$

*Proof.* The first assertion is general and contained in Corollary 2.13. To prove the second assertion, we divide the components of  $\partial M$  into two sets: the components  $\Gamma'_i, 1 \leq i \leq p$ , which meet  $\mathcal{Z}(u)$ , and the components  $\Gamma''_j, 1 \leq j \leq q$ , which do not meet  $\mathcal{Z}(u)$ . Let  $\Gamma(u) = \cup_{i=1}^p \Gamma'_i$ . Clearly, we have the relation

$$b_0(\mathcal{Z}(u) \cup \partial M) - b_0(\partial M) = b_0(\mathcal{Z}(u) \cup \Gamma(u)) - b_0(\Gamma(u)).$$

On the other-hand, according to (2.18), for each  $1 \leq i \leq p$ , we have

$$\sum_{z \in \mathcal{S}_b(u) \cap \Gamma'_i} \rho(z) \geq 2.$$

Relation (2.19) follows from the fact that  $b_0(\mathcal{Z}(u) \cup \Gamma(u)) \geq 1$ . □

### 2.3. Proof of the Local Structure Theorem at an Interior Point

In this section, we provide a proof of the local structure theorem for the nodal set of an eigenfunction  $u$  in the neighborhood of an interior singular point (alias critical zero)  $x$ , see Theorem 2.8, Assertion (i). Cheng [Chen1976] states a more precise result<sup>3</sup>, the existence of a local diffeomorphism which sends the nodal set of  $u$  in a neighborhood of  $x$  onto the nodal set of the lower order term in the Taylor expansion of  $u$  at  $x$  (a harmonic polynomial), which consists of rays. Our proof has the advantage of being more quantitative in particular when applied to eigenfunctions depending on a parameter. This proof is probably known although we did not find it explicitly in the literature. In [Bess1980], Besson refers to § 128 of the book [Vali1966].

Let  $(M, g)$  be a  $C^\infty$  compact Riemannian surface, and let  $V : M \rightarrow \mathbb{R}$  be a real valued  $C^\infty$  potential. Let  $u \neq 0$  be a real valued function, satisfying

$$(2.20) \quad (-\Delta_g + V)u = \lambda u$$

for some real number  $\lambda$ . Here  $\Delta_g$  denotes the Laplace-Beltrami operator of  $(M, g)$ . Let  $x$  be a given (interior) point of  $M$  (in case  $M$  has a boundary).

Choose some  $r_0 > 0$  such that the exponential map  $\exp_x : T_x M \rightarrow M$  is a diffeomorphism from the disk  $D(2r_0)$ , with center 0 and radius  $2r_0$  in  $T_x M$ , onto the geodesic disk  $D(x, 2r_0)$ , with center  $x$  and radius  $2r_0$  in  $M$ . Choose an orthonormal frame in  $T_x M$ , call  $(\xi_1, \xi_2)$  the corresponding coordinates in  $T_x M$ , and  $(r, \omega)$  the associated polar coordinates. In the normal coordinates  $(\xi_1, \xi_2)$ , the Riemannian metric is given by the  $2 \times 2$  matrix  $G = (g_{ij})$ , where  $g_{ij} = g(\frac{\partial}{\partial \xi_i}, \frac{\partial}{\partial \xi_j})$ ; the Riemannian measure is given by  $v_g d\xi_1 d\xi_2$ , where  $v_g = \sqrt{\det G}$ . Write the matrix  $G^{-1}$  as  $G^{-1} = (g^{ij})$ . Then (see for example [GaHuLa2004, § 2.89bis, p. 87]),

$$(2.21) \quad \begin{cases} G(0, 0) = \text{Id}, & \text{i.e., } g_{ij}(0, 0) = \delta_{ij}, & 1 \leq i, j \leq 2, \\ \frac{\partial G}{\partial \xi_k}(0, 0) = 0, & \text{i.e., } \frac{\partial g_{ij}}{\partial \xi_k}(0, 0) = 0, & 1 \leq i, j, k \leq 2. \end{cases}$$

It follows that

$$(2.22) \quad \begin{cases} v_g(0, 0) = 1, \\ G^{-1}(0, 0) = \text{Id}, & \text{i.e., } g^{ij}(0, 0) = \delta_{ij}, & 1 \leq i, j \leq 2, \\ \frac{\partial v_g}{\partial \xi_k}(0, 0) = 0, & 1 \leq k \leq 2. \\ \frac{\partial G^{-1}}{\partial \xi_k}(0, 0) = 0, & \text{i.e., } \frac{\partial g^{ij}}{\partial \xi_k}(0, 0) = 0, & 1 \leq i, j, k \leq 2. \end{cases}$$

Given a function  $u$  on  $M$ , let  $f = u \circ \exp_x$ . In the local coordinates  $(\xi_1, \xi_2)$ , the Laplace-Beltrami operator  $\Delta_g$  is given (see [BeGM1971, §G.III, p. 126]) by

$$(2.23) \quad \begin{cases} \Delta_g f &= v_g^{-1} \sum_{1 \leq i, j \leq 2} \frac{\partial}{\partial \xi_i} \left( v_g g^{ij} \frac{\partial f}{\partial \xi_j} \right), \\ &= \sum_{1 \leq i, j \leq 2} g^{ij} \frac{\partial^2 f}{\partial \xi_i \partial \xi_j} + \sum_{1 \leq j \leq 2} b_j \frac{\partial f}{\partial \xi_j}, \\ &\text{where } b_j = \sum_{1 \leq i \leq 2} v_g^{-1} \frac{\partial}{\partial \xi_i} (v_g g^{ij}), & 1 \leq j \leq 2. \end{cases}$$

Letting  $\Delta_0 = \sum_{1 \leq j \leq 2} \frac{\partial^2}{\partial \xi_j^2}$  denote the Laplacian in the Euclidean space  $(T_x M, g_x)$ , and taking relations (2.21) and (2.22) into account, we obtain the following expression

<sup>3</sup>The validity of the proof of Cheng's statement is questioned in K. Pagani's thesis [Paga1990], Bemerkungen 2.9.3, p. 34. We thank V. Bobkov for pointing out this fact.



for the Laplace-Beltrami operator,

$$(2.24) \quad \begin{cases} \Delta_g = \Delta_0 + \sum_{1 \leq i, j \leq 2} a_{ij} \frac{\partial^2}{\partial \xi_i \partial \xi_j} + \sum_{1 \leq j \leq 2} b_j \frac{\partial}{\partial \xi_j}, \\ \text{where } \text{ord}(a_{ij}, (0, 0)) \geq 2 \text{ and } \text{ord}(b_j, (0, 0)) \geq 1. \end{cases}$$

If  $u$  satisfies (2.20) and  $u(x) = 0$ , the unique continuation theorem [Aron1957, DoFe1990a] implies that  $f$  does not vanish at infinite order at 0.

If  $\text{ord}(u, x) = \text{ord}(f, 0) = p$ , Taylor's formula at 0, gives

$$(2.25) \quad \begin{cases} f(\xi_1, \xi_2) = \sum_{|\alpha|=p} \frac{1}{\alpha!} D^\alpha f(0, 0) (\xi_1, \xi_2)^\alpha + R_{p+1}(\xi_1, \xi_2), \text{ where} \\ R_{p+1}(\xi_1, \xi_2) = \sum_{|\alpha|=p+1} \frac{p+1}{\alpha!} (\xi_1, \xi_2)^\alpha \int_0^1 (1-t)^p D^\alpha f(t \xi_1, t \xi_2) dt. \end{cases}$$

Here, as usual,

$$(2.26) \quad \begin{cases} \alpha = (\alpha_1, \alpha_2), \quad |\alpha| = \alpha_1 + \alpha_2, \quad (\xi_1, \xi_2)^\alpha = \xi_1^{\alpha_1} \xi_2^{\alpha_2}, \text{ and} \\ D^\alpha f = \frac{\partial^{|\alpha|} f}{\partial \xi_1^{\alpha_1} \partial \xi_2^{\alpha_2}}. \end{cases}$$

Using relations (2.20) and (2.24), and identifying the terms with lowest order, we find that the polynomial  $P_p(\xi_1, \xi_2) := \sum_{|\alpha|=p} \frac{1}{\alpha!} D^\alpha f(0, 0) (\xi_1, \xi_2)^\alpha$  is homogenous of degree  $p$ , and harmonic with respect to  $\Delta_0$ .

REMARK 2.30. As a matter of fact, we may write a 2-term Taylor formula for the function  $f$ ,

$$f(\xi_1, \xi_2) = P_p(\xi_1, \xi_2) + P_{p+1}(\xi_1, \xi_2) + R_{p+2}(\xi_1, \xi_2),$$

where  $P_p$  and  $P_{p+1}$  are homogeneous polynomials of degrees  $p$  and  $(p+1)$  respectively, and where the remainder term  $R_{p+2}$  vanishes at order at least  $(p+2)$ . Then, we actually have that  $\Delta_0 P_p = 0$  and  $\Delta_0 P_{p+1} = 0$ .

Writing the harmonicity condition  $\Delta_0 P_p = 0$  in polar coordinates  $(r, \omega)$  in  $T_x M$ , we find that the polynomial  $P_p$  has the form

$$(2.27) \quad P_p(r \cos \omega, r \sin \omega) = a r^p \sin(p \omega - \omega_0).$$

for some  $0 \neq a \in \mathbb{R}$  and some  $\omega_0 \in [0, 2\pi]$ .

Multiplying the function  $f$  by some constant, and rotating the coordinates  $(\xi_1, \xi_2)$  in  $\mathbb{R}^2$  if necessary, we can assume that  $a = 1$  and  $\omega_0 = 0$ . It follows that  $f$  can be written as

$$(2.28) \quad f(r \cos \omega, r \sin \omega) = r^p \sin(p \omega) + r^{p+1} T_{p+1}(r \cos \omega, r \sin \omega),$$

where  $T_{p+1}$  is given by

$$(2.29) \quad \sum_{|\alpha|=p+1} \frac{p+1}{\alpha!} (\cos \omega, \sin \omega)^\alpha \int_0^1 (1-t)^p D^\alpha f(tr \cos \omega, tr \sin \omega) dt.$$

Define

$$(2.30) \quad W(r, \omega) := \sin(p \omega) + r T_{p+1}(r, \omega).$$

The function  $W(0, \omega)$  vanishes precisely for the values

$$(2.31) \quad \omega_j := j \frac{\pi}{p}, \quad j \in \{0, \dots, 2p-1\}.$$

Choose  $\alpha_1 \in (0, \frac{\pi}{8})$  and define  $\alpha_p := \frac{\alpha_1}{p}$ . We have the following relations.

$$(2.32) \quad \begin{cases} \sin(p(\omega_j \pm \alpha_p)) = \pm(-1)^j \sin(\alpha_1), \\ |\sin(p\omega)| \geq \sin \alpha_1, \text{ for } \omega \notin \bigcup_{j=0}^{2p-1} (\omega_j - \alpha_p, \omega_j + \alpha_p) \end{cases}$$

Define

$$(2.33) \quad r_1 := \min \left\{ r_0, \frac{1}{2} \sin(\alpha_1) \|T_{p+1}\|_{\infty, D(r_0)}^{-1}, \frac{1}{2} \cos(\alpha_1) \|\partial_\omega T_{p+1}\|_{\infty, D(r_0)}^{-1} \right\},$$

where  $\|\cdot\|_{\infty, D(\frac{1}{2})}$  denotes the  $L^\infty$  norm of functions in the disk  $D(r_0)$  of radius  $r_0$  in  $T_x M$ .

**PROPOSITION 2.31.** *For any  $0 \leq r \leq r_1$ ,*

(i) *the function  $\omega \mapsto W(r, \omega)$  does not vanish in*

$$[0, 2\pi] \setminus \bigcup_{j=0}^{2p-1} (\omega_j - \alpha_p, \omega_j + \alpha_p) = \bigcup_{j=0}^{2p-1} [\omega_j + \alpha_p, \omega_{j+1} - \alpha_p];$$

(ii) *for each  $j \in \{0, \dots, 2p-1\}$ , the function  $\omega \mapsto W(r, \omega)$  has exactly one zero  $\tilde{\omega}_j(r) \in (\omega_j - \alpha_p, \omega_j + \alpha_p)$ ;*

(iii) *for each  $j \in \{0, \dots, 2p-1\}$ , the function  $r \mapsto \tilde{\omega}_j(r)$  is  $C^\infty$  in  $(0, r_1)$  and tends to  $\omega_j$  as  $r$  tends to zero;*

(iv) *for each  $j \in \{0, \dots, 2p-1\}$ , the curve*

$$(0, r_1) \ni r \mapsto a_j(r) = (r \cos(\tilde{\omega}_j(r)), r \sin(\tilde{\omega}_j(r)))$$

*is smooth and has semi-tangent  $\omega_j$  at the origin.*

*Proof.* To prove (i), we observe that in each interval  $\{r\} \times [\omega_j + \alpha_p, \omega_{j+1} - \alpha_p]$ ,  $|W(r, \omega)| \geq \frac{1}{2} \sin(\alpha_1)$ . To prove (ii), we observe that the function  $W(r, \omega)$  changes sign in  $\{r\} \times (\omega_j - \alpha_p, \omega_j + \alpha_p)$  and that its partial derivative with respect to  $\omega$  does not vanish. Assertion (iii) follows from the implicit function theorem. Assertion (iv) follows from the previous ones.  $\square$

**REMARK 2.32.** Assume that there exist two eigenfunctions  $v_1$  and  $v_2$  of (2.20) such that the functions  $f_i = v_i \circ \exp_x$  satisfy the relations

$$(2.34) \quad \begin{cases} f_1(r \cos \omega, r \sin \omega) = r^p \sin(p\omega) + R_{1,p+1}(r \cos \omega, r \sin \omega), \\ f_2(r \cos \omega, r \sin \omega) = r^p \cos(p\omega) + R_{2,p+1}(r \cos \omega, r \sin \omega). \end{cases}$$

Defining the family of functions  $w_\theta = \cos \theta v_1 - \sin \theta v_2$ , the associated family of functions  $f_\theta = w_\theta \circ \exp_x$ , satisfies

$$(2.35) \quad \begin{cases} f_\theta(r \cos \omega, r \sin \omega) = r^p \sin(p\omega - \theta) + R_{\theta,p+1}(r \cos \omega, r \sin \omega), \text{ with} \\ R_{\theta,p+1} = \cos \theta R_{1,p+1} - \sin \theta R_{2,p+1}. \end{cases}$$

Then, Proposition 2.31 remains valid for the family  $f_\theta$ , uniformly with respect to the variable  $\theta \in [0, 2\pi]$ , with  $\omega_j$  replaced by  $\omega_{j,\theta} + \frac{\theta}{p}$ , and the corresponding functions  $r \mapsto \tilde{\omega}_j(r, \theta)$  and  $r \mapsto a_j(r, \theta)$  are smooth in  $(r, \theta)$ .

**REMARK 2.33.** Proposition 2.31 tells us that, in a neighborhood of the critical zero  $u$  of  $u$ , the nodal set  $\mathcal{Z}(u)$  consists of  $p$  smooth semi-arcs emanating from  $x$  tangentially to the rays  $\omega_j$ .

## 2.4. Proof of the Local Structure Theorem at a Boundary Point

**2.4.1. Preamble.** Let  $\Omega \subset \mathbb{R}^2$  be a bounded domain with  $C^\infty$  boundary  $\Gamma := \partial\Omega$ . We consider the eigenvalue problem

$$(2.36) \quad \begin{cases} (-\Delta + V)u = \lambda u & \text{in } \Omega \\ B(u) = 0 & \text{on } \Gamma, \end{cases}$$

where  $V$  is a real valued function in  $C^\infty(\overline{\Omega})$ ,  $\Delta$  the usual Laplacian of  $\mathbb{R}^2$ , and  $B(u)$  one of the following boundary conditions on  $\Gamma$ ,

$$(2.37) \quad \begin{cases} B(u) := u|_\Gamma & \text{the Dirichlet boundary condition} \\ B(u) := \partial_{\nu_i} u & \text{the Neumann boundary condition} \\ B(u) := \partial_{\nu_i} u - h u|_\Gamma & \text{the } h\text{-Robin boundary condition,} \end{cases}$$

with  $\partial_{\nu_i} u$  the derivative of  $u$  with respect to the unit normal along  $\Gamma$ , pointing inwards, and  $h$  a  $C^\infty$  function on  $\Gamma$ .

The purpose of this section is to describe the local structure of the nodal set  $\mathcal{Z}(u)$  of an eigenfunction  $u$  of (2.36)-(2.37) near a boundary singular point of  $u$ , i.e., a point  $y \in \Gamma$  at which the nodal set hits the boundary. For the sake of simplicity, throughout this section, we assume that

ASSUMPTION 2.34.  $\Omega$  is simply connected.

We explain how to deal with non simply connected domains in Remark 2.39 and Subsection 2.4.7.

**2.4.2. Notation.** We use the following notation.

Without loss of generality, we assume that the length of  $\Gamma$  is  $2\pi$ . The orientation of  $\mathbb{R}^2$  induces a natural orientation of  $\Gamma$ , and we fix an arc length parametrization of  $\Gamma$  compatible with this orientation:

$$(2.38) \quad \begin{cases} \gamma : [0, 2\pi] \rightarrow \mathbb{R}^2 \text{ with } \gamma([0, 2\pi]) = \Gamma \\ \vec{\tau}_{\gamma(t)} = \dot{\gamma}(t) \text{ is the unit tangent vector} \\ \vec{\nu}_{\gamma(t)} \text{ is the unit normal vector pointing inwards} \\ \{\vec{\tau}, \vec{\nu}\} \text{ is a direct frame.} \end{cases}$$

Introduce the notation

$$(2.39) \quad \begin{cases} \mathbb{H} := \{(\xi_1, \xi_2) \in \mathbb{R}^2 \mid \xi_2 > 0\} \\ \overline{\mathbb{H}} := \{(\xi_1, \xi_2) \in \mathbb{R}^2 \mid \xi_2 \geq 0\}. \end{cases}$$

$$(2.40) \quad \begin{cases} \mathbb{D} := \{(\xi_1, \xi_2) \in \mathbb{R}^2 \mid \xi_1^2 + \xi_2^2 < 1\} \\ \overline{\mathbb{D}} := \{(\xi_1, \xi_2) \in \mathbb{R}^2 \mid \xi_1^2 + \xi_2^2 \leq 1\}. \end{cases}$$

Given  $y = (y_1, y_2) \in \mathbb{R}^2$  and  $r > 0$ , define the disks

$$(2.41) \quad \begin{cases} D(y, r) := \{(z_1, z_2) \in \mathbb{R}^2 \mid (y_1 - z_1)^2 + (y_2 - z_2)^2 < r^2\} \\ \overline{D}(y, r) := \{(z_1, z_2) \in \mathbb{R}^2 \mid (y_1 - z_1)^2 + (y_2 - z_2)^2 \leq r^2\}. \end{cases}$$

Similarly, given  $\eta \in \partial\mathbb{H}$ , define the half-disks  $D_+(\eta, r)$  and  $\overline{D}_+(\eta, r)$

$$(2.42) \quad \begin{cases} D_+(\eta, r) := \{(\xi_1, \xi_2) \in \mathbb{H} \mid (\eta_1 - \xi_1)^2 + (\eta_2 - \xi_2)^2 < r^2\} \\ \overline{D}_+(\eta, r) := \{(\xi_1, \xi_2) \in \mathbb{H} \mid (\eta_1 - \xi_1)^2 + (\eta_2 - \xi_2)^2 \leq r^2\}. \end{cases}$$

### 2.4.3. Preparation.

#### 2.4.3.1. Regularity of conformal mappings at the boundary.

LEMMA 2.35. *Let  $\Omega$  be a  $C^\infty$  simply connected domain of  $\mathbb{R}^2$  with boundary  $\Gamma$ . Let  $y_0, z_0$  and  $y_*$  be distinct points in  $\Gamma$ . Then, there exists a conformal diffeomorphism  $F : \Omega \rightarrow \mathbb{H}$  which extends as a  $C^\infty$  map up to the boundary, and  $F|_\Gamma$  sends  $\Gamma \setminus \{y_*\}$  diffeomorphically onto  $\partial\mathbb{H}$ ,  $y_0$  to  $(0, 0)$  and  $z_0$  to some  $(\zeta_0, 0)$  at finite distance in  $\partial\mathbb{H}$ .*

*Proof.* The existence of a conformal diffeomorphism  $F_1 : \Omega \rightarrow \mathbb{D}$  is given by the Riemann mapping theorem. The fact that this diffeomorphism is  $C^\infty$  up to the boundary and sends  $\Gamma$  diffeomorphically onto  $\partial\mathbb{D}$  is explained in [BeKr1987].

Since  $F_1(y_*) \in \partial\mathbb{D}$ , the map  $F_2 = \overline{F_1(y_*)} F_1$  is a conformal map from  $\Omega$  onto  $\mathbb{D}$  which extends smoothly to the boundary, sends  $\Gamma$  diffeomorphically onto  $\partial\mathbb{D}$ , and  $y_*$  to the point 1. The map  $F_3 : w \mapsto i \frac{1+w}{1-w}$  maps  $\mathbb{D}$  onto  $\mathbb{H}$ , is smooth up to the boundary, maps  $\partial\mathbb{D} \setminus \{1\}$  onto  $\partial\mathbb{H}$ , and 1 to infinity. Taking  $F_4$  a suitable horizontal translation in  $\mathbb{H}$ , the map  $F := F_4 \circ F_3 \circ F_2$  has the required properties.  $\square$

2.4.3.2. *Eigenfunctions.* The conformal diffeomorphism  $E := F^{-1} : \mathbb{H} \rightarrow \Omega$  is  $C^\infty$  up to the boundary, sends  $\partial\mathbb{H}$  onto the boundary  $\Gamma$  minus the point  $y_*$ , and the point 0 to  $y_0$ .

If  $\xi = (\xi_1, \xi_2)$  and  $E(\xi) = (E_1(\xi_1, \xi_2), E_2(\xi_1, \xi_2))$ , the Jacobian of  $E$  is given by

$$\text{Jac}(E)(\xi) = \begin{pmatrix} \partial_{\xi_1} E_1(\xi) & \partial_{\xi_2} E_1(\xi) \\ \partial_{\xi_1} E_2(\xi) & \partial_{\xi_2} E_2(\xi) \end{pmatrix}.$$

where  $\partial_{\xi_i}$  stands for  $\frac{\partial}{\partial \xi_i}$ .

Since  $E$  is conformal, we have  $|\nabla E_1| = |\nabla E_2|$ ,  $\langle \nabla E_1, \nabla E_2 \rangle = 0$ . The determinant of the Jacobian of  $E$  is given by

$$(2.43) \quad J_E := \det(\text{Jac}(E)) = |\nabla E_1|^2 = |\nabla E_2|^2.$$

Let  $u$  be a  $C^\infty$  function in  $\Omega$ . The Laplacian  $\Delta_\xi$  of the function  $u \circ E$  is given by the following formula in the variables  $(\xi_1, \xi_2)$  of  $\mathbb{H}$

$$(2.44) \quad \Delta_\xi(u \circ E) = J_E ((\Delta_x u) \circ E),$$

where  $\Delta_x$  is the Laplacian of  $u$  in the variables  $(x_1, x_2)$  of  $\Omega$ .

Let  $u$  be a nontrivial eigenfunction of (2.36)–(2.37), and let  $y_0 \in \Gamma$ . Choose  $E$  so that  $E(0, 0) = y_0$ . We now work with the function

$$(2.45) \quad v = u \circ E.$$

Define the functions

$$(2.46) \quad \begin{cases} V_E := J_E (V \circ E), \text{ and} \\ h_E := \sqrt{J_E} (h \circ E). \end{cases}$$

The function  $v$  satisfies

$$(2.47) \quad \begin{cases} (-\Delta_\xi v + V_E)v = \lambda J_E v & \text{in } \mathbb{H} \\ B_E v = 0 & \text{on } \partial\mathbb{H}, \end{cases}$$

where the boundary condition  $B_E v$  is given by

$$(2.48) \quad \begin{cases} B_E v = v|_{\partial\mathbb{H}} & \text{in the Dirichlet case} \\ B_E v = \partial_{\xi_2} v|_{\partial\mathbb{H}} & \text{in the Neumann case} \\ B_E v = (\partial_{\xi_2} v - h_E v)|_{\partial\mathbb{H}} & \text{in the Robin case.} \end{cases}$$

To determine the local properties of  $u$  near  $y_0 \in \partial\mathbb{H}$ , it is sufficient to determine the local properties of  $v$  in  $\overline{D}_+(0, r_0) \cap \mathbb{H}$ , for some  $r_0 > 0$ .

#### 2.4.4. The unique continuation property at the boundary.

PROPERTY 2.36. *The eigenfunctions of (2.36)-(2.37) are in  $C^\infty(\overline{\Omega})$ .*

This property follows from elliptic regularity, see [GiTr1977], Sections 6.4 and 6.7, or [Mikh1978], Chap. 4.2, page 217.

PROPOSITION 2.37. *A nontrivial eigenfunction  $u$  of (2.36)-(2.37) cannot vanish at infinite order at any point  $y \in \Gamma$ .*

*Proof.* We follow the proof of Lemma 2.1 in Melas' paper [Mela1992]. He only considers the Dirichlet boundary condition, and deals with convex domains. His proof can be adapted to the Neumann boundary condition, and the part of the proof we are interested in does actually not use the convexity assumption. For completeness, we give a complete proof here. We use the framework described in Paragraph 2.4.3.2.

Let  $u$  be a nontrivial eigenfunction of (2.36). Then  $u \in C^\infty(\overline{\Omega})$ , and the function  $v = u \circ E$  is in  $C^\infty(\overline{\mathbb{H}})$ . Furthermore,  $u$  vanishes at infinite order at  $y_0$  if and only if  $v$  vanishes at infinite order at 0.

We now restrict  $v$  to some neighborhood  $\overline{D}_+(0, r_0) \cap \overline{\mathbb{H}}$  of  $0 \in \overline{\mathbb{H}}$ , and correspondingly  $u$  to the image  $\overline{D}_E(y_0, r_0) := E(\overline{D}_+(0, r_0) \cap \overline{\mathbb{H}})$ .

Since  $E$  is conformal, the function  $v$  satisfies the equation

$$\Delta_\xi v = J_E ((\Delta_x u) \circ E) = (V_E - J_E \lambda) v,$$

where the function  $V_E$  is  $C^\infty$  and bounded in  $\overline{D}_+(0, r_0) \cap \mathbb{H}$ . Furthermore,  $v$  satisfies the Dirichlet (resp. the Neumann, or a Robin) boundary condition on  $\overline{D}_+(0, r_0) \cap \partial\mathbb{H}$  when the function  $u$  satisfies the Dirichlet boundary condition on  $\overline{D}_E(y_0, r_0) \cap \Gamma$  (resp. the Neumann, or a Robin boundary condition).

We now work with the function  $v$  restricted to  $\overline{D}_+(0, r_0) \cap \overline{\mathbb{H}}$ , and we consider three cases separately:  $v$  satisfies the Dirichlet boundary condition,  $v$  satisfies the Neumann boundary condition, or  $v$  satisfies a Robin boundary condition on  $\overline{D}_+(0, r_0) \cap \partial\mathbb{H}$ .

◇ *Dirichlet boundary condition.* We define the function  $w$  on  $D_+(0, r_0)$  by

$$(2.49) \quad w(\xi_1, \xi_2) := \begin{cases} v(\xi_1, \xi_2) & \text{if } \xi_2 > 0 \\ -v(\xi_1, -\xi_2) & \text{if } \xi_2 < 0 \\ 0 & \text{if } \xi_2 = 0. \end{cases}$$

Since  $v$  extends to the boundary and vanishes on the boundary, the function  $w$  is well defined and continuous in  $D_+(0, r_0)$ , with  $w(\xi_1, 0) = 0$  for all  $\xi_1 \in (-r_0, r_0)$ .

The function  $w$  has first partial derivatives given as follows:

a)

$$\partial_{\xi_1} w(\xi_1, \xi_2) := \begin{cases} \partial_{\xi_1} v(\xi_1, \xi_2) & \text{if } \xi_2 > 0 \\ -\partial_{\xi_1} v(\xi_1, -\xi_2) & \text{if } \xi_2 < 0 \\ 0 & \text{if } \xi_2 = 0, \end{cases}$$

where the third line follows from the fact that  $v(\xi_1, 0) \equiv 0$  on  $(-r_0, r_0)$ .

b)

$$\partial_{\xi_2} w(\xi_1, \xi_2) := \begin{cases} \partial_{\xi_2} v(\xi_1, \xi_2) & \text{if } \xi_2 > 0 \\ \partial_{\xi_2} v(\xi_1, -\xi_2) & \text{if } \xi_2 < 0 \\ \partial_{\xi_2} v(\xi_1, 0) & \text{if } \xi_2 = 0, \end{cases}$$

where the third line is computed using the definition of the derivative of  $w$  at the point  $(\xi_1, 0)$ .

Since  $v$  is  $C^\infty$  up to the boundary, the first partial derivatives of  $w$  are continuous. The second derivatives of  $w$  are given as follows:

a)

$$\partial_{\xi_1}^2 w(\xi_1, \xi_2) := \begin{cases} \partial_{\xi_1}^2 v(\xi_1, \xi_2) & \text{if } \xi_2 > 0 \\ -\partial_{\xi_1}^2 v(\xi_1, -\xi_2) & \text{if } \xi_2 < 0 \\ 0 & \text{if } \xi_2 = 0, \end{cases}$$

where the third line follows from the fact that  $\partial_{\xi_1} w(\xi_1, 0) \equiv 0$  on  $(-r_0, r_0)$ .

Since  $v$  is  $C^\infty$  up to the boundary, this second derivative is continuous.

b)

$$\partial_{\xi_2 \xi_1}^2 w(\xi_1, \xi_2) := \begin{cases} \partial_{\xi_2 \xi_1}^2 v(\xi_1, \xi_2) & \text{if } \xi_2 > 0 \\ \partial_{\xi_2 \xi_1}^2 v(\xi_1, -\xi_2) & \text{if } \xi_2 < 0 \\ \partial_{\xi_2 \xi_1}^2 v(\xi_1, 0) & \text{if } \xi_2 = 0, \end{cases}$$

where the third line follows from the definition of the derivative of  $\partial_{\xi_1} w$  with respect to  $\xi_2$  at some point  $(\xi_1, 0)$ . Since  $v$  is  $C^\infty$  up to the boundary, this second derivative is continuous.

c) From the formula for  $\partial_{\xi_2} w$  we immediately obtain

$$\partial_{\xi_1 \xi_2}^2 w(\xi_1, \xi_2) := \begin{cases} \partial_{\xi_1 \xi_2}^2 v(\xi_1, \xi_2) & \text{if } \xi_2 > 0 \\ \partial_{\xi_1 \xi_2}^2 v(\xi_1, -\xi_2) & \text{if } \xi_2 < 0 \\ \partial_{\xi_1 \xi_2}^2 v(\xi_1, 0) & \text{if } \xi_2 = 0. \end{cases}$$

Since  $v$  is  $C^\infty$  up to the boundary, this second derivative is continuous, and we have  $\partial_{\xi_1 \xi_2}^2 w = \partial_{\xi_2 \xi_1}^2 w$ .

d)

$$\partial_{\xi_2}^2 w(\xi_1, \xi_2) := \begin{cases} \partial_{\xi_2}^2 v(\xi_1, \xi_2) & \text{if } \xi_2 > 0 \\ -\partial_{\xi_2}^2 v(\xi_1, -\xi_2) & \text{if } \xi_2 < 0 \\ \pm \partial_{\xi_2}^2 v(\xi_1, 0) & \text{if } \xi_2 = 0, \end{cases}$$

where the third line follows from a direct computation of the right/left partial derivative of  $\partial_{\xi_2} w$  with respect to  $\xi_2$  at a point  $(\xi_1, 0)$ . The sign indicates the value for the right/left derivatives.

It follows from (2.47) that  $\Delta_{\xi} v(\xi_1, 0) \equiv 0$  because  $v$  satisfies the Dirichlet boundary condition. Since we already have  $\partial_{\xi_1}^2 v(\xi_1, 0) \equiv 0$ , we conclude that  $\partial_{\xi_2}^2 v(\xi_1, 0) \equiv 0$  as well, and hence that the second derivative  $\partial_{\xi_2}^2 w$  is well defined and continuous.

We have just shown that the function  $w$  is in  $C^2(D_+(0, r_0))$ . Furthermore, we have

$$(2.50) \quad \Delta_{\xi} w(\xi_1, \xi_2) = \begin{cases} \Delta_{\xi} v(\xi_1, \xi_2) & \text{if } \xi_2 > 0 \\ -\Delta_{\xi} v(\xi_1, -\xi_2) & \text{if } \xi_2 < 0 \\ 0 & \text{if } \xi_2 = 0, \end{cases}$$

and hence, by (2.47),

$$(2.51) \quad |\Delta_{\xi} w| \leq C |w| \text{ in } D_+(0, r_0).$$

Recall the *strong unique continuation property* for the operator  $P = -\Delta + V$  in the open domain  $\Omega \subset \mathbb{R}^2$  where  $V \in L^\infty(\Omega)$ .

**THEOREM 2.38.** *Assume that  $u \in H^2(\Omega)$  and that  $|\Delta u| \leq C(|\nabla u| + |u|)$  almost everywhere in  $\Omega$ . If  $u$  vanishes to infinite order at some  $x_0 \in \Omega$  in the sense that  $\lim_{r \rightarrow 0} r^{-N} \int_{B(x_0, r)} |u|^2 dx = 0$  for all  $N \geq 0$ , then  $u$  vanishes identically in  $\Omega$ .*

For this theorem, we refer to [Sal014] (Theorem 1.2 and Remark 4 on page 4), or Aronszajn [Aron1957].

Since  $w \not\equiv 0$ , in view of (2.51), the strong unique continuation property implies that  $w$  does not vanish at infinite order at 0, so that  $v$  does not vanish at 0 at infinite order either. This proves that the eigenfunction  $u$  cannot vanish at infinite order at the boundary point  $y$ .

◇ *Neumann boundary condition.* We define the function  $w$  on  $D_+(0, r_0)$  by

$$(2.52) \quad w(\xi_1, \xi_2) := \begin{cases} v(\xi_1, \xi_2) & \text{if } \xi_2 > 0 \\ v(\xi_1, -\xi_2) & \text{if } \xi_2 < 0 \\ v(\xi_1, 0) & \text{if } \xi_2 = 0. \end{cases}$$

Since  $v$  is  $C^\infty$  up to the boundary, the function  $w$  is well defined and continuous in  $D_+(0, r_0)$ , with  $w(\xi_1, 0) = v(\xi_1, 0)$  for all  $\xi_1 \in (-r_0, r_0)$ .

The function  $w$  has first partial derivatives given as follows:

a)

$$\partial_{\xi_1} w(\xi_1, \xi_2) := \begin{cases} \partial_{\xi_1} v(\xi_1, \xi_2) & \text{if } \xi_2 > 0 \\ \partial_{\xi_1} v(\xi_1, -\xi_2) & \text{if } \xi_2 < 0 \\ \partial_{\xi_1} v(\xi_1, 0) & \text{if } \xi_2 = 0. \end{cases}$$

b)

$$\partial_{\xi_2} w(\xi_1, \xi_2) := \begin{cases} \partial_{\xi_2} v(\xi_1, \xi_2) & \text{if } \xi_2 > 0 \\ -\partial_{\xi_2} v(\xi_1, -\xi_2) & \text{if } \xi_2 < 0 \\ 0 & \text{if } \xi_2 = 0, \end{cases}$$

where the third line is computed using the definition of the derivative, and the fact that the function  $v$  satisfies the Neumann boundary condition  $\partial_{\xi_2} v(\xi_1, 0) \equiv 0$  in  $(-r_0, r_0)$ .

Since  $v$  is  $C^\infty$  up to the boundary, the first partial derivatives of  $w$  are continuous.

The second derivatives of  $w$  are given as follows:

a)

$$\partial_{\xi_1}^2 w(\xi_1, \xi_2) := \begin{cases} \partial_{\xi_1}^2 v(\xi_1, \xi_2) & \text{if } \xi_2 > 0 \\ \partial_{\xi_1}^2 v(\xi_1, -\xi_2) & \text{if } \xi_2 < 0 \\ \partial_{\xi_1}^2 v(\xi_1, 0) & \text{if } \xi_2 = 0, \end{cases}$$

where the third line follows from the fact that  $\partial_{\xi_1} v(\xi_1, 0)$  is  $C^\infty$ . Since  $v$  is  $C^\infty$  up to the boundary, this second derivative is continuous.

b)

$$\partial_{\xi_2 \xi_1}^2 w(\xi_1, \xi_2) := \begin{cases} \partial_{\xi_2 \xi_1}^2 v(\xi_1, \xi_2) & \text{if } \xi_2 > 0 \\ -\partial_{\xi_2 \xi_1}^2 v(\xi_1, -\xi_2) & \text{if } \xi_2 < 0 \\ \pm \partial_{\xi_2 \xi_1}^2 v(\xi_1, 0) & \text{if } \xi_2 = 0, \end{cases}$$

where the third line follows from the definition of the right/left derivatives of  $\partial_{\xi_1} w$  with respect to  $\xi_2$  at the point  $(\xi_1, 0)$ . The term in the third line is actually zero due to the Neumann boundary conditions and the fact that  $\partial_{\xi_2 \xi_1}^2 v(\xi_1, 0) = \partial_{\xi_1 \xi_2}^2 v(\xi_1, 0)$ . Since  $v$  is  $C^\infty$  up to the boundary, this second derivative is continuous.

c) From the formula for  $\partial_{\xi_2} w$  we immediately obtain

$$\partial_{\xi_1 \xi_2}^2 w(\xi_1, \xi_2) := \begin{cases} \partial_{\xi_1 \xi_2}^2 v(\xi_1, \xi_2) & \text{if } \xi_2 > 0 \\ -\partial_{\xi_1 \xi_2}^2 v(\xi_1, -\xi_2) & \text{if } \xi_2 < 0 \\ 0 & \text{if } \xi_2 = 0. \end{cases}$$

Since  $v$  is  $C^\infty$  up to the boundary, this second derivative is continuous, and we have  $\partial_{\xi_1 \xi_2}^2 w = \partial_{\xi_2 \xi_1}^2 w$ .

d)

$$\partial_{\xi_2}^2 w(\xi_1, \xi_2) := \begin{cases} \partial_{\xi_2}^2 v(\xi_1, \xi_2) & \text{if } \xi_2 > 0 \\ \partial_{\xi_2}^2 v(\xi_1, -\xi_2) & \text{if } \xi_2 < 0 \\ \partial_{\xi_2}^2 v(\xi_1, 0) & \text{if } \xi_2 = 0. \end{cases}$$

We have shown that the function  $w$  is continuous, with continuous first and second derivatives. Furthermore, we have

$$(2.53) \quad \Delta_\xi w(\xi_1, \xi_2) = \begin{cases} \Delta_\xi v(\xi_1, \xi_2) & \text{if } \xi_2 > 0 \\ \Delta_\xi v(\xi_1, -\xi_2) & \text{if } \xi_2 < 0 \\ \Delta_\xi v(\xi_1, 0) & \text{if } \xi_2 = 0, \end{cases}$$

and hence, by (2.47),

$$(2.54) \quad |\Delta_\xi w| \leq C |w| \text{ in } D_+(0, r_0).$$

We can apply Aronszajn's theorem to  $w$  and, since  $w \not\equiv 0$ , conclude that  $w$  does not vanish at infinite order at 0 in  $L^1$ -norm, so that  $v$  does not vanish at infinite order in  $L^1$ -norm either. This proves that  $u$  cannot vanish at infinite order at the boundary point  $y$ .



◇ *Robin boundary condition.*

According to the third line in (2.48), we have  $\partial_{\xi_2} v(\xi_1, 0) - g(\xi_1)v(\xi_1, 0) \equiv 0$ , where  $g(\xi_1) := h(\xi_1) \sqrt{J_E}(\xi_1, 0)$ . Introduce the function

$$(2.55) \quad v_1(\xi_1, \xi_2) := e^{-g(\xi_1)\xi_2} v(\xi_1, \xi_2).$$

Then,

$$(2.56) \quad \begin{cases} \partial_{\xi_1} v_1(\xi_1, \xi_2) = e^{-g(\xi_1)\xi_2} \partial_{\xi_1} v(\xi_1, \xi_2) - g'(\xi_1)\xi_2 v_1(\xi_1, \xi_2) \\ \partial_{\xi_2} v_1(\xi_1, \xi_2) = e^{-g(\xi_1)\xi_2} \partial_{\xi_2} v(\xi_1, \xi_2) - g(\xi_1) v_1(\xi_1, \xi_2), \end{cases}$$

and hence,

$$(2.57) \quad \begin{cases} v_1(\xi_1, 0) = v(\xi_1, 0) \\ \partial_{\xi_2} v_1(\xi_1, 0) = \partial_{\xi_2} v(\xi_1, 0) - g(\xi_1) v(\xi_1, 0) \equiv 0, \end{cases}$$

so that the function  $v$  satisfies the Neumann boundary condition. Then,

$$(2.58) \quad \begin{cases} \partial_{\xi_1}^2 v_1(\xi_1, \xi_2) = e^{-g(\xi_1)\xi_2} \partial_{\xi_1}^2 v(\xi_1, \xi_2) - 2g'(\xi_1)\xi_2 \partial_{\xi_1} v_1 \\ \quad - [g''(\xi_1)\xi_2 - (\xi_2 g'(\xi_1))^2] v_1 \\ \partial_{\xi_2}^2 v_1(\xi_1, \xi_2) = e^{-g(\xi_1)\xi_2} \partial_{\xi_2}^2 v(\xi_1, \xi_2) - 2g(\xi_1) \partial_{\xi_2} v_1(\xi_1, \xi_2) - g^2(\xi_1) v_1. \end{cases}$$

It follows that the function  $v_1$  satisfies

$$(2.59) \quad \begin{cases} \Delta_{\xi} v_1 + a_1 \partial_{\xi_1} v_1 + a_2 \partial_{\xi_2} v_1 + A v_1 = 0 \\ \partial_{\xi_2} v_1(\xi_1, 0) = 0, \end{cases}$$

where the functions  $a_1, a_2$  and  $A$  are  $C^\infty$  and bounded in the neighborhood in which we work.

We can now repeat the arguments of the Neumann case, using the inequality

$$|\Delta v_1| \leq C(|\nabla v_1| + |v_1|)$$

and apply Theorem 2.38.

This concludes the proof of Proposition 2.37.  $\square$

**REMARK 2.39.** We have proved Proposition 2.37 under the additional assumption that  $\Omega$  is simply connected. In the general case, since the property we are interested in is local, it suffices to first reduce to a simply-connected neighborhood  $\Omega_1$  of the point  $y_0$ . Indeed, in a neighborhood of  $y_0$ , the boundary  $\Gamma$  is a graph above the tangent to  $\Gamma$  at  $y_0$  which we can choose as the first coordinate axis  $x_1$ . Then, for  $r$  small enough,  $\Omega_1 := \Omega \cap D_x(y_0, r)$  will be simply connected, and we will choose a conformal diffeomorphism from  $\mathbb{H}$  to  $\Omega_1$ , as given in Lemma 2.35.

In the general case of a compact surface with boundary, we can use [YaZh2021, Section 2] or [PiVe2020].

We also have the following relations in the sense of distributions.

$$(2.60) \quad \partial_{\xi_1} w(\xi_1, \xi_2) \stackrel{\mathcal{D}'}{=} \begin{cases} \partial_{\xi_1} v(\xi_1, \xi_2) & \text{if } \xi_2 > 0 \\ \partial_{\xi_1} v(\xi_1, -\xi_2) & \text{if } \xi_2 < 0. \end{cases}$$

$$(2.61) \quad \partial_{\xi_2} w(\xi_1, \xi_2) \stackrel{\mathcal{D}'}{=} \begin{cases} \partial_{\xi_2} v(\xi_1, \xi_2) & \text{if } \xi_2 > 0 \\ -\partial_{\xi_2} v(\xi_1, -\xi_2) & \text{if } \xi_2 < 0. \end{cases}$$

$$(2.62) \quad \partial_{\xi_1}^2 w(\xi_1, \xi_2) \stackrel{\mathcal{D}'}{=} \begin{cases} \partial_{\xi_1}^2 v(\xi_1, \xi_2) & \text{if } \xi_2 > 0 \\ \partial_{\xi_1}^2 v(\xi_1, -\xi_2) & \text{if } \xi_2 < 0. \end{cases}$$

$$(2.63) \quad \partial_{\xi_2}^2 w(\xi_1, \xi_2) \stackrel{\mathcal{D}'}{=} \begin{cases} \partial_{\xi_2}^2 v(\xi_1, \xi_2) & \text{if } \xi_2 > 0 \\ \partial_{\xi_2}^2 v(\xi_1, -\xi_2) & \text{if } \xi_2 < 0. \end{cases}$$

$$(2.64) \quad \partial_{\xi_1 \xi_2}^2 w(\xi_1, \xi_2) \stackrel{\mathcal{D}'}{=} \partial_{\xi_2 \xi_1}^2 w(\xi_1, \xi_2) \stackrel{\mathcal{D}'}{=} \begin{cases} \partial_{\xi_1 \xi_2}^2 v(\xi_1, \xi_2) & \text{if } \xi_2 > 0 \\ -\partial_{\xi_1 \xi_2}^2 v(\xi_1, -\xi_2) & \text{if } \xi_2 < 0. \end{cases}$$

#### 2.4.5. Proof of the Local Structure Theorem at the Boundary.

Let  $y_0$  be a boundary singular point of an eigenfunction  $u$  of (2.36). To analyze  $u$  in a neighborhood of  $y_0$ , we apply Lemma 2.35 and work with the function  $v = u \circ E$  which satisfies (2.47).

From Subsection 2.4.4, we know that the function  $v$  does not vanish at infinite order at 0. Let  $p := \text{ord}(v, 0)$ . Applying Taylor's formula to the function  $v$  at the point 0, in the half-disk  $\bar{D}_+(0, r_0)$  for some  $r_0 > 0$ , gives

$$(2.65) \quad \begin{cases} v(\xi_1, \xi_2) = \sum_{|\alpha|=p} \frac{1}{\alpha!} D^\alpha v(0, 0) (\xi_1, \xi_2)^\alpha + R_{p+1}(\xi_1, \xi_2), \text{ where} \\ R_{p+1}(\xi_1, \xi_2) = \sum_{|\beta|=p+1} \frac{|\beta|}{\beta!} (\xi_1, \xi_2)^\beta \int_0^1 (1-s)^{|\beta|-1} D^\beta v(s\xi_1, s\xi_2) ds. \end{cases}$$

Here, as usual,

$$(2.66) \quad \alpha = (\alpha_1, \alpha_2), \quad |\alpha| = \alpha_1 + \alpha_2, \quad (\xi_1, \xi_2)^\alpha = \xi_1^{\alpha_1} \xi_2^{\alpha_2}, \quad D^\alpha v = \frac{\partial^{|\alpha|} v}{\partial \xi_1^{\alpha_1} \partial \xi_2^{\alpha_2}}.$$

Using (2.47), and identifying the terms with lowest order, we find that the polynomial  $P_p(\xi_1, \xi_2) := \sum_{|\alpha|=p} \frac{1}{\alpha!} D^\alpha v(0, 0) (\xi_1, \xi_2)^\alpha$  is homogenous of degree  $p$ , and harmonic (with respect to  $\Delta_\xi$ ) in  $\mathbb{H}$ . Writing the harmonicity condition in polar coordinates  $(\rho, \omega)$  at the point 0 in  $\mathbb{R}^2$ , we find that the polynomial  $P_p$  has the form

$$(2.67) \quad P_p(\rho \cos \omega, \rho \sin \omega) = \rho^p Q_p(\omega),$$

with the function  $Q_p$  satisfying  $Q_p''(\omega) + p^2 Q_p(\omega) \equiv 0$  in  $(0, \pi)$ . It follows that  $v$  can be written as

$$(2.68) \quad v(\rho \cos \omega, \rho \sin \omega) = \rho^p Q_p(\omega) + \rho^{p+1} T_{p+1}(\rho, \omega),$$

where

$$(2.69) \quad T_{p+1}(\rho, \omega) = \sum_{|\beta|=p+1} \frac{|\beta|}{\beta!} (\cos \omega, \sin \omega)^\beta \int_0^1 (1-s)^{|\beta|-1} D^\beta v(s\rho \cos \omega, s\rho \sin \omega) ds.$$

Depending on the boundary condition satisfied by  $u$ , the function  $v$  satisfies

- (1) the Dirichlet condition  $v(\xi_1, 0) = 0$ ,
- (2) the Neumann condition  $\partial_{\xi_2} v(\xi_1, 0) = 0$ , or
- (3) the Robin condition  $\partial_{\xi_2} v(\xi_1, 0) - h(\xi_1) \sqrt{J_E}(\xi_1, 0) v(\xi_1, 0) = 0$ ,

see (2.48).

We now express the normal derivative  $\partial_{\xi_2}$  in terms of the  $\rho$  and  $\omega$  derivatives,

$$(2.70) \quad \partial_{\xi_2} = \sin \omega \partial_\rho + \cos \omega \frac{1}{\rho} \partial_\omega.$$

In polar coordinates, the relation  $\xi_2 = 0$  is equivalent to  $\omega \in \{0, \pi\}$ . For  $\omega_0 \in \{0, \pi\}$ , we have

$$v(\rho \cos \omega_0, 0) = \rho^p Q_p(\omega_0) + \mathcal{O}(\rho^{p+1})$$

and

$$\partial_{\xi_2} v(\rho \cos \omega_0, 0) = \rho^{p-1} \cos(\omega_0) Q'_p(\omega_0) + \mathcal{O}(\rho^p)$$

so that

$$\partial_{\xi_2} v(\rho \cos \omega_0, 0) - h_E(\rho \cos \omega_0) v(\rho \cos \omega_0, 0) = \rho^{p-1} \cos(\omega_0) Q'_p(\omega_0) + \mathcal{O}(\rho^p).$$

From these relations, we conclude that

(1) if  $v$  satisfies the *Dirichlet condition*, then  $Q_p(0) = Q_p(\pi) = 0$ , and hence

$$(2.71) \quad v(\rho \cos \omega, \rho \sin \omega) = a_v \rho^p \sin(p\omega) + \rho^{p+1} T_{p+1}(\rho, \omega),$$

(2) if  $v$  satisfies the *Neumann or Robin condition*, then  $Q'_p(0) = Q'_p(\pi) = 0$ , and hence

$$(2.72) \quad v(\rho \cos \omega, \rho \sin \omega) = a_v \rho^p \cos(p\omega) + \rho^{p+1} T_{p+1}(\rho, \omega),$$

where  $a_v$  is a nonzero scalar. For an alternative proof, see Subsection 2.4.6.

Define

$$(2.73) \quad \begin{cases} V_d(\rho, \omega) := \sin(p\omega) + a_v^{-1} \rho T_{p+1}(\rho, \omega) \\ V_n(\rho, \omega) := \cos(p\omega) + a_v^{-1} \rho T_{p+1}(\rho, \omega). \end{cases}$$

◇ *Dirichlet boundary condition.* Define the values

$$(2.74) \quad \omega_j := j \frac{\pi}{p}, \quad j \in \{0, \dots, p\},$$

$$(2.75) \quad \alpha_1 \in \left(0, \frac{\pi}{8}\right) \text{ and } \alpha_p := \frac{\alpha_1}{p}.$$

In the interval  $(0, \pi)$ , the function  $V_d(0, \omega)$  vanishes precisely for the values  $\omega_j$  with  $j \in \{1, \dots, p-1\}$ . The following relations hold.

$$(2.76) \quad \begin{cases} \sin(p(\omega_j \pm \alpha_p)) = \pm(-1)^j \sin(\alpha_1) \\ |\sin(p\omega)| \geq \sin \alpha_1, \text{ for } \omega \in \bigcup_{j=0}^{p-1} [\omega_j + \alpha_p, \omega_{j+1} - \alpha_p]. \end{cases}$$

On the other hand, we have

$$\partial_\omega V_d(\rho, \omega) = p \cos(p\omega) + |a_v|^{-1} \rho \partial_\omega T_{p+1}(\rho, \omega), \text{ and}$$

$$(2.77) \quad |\cos(p\omega)| \geq \cos(\alpha_1) \quad \forall \omega \in [0, \alpha_p] \cup [\pi - \alpha_p, \pi] \cup \bigcup_{j=1}^{p-1} [\omega_j - \alpha_p, \omega_j + \alpha_p].$$

Define

$$(2.78) \quad r_{d,1} := \frac{1}{2} \min \left\{ r_0, |a_v| \sin(\alpha_1) \|T_{p+1}\|_{\infty, \frac{r_0}{2}}^{-1}, p |a_v| \cos(\alpha_1) \|\partial_\omega T_{p+1}\|_{\infty, \frac{r_0}{2}}^{-1} \right\},$$

where  $\|\cdot\|_{\infty, \frac{r_0}{2}}$  denotes the  $L^\infty$  norm of functions in  $D_+(0, \frac{r_0}{2})$ . Then, for all  $r \leq r_{d,1}$ ,

$$(2.79) \quad \begin{cases} \pm (-1)^j V_d(r, \omega_j \pm \alpha_p) \geq \frac{1}{2} \sin(\alpha_1) & \text{for all } 1 \leq j \leq p-1 \\ |\partial_\omega V_d(r, \omega)| \geq \frac{p}{2} \cos(\alpha_1) & \text{for all} \\ \omega \in [0, \alpha_p] \cup [\pi - \alpha_p, \pi] \cup \bigcup_{j=1}^{p-1} [\omega_j - \alpha_p, \omega_j + \alpha_p], \\ |V_d(r, \omega)| \geq \frac{1}{2} \sin(\alpha_1) & \text{for all } \omega \in \bigcup_{j=0}^{p-1} [\omega_j + \alpha_p, \omega_{j+1} - \alpha_p]. \end{cases}$$

PROPOSITION 2.40. *Assume that  $\rho \leq r_{d,1}$ . The following properties hold.*

(i) *The function  $\omega \mapsto V_d(\rho, \omega)$  does not vanish in*

$$\bigcup_{j=0}^{p-1} [\omega_j + \alpha_p, \omega_{j+1} - \alpha_p].$$

(ii) *For each  $j \in \{1, \dots, p-1\}$ , the function  $\omega \mapsto V_d(\rho, \omega)$  has exactly one zero  $\tilde{\omega}_j(\rho) \in (\omega_j - \alpha_p, \omega_j + \alpha_p)$ , and does not vanish in  $(0, \alpha_p] \cup [\pi - \alpha_p, \pi)$ .*

(iii) *For each  $j \in \{1, \dots, p-1\}$ , the function  $\rho \mapsto \tilde{\omega}_j(\rho)$  is  $C^\infty$  in the interval  $(0, r_1)$  and tends to  $\omega_j$  as  $\rho$  tends to zero.*

(iv) *For each  $j \in \{1, \dots, p-1\}$ , the curve*

$$(0, r_{d,1}) \ni \rho \mapsto a_j(\rho) = (\rho \cos \tilde{\omega}_j(\rho), \rho \sin \tilde{\omega}_j(\rho))$$

*is smooth and has semi-tangent  $\omega_j$  at the origin.*

In the Dirichlet case, recall that  $p := \text{ord}(v, 0)$  and  $\rho(v, 0) = p - 1$ .

*Proof.* For the proof, we use (2.79). To prove (i), we observe that in each set  $\{\rho\} \times [\omega_j + \alpha_p, \omega_{j+1} - \alpha_p]$ , with  $0 < \rho \leq r_{d,1}$  and  $j = 0 \dots (p-1)$ ,  $|V_d(\rho, \omega)| \geq \frac{1}{2} \sin(\alpha_1)$ . To prove (ii), we observe that the function  $V_d(\rho, \omega)$  changes sign in  $\{\rho\} \times (\omega_j - \alpha_p, \omega_j + \alpha_p)$ , and that its partial derivative with respect to  $\omega$  does not vanish. We use a similar reasoning in  $(0, \alpha_p] \cup [\pi - \alpha_p, \pi)$ , taking into account the fact that  $V_d(\rho, \omega)$  vanishes for  $\omega = 0$  or  $\pi$ . The first part of Assertion (iii) follows from the implicit function theorem; the second part from the fact that  $\alpha_1$  can be chosen as small as we want. Assertion (iv) follows from the previous ones.  $\square$

Introduce the following notation (“colored arcs”).

$$(2.80) \quad \begin{cases} [r, \omega] := (r \cos \omega, r \sin \omega), \\ C_+(0, r) := \{[r, \omega] \mid \omega \in (0, \pi)\}, \\ \mathcal{G}_d(r, j) := \{[r, \omega] \mid \omega \in (\omega_j - \alpha_p, \omega_j + \alpha_p)\}, \text{ for } 1 \leq j \leq (p-1), \\ \mathcal{R}_d(r, j) := \{[r, \omega] \mid \omega \in [\omega_j + \alpha_p, \omega_{j+1} - \alpha_p]\}, \text{ for } 0 \leq j \leq (p-1), \\ \mathcal{B}_d(r, 0) := \{[r, \omega] \mid \omega \in (0, \alpha_p)\}, \\ \mathcal{B}_d(r, p) := \{[r, \omega] \mid \omega \in [\pi - \alpha_p, \pi)\}. \end{cases}$$

The above arcs are illustrated in Figure 2.2, left image, in the Dirichlet case, with  $p = 8$ . For  $r \leq r_{d,1}$ , the nodal set  $\mathcal{Z}(v)$  meets each “green” arc precisely once, and does not meet the “red” or “blue” arcs.

More precisely, for  $0 < r \leq r_{d,1}$ , we have the following properties.

$$(2.81) \quad \left\{ \begin{array}{l} \pm (-1)^j \operatorname{sgn}(a_v) v([r, \omega_j \pm \alpha_p]) \geq \frac{1}{2} |a_v| \sin(\alpha_1) r^p. \\ \text{In } \mathcal{G}_d(r, j), 1 \leq j \leq (p-1), |\partial_\omega v(r, \omega)| \geq \frac{p}{2} |a_v| \cos(\alpha_1) r^p \\ \quad \text{and } v(r, \omega) \text{ vanishes precisely once.} \\ \text{In } \mathcal{B}_d(r, 0) \cup \mathcal{B}_d(r, p), |\partial_\omega v(r, \omega)| \geq \frac{p}{2} |a_v| \cos(\alpha_1) r^p \\ \quad \text{and } v(r, \omega) \text{ does not vanish.} \\ \text{In } \mathcal{R}_d(r, j), 0 \leq j \leq (p-1), |v(r, \omega)| \geq \frac{1}{2} |a_v| \sin(\alpha_1) r^p \\ \quad \text{and } v(r, \omega) \text{ does not vanish.} \end{array} \right.$$

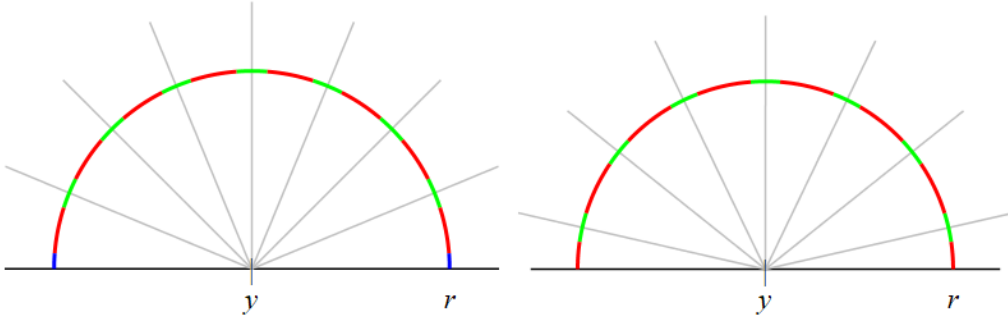


FIGURE 2.2. Colored intervals for  $v$  (Dirichlet/Robin), here  $\rho(v, 0) = 7$

◇ *Neumann or Robin boundary condition.* We introduce the values

$$(2.82) \quad \omega'_j := (j - \frac{1}{2}) \frac{\pi}{p}, \quad j \in \{1, \dots, p\},$$

$$(2.83) \quad \alpha_1 \in \left(0, \frac{\pi}{8}\right) \text{ and } \alpha_p := \frac{\alpha_1}{p}.$$

In the interval  $(0, \pi)$ , the function  $V_n(0, \omega)$  vanishes precisely for the values  $\omega'_j$ ,  $1 \leq j \leq p$ . The following relations hold.

$$(2.84) \quad \left\{ \begin{array}{l} \cos(p(\omega'_j \pm \alpha_p)) = \pm (-1)^j \sin(\alpha_1) \text{ for } 1 \leq j \leq p \\ |\cos(p\omega)| \geq \sin \alpha_1 \text{ for all} \\ \omega \in [0, \omega'_1 - \alpha_p] \cup [\omega'_p + \alpha_p, \pi] \cup \bigcup_{j=1}^{p-1} [\omega'_j + \alpha_p, \omega'_{j+1} - \alpha_p]. \end{array} \right.$$

On the other hand, we have

$$\partial_\omega V_n(\rho, \omega) = -p \sin(p\omega) + |a_v|^{-1} \rho \partial_\omega T_{p+1}(\rho, \omega), \text{ and}$$

$$(2.85) \quad |\sin(p\omega)| \geq \cos(\alpha_1), \quad \forall \omega \in \bigcup_{j=1}^p [\omega'_j - \alpha_p, \omega'_j + \alpha_p].$$

Define

$$(2.86) \quad r_{n,1} := \frac{1}{2} \min \left\{ r_0, |a_v| \sin(\alpha_1) \|T_{p+1}\|_{\infty, \frac{r_0}{2}}^{-1}, p |a_v| \cos(\alpha_1) \|\partial_\omega T_{p+1}\|_{\infty, \frac{r_0}{2}}^{-1} \right\},$$

where  $\|\cdot\|_{\infty, \frac{r_0}{2}}$  denotes the  $L^\infty$  norm of functions on the disk  $D_+(0, \frac{r_0}{2})$ .

Then, for all  $r \leq r_{n,1}$ ,

$$(2.87) \quad \begin{cases} \pm (-1)^j V_n(r, \omega'_j \pm \alpha_p) \geq \frac{1}{2} \sin(\alpha_1) & \text{for } 1 \leq j \leq p \\ |\partial_\omega V_n(r, \omega)| \geq \frac{p}{2} \cos(\alpha_1) & \text{for all} \\ \omega \in \bigcup_{j=1}^p [\omega'_j - \alpha_p, \omega'_j + \alpha_p], \\ |V_n(r, \omega)| \geq \frac{1}{2} \sin(\alpha_1) & \text{for all} \\ \omega \in [0, \omega'_1 - \alpha_p] \cup [\omega'_p + \alpha_p, \pi] \cup \bigcup_{j=1}^{p-1} [\omega'_j + \alpha_p, \omega'_{j+1} - \alpha_p]. \end{cases}$$

PROPOSITION 2.41. *Assume that  $\rho \leq r_{n,1}$ . The following properties hold.*

(i) *The function  $\omega \mapsto V_n(\rho, \omega)$  does not vanish in*

$$[0, \omega'_1 - \alpha_p] \cup [\omega'_p + \alpha_p, \pi] \cup \bigcup_{j=1}^{p-1} [\omega'_j + \alpha_p, \omega'_{j+1} - \alpha_p].$$

(ii) *For each  $j \in \{1, \dots, p\}$ , the function  $\omega \mapsto V_n(\rho, \omega)$  has exactly one zero  $\tilde{\omega}'_j(\rho) \in (\omega'_j - \alpha_p, \omega'_j + \alpha_p)$ .*

(iii) *For each  $j \in \{1, \dots, p\}$ , the function  $\rho \mapsto \tilde{\omega}'_j(\rho)$  is  $C^\infty$  in the interval  $(0, r_{n,1})$  and tends to  $\omega'_j$  as  $\rho$  tends to zero.*

(iv) *For each  $j \in \{1, \dots, p\}$ , the curve*

$$(0, r_{n,1}) \ni \rho \mapsto a_j(\rho) = (\rho \cos(\tilde{\omega}'_j(\rho)), \rho \sin(\tilde{\omega}'_j(\rho)))$$

*is smooth and has semi-tangent  $\omega'_j$  at the origin.*

Recall that, in the Robin case,  $p := \text{ord}(v, 0) = \rho(v, 0) =: q$ .

*Proof.* The proof is similar to the previous one. □

Introduce the following notation (“colored arcs”).

$$(2.88) \quad \begin{cases} [r, \omega] := (r \cos \omega, r \sin \omega), \\ C_+(0, r) := \{[r, \omega] \mid \omega \in (0, \pi)\}, \\ \mathcal{G}_n(r, j) := \{[r, \omega] \mid \omega \in (\omega'_j - \alpha_p, \omega'_j + \alpha_p)\}, \text{ for } 1 \leq j \leq p, \\ \mathcal{R}_n(r, j) := \{[r, \omega] \mid \omega \in [\omega'_j + \alpha_p, \omega'_{j+1} - \alpha_p]\}, \text{ for } 1 \leq j \leq (p-1), \\ \mathcal{R}_n(r, 0) := \{[r, \omega] \mid \omega \in (0, \omega'_1 - \alpha_p]\}, \\ \mathcal{R}_n(r, p) := \{[r, \omega] \mid \omega \in [\omega'_p + \alpha_p, \pi)\}. \end{cases}$$

The above arcs are illustrated in Figure 2.2, right image, for the Robin case, with  $p = 7$ . For  $0 < r < r_{n,1}$ , the nodal set  $\mathcal{Z}(v)$  meets each “green” arc precisely once, and does not meet the “red” arcs.

More precisely, for  $0 < r \leq r_{n,1}$ , we have the following properties.

$$(2.89) \quad \left\{ \begin{array}{l} \mp (-1)^j \operatorname{sgn}(a_v) v([r, \omega'_j \pm \alpha_p]) \geq \frac{1}{2} |a_v| \sin(\alpha_1) r^p. \\ \text{In } \mathcal{G}_n(r, j), 1 \leq j \leq p, |\partial_\omega v(r, \omega)| \geq \frac{p}{2} |a_v| \cos(\alpha_1) r^p \\ \quad \text{and } v(r, \omega) \text{ vanishes precisely once.} \\ \text{In } \mathcal{R}_n(r, 0) \cup \mathcal{R}_n(r, p), |v(r, \omega)| \geq \frac{1}{2} |a_v| \sin(\alpha_1) r^p \\ \quad \text{and } v(r, \omega) \text{ does not vanish.} \\ \text{In } \mathcal{R}_n(t, j), 1 \leq j \leq (p-1), |v(r, \omega)| \geq \frac{1}{2} |a_v| \sin(\alpha_1) r^p \\ \quad \text{and } v(r, \omega) \text{ does not vanish.} \end{array} \right.$$

REMARK 2.42. Translated into properties of the eigenfunction  $u$ , Propositions 2.40, resp. 2.41, tell us that, in a neighborhood of a singular point  $y_0$  of  $u$ , the nodal set  $\mathcal{Z}(u)$  consists of  $(p-1)$ , resp.  $p$ , smooth semi-arcs emanating from  $y_0$  tangentially to the rays  $\omega_j$ , resp.  $\omega'_j$ . These arcs are contained in the image under  $E$  of conical neighborhoods of the rays (controlled by the parameter  $\alpha_1$ ).

#### 2.4.6. A refined Taylor formula near a boundary singular point.

Let  $v = u \circ E$  as in Subsection 2.4.5, and  $p = \operatorname{ord}(v, 0)$ . Applying Taylor's formula at order  $(p+1)$  to the function  $v$  at the point 0 in the half-disk  $\overline{D}_+(0, r_0)$ , gives

$$(2.90) \quad \left\{ \begin{array}{l} v(\xi_1, \xi_2) = \sum_{|\alpha|=p} \frac{1}{\alpha!} D^\alpha v(0) (\xi_1, \xi_2)^\alpha + \sum_{|\alpha|=p+1} \frac{1}{\alpha!} D^\alpha v(0) (\xi_1, \xi_2)^\alpha \\ \quad + \sum_{|\beta|=p+2} R_\beta(\xi_1, \xi_2) (\xi_1, \xi_2)^\beta, \text{ where} \\ R_\beta(\xi_1, \xi_2) = \frac{|\beta|}{\beta!} \int_0^1 (1-s)^{|\beta|-1} D^\beta v(s \xi_1, s \xi_2) ds. \end{array} \right.$$

Then, both

$$(2.91) \quad \left\{ \begin{array}{l} p_0(\xi_1, \xi_2) := \sum_{|\alpha|=p} \frac{1}{\alpha!} D^\alpha v(0) (\xi_1, \xi_2)^\alpha \text{ and} \\ p_1(\xi_1, \xi_2) := \sum_{|\alpha|=p+1} \frac{1}{\alpha!} D^\alpha v(0) (\xi_1, \xi_2)^\alpha \end{array} \right.$$

are homogeneous *harmonic* polynomials, respectively of degree  $p$  and  $(p+1)$ .

Harmonic homogenous polynomials of degree  $n \geq 1$  in two variables form a two dimensional vector space  $\mathcal{H}_n$ . Writing

$$(2.92) \quad (\xi_1 + i \xi_2)^n = C_n(\xi_1, \xi_2) + i S_n(\xi_1, \xi_2),$$

where

$$(2.93) \quad \left\{ \begin{array}{l} C_n(\xi_1, \xi_2) = \sum_{k=0, \text{ even}}^n (-1)^{\frac{k}{2}} \binom{n}{k} \xi_1^{n-k} \xi_2^k \\ \quad = \xi_1^n - \binom{n}{2} \xi_1^{n-2} \xi_2^2 + \binom{n}{4} \xi_1^{n-4} \xi_2^4 - \dots \\ S_n(\xi_1, \xi_2) = \sum_{k=0, \text{ odd}}^n (-1)^{\lfloor \frac{k}{2} \rfloor} \binom{n}{k} \xi_1^{n-k} \xi_2^k \\ \quad = n \xi_1^{n-1} \xi_2 - \binom{n}{3} \xi_1^{n-3} \xi_2^3 + \binom{n}{5} \xi_1^{n-5} \xi_2^5 - \dots \end{array} \right.$$

we obtain a basis  $\{C_n, S_n\}$  of  $\mathcal{H}_n$ . In polar coordinates, we have

$$(2.94) \quad \left\{ \begin{array}{l} C_n(\rho \cos \omega, \rho \sin \omega) = \rho^n \cos(n\omega) \\ S_n(\rho \cos \omega, \rho \sin \omega) = \rho^n \sin(n\omega). \end{array} \right.$$

We list the following relations for later use.

$$(2.95) \quad \begin{cases} \partial_{\xi_1} C_n(\xi_1, \xi_2) &= n C_{n-1}(\xi_1, \xi_2) \\ &= n \xi_1^{n-1} - (n-2) \binom{n}{2} \xi_1^{n-3} \xi_2^2 + \dots \\ \partial_{\xi_1} S_n(\xi_1, \xi_2) &= n S_{n-1}(\xi_1, \xi_2) \\ &= n(n-1) \xi_1^{n-2} \xi_2 - n \binom{n-1}{3} \xi_1^{n-4} \xi_2^3 + \dots \end{cases}$$

$$(2.96) \quad \begin{cases} \partial_{\xi_2} C_n(\xi_1, \xi_2) &= -n S_{n-1}(\xi_1, \xi_2) \\ &= -2 \binom{n}{2} \xi_1^{n-2} \xi_2 + 4 \binom{n}{4} \xi_1^{n-4} \xi_2^3 + \dots \\ \partial_{\xi_2} S_n(\xi_1, \xi_2) &= n C_{n-1}(\xi_1, \xi_2) \\ &= n \xi_1^{n-1} - 3 \binom{n}{3} \xi_1^{n-3} \xi_2^2 + \dots \end{cases}$$

$$(2.97) \quad \begin{cases} C_n(\xi_1, 0) = \xi_1^n & \& S_n(\xi_1, 0) = 0 \\ \partial_{\xi_1} C_n(\xi_1, 0) = n \xi_1^{n-1} & \& \partial_{\xi_1} S_n(\xi_1, 0) = 0 \\ \partial_{\xi_2} C_n(\xi_1, 0) = 0 & \& \partial_{\xi_2} S_n(\xi_1, 0) = n \xi_1^{n-1}. \end{cases}$$

Coming back to the Taylor formula at order  $(p+1)$  for the function  $v$ , and using the preceding relations, we rewrite (2.90) as

$$(2.98) \quad \begin{aligned} v(\xi_1, \xi_2) &= c_{v,p} C_p(\xi_1, \xi_2) + s_{v,p} S_p(\xi_1, \xi_2) \\ &+ c_{v,p+1} C_{p+1}(\xi_1, \xi_2) + s_{v,p+1} S_{p+1}(\xi_1, \xi_2) \\ &+ \sum_{|\beta|=p+2} R_\beta(\xi_1, \xi_2) (\xi_1, \xi_2)^\beta. \end{aligned}$$

◇ *Dirichlet boundary condition.* In this case, we have  $v(\xi_1, 0) \equiv 0$ . Using (2.97), we obtain

$$0 \equiv c_{v,p} \xi_1^p + c_{v,p+1} \xi_1^{p+1} + \mathcal{O}(\xi_1^{p+2}),$$

which implies that  $c_{v,p} = c_{v,p+1} = 0$ .

◇ *Neumann boundary condition.* In this case, we have  $\partial_{\xi_2} v(\xi_1, 0) \equiv 0$ . Using (2.97), we obtain

$$0 \equiv p s_{v,p} \xi_1^{p-1} + (p+1) s_{v,p+1} \xi_1^p + \mathcal{O}(\xi_1^{p+1}),$$

which implies that  $s_{v,p} = s_{v,p+1} = 0$ .

◇ *Robin boundary condition.* In this case, we have  $\partial_{\xi_2} v(\xi_1, 0) \equiv h_E(\xi_1) v(\xi_1, 0)$ . Using (2.97), we obtain

$$p s_{v,p} \xi_1^{p-1} + (p+1) s_{v,p+1} \xi_1^p + \mathcal{O}(\xi_1^{p+1}) \equiv h_E(0) c_{v,p} \xi_1^p + \mathcal{O}(\xi_1^{p+1})$$

which implies that  $s_{v,p} = 0$  and  $(p+1) s_{v,p+1} = h_E(0) c_{v,p}$ .

We have proved the following lemma.

LEMMA 2.43. *For the function  $v$  such that  $\text{ord}(v, 0) = p$ , the Taylor formula at the point 0 and at order  $(p+1)$  is given, depending on the boundary condition, as follows:*

Dirichlet case:

$$v(\xi_1, \xi_2) = s_{v,p} S_p(\xi_1, \xi_2) + s_{v,p+1} S_{p+1}(\xi_1, \xi_2) + R_{p+2}(\xi_1, \xi_2),$$



Neumann case:

$$v(\xi_1, \xi_2) = c_{v,p} C_p(\xi_1, \xi_2) + c_{v,p+1} C_{p+1}(\xi_1, \xi_2) + R_{p+2}(\xi_1, \xi_2),$$

Robin case:

$$v(\xi_1, \xi_2) = c_{v,p} C_p(\xi_1, \xi_2) + c_{v,p+1} C_{p+1}(\xi_1, \xi_2) + \frac{c_{v,p} h_E(0)}{p+1} S_{p+1}(\xi_1, \xi_2) + R_{p+2}(\xi_1, \xi_2),$$

where the remainder term  $R_{p+2}(\xi_1, \xi_2) = \sum_{|\beta|=p+2} R_\beta(\xi_1, \xi_2) (\xi_1, \xi_2)^\beta$  vanishes at order at least  $(p+2)$  at zero.

REMARK 2.44. Note that one recovers the Neumann case from the Robin case. Note also that one recovers the formulas in polar coordinates form given in (2.71) and (2.72).

### 2.4.7. Non simply connected domains.

Let  $\Omega \subset \mathbb{R}^2$  be a smooth bounded domain, contained in some open disk  $D(0, r)$ . The boundary  $\Gamma$  of  $\Omega$  is a compact 1-manifold without boundary, so that it has finitely many components,  $\Gamma_1, \dots, \Gamma_k$ ,  $1 \leq k < \infty$ , which are all diffeomorphic to  $\mathbb{S}^1$ , and hence are Jordan curves. Each curve  $\Gamma_j$  separates the plane into two components, one bounded  $B_j$ , the other one unbounded  $D_j$ .

**Claim.** Relabeling the components  $\Gamma_j$  is necessary,

$$\Omega = B_1 \setminus \bigcup_{j=2}^k B_j.$$

*Sketch of the proof.*

Fact 1: For all  $j$ ,  $1 \leq j \leq k$ ,  $\Omega \subset B_j$  or  $\Omega \subset D_j$ .

Assume this is not the case. Then, for some  $j$ , there exists  $b, d \in \Omega$  with  $b \in B_j$  and  $d \in D_j$ . Since  $\Omega$  is connected, there exists a continuous path from  $b$  to  $d$  entirely contained in  $\Omega$ . On the other hand, this path would have to intersect  $\Gamma_j$ , a contradiction.

Fact 2: There exists at most one  $j$  such that  $\Omega \subset B_j$ .

Assume this is not the case, and that  $\Omega \subset B_1 \cap B_2$ . Since  $\Gamma_2$  does not intersect  $\Gamma_1$ , it must be contained in  $B_1$  or in  $D_1$ . If  $\Gamma_2 \subset D_2$  then  $B_1 \cap B_2 = \emptyset$ , a contradiction. If  $\Gamma_2 \subset B_1$ , we reach a contradiction with the fact that we have point in  $\Omega$  as close as we want from  $\Gamma_1$  although  $B_1$  is at positive distance from  $\Gamma_1$ .

Fact 3: There exists some  $j$  such that  $\Omega \subset B_j$ .

Take some  $x_0 \in \Omega$ , and consider  $r_0 := \sup \{d(x_0, x) \mid x \in \Omega\}$ . Then  $r_0$  is finite and the supremum is achieved at some  $x_1 \in \Gamma$ , and  $\Omega \subset \overline{B(x_0, r_1)}$ . If  $x_1 \in \Gamma_j$  then  $\Omega \subset B_j$ .

Fact 4: Up to relabeling the boundary components, we have  $\Omega \subset B_1$  and  $\Omega \subset D_j$  for all  $j = 2, \dots, k$ , and

$$\Omega = B_1 \cap \bigcap_{j=2}^k D_j = B_1 \setminus \bigcup_{j=2}^k B_j.$$

The inclusion  $\subset$  is clear. If the inclusion  $\supset$  were not true, we would find a point  $x \in B_1 \cap \bigcap_{j=2}^k D_j$ , not in  $\Omega$ . The largest disk  $B(x, r)$  contained in  $B_1 \cap \bigcap_{j=2}^k D_j$  would touch one of the  $\Gamma_j$  and this would yield a contradiction since there is a one-sided neighborhood of each  $\Gamma_j$  contained in  $\Omega$ .

✓

The domain  $B_1$  is simply connected and its boundary  $\Gamma_1$  is called the *outer boundary* of  $\Omega$ . We say that  $B_1$  is obtained from  $\Omega$  by *filling the holes*.

Given any component  $\Gamma_j$  of  $\Gamma$  there exists a diffeomorphism  $\Psi$  of  $\mathbb{R}^2$  such that the outer boundary of  $\Psi(\Omega)$  is  $\Psi(\Gamma_1)$ . For this purpose, it suffices to use two stereographic projections from  $\mathbb{S}^2$  to  $\mathbb{R}^2$ , using adhoc points on  $\mathbb{S}^2$ . As explained in [BeKr1987, p. 24] using the outer boundary and applying Lemma 2.35 several times, one can construct a conformal diffeomorphism from  $B_1$  to the unit disc  $\mathbb{D}$  sending the outer boundary of  $\Omega$  to  $\partial\mathbb{D}$ , and the other boundary components to analytic Jordan curves in  $\mathbb{D}$ .

REMARK 2.45. As far as the local boundary behavior of an eigenfunction is concerned, we could use the following alternative argument. Given a point  $m_0 \in \Gamma$ , choose the coordinate system  $(x_1, x_2)$  in  $\mathbb{R}^2$  such that  $m_0 = (0, 0)$  and the  $x_1$ -axis is tangent to  $\Gamma$  at 0. Choose  $a > 0$  small enough so that  $\Omega_a := \Omega \cap D_x(0, a)$  is simply connected and  $\Gamma \cap D_x(0, a)$  is a graph above the segment  $(-a, a) \times \{0\}$ .

Since  $\Omega_a$  is simply connected, there exists a conformal diffeomorphism  $E$  from  $\mathbb{H}$  onto  $\Omega_a$ , and this map is smooth up to the boundary except around the intersection points of  $\partial D_x(0, a)$  with  $\Gamma$ . We may also assume that  $E(0, 0) = (0, 0)$ . Choose  $r_0 > 0$  small enough so that  $E|_{D_+(0, r_0) \cap \mathbb{H}}$  is  $C^\infty$  up to the boundary.

## Eigenvalue Bounds for Riemannian Spheres with Potential

### 3.1. Revisiting the Multiplicity Bounds for Riemannian Spheres

**3.1.1. Introduction.** In this chapter, we revisit the paper [HoHN1999] by M. and T. Hoffmann-Ostenhof and N. Nadirashvili, in which the authors consider Riemannian spheres with potential  $(M, g, V)$ . This means that  $M$  is a  $C^\infty$  surface homeomorphic to the sphere, and that it is equipped with a  $C^\infty$  Riemannian metric  $g$ , and with a  $C^\infty$  real valued potential  $V$ . We denote the eigenvalues of the Schrödinger operator  $-\Delta + V$  on  $M$  by  $\{\lambda_k\}_{k=1}^\infty$ , with first label 1, see Section 2.1, Equation (2.1).

According to Cheng [Chen1976], for  $(M, g, 0)$ ,  $\text{mult}(\lambda_2) \leq 3$ , and this bound is sharp, achieved for the round metric on the sphere. Nadirashvili [Nadi1987], proved that  $\text{mult}(\lambda_k) \leq (2k - 1)$ , for any  $k \geq 1$ , and for any such  $(M, g, V)$ . In [HoHN1999], M. and T. Hoffmann-Ostenhof and Nadirashvili, prove the following result.

**THEOREM 3.1** ([HoHN1999], Theorem 1). *For any smooth Riemannian metric  $g$ , and any smooth real valued potential  $V$  on the sphere  $M$ , the eigenvalues of the operator  $-\Delta + V$  satisfy  $\text{mult}(\lambda_k) \leq (2k - 3)$  for any  $k \geq 3$ .*

*Sketch of the proof of Theorem 3.1.* Fix some  $x \in M$ . Consider the eigenspace  $U(\lambda_k)$ . We first prove Nadirashvili's estimate,

$$(3.1) \quad \text{for } (M, g, V), \quad \text{mult}(\lambda_k) \leq (2k - 1) \text{ for all } k \geq 1.$$

The estimate is clear for  $k = 1$ . Assume, by contradiction, that  $\text{mult}(\lambda_k) = \dim U(\lambda_k) \geq 2k$  for some integer  $k \geq 2$ . Then, according to Lemma 2.14, there exists a function  $0 \neq u \in U(\lambda_k)$  such that  $\nu(u, x) \geq 2k$ . By Courant's theorem, Theorem 2.4, the number of nodal domains of  $u$  satisfies  $\kappa(u) \leq k$ . Since  $M$  is topologically a sphere, we can apply Euler's formula (2.17) to the nodal set  $\mathcal{Z}(u)$  of the function  $u$ ,

$$(3.2) \quad \kappa(u) = 1 + b_0(\mathcal{Z}(u)) + \frac{1}{2} \sum_{z \in \mathcal{S}(u)} (\nu(u, z) - 2).$$

Summing up the above information, we obtain

$$(3.3) \quad 0 \geq \kappa(u) - k = \{b_0(\mathcal{Z}(u)) - 1\} + \sum_{\substack{z \in \mathcal{S}(u) \\ z \neq x}} \frac{\nu(u, z) - 2}{2} + \left\{ \frac{\nu(u, x)}{2} - k + 1 \right\} \geq 1,$$

a contradiction.

Note that inequality (3.1) is sharp for  $k = 1$  and 2, see Table 1.1 in Section 1.2.

In view of (3.1), to prove Theorem 3.1, it suffices to show that the cases  $\dim U(\lambda_k) = (2k - 1)$ , and  $\dim U(\lambda_k) = (2k - 2)$  cannot occur when  $k \geq 3$ . This is the purpose of the following two subsections, in which we revisit the arguments of [HoHN1999].

More precisely, in Subsection 3.1.2, we assume that  $\dim U(\lambda_k) = (2k - 1)$  for some  $k \geq 3$ , and we reach a contradiction using an argument which will be recurrent in this paper, the *rotating function argument*, see Paragraph 3.1.2.3. In Subsection 3.1.3, we assume that  $\dim U(\lambda_k) = (2k - 2)$  for some  $k \geq 3$ , and we reach a contradiction by using both the *rotating function argument* and the Poincaré-Hopf theorem, see [Miln1997, Chap. 6, p. 35]

### 3.1.2. Riemannian spheres with potential, $\dim U(\lambda_k) \leq (2k - 2)$ for $k \geq 3$ .

The proof of this upper bound is by contradiction. Taking (3.1) into account, we assume that:

$$(3.4) \quad \text{There exists some } k \geq 3 \text{ such that } \dim U(\lambda_k) = (2k - 1).$$

Fixing some  $x \in M$ , we introduce the subspace

$$(3.5) \quad W_x := \{u \in U(\lambda_k) \mid \nu(u, x) \geq 2(k - 1)\}.$$

Fix a direct orthonormal frame  $\{\vec{e}_1, \vec{e}_2\}$  in  $T_x M$ , and the associated polar coordinates  $(r, \omega)$ , via the exponential map  $\exp_x$ .

3.1.2.1. *Structure of the nodal set  $\mathcal{Z}(u)$ , for  $0 \neq u \in W_x$ .*

PROPERTIES 3.2. *Assume that  $\dim U(\lambda_k) = (2k - 1)$  for some  $k \geq 3$ . The linear subspace*

$$W_x = \{u \in U(\lambda_k) \mid \nu(u, x) \geq 2(k - 1)\}$$

*has the following properties. For any  $0 \neq u \in W_x$ ,*

- (i)  $\nu(u, x) = 2(k - 1)$ , and  $x$  is the only singular point of the function  $u$ ;
- (ii)  $\mathcal{Z}(u)$  is connected;
- (iii)  $\kappa(u) = k$ .

*Furthermore,  $\dim W_x = 2$ , and there exists a basis  $\{v_1, v_2\}$  of  $W_x$  such that, in the local polar coordinates  $(r, \omega)$  centered at  $x$ ,*

$$(3.6) \quad \begin{cases} v_1(r, \omega) = r^{k-1} \sin((k - 1)\omega) + \mathcal{O}(r^k), \\ v_2(r, \omega) = r^{k-1} \cos((k - 1)\omega) + \mathcal{O}(r^k). \end{cases}$$

*Proof.* According to Lemma 2.14 (ii), there exist two linearly independent functions  $u_1, u_2 \in U(\lambda_k)$ , with  $\nu(u_i, x) \geq 2(k - 1)$ , for  $i = 1, 2$ , so that  $\dim W_x \geq 2$ . Given any  $0 \neq u \in W_x$ , we can apply Inequality (3.3) to  $u$ ,

$$(3.7) \quad 0 \geq \kappa(u) - k = \{b_0(\mathcal{Z}(u)) - 1\} + \sum_{\substack{z \in \mathcal{S}(u) \\ z \neq x}} \frac{\nu(u, z) - 2}{2} + \left\{ \frac{\nu(u, x)}{2} - k + 1 \right\}.$$

The three terms in the right-hand side of (3.7) are nonnegative, and their sum is nonpositive. They must all vanish. This proves Assertions (i)–(iii).

We already know that  $W_x$  has dimension at least 2. Assume that it has dimension at least 3, and let  $v_1, v_2, v_3$  be three linearly independent functions in  $W_x$ . Since  $\nu(v_i, x) = 2(k - 1)$ , Lemma 2.17 implies the existence of a nontrivial linear combination  $v$  of these functions with  $\nu(v, x) \geq 2k$ , contradicting Assertion (i). Hence,  $\dim W_x = 2$ .

For any  $0 \neq u \in W_x$  and  $\xi \in T_x M$ , we have

$$u(\exp_x(t\xi)) = t^{(k-1)} h_{x,u}(\xi) + \mathcal{O}(t^k),$$

where  $h_{x,u}$  is a harmonic homogeneous polynomial of degree  $(k-1)$  in  $\xi$ . On  $W_x$ , the map  $u \mapsto h_{x,u}$  is linear and injective. Since the space  $\mathcal{H}_{x,(k-1)}$  of harmonic homogeneous polynomials of degree  $(k-1)$  has dimension 2, this map is bijective. The space  $\mathcal{H}_{x,(k-1)}$  is generated by the polynomials  $r^{(k-1)} \sin((k-1)\omega)$  and  $r^{(k-1)} \cos((k-1)\omega)$  in the polar coordinates  $(r, \omega)$ . This proves the existence of the basis  $\{v_1, v_2\}$  satisfying (3.6). This proves the last assertion.

The proof of Properties 3.2 is now complete.  $\square$

Let  $0 \neq u \in W_x$ . The local structure theorem – Corollary 2.9 (i) – implies that, in a neighborhood of  $x$ , the nodal set  $\mathcal{Z}(u)$  consists of  $2(k-1)$  nodal semi-arcs which emanate from  $x$ , tangentially to  $2(k-1)$  rays dividing the unit circle in  $T_x M$  into equal parts. Since  $\mathcal{S}(u) = \{x\}$ , if we follow a nodal semi-arc emanating from  $x$ , we will eventually come back to  $x$ . Using the fact that  $\mathcal{S}(u) = \{x\}$  and the connectedness of  $\mathcal{Z}(u)$ , we conclude that  $\mathcal{Z}(u)$  consists of  $(k-1)$  simple loops at  $x$ , and that these loops only intersect each other at  $x$ .

**DEFINITION 3.3.** A *p-bouquet of loops at  $x$*  is a collection of  $p$  piecewise  $C^1$  loops at  $x$ , which do not intersect away from  $x$ , and whose semi-tangents at  $x$  are pairwise transverse in  $T_x M$ .

Therefore, for any  $0 \neq u \in W_x$ , the nodal set  $\mathcal{Z}(u)$  is a  $(k-1)$ -bouquet of loops at the point  $x$ .

3.1.2.2. *Combinatorial type of the nodal set  $\mathcal{Z}(u)$ , for  $0 \neq u \in W_x$ .* Using the frame  $\{\vec{e}_1, \vec{e}_2\}$  in  $T_x M$ , we label the rays tangent to  $\mathcal{Z}(u)$  at  $x$  counter-clockwise, according to their angle with respect to  $\vec{e}_1$  (two consecutive rays making an angle  $\frac{\pi}{k-1}$ ), so that we obtain an ordered list

$$\{0 \leq \vartheta_0 < \dots < \vartheta_{(2k-3)} < 2\pi\} .$$

The loops in the  $(k-1)$ -bouquet of loops  $\mathcal{Z}(u)$  can now be described by a map

$$(3.8) \quad \tau_{x,u} : \{0, \dots, (2k-3)\} \rightarrow \{0, \dots, (2k-3)\} ,$$

which is defined in the following way: for  $j \in \{0, \dots, (2k-3)\}$ , we consider the nodal arc which emanates from  $x$  tangentially to the ray  $\vartheta_j$ , and define  $\tau_{x,u}(j)$  as the label of the ray tangent to the nodal arc when it arrives back at  $x$ , forming a loop at  $x$ , with semi-tangents the rays  $\vartheta_j$  and  $\vartheta_{\tau_{x,u}(j)}$ . We denote this loop by  $\gamma_{j, \tau_{x,u}(j)}^{x,u}$ .

**DEFINITION 3.4 (Combinatorial type).** The map  $\tau_{x,u}$  is called the *combinatorial type* of the function  $u$ , or of the nodal set  $\mathcal{Z}(u)$ , at the point  $x$ .

We shall write  $\tau$  instead of  $\tau_{x,u}$  when there is no ambiguity. The properties of nodal sets imply that

$$(3.9) \quad \begin{cases} \tau_{x,u}(j) \neq j & \text{for all } j \in \{0, \dots, (2k-3)\} , \\ \tau_{x,u}^2 = \text{Id} . \end{cases}$$

Note that changing the frame  $\{\vec{e}_1, \vec{e}_2\}$  at  $x$ , keeping the orientation, amounts to conjugating the map  $\tau_{x,u}$  by a circular permutation of the set  $\{0, \dots, (2k-3)\}$ .

3.1.2.3. *The rotating function argument.* Fix the basis  $\{v_1, v_2\}$  of  $W_x$  provided by Properties 3.2, using the direct frame  $\{\vec{e}_1, \vec{e}_2\}$  in  $T_x M$  and the associated local polar coordinates  $(r, \omega)$  at  $x$  such that (3.6) holds.

We now analyze the nodal sets of the one-parameter family,

$$(3.10) \quad w_\theta = \cos((k-1)\theta) v_1 - \sin((k-1)\theta) v_2,$$

for  $\theta \in [0, \frac{\pi}{k-1}]$ . In particular, we have

$$(3.11) \quad v_1 = w_0 = -w_{\frac{\pi}{k-1}} \quad \text{and} \quad v_2 = -w_{\frac{\pi}{2(k-1)}},$$

and

$$(3.12) \quad w_\theta(r, \omega) = r^{k-1} \sin((k-1)(\omega - \theta)) + \mathcal{O}(r^k).$$

Properties 3.2 state that  $x$  is the sole singular point of the eigenfunction  $w_\theta$ , and that the nodal set  $\mathcal{Z}(w_\theta)$  is connected. With respect to the frame  $\{\vec{e}_1, \vec{e}_2\}$  in  $T_x M$ , there are  $2(k-1)$  nodal semi-arcs which emanate from  $x$ , tangentially to the  $2(k-1)$  rays  $\{\omega = \omega_j(\theta) := \omega_j + \theta\}$ , where  $\omega_j := j \frac{\pi}{k-1}$ ,  $j \in \{0, \dots, (2k-3)\}$ . We call these rays  $\omega_j(\theta)$  for short, and we view  $j$  as defined modulo  $2(k-1)$ .

The nodal set  $\mathcal{Z}(w_\theta)$  is a  $(k-1)$ -bouquet of loops described by the map  $\tau_{x, w_\theta}$  associated with the rays  $\{\omega_j(\theta)\}$ . Call this map  $\tau_\theta$  for short, and call  $\gamma_{j, \tau_\theta(j)}^\theta$  the corresponding loops at  $x$ .

**PROPERTY 3.5.** *Assume that  $k \geq 3$ , and  $\dim U(\lambda_k) = (2k-1)$ . Choose some  $j \in \{0, \dots, (2k-3)\}$ . Considering  $\tau_\theta(j)$  instead of  $j$  if necessary, we can assume that  $0 \leq j < \tau_\theta(j) \leq 2k-3$ . The loop  $\gamma_{j, \tau_\theta(j)}^\theta$  separates (the topological sphere)  $M$  into two components. The rays  $\omega_k(\theta)$  such that  $j < k < \tau_\theta(j)$  point inside one of the two components; the rays  $\omega_k(\theta)$  with  $k < j$  or  $k > \tau_\theta(j)$  point inside the other component. In particular,  $\tau_\theta(j) - j$  is an odd integer.*

The proof of this property is clear.

**PROPERTY 3.6.** *Assume that  $k \geq 3$ , and  $\dim U(\lambda_k) = (2k-1)$ . The combinatorial type  $\tau_\theta$  of the function  $w_\theta = \cos((k-1)\theta) v_1 - \sin((k-1)\theta) v_2$  does actually not depend on  $\theta$ . More precisely, for any  $j \in \{0, \dots, (2k-3)\}$ , and for any  $\theta \in [0, \frac{\pi}{k-1}]$ , the loop which emanates from  $x$  tangentially to the ray  $\omega_j(\theta)$  arrives at  $x$  tangentially to the ray  $\omega_{\tau_\theta(j)}(\theta)$ . We shall henceforth denote this map by  $\tau$ .*

*Proof.* Since all the functions  $w_\theta$  share the same properties, it suffices to show that  $\tau_\theta = \tau_0$  for  $\theta$  small enough. Assume the contrary. Then, there exists a sequence  $\theta_n$  tending to zero, and a sequence  $\{j_n\} \subset \{0, \dots, 2k-3\}$  such that  $\tau_{\theta_n}(j_n) \neq \tau_0(j_n)$ . Since the sequence  $\{j_n\}$  takes finitely many values, we can find a constant subsequence  $\{j_{n,1}\} \subset \{j_n\}$ . Similarly, there exists subsequence  $\{j_{n,2}\} \subset \{j_{n,1}\}$  such that  $\tau_{\theta_{n,2}}(j_{n,2})$  is constant. Hence, there exists some  $\ell \in \{0, \dots, 2k-3\}$ , and a sequence  $\theta_n$  such that  $\tau_{\theta_n}(\ell) \neq \tau_0(\ell)$ . Without loss of generality, we may assume that  $\ell = 0$ , so that there exists a sequence  $\theta_n$  tending to zero such that  $\tau_{\theta_n}(0) \equiv \ell_0 \neq \tau(0)$ .

We now use a more precise version of the local structure theorem, see Section 2.3. For any  $\alpha > 0$  small enough, there exists  $r_0 > 0$  such that, for all  $\theta$ ,  $\mathcal{Z}(w_\theta) \cap B(x, 2r_0)$  consists of  $2(k-1)$  nodal semi-arcs

$$(3.13) \quad A_j(r, \theta) : (0, 2r_0) \ni r \mapsto \exp_x(r \tilde{\omega}_j(r, \theta)) \in B(x, 2r_0),$$

for  $j \in \{0, \dots, 2k-3\}$ . Here, we assume that an orthonormal frame  $\{e_1, e_2\}$  has been chosen in  $T_x M$ , in such a way that the vector  $e_1$  directs the ray  $\omega_0$ . In the polar coordinates  $(r, \omega)$  associated with this frame, we identify the angle  $\omega$  with a point on the unit circle. Furthermore, the functions  $\tilde{\omega}_j$  are smooth in  $(r, \theta) \in (0, 2r_0) \times [0, 2\pi]$ , and they satisfy,

$$(3.14) \quad \begin{cases} \tilde{\omega}_j(r, \theta) \in (\omega_j + \theta - \alpha, \omega_j + \theta + \alpha) , \\ \lim_{r \rightarrow 0} \tilde{\omega}_j(r, \theta) = \omega_j + \theta , \end{cases}$$

for all  $j, 0 \leq j \leq 2k-3$ . The semi-arc  $A_j(r, \theta)$  is semi-tangent to the ray  $\omega_j + \theta$  at the point  $x$ .

We now reason as in the proof of Lemma 2.20. In the closed ball  $\overline{B}(x, r_0)$ , the nodal set  $\mathcal{Z}(w_{\theta_n})$  consists of  $2(k-1)$  nodal semi-arcs  $A_j(\cdot, \theta_n)$ , with end points  $x$  and  $\exp_x(r_0 \tilde{\omega}_j(r_0, \theta_n))$  which converge to the corresponding semi-arcs  $A_j(\cdot, 0)$  with end points  $x$  and  $\exp_x(r_0 \tilde{\omega}_j(r_0, 0))$ .

In the compact set  $M \setminus B(x, r_0)$ , the nodal set  $\mathcal{Z}(w_{\theta_n})$  consists of  $(k-1)$  disjoint connected nodal arcs  $C_j(r_0, \theta_n)$  with two end points  $\exp_x(r_0 \tilde{\omega}_j(r_0, \theta_n))$  and  $\exp_x(r_0 \tilde{\omega}_{\tau(j)}(r_0, \theta_n))$ , which correspond to the intersections of the loops in  $\mathcal{Z}(w_{\theta_n})$  with  $M \setminus B(x, r_0)$ . We look more precisely at the arcs  $C_0(r_0, \theta_n)$ . From this sequence of compact connected subsets of  $M \setminus B(x, r_0)$ , we can extract a subsequence which converges in the Hausdorff distance to some compact connected set  $C_0$ . Since any  $z \in C_0$  is the limit of a sequence  $z_n \in C_0(r_0, \theta_n)$ , and since  $w_{\theta_n}$  tends to  $w_0$  uniformly on  $M$ , we conclude that  $w_0(z) = 0$ , i.e., that  $C_0 \subset \mathcal{Z}(w_0)$ . The set  $C_0$  contains the points  $\exp_x(r_0 \tilde{\omega}_0(r_0, 0))$  and  $\exp_x(r_0 \tilde{\omega}_{\ell_0}(r_0, 0))$ . Since  $C_0$  is connected and contained in  $\mathcal{Z}(w_0)$ , and in view of the structure of  $\mathcal{Z}(w_0)$ , we must have  $\ell_0 = \tau(0)$ , and we reach a contradiction. The proof of Property 3.6 is complete.  $\square$

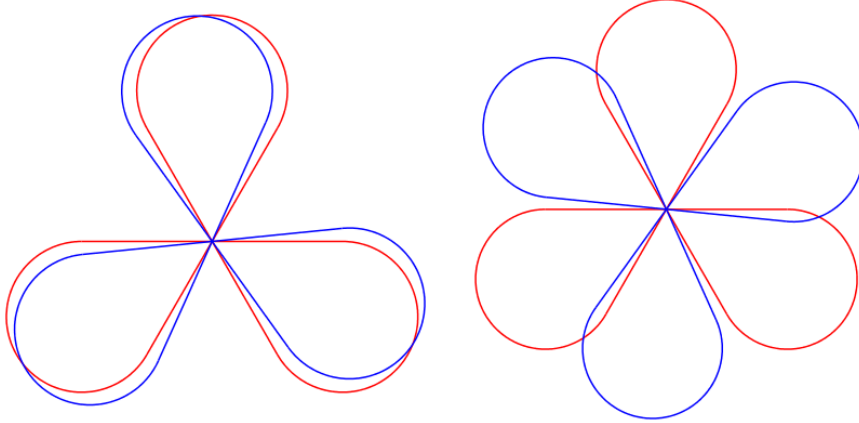


FIGURE 3.1. Example 1:  $k = 4$ ,  $\theta \simeq 0$  (left) and  $\theta \simeq \frac{\pi}{3}$  (right)

*Conclusion of the rotating function argument.* Under the assumption that  $k \geq 3$ , and  $\dim U(\lambda_k) = (2k-1)$ , we can apply the previous construction.

Since  $w_{\frac{\pi}{k-1}} = -v_1$ , we infer from Property 3.6 that  $\gamma_{0, \tau(0)}^{\frac{\pi}{k-1}} = \gamma_{1, \tau(0)+1}^0$ . Since there is only one nodal semi-arc tangent to a given ray at  $x$ , we conclude that  $\tau(0) \neq 1$  and  $\tau(0) \neq 2k-3$ . It follows that  $0 < 1 < \tau(0)$ , and that  $\tau(0) < \tau(0)+1 = \tau(1) \leq 2k-3$  (here we have used the assumption  $k \geq 3$ ). This contradicts Property 3.5, and proves

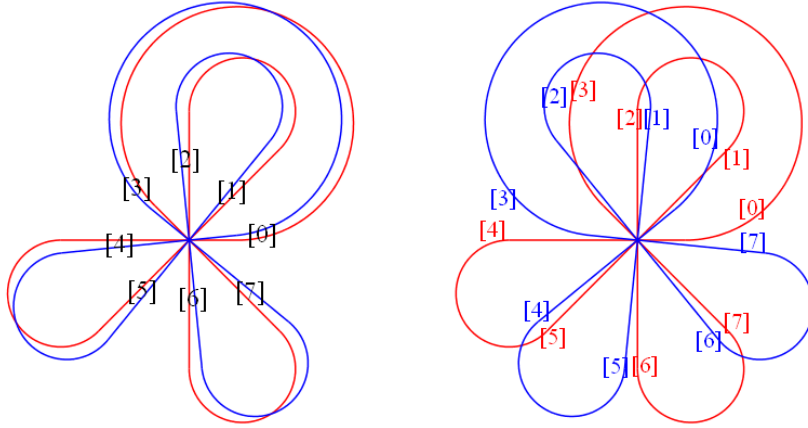


FIGURE 3.2. Example 2:  $k = 5$ ,  $\theta \simeq 0$  (left) and  $\theta \simeq \frac{\pi}{4}$  (right)

that  $\dim U(\lambda_k) = (2k - 1)$  cannot occur. This is illustrated in Figures 3.1 and 3.2 (with  $k = 4$ ). The nodal set of  $w_0$  is displayed in red, the nodal set of  $w_\theta$  is displayed in blue. In the left sub-figures,  $\theta$  is close to 0, in the right sub-figures  $\theta$  is close to  $\frac{\pi}{k-1}$ . In the second figure, the numbers in brackets are the labels of the rays.

We have proved the inequality

$$(3.15) \quad \text{mult}(\lambda_k) \leq (2k - 2), \text{ for any } k \geq 3.$$

□

REMARK 3.7. As far as we know, the idea to consider the family of functions  $w_\theta$  was introduced by Besson [Bess1980], in the proof of his Theorem 3.C.1 in which he improves the upper bound for the multiplicity of the second eigenvalue of a torus from 7 to 6. A similar idea was used by Nadirashvili [Nadi1987], p. 231 lines 1–8, for higher eigenvalues as well. It is used in [HoHN1999, HoMN1999, Berd2018] also, and will appear several times, in one form or another, in the present paper.

REMARK 3.8. In the next section, we will introduce the *combinatorial type* for different kinds of nodal sets on a compact surface  $M$  with boundary, and we will repeatedly use a *rotating function argument*.

### 3.1.3. Riemannian spheres with potential, $\dim U(\lambda_k) \leq (2k - 3)$ for $k \geq 3$ .

The proof of this upper bound is by contradiction. Taking Subsection 3.1.2 into account, we assume that  $\dim U(\lambda_k) = (2k - 2)$ .

As in the previous subsection, fix some  $x \in M$ , a direct orthonormal frame  $\{\vec{e}_1, \vec{e}_2\}$  in  $T_x M$ , and the associated polar coordinates  $(r, \omega)$ , via the exponential map  $\exp_x$ .

PROPERTIES 3.9. Assume that  $\dim U(\lambda_k) = (2k - 2)$  for some  $k \geq 3$ . Then, the linear subspace

$$W_x = \{u \in U(\lambda_k) \mid \nu(u, x) \geq 2(k - 1)\}$$

has the following properties.

- (i)  $\dim W_x = 1$  and, for any  $0 \neq u \in W_x$ ,
- (ii)  $\nu(u, x) = 2(k - 1)$ , and  $x$  is the only singular point of the eigenfunction  $u$ ;
- (iii)  $\mathcal{Z}(u)$  is connected;
- (iv)  $\kappa(u) = k$ .



*Proof.* By Lemma 2.14,  $\dim W_x \geq 1$ . Given any  $0 \neq u \in W_x$ , Euler's formula gives

$$(3.16) \quad 0 \geq \kappa(u) - k = \{b_0(\mathcal{Z}(u)) - 1\} + \sum_{\substack{z \in \mathcal{S}(u) \\ z \neq x}} \frac{\nu(u, z) - 2}{2} + \left\{ \frac{\nu(u, x)}{2} - k + 1 \right\},$$

and we conclude that (ii)–(iv) hold. To prove (v), assuming that  $\dim W_x \geq 2$ , we can repeat the arguments of Subsection 3.1.2, and reach a contradiction.  $\square$

**PROPERTY 3.10.** *Assume that  $\dim U(\lambda_k) = (2k - 2)$  for some  $k \geq 3$ . Let  $[W_x]$  denote the line  $W_x$  as a point in the projective space  $\mathbb{P}(U)$  of  $U$ . Then, the map  $x \mapsto [W_x]$  from  $M$  to  $\mathbb{P}(U)$  is  $C^\infty$ .*

*Proof.* Since  $(-\Delta + V)w_x = \lambda_k w_x$ , the condition that  $\text{ord}(w_x, x) \geq (k - 1)$  is equivalent to  $(2k - 3)$  linear equations in the derivatives of  $w_x$  at  $x$  (cf. the proof of Lemma 2.14). Choosing a basis  $\{\phi_j\}_{j=1}^{(2k-2)}$  of  $U$ , and writing  $w_x$  as  $w_x = \sum_{j=1}^{2k-2} \alpha_j(x)\phi_j$ , we obtain a system of  $(2k - 3)$  linear equations in the  $(2k - 2)$  unknowns  $\{\alpha_j(x)\}_{j=1}^{(2k-2)}$ . Call  $\mathcal{M}(x)$  the associated matrix. The system reads  $\mathcal{M}(x)\mathcal{A}(x) = 0$  where  $\mathcal{A}(x)$  is the vector associated with the coefficients  $\alpha_j(x)$ . Since  $\dim W_x = 1$  for all  $x \in M$ , this linear system has constant rank  $(2k - 3)$ . Given some  $x_0 \in M$ , there exists a  $(2k - 3) \times (2k - 3)$  sub-matrix  $\mathcal{M}'_{x_0}$  which is invertible, and the same is true for the sub-matrix  $\mathcal{M}'_x$  provided that  $x$  is close enough to  $x_0$ . We can now find  $w_x$ , alias the coefficients  $\alpha_j(x)$ , by solving a linear system of the form  $\mathcal{M}'_x \mathcal{A}'(x) = \mathcal{B}(x)$  in a neighborhood of  $x_0$ . In view of Cramer's method, the coefficients of  $\mathcal{A}'(x)$  are given as quotients of determinants whose coefficients are  $C^\infty$  in  $x$ , and the determinant at the denominator is nonzero.  $\square$

Since  $M$  is simply connected, the map  $x \mapsto [W_x]$  can be lifted to a smooth map  $x \mapsto w_x$ , from  $M$  to  $\mathbb{S}(U(\lambda_k))$ , the unit sphere of  $U(\lambda_k)$  (for example with respect to the  $L^2$  norm).

To each  $x \in M$ , we associate the homogeneous polynomial of degree  $(k - 1)$ ,  $h_{x, w_x}$  on  $T_x M$  defined by  $p_x := h_{x, w_x} : T_x M \ni \xi \mapsto \frac{d^{k-1}}{dt^{k-1}} w_x(\exp_x(t\xi))$ . It is harmonic with respect to the Riemannian metric  $g_x$  in  $T_x M$ . The map  $x \mapsto p_x$  is smooth. The restriction of the polynomial  $p_x$  to the unit circle  $S_x M$  in  $(T_x M, g_x)$  has simple zeros. Choose some  $x_0 \in M$ , and some root  $e_{x_0}$  of  $p_{x_0}$  in  $S_{x_0} M$ . Given any  $x_1 \in M$ , and any curve  $c$  from  $x_0$  to  $x_1$ , we can follow this root by continuity along the curve  $c$  so that  $e_{c(t)}$  is a root of  $p_{c(t)}$ . Since the set of roots is discrete, and since  $M$  is simply connected, the root  $e_{c(1)}$  at  $x_1$  does not depend on the choice of the curve  $c$ .

It follows that we have defined a continuous unit vector-field  $x \mapsto e_x$  on  $M$ , contradicting the Poincaré-Hopf theorem (see below). Here, we have indeed a vector-field without zero, and  $\chi(M) = 2$ . We have proved that the assumption  $\dim U(\lambda_k) = (2k - 2)$  leads to a contradiction, and hence that  $\dim U(\lambda_k) \leq (2k - 3)$ .  $\square$

For the sake of completeness, we recall the statement of the Poincaré-Hopf theorem.

**THEOREM 3.11** ([Miln1997], p. 35). *Let  $X$  be a closed manifold. Let  $w$  be a  $C^\infty$  vector-field on  $X$  with isolated zeros. Then, the sum of the indices at the zeros of  $w$  is equal to the Euler characteristic of  $X$ .*

### 3.2. Spheres: Labeling Nodal Loops and Nodal Domains

**3.2.1. Preamble.** In Section 3.1, we have used the notion of *combinatorial type* to study the eigenvalue multiplicity problem on Riemannian spheres with potential,  $(M, g, V)$ . More precisely, we have introduced the combinatorial type of very special eigenfunctions, namely eigenfunctions  $u \in U(\lambda_k)$ , with only one singular point  $x \in M$ , and whose nodal set  $\mathcal{Z}(u)$  is a  $(k-1)$ -bouquet of loops at  $x$ , see Properties 3.2 and 3.9. The combinatorial type  $\tau_u$  of  $\mathcal{Z}(u)$  describes how the loops are organized in the bouquet  $\mathcal{Z}(u)$ .

In this section, we introduce the *nodal word*  $\mathcal{W}_u$  in order to describe how the nodal domains of  $u$  are organized around  $x$ , by looking at their intersections with a small geodesic circle  $S_x(r)$  with center  $x$  and radius  $r$ . We prove that the nodal word  $\mathcal{W}_u$  determines the combinatorial type  $\tau_u$  and vice-versa.

Similar considerations will be applied to smooth bounded domains in  $\mathbb{R}^2$ , see Section 5.5.

We make the following assumptions through out this section.

ASSUMPTIONS 3.12.

- (i)  $(M, g, V)$  is a Riemannian sphere  $M$  with  $C^\infty$  Riemannian metric  $g$  and  $C^\infty$  real valued potential  $V$ .
- (ii)  $u$  is an eigenfunction of the Schrödinger operator  $(-\Delta + V)$  on  $M$ , with a unique critical zero  $x \in M$  such that  $\text{ord}(u, x) = p$  for some  $p \geq 2$ .
- (iii)  $\mathcal{Z}(u)$  is connected.

For convenience, we fix

- ◇ an orientation of  $T_x M$ ,
- ◇ a ray  $\omega_0$  in  $T_x M$ , tangent to  $\mathcal{Z}(u)$  at  $x$ ,
- ◇ the direct orthonormal frame  $\mathcal{E}(\omega_0) := \{e_{0,1}, e_{0,2}\}$  in  $T_x M$  whose first vector  $e_{0,1}$  is supported by  $\omega_0$ ,

and we denote

- ◇ the rays tangent to  $\mathcal{Z}(u)$  at  $x$  by  $\omega_0, \omega_1, \dots, \omega_{(2p-1)}$ , counter-clockwise,
- ◇ the polar coordinates associated with  $\mathcal{E}(\omega_0)$  in  $T_x M$  by  $(r, \omega)$ ,
- ◇ the combinatorial type of  $\mathcal{Z}(u)$  with respect to the rays  $\{\omega_0, \dots, \omega_{(2p-1)}\}$ , by  $\tau_u$  (see Definition 3.4).

Let  $u$  be an eigenfunction satisfying Assumptions 3.12.

*Fact 1.* The nodal set  $\mathcal{Z}(u)$  is a  $p$ -bouquet of loops described by the pair  $(L, \tau)$ , where  $L = \{0, \dots, (2p-1)\}$  and  $\tau = \tau_u$  is the combinatorial type of  $u$ . We now denote this bouquet by  $\mathcal{B}_L$ .

Indeed, in a small neighborhood of  $x$ , the nodal set  $\mathcal{Z}(u)$  consists of  $2p$  nodal semi-arcs emanating from  $x$ , tangentially to  $2p$  distinct<sup>1</sup> rays  $\omega_0, \dots, \omega_{2p-1}$ . Since nodal arcs can only meet at critical zeros, and since  $\mathcal{S}(u) = \{x\}$ , the nodal interval emanating from  $x$  tangentially to the ray  $\omega_j$  must end up at  $x$ , arriving tangentially to some (different) ray  $\omega_{\tau(j)}$ , thus forming a loop  $\gamma_{j, \tau(j)}$  at  $x$ . This defines the map  $\tau$ ,

$$(3.17) \quad \tau : L \rightarrow L,$$

<sup>1</sup>The rays actually form an equiangular system, but this is not needed here.

with the following properties,

$$(3.18) \quad \begin{cases} \tau^2 = \text{Id}, \\ \tau(j) \neq j, \quad \forall j \in L, \\ \tau(j) - j \text{ is odd}, \quad \forall j \in L. \end{cases}$$

The first property is clear. The second and third ones follow from the local structure theorem and from the fact that  $M$  is a sphere, see Property 3.5.

*Fact 2.* *The eigenfunction  $u$  has  $(p + 1)$  nodal domains.*

This property is a consequence of the following lemma; it is related to the fact that the eigenfunctions in Properties 3.2 and 3.9 are *Courant-sharp*, i.e., they have the maximum number of nodal domains allowed by Courant's nodal domain theorem, see Section 6.2.

LEMMA 3.13. *The complement of a  $p$ -bouquet of loops  $\mathcal{B}$  in the sphere  $M$  has  $(p + 1)$  components.*

*Proof.* We can turn the  $p$ -bouquet of loops  $\mathcal{B}$  into a (simple) graph  $\mathcal{G}_{\mathcal{B}}$  on the sphere by vertex-edge additions as explained in Section 2.2. Then, the number of components in the complement of the bouquet  $\mathcal{B}$  is the same as the number of components in the complement of the graph  $\mathcal{G}_{\mathcal{B}}$ . Using the notation of Section 2.2, Euler's formula for the graph  $\mathcal{G}_{\mathcal{B}}$  reads

$$r(\mathcal{G}_{\mathcal{B}}) = \alpha_1(\mathcal{G}_{\mathcal{B}}) - \alpha_0(\mathcal{G}_{\mathcal{B}}) + c(\mathcal{G}_{\mathcal{B}}) + 1$$

as in Equation (2.16). It is easy to see that  $\alpha_1(\mathcal{G}_{\mathcal{B}}) - \alpha_0(\mathcal{G}_{\mathcal{B}}) = (p - 1)$ . Since  $c(\mathcal{G}_{\mathcal{B}}) = 1$ , the result follows.  $\square$

In the polar coordinates  $(r, \omega)$ , and for  $r$  small enough, the nodal semi-arcs emanating from  $x$  are given by equations  $r \mapsto \exp_x(r \tilde{\omega}_j(r))$ ,  $0 \leq j \leq 2p - 1$ , see Section 2.3. These arcs determine  $2p$  intervals (sub-arcs)

$$(3.19) \quad I_j(r) := \{\exp_x(r \omega) \mid \omega \in (\tilde{\omega}_j(r), \tilde{\omega}_{j+1}(r))\}, \quad 0 \leq j \leq 2p - 1,$$

on the geodesic circle  $S_x(r) = \{\exp_x(r \omega) \mid \omega \in [0, 2\pi]\}$ . The function  $u$  does not vanish in these open intervals, and changes sign while crossing an end point  $\exp_x(r \tilde{\omega}_j(r))$  along the circle.

*Fact 3.* *Each open interval  $I_j(r)$  is contained in a unique nodal domain, and two contiguous intervals are contained in different nodal domains. Each nodal domain of  $u$  contains at least one interval (for  $r$  small enough).*

DEFINITION 3.14. Let  $\mathcal{D}(u)$  be the set of nodal domains of  $u$ .

A bijection  $d : \{1, \dots, (p + 1)\} \rightarrow \mathcal{D}(u)$  is called a *labeling of the nodal domains* of  $u$ . Using this labeling, we describe  $\mathcal{D}(u)$  as  $\mathcal{D}(u) = \{\Omega_{d(1)}, \dots, \Omega_{d(p+1)}\}$ . The *nodal word*  $\mathcal{W}_{u,d}$  of  $u$ , associated with the labeling  $d$  of  $\mathcal{D}(u)$ , is the map  $\mathcal{W}_{u,d} : \{0, \dots, (2p - 1)\} \rightarrow \{1, \dots, (p + 1)\}$

$$\mathcal{W}_{u,d} = \begin{pmatrix} 0 & 1 & \dots & (2p - 2) & (2p - 1) \\ a_0 & a_1 & \dots & a_{2p-2} & a_{2p-1} \end{pmatrix},$$

also written as the word

$$\mathcal{W}_{u,d} = |a_0|a_2| \dots |a_{(2p-1)}|,$$

where the letter  $a_j$  is the label  $d(k)$  of the nodal domain which contains  $I_j(r)$ ,

$$\mathcal{W}_{u,d}(j) = d(k) \Leftrightarrow I_j(r) \subset \Omega_{d(k)}.$$

The word  $\mathcal{W}(u, d)$  has length  $2p$ , the letters of the word are the labels of the nodal domains (they are separated by vertical bars in the second formula for notational convenience).

*Fact 4.* Given  $\mathcal{W}_{u,d}$  a nodal word, we recover the labeling  $d$  as follows,

- (1)  $d(1) = a_0$  and  $d(2) = a_1$
- (2) if  $m_3 := \min \{j \mid a_j \notin \{d(1), d(2)\}\}$ , then  $\Omega_{d(3)}$  is the nodal domain which contains  $I_{m_3}(r)$ , i.e.  $d(3) = a_{m_3}$ .
- (3) ...

It is convenient to describe a procedure to produce a “standard nodal word”  $\mathcal{W}_u$ , and a “standard labeling”  $d_s$  of the nodal domains of an eigenfunction  $u$  satisfying Assumptions 3.12.

DEFINITION 3.15. The *standard nodal word*  $\mathcal{W}_u$  of  $u$  is the map

$$\mathcal{W}_u : L \rightarrow \{1, \dots, (p+1)\}$$

defined as follows.

- (1) Let  $\mathcal{W}_u(1) = 1$ . Equivalently, call  $\Omega_1$  the nodal domain which contains the interval  $I_0(r)$ . Let  $\mathcal{W}_u(j) = 1$  whenever  $I_j(r) \subset \Omega_1$ .
- (2) Let  $\mathcal{W}_u(2) = 2$ . Equivalently, call  $\Omega_2$  the nodal domain which contains the interval  $I_1(r)$ . Let  $\mathcal{W}_u(j) = 2$  whenever  $I_j(r) \subset \Omega_2$ .
- (3) Assume that  $k$  nodal domains have been labeled, with the labels given in increasing order,  $1, 2, \dots, k$ . Since all nodal domains intersect any neighborhood of  $x$ , the set  $\{j \mid I_j(r) \not\subset \bigcup_{j=1}^k \Omega_j\}$  is not empty. Let  $m_{k+1}$  be its infimum. Call  $\Omega_{k+1}$  the nodal domain which contains  $I_{m_{k+1}}(r)$ . Let  $\mathcal{W}_u(j) = (k+1)$  whenever  $I_j(r) \subset \Omega_{k+1}$ .
- (4) After at most  $p$  steps, all nodal domains will be labeled.

**3.2.2. Sub-bouquets of loops.** As stated in the previous subsection, the nodal set  $\mathcal{Z}(u)$  is a  $p$ -bouquet of loops  $\mathcal{B}_L$  at  $x$ , i.e.,  $p$  simple loops at  $x$  which do not intersect away from  $x$ , and which meet transversally at  $x$ .

Take any loop,  $\gamma_{j,\tau(j)}$ . Exchanging,  $j$  and  $\tau(j)$  if necessary, we may assume that  $j < \tau(j)$ . Consider the subsets

$$(3.20) \quad \begin{cases} L_j := \{j, (j+1), \dots, (\tau(j)-1), \tau(j)\} \subset L, \\ L'_j := L_j \setminus \{j, \tau(j)\}. \end{cases}$$

Since  $M$  is a sphere,  $M \setminus \{\gamma_{j,\tau(j)}\}$  has two components. The local structure of  $\mathcal{Z}(u)$  at  $x$  shows that the rays  $\omega_k, k \in L'_j$ , point inside one of the components, call it  $C'_j$ . If  $L'_j$  is empty, choose  $C'_j$  to be the component which is a nodal domain of  $u$ . For  $\ell \leq j \leq \tau(\ell) - 1$ , the nodal interval  $I_j(r)$  is contained in  $C'_j$ , and the subsets  $L_j, L'_j$  are invariant under  $\tau$ , and correspond to bouquets of loops  $\mathcal{B}_{L_j}$  and  $\mathcal{B}_{L'_j} \subset C'_j$ .

Similarly, the rays  $\omega_k, k \in L \setminus L_j$ , point inside the other component, call it  $C''_j$ . The corresponding nodal intervals are contained in  $C''_j$ , so that  $L \setminus L_j$  is invariant under  $\tau$ , and corresponds to a bouquet of loops  $\mathcal{B}_{L \setminus L_j} \subset C''_j$ . Note that if  $L_j = L$ , then  $C''_j$  is a nodal domain of  $u$ .

### 3.2.3. Nodal word of $u$ vs combinatorial type of $u$ .

PROPERTY 3.16. *Once we have chosen an orientation in  $T_x M$ , an initial ray  $\omega_0$ , and labeled the other rays counter-clockwise, the combinatorial type  $\tau_u : L \rightarrow L$  of  $u$  determines the standard nodal word  $\mathcal{W}_u : L \rightarrow \{1, \dots, (p+1)\}$  of the nodal domains of  $u$ . Conversely, given a standard nodal word  $\mathcal{W}_u$  as defined in Definition 3.15, we can recover the nodal type  $\tau_u$ .*

3.2.3.1. *Proof of Property 3.16 on a simple example.* For the example, we choose  $p = 8$ , so that  $L = \{0, 1, 2, 3, 4, 5, 6, 7, 8, 9, 10, 11, 12, 13, 14, 15\}$ , and the map  $\tau$

$$(3.21) \quad \tau = \begin{pmatrix} 0 & 1 & 2 & 3 & 4 & 5 & 6 & 7 & 8 & 9 & 10 & 11 & 12 & 13 & 14 & 15 \\ 3 & 2 & 1 & 0 & 9 & 8 & 7 & 6 & 5 & 4 & 15 & 12 & 11 & 14 & 13 & 10 \end{pmatrix}$$

written in matrix form:  $\tau$  maps the first line to the second line.

We view the pair  $(L, \tau)$  as describing an abstract bouquet of loops  $\mathcal{B}_L$  which satisfies the properties explained in Subsection 3.2.2, see Figure 3.3 for a representation in  $\mathbb{R}^2$ . The numbers between brackets are the labels of the rays or nodal arcs emanating from  $x$ . Since we may think of  $\mathcal{B}_L$  as the zero set of some function, we still call the components  $\Omega_j$  of  $M \setminus \mathcal{B}_L$  “nodal domains of  $\mathcal{B}_L$ ”.

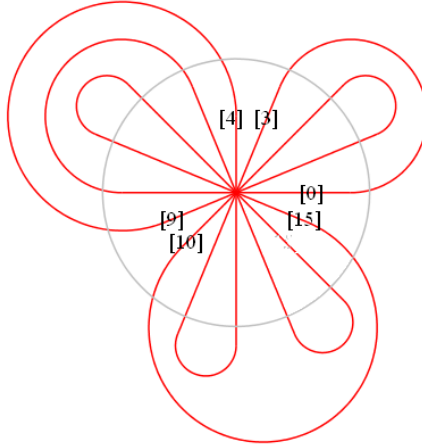


FIGURE 3.3. The bouquet  $\mathcal{B}_L$  with  $\tau$  given by (3.21)

We first partition the set  $L$  into  $\tau$ -invariant subsets with the same notation as in Equation (3.20).

- ◇ Since  $\tau(0) = 3$ , we have the  $\tau$ -invariant subset  $L_0 = \{0, 1, 2, 3\}$ , the “big” loop  $\gamma_{0,3}$  and  $C'_0$  the connected component of  $M \setminus \gamma_{0,3}$  which contains  $\mathcal{B}_{L'_0}$ .
- ◇ Since  $\tau(4) = 9$ , we have the  $\tau$ -invariant subset  $L_4 = \{4, 5, 6, 7, 8, 9\}$ , the “big” loop  $\gamma_{4,9}$  and  $C'_4$  the corresponding component of  $M \setminus \gamma_{4,9}$ .
- ◇ Since  $\tau(10) = 15$ , we have the  $\tau$ -invariant subset  $L_{10} = \{10, 11, 12, 13, 14, 15\}$ , the “big” loop  $\gamma_{10,15}$  and  $C'_{10}$  the corresponding component of  $M \setminus \gamma_{10,15}$ .

The set  $L$  has been partitioned into three  $\tau$ -invariant subsets  $L_0 = \{0, 1, 2, 3\}$ ,  $L_4 = \{4, 5, 6, 7, 8, 9\}$  and  $L_{10} = \{10, 11, 12, 13, 14, 15\}$ . Accordingly, the matrix representing  $\tau$  can be decomposed into three blocks,

$$\tau = \left( \begin{array}{cccc|cccccc|cccccc} 0 & 1 & 2 & 3 & 4 & 5 & 6 & 7 & 8 & 9 & 10 & 11 & 12 & 13 & 14 & 15 \\ 3 & 2 & 1 & 0 & 9 & 8 & 7 & 6 & 5 & 4 & 15 & 12 & 11 & 14 & 13 & 10 \end{array} \right).$$

The set  $M \setminus (C'_0 \cup C'_4 \cup C'_{10})$  is a nodal domain of  $\mathcal{B}_L$  which we call the *exterior* of  $\mathcal{B}_L$ . Any other nodal domain of  $\mathcal{B}_L$  is contained in either  $C'_0, C'_4$  or  $C'_{10}$ . It now suffices to define  $\mathcal{W}_u$  on each of the invariant subsets or, equivalently, to find the labels of the exterior of  $\mathcal{B}_L$  and of the nodal domains contained in  $C'_0, C'_4$  or  $C'_{10}$ .

We first label the nodal domains inside  $C'_0$ . We have  $I_j(r) \subset C'_0$  for  $j \in \{0, 1, 2\}$ . According to Definition 3.15,  $\mathcal{W}(0) = 1$ , and  $\mathcal{W}(1) = 2$ . Following  $S_x(r)$  from  $\exp_x(r\tilde{\omega}_0(r))$  to  $\exp_x(r\tilde{\omega}_3(r))$  and exiting  $C'_0$ , we conclude that  $\mathcal{W}(2) = 1$  and  $\mathcal{W}(3) = 3$ . This implies that the exterior of  $\mathcal{B}_L$  is the nodal domain  $\Omega_3$  and this also implies that  $\mathcal{W}(9) = \mathcal{W}(15) = 3$  because  $I_9(r)$  and  $I_{15}(r)$  are both contained in the exterior of  $\mathcal{B}_L$ .

We now label the nodal domains inside  $C'_4$ . We have  $I_j(r) \subset C'_4$  for  $j \in \{4, 5, 6, 7, 8\}$ . According to Definition 3.15, we set  $\mathcal{W}(4) = 4$ . Following  $S_x(r)$  from  $\exp_x(r\tilde{\omega}_4(r))$  to  $\exp_x(r\tilde{\omega}_9(r))$  and exiting  $C'_4$ , we conclude that  $\mathcal{W}(8) = 4$  and  $\mathcal{W}(10) = 7$  because  $C'_4$  contains 3 nodal domains. It remains to label the nodal domains in  $L'_4$ . This is similar to the first step (with different labels though) and we find that  $\mathcal{W}(5) = \mathcal{W}(7) = 5$  and  $\mathcal{W}(6) = 6$  because we have one loop  $\gamma_{6,7}$  inside the loop  $\gamma_{5,8}$ .

It remains to label the nodal domains inside  $C'_{10}$ , starting from  $\mathcal{W}(10) = 7$ . Because there are two loops  $\gamma_{11,12}$  and  $\gamma_{13,15}$  inside the loop  $\gamma_{10,15}$ , we find that  $\mathcal{W}(10) = \mathcal{W}(12) = \mathcal{W}(14) = 7$ ,  $\mathcal{W}(11) = 8$  and  $\mathcal{W}(13) = 9$ .

Finally, the map  $\mathcal{W}$  is given by the matrix

$$(3.22) \quad \mathcal{W} = \begin{pmatrix} 0 & 1 & 2 & 3 & 4 & 5 & 6 & 7 & 8 & 9 & 10 & 11 & 12 & 13 & 14 & 15 \\ 1 & 2 & 1 & 3 & 4 & 5 & 6 & 5 & 4 & 3 & 7 & 8 & 7 & 9 & 7 & 3 \end{pmatrix},$$

where  $\mathcal{W}$  sends the entry  $j \in L$  in the first line, the label of the interval  $I_j(r)$ , to the entry  $\mathcal{W}(j)$  in the second line, the label of the nodal domain which contains  $I_j(r)$ .

• *Proof that one can recover  $\tau$  from  $\mathcal{W}$ .* We use the fact that the nodal domains come in disjoint families separated by loops.

The boundary of the domain  $\Omega_1$  contains the loop  $\gamma_{0,\tau(0)}$ . To determine  $\tau(0)$ , we look at the largest integer  $\ell$  such that  $\mathcal{W}(\ell) = 1$ : this is 2 and we conclude that  $\tau(0) = 3$ . Looking at the second row of the matrix of  $\mathcal{W}$  in (3.22), we infer that  $\Omega_2$  is bounded by a single loop, so that  $\tau(1) = 2$ . We have determined a  $\tau$ -invariant subset  $L_0 = \{0, 1, 2, 3\}$ , and that  $\tau$  satisfies

$$\tau|_{L_0} = \begin{pmatrix} 0 & 1 & 2 & 3 \\ 3 & 2 & 1 & 0 \end{pmatrix}.$$

The next nodal domain is  $\Omega_3$  and we have  $\mathcal{W}(3) = \mathcal{W}(9) = \mathcal{W}(15) = 3$ . Taking into account how we constructed  $\mathcal{W}$  from  $\tau$ , it follows that  $\Omega_3$  is the “exterior” of  $\mathcal{B}_L$ .

The next nodal domain which appears is  $\Omega_4$ . To determine  $\tau(4)$ , we look at the largest integer  $\ell$  such that  $\mathcal{W}(\ell) = 4$ : this is 8. This means that  $\tau(4) = 9$ , and we have a loop  $\gamma_{4,9}$  whose complement in  $M$  has two connected components  $C''_4$  and  $C'_4$ , with the rays labeled 5 to 8 pointing inside  $C''_4$ . We have the  $\tau$ -invariant subset  $L_4 = \{4, 5, 6, 7, 8, 9\}$ . In  $C'_4$ , the nodal domain label 4 occurs twice, the label 5 occurs twice as well, and the label 6 once. We conclude that

$$\tau|_{L_4} = \begin{pmatrix} 4 & 5 & 6 & 7 & 8 & 9 \\ 9 & 8 & 7 & 6 & 5 & 4 \end{pmatrix}.$$

The two next nodal domain to appear are  $\Omega_3$  again and  $\Omega_7$ . Reasoning as above, we find that  $\tau(10) = 15$  and we have the  $\tau$ -invariant subset  $L_{10} = \{10, 11, 12, 13, 14, 15\}$ . Finally,

$$\tau|_{L_{10}} = \begin{pmatrix} 10 & 11 & 12 & 13 & 14 & 15 \\ 15 & 12 & 11 & 14 & 13 & 10 \end{pmatrix}.$$

We have recovered the map  $\tau$  from the map  $\mathcal{W}$  in the example at hand.  $\square$

### 3.2.3.2. Proof of Property 3.16 in general.

• *Proof that  $\tau$  determines  $\mathcal{W}$ .*

◇ We begin by partitioning  $L$  into invariant subsets.

First we define  $\ell_1 := 0$ . Then  $\ell_1 < \tau(\ell_1) \leq (2p - 1)$  and the subset  $L_{\ell_1} = \{\ell_1, \dots, \tau(\ell_1)\}$  is  $\tau$ -invariant. If  $\tau(\ell_1) = (2p - 1)$ ,  $M \setminus \gamma_{\ell_1, \tau(\ell_1)}$  has two components, one of them  $C''_{\ell_1}$  is a nodal domain of  $\mathcal{B}_L$ , and we define  $\mathcal{W}(2p - 1) = (p + 1)$ . The other component  $C'_{\ell_1}$  of  $M \setminus \gamma_{\ell_1, \tau(\ell_1)}$  contains all the nodal domains of  $\mathcal{B}_L$ , except the nodal domain  $\Omega_{p+1}$ . If  $\tau(\ell_1) \neq (2p - 1)$ ,  $\tau(\ell_1) \leq (2p - 3)$ , and we introduce  $\ell_2 := \tau(\ell_1) + 1$ . The subset  $L_{\ell_2} = \{\ell_2, \dots, \tau(\ell_2)\}$  is  $\tau$ -invariant, and we can repeat the procedure. After at most  $|L|/2$  steps, we obtain a sequence  $\ell_1 < \dots < \ell_m$  such that  $\ell_{j+1} = \tau(\ell_j) + 1$  and  $\tau(\ell_m) = (2p - 1)$ . Then, we have a partition,  $L = \bigsqcup_{j=1}^m L_{\ell_j}$ , of  $L$ . A nodal domain of  $\mathcal{B}_L$  is either contained in one of the components  $C'_{\ell_j}$ , or is equal to the *exterior nodal domain* of  $\mathcal{B}_L$ , the set  $M \setminus \bigcup_{j=1}^m C'_{\ell_j}$ .

◇ Consider a loop  $\gamma_{\ell_j, \tau(\ell_j)}$ , with

$$(3.23) \quad \begin{cases} L_{\ell_j} = \{\ell_j, \dots, \tau(\ell_j)\} \text{ and } L'_{\ell_j} = L_{\ell_j} \setminus \{\ell_j, \tau(\ell_j)\}, \\ k_{\ell_j} = \frac{1}{2}|L_{\ell_j}|. \end{cases}$$

Taking into account Subsection 3.2.2 and Lemma 3.13, with the set  $L_{\ell_j}$  we associate a  $k_{\ell_j}$ -bouquet of loops  $\mathcal{B}_{L_{\ell_j}}$ , whose complement in  $M$  has  $(k_{\ell_j} + 1)$  components. Similarly, with the set  $L'_{\ell_j}$  we associate a  $(k_{\ell_j} - 1)$ -bouquet  $\mathcal{B}_{L'_{\ell_j}}$  which is contained in  $C'_{\ell_j}$ , and whose complement in  $C'_{\ell_j}$  has  $k_{\ell_j}$  components which are actually nodal domains of  $\mathcal{B}_L$ .

◇ The  $k_{\ell_1}$  nodal domains contained in  $C'_{\ell_1}$  are labeled from 1 to  $k_{\ell_1}$ . The intervals  $I_j(r)$ ,  $\ell_1 \leq j \leq \tau(\ell_1) - 1$  are contained in  $C'_{\ell_1}$ ; the intervals  $I_j(r)$ ,  $\tau(\ell_1) \leq j$  are contained in  $C''_{\ell_1}$ . From these facts, we infer that

$$(3.24) \quad \begin{cases} \mathcal{W}(0) = \mathcal{W}(\tau(\ell_1) - 1) = 1, \\ \mathcal{W}(1) = 2, \\ \mathcal{W}(\tau(\ell_1)) = k_{\ell_1} + 1, \\ \mathcal{W}(\tau(\ell_1) + 1) = k_{\ell_1} + 2. \end{cases}$$

The label  $\mathcal{W}(\tau(\ell_1))$  plays a special role. Indeed, this is the label of the exterior of  $\mathcal{B}_L$ ,  $M \setminus \bigcup_{j=1}^m C'_{\ell_j}$ . It follows that the nodal domains of  $\mathcal{B}_L$  will be labeled as follows:

- 1) The  $k_{\ell_1}$  nodal domains contained in  $C'_{\ell_1}$  are labeled from 1 to  $k_{\ell_1}$ .
- 2) The exterior nodal domain of  $\mathcal{B}_L$  is labeled  $(k_{\ell_1} + 1)$ .
- 3) The  $k_{\ell_2}$  nodal domains contained in  $C'_{\ell_2}$  are labeled from  $(k_{\ell_1} + 2)$  to  $(k_{\ell_1} + k_{\ell_2} + 1)$ .
- 4) The  $k_{\ell_3}$  nodal domains contained in  $C'_{\ell_3}$  are labeled from  $(k_{\ell_1} + k_{\ell_2} + 2)$  to  $(k_{\ell_1} + k_{\ell_2} + k_{\ell_3} + 1)$ .
- 5) ... and so on.

Once we know the label of the exterior domain, and which label sets to use for the domains contained in the sets  $C'_{\ell_j}$ , it suffices to determine  $\mathcal{W}$  on each set  $L_{\ell_j}$  independently, and we can reason by induction on the size of  $|L|$ .

◇ Given  $\ell \in \{\ell_1, \dots, \ell_m\}$ , the connected component  $C'_{\ell_1}$  of  $M \setminus \gamma_{\ell, \tau(\ell)}$  is simply connected, with boundary  $\gamma_{\ell, \tau(\ell)}$ . The nodal domains inside  $C'_\ell$  are numbered from  $K_\ell$  to  $K_\ell + k_\ell - 1$ , according to the above list. The interval  $I_\ell(r)$  is the first interval contained in  $C'_\ell$  to be labeled,  $\mathcal{W}(\ell) = K_\ell$ , and we must have  $\mathcal{W}(\ell + 1) = (K_\ell + 1)$ . Since  $|L_\ell| < |L|$  we can now apply the induction hypothesis, and  $\mathcal{W}|_{L_\ell}$  is well defined.

• *Proof that one can recover  $\tau$  from  $\mathcal{W}$  in general.*

◇ Assume that we are given some  $L := \{0, \dots, (2p - 1)\}$  and some map  $\mathcal{W} : L \rightarrow \{1, \dots, (p + 1)\}$  associated with a  $p$ -bouquet of loops  $\mathcal{B}_L$  as in Definition 3.15. Let  $\tau : L \rightarrow L$  be the combinatorial type of the  $p$ -bouquet  $\mathcal{B}_L$ .

In order to recover  $\tau$  from  $\mathcal{W}$ , the idea is to recover the  $\tau$ -invariant subsets  $L_{\ell_j}$  introduced above, and to reason by induction on the size of the bouquets, i.e., on  $|L|$ .

◇ We first look at the nodal domain  $\Omega_1$ , with label  $\mathcal{W}(0) = 1$ , and at the set  $\mathcal{W}^{-1}(1)$ . If  $\mathcal{W}^{-1}(1) = \{0\}$ , then we must have  $\tau(0) = 1$ , the loop  $\gamma_{0,1}$  bounds  $\Omega_1$ ,  $\tau(0) = 1$ , and  $\Omega_2$  is the exterior domain of  $\mathcal{B}_L$ .

If  $|\mathcal{W}^{-1}(1)| > 1$ , we look at  $m_1 := \max \mathcal{W}^{-1}(1)$ . Then, the only possibility is that  $\tau(0) = m_1 + 1$ . According to Subsection 3.2.2, the subsets  $L_0 := \{0, \dots, (m_1 + 1)\}$ ,  $L'_0 := \{1, \dots, m_1\}$ , and  $L \setminus L_0$  are  $\tau$  invariant. Defining  $C'_0$  and  $C''_0$  as above, there are exactly  $k_0$  nodal domains inside  $C'_0$ , where  $2k_0 = |L_0|$ ,  $\mathcal{W}(m_1 + 1) = (k_0 + 1)$ , and the domain  $\Omega_{\mathcal{W}(m_1+1)}$  is the exterior domain of  $\mathcal{B}_L$ . Looking at  $\mathcal{W}^{-1}(k_0 + 1)$ , we obtain the partition of  $L$  into  $\tau$ -invariant subsets which we used to deduce the word  $\mathcal{W}$  from the combinatorial type  $\tau$ .

Example: If we look back at the example given by Equation (3.21) and at the corresponding map  $d$  given by Equation (3.22), we find that  $m_1 = 2$ , and that  $k_1 + 1 = 3$ , and we recover the fact that

$$L = \{0, \dots, 3\} \sqcup \{4, \dots, 9\} \sqcup \{10, \dots, 15\}$$

and the fact that  $\Omega_3$  is the exterior domain of  $\mathcal{B}_L$ .

◇ To conclude in the general case, it suffices to determine  $\tau$  in each of the invariant subsets, so that we can now use an induction argument on  $|L|$ .



## CHAPTER 4

### Plane Domains: the Estimate $\text{mult}(\lambda_k) \leq (2k - 2)$ for $k \geq 3$

Let  $\Omega$  be a regular (i.e.,  $C^\infty$ ) bounded domain<sup>1</sup> in  $\mathbb{R}^2$ . We are interested in the eigenvalue problem for the Laplacian or for a Schrödinger operator of the form  $-\Delta + V$  in  $\Omega$ , with Dirichlet, Neumann or  $h$ -Robin boundary condition, see (2.3). As indicated in the introduction, we do not consider the Steklov problem. In this chapter, we prove the following result.

**THEOREM 4.1.** *The multiplicities of the eigenvalues of the operator  $-\Delta + V$  in  $\Omega$ , with the Dirichlet, Neumann or  $h$ -Robin boundary condition, satisfy the estimate  $\text{mult}(\lambda_k) \leq (2k - 2)$  for any  $k \geq 3$ .*

In the next chapter, we will discuss the proof of the sharper estimate  $\text{mult}(\lambda_k) \leq (2k - 3)$  for any  $k \geq 3$ , under the additional assumption that  $\Omega$  is *simply connected*, and relate this estimate to [HoMN1999, Theorem A].

#### 4.1. Bounding $\text{mult}(\lambda_k)$ from Above

**4.1.1. Introduction.** As in [HoMN1999], our proof of Theorem 4.1 consists of three steps.

- The first step is to prove the upper bound  $\text{mult}(\lambda_k) \leq (2k - 1)$  for all  $k \geq 1$ . This upper bound follows easily from Courant's nodal domain theorem, Theorem 2.4, and Euler's formula for nodal sets, see Subsection 4.1.3. It is sharp for  $k = 1$  since  $\text{mult}(\lambda_1) = 1$  for any domain. The inequality  $\text{mult}(\lambda_2) \leq 3$  turns out to be sharp either. This is related to the *nodal line conjecture*, see Section 6.1.
- In a second step, we prove that  $\text{mult}(\lambda_k)$  cannot be equal to  $(2k - 1)$  for  $k \geq 3$ . This is done in Section 4.2, under the simplifying assumption that  $\Omega$  is simply-connected, and in Section 4.3 in the general case.

**REMARK 4.2.** As far as we know, for the Neumann and  $h$ -Robin boundary condition, the upper bound on the eigenvalue multiplicities given in Theorem 4.1 is new.

**4.1.2. Notation.** Let us fix some notation for Sections 4.1–5.4.

Let  $U$  denote a linear subspace of an eigenspace of the eigenvalue problem for  $-\Delta + V$  in  $\Omega$ , see (2.3). We assume that  $U$  satisfies the inequality

$$(4.1) \quad \max \{ \kappa(u) \mid 0 \neq u \in U \} \leq \ell, \quad \text{for some integer } \ell \geq 2.$$

We denote  $\partial\Omega$  by  $\Gamma$ , and write it as the union of its components,

$$\Gamma = \bigcup_{j=1}^q \Gamma_j, \quad \text{with } q \geq 1.$$

---

<sup>1</sup>By “domain”, we mean a connected open subset.

Given  $0 \neq u \in U$ , define the sets

$$(4.2) \quad \begin{cases} J(u) & := \{j \mid \Gamma_j \cap \mathcal{Z}(u) \neq \emptyset\}, \\ \Gamma(u) & := \cup_{j \in J(u)} \Gamma_j. \end{cases}$$

Given a function  $0 \neq u \in U$ ,  $[u]$  denotes the line

$$(4.3) \quad [u] := \{a u \mid a \in \mathbb{R} \setminus \{0\}\}$$

in the projective space  $\mathbb{P}(U)$ . We will say that  $u$  is a generator of the line  $[u]$ . If a function  $u$  is uniquely determined by some condition, up to multiplication by a nonzero scalar, we will say that  $u$  is uniquely determined *up to scaling* or, equivalently, that  $[u]$  is uniquely determined.

**4.1.3. The initial inequalities.** We shall make an extensive use of Euler's formula for the nodal set  $\mathcal{Z}(u)$  of an eigenfunction  $u$ , see Subsection 2.2.2. Taking into account the assumption (4.1) on  $U$ , we have

$$(4.4) \quad \ell \geq \kappa(u) = 1 + \beta(u) + \sigma_i(u) + \sigma_b(u),$$

where,

$$(4.5) \quad \begin{cases} \beta(u) & := b_0(\mathcal{Z}(u) \cup \Gamma) - b_0(\Gamma) \\ & = b_0(\mathcal{Z}(u) \cup \Gamma(u)) - b_0(\Gamma(u)), \end{cases}$$

$$(4.6) \quad \begin{cases} \sigma_i(u) & = \frac{1}{2} \sum_{z \in \mathcal{S}_i(u)} (\nu(u, z) - 2), \\ \sigma_b(u) & = \frac{1}{2} \sum_{z \in \mathcal{S}_b(u)} \rho(u, z) = \sum_{j \in J(u)} \frac{1}{2} \sum_{z \in \mathcal{S}_b(u) \cap \Gamma_j} \rho(u, z). \end{cases}$$

From the nodal character, using Proposition 2.29 and the definition of  $J(u)$ , we also have

$$(4.7) \quad \forall j \in J(u), \quad \sum_{z \in \mathcal{S}_b(u) \cap \Gamma_j} \rho(u, z) \text{ is even and } \geq 2.$$

We now rewrite the Euler inequality (4.4) in the form,

$$(4.8) \quad \begin{cases} 0 \geq \kappa(u) - \ell = & [b_0(\mathcal{Z}(u) \cup \Gamma(u)) - 1] + \frac{1}{2} \sum_{z \in \mathcal{S}_i(u)} (\nu(u, z) - 2) \\ & + \sum_{j \in J(u)} \frac{1}{2} \left( \sum_{z \in \mathcal{S}_b(u) \cap \Gamma_j} \rho(u, z) - 2 \right) - (\ell - 2). \end{cases}$$

We will apply this inequality to eigenfunctions with prescribed singular points.

Fix some  $x \in \Gamma_1$ , and let  $m := \dim U$ . By Lemma 2.15, there exists  $0 \neq u \in U$  such that  $\rho(u, x) \geq (m - 1)$ . Rewrite (4.8) as,

$$(4.9) \quad \begin{cases} 0 \geq \kappa(u) - \ell = & [b_0(\mathcal{Z}(u) \cup \Gamma(u)) - 1] + \frac{1}{2} \sum_{z \in \mathcal{S}_i(u)} (\nu(z) - 2) \\ & + \sum_{j \in J(u), j \neq 1} \frac{1}{2} \left( \sum_{z \in \mathcal{S}_b(u) \cap \Gamma_j} \rho(u, z) - 2 \right) \\ & + \frac{1}{2} \sum_{z \in \mathcal{S}_b(u) \cap \Gamma_1} \rho(u, z) - \ell + 1. \end{cases}$$

The first three terms in the right-hand side of the equality are nonnegative. It follows that

$$2\ell - 2 \geq \sum_{z \in \mathcal{S}_b(u) \cap \Gamma_1} \rho(u, z) \geq m - 1,$$

so that

$$(4.10) \quad \dim U = m \leq (2\ell - 1).$$

Courant's nodal domain theorem states that  $\max \{\kappa(u) \mid 0 \neq u \in U(\lambda_k)\} \leq k$ . Choosing  $U = U(\lambda_k)$ , inequality (4.10) yields the following estimate.

PROPOSITION 4.3 ([Nadi1987], Theorem 2). *Let  $\Omega \subset \mathbb{R}^2$  be a bounded domain with smooth boundary. Let  $\{\lambda_k, k \geq 1\}$  be the eigenvalues of the operator  $-\Delta + V$  in  $\Omega$ , with Dirichlet or Robin boundary condition. Then, for any  $k \geq 1$ ,*

$$\text{mult}(\lambda_k) \leq (2k - 1).$$

In view of Proposition 4.3, in order to prove Theorem 4.1, it suffices to show that the equality  $\dim U(\lambda_k) = (2k - 1)$  cannot occur for  $k \geq 3$ . This is the purpose of Sections 4.2 and 4.3 in which we revisit and extend the arguments of [HoMN1999] for the three boundary conditions (2.4).

REMARK 4.4. According to Pleijel [Plej1956], Courant's Theorem 2.4 is sharp for finitely many Dirichlet eigenvalues only. The eigenvalue  $\lambda_k$  is called *Courant-sharp* whenever the associated eigenspace  $U(\lambda_k)$  contains an eigenfunction with  $k$  nodal domains, the maximum number allowed by Courant's nodal domain theorem. If  $\lambda_k$  is not a Courant-sharp eigenvalue, we have  $\max \{\kappa(u) \mid 0 \neq u \in U(\lambda_k)\} \leq (k - 1)$  and hence  $\text{mult}(\lambda_k) \leq (2k - 3)$ , improving the inequality in Proposition 4.3 by 2. We refer to Section 6.2 for more details and references on Courant-sharp eigenvalues, and results à la Pleijel.

REMARK 4.5. In the forthcoming sections, under the assumptions that  $\ell = k \geq 3$  and  $\text{mult}(\lambda_k) = (2k - 1)$  or  $\text{mult}(\lambda_k) = (2k - 2)$ , we will prescribe eigenfunctions  $u$  with a singular set  $\mathcal{S}(u)$  such that equality holds in (4.9), implying that  $\kappa(u) = k$ , and hence that  $\lambda_k$  is Courant-sharp. We will actually not use this information in the proofs, but rather carefully analyze the nodal sets  $\mathcal{Z}(u)$  to reach a topological contradiction.

## 4.2. $\Omega$ Simply Connected: the Estimate $\text{mult}(\lambda_k) \leq (2k - 2)$ for $k \geq 3$

**4.2.1. Introduction.** In this section, we provide detailed proofs of the statements in [HoMN1999, Section 2]. The general idea is to prove that an a priori upper bound on the number of nodal domains of eigenfunctions in a given subspace  $U$  implies an upper bound on  $\dim U$ . Indeed, the bigger the dimension of  $U$ , the easier to construct eigenfunctions with prescribed high order singular points and, by Euler's formula, with more nodal domains.

The inequality in the title is valid for *any* smooth bounded domain  $\Omega \subset \mathbb{R}^2$ . Note that it is not true for  $k = 1$  and  $k = 2$ . In order to simplify the presentation, we shall however give the proof under *the additional assumption that  $\Omega$  is simply connected*, see Proposition 4.16. In Remark 4.17, we explain how to deal with the general case, referring to Section 4.3 for complete proofs.

The proof of the inequality is by contradiction. Taking Proposition 4.3 into account, we will assume that  $\dim U(\lambda_k) = (2k - 1)$  for some  $k \geq 3$ , and reach a contradiction. In this section, we make the following assumptions.

ASSUMPTIONS 4.6.

- i)  $\Omega$  is simply connected.
- ii)  $U$  is a linear subspace of an eigenspace  $U(\lambda)$  of  $-\Delta + V$  in  $\Omega$ , with Dirichlet or Robin boundary condition, see (2.3).

iii) For some  $\ell \geq 2$ ,

$$\begin{cases} \sup \{ \kappa(u) \mid 0 \neq u \in U \} \leq \ell & \text{and} \\ \dim U = (2\ell - 1). \end{cases}$$

#### 4.2.2. Eigenfunctions with two prescribed boundary singular points.

We use the notation of Subsection 4.1.2, and work under Assumptions 4.6.

For  $y \neq z \in \Gamma$ , we introduce the subspace

$$V_{y,z} := \{ u \in U \mid \rho(u, y) \geq (2\ell - 3) \text{ and } \rho(u, z) \geq 1 \}.$$

According to Lemma 2.16,  $V_{y,z} \neq \{0\}$ . The purpose of this subsection is to investigate the properties of the functions  $u \in V_{y,z}$ , precise order of vanishing, and structure of their nodal sets.

##### 4.2.2.1. Properties of $V_{y,z}$ .

LEMMA 4.7. *Assume that  $\Omega$  is simply connected. Let  $U$  be a linear subspace of an eigenspace of  $-\Delta + V$  in  $\Omega$ , such that  $\sup \{ \kappa(u) \mid 0 \neq u \in U \} \leq \ell$  for some  $\ell \geq 2$ , and  $\dim U = (2\ell - 1)$ . Let  $y \neq z \in \Gamma$ . The subspace*

$$V_{y,z} := \{ u \in U \mid \rho(u, y) \geq (2\ell - 3) \text{ and } \rho(u, z) \geq 1 \}.$$

has the following properties.

- (i)  $\dim V_{y,z} = 1$  and, for any  $0 \neq u \in V_{y,z}$ ;
- (ii)  $\mathcal{S}_i(u) = \emptyset$  and  $\mathcal{S}_b(u) = \{y, z\}$ ;
- (iii)  $\rho(u, y) = (2\ell - 3)$  and  $\rho(u, z) = 1$ ;
- (iv)  $\kappa(u) = \ell$ ;
- (v) the set  $\mathcal{Z}(u) \cup \Gamma$  is connected.

A generator of  $V_{y,z}$  will be denoted by  $v_{y,z}$  (defined up to scaling).

*Proof.* For simplicity, in the proof, we write  $\nu(z)$  for  $\nu(u, z)$ ,  $\dots$

The fact that  $\dim V_{y,z} \geq 1$  follows from Lemma 2.16. In view of our assumptions, for any  $0 \neq u \in U$ , Euler's formula (4.9) gives,

$$(4.11) \quad 0 \geq \kappa(u) - \ell = (b_0(\mathcal{Z}(u) \cup \Gamma) - 1) + \frac{1}{2} \sum_{x \in \mathcal{S}_i(u)} (\nu(x) - 2) + \frac{1}{2} \sum_{x \in \mathcal{S}_b(u), x \neq y, z} \rho(x) + \frac{1}{2} (\rho(y) + \rho(z) - 2\ell + 2).$$

Each term in the right-hand side of the equality being nonnegative, the inequality implies that each term is zero, thus proving Assertions (ii)–(v).

To prove the first assertion, assume that there exist two linearly independent functions  $u_1$  and  $u_2$  in  $U$ . By Assertion (iii) they both satisfy  $\rho(u_i, y) = (2\ell - 3)$  and  $\rho(u_i, z) = 1$ . Applying Lemma 2.17 at the point  $z$ , we find a nontrivial linear combination  $\tilde{u}$  of  $u_1$  and  $u_2$  such that  $\rho(\tilde{u}, z) \geq 2$  and  $\rho(\tilde{u}, y) \geq (2\ell - 3)$ , contradicting Assertion (iii).  $\square$

DEFINITION 4.8. By a *nodal pattern*, we mean a nodal set, up to continuous deformations under which singular points may move, but neither appear nor disappear (singular points occur when the nodal set has self-intersections, or when it hits the boundary.)

REMARK 4.9. The *nodal patterns* displayed in Figure 4.1 are valid for both the Dirichlet and Robin boundary conditions. Unless otherwise stated this remark applies to all figures of this section.

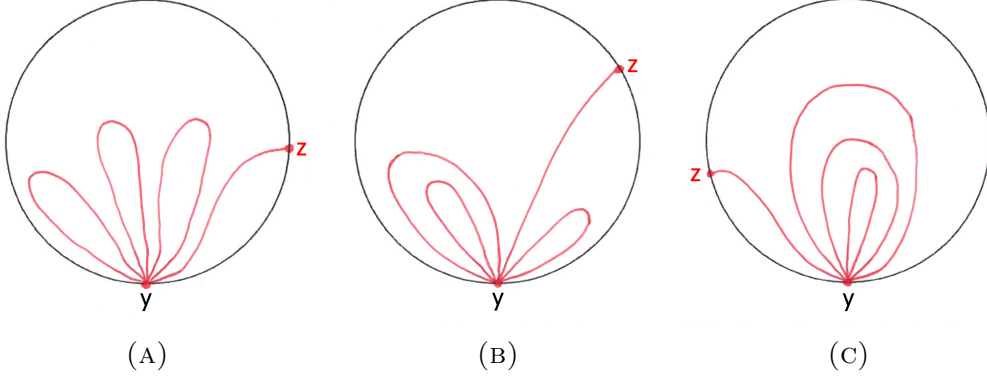


FIGURE 4.1.  $\Omega$  simply connected: some possible nodal patterns for  $v_{y,z}$

4.2.2.2. *Structure and combinatorial type of nodal sets in  $V_{y,z}$ .* Fix  $y \neq z \in \Gamma$ . Under the assumptions of Lemma 4.7, the nodal set of an eigenfunction  $u \in V_{y,z}$  can be described as follows, using the notation of Section 2.4.

For  $r_0$  small enough, in the neighborhood  $D_+(y, r_0)$  of  $y$ , the nodal set  $\mathcal{Z}(u)$  consists of  $(2\ell - 3)$  nodal semi-arcs  $\delta_j$  emanating from  $y$ , tangentially to the rays  $\omega_j$ ,  $1 \leq j \leq (2\ell - 3)$  (they actually depend on  $y, z$  as well). Choosing any  $j$ , we follow the nodal semi-arc  $\delta_j$  along  $\mathcal{Z}(u)$ , until we reach a singular point of  $u$ . Otherwise stated, we consider the component of  $\mathcal{Z}(u) \setminus \mathcal{S}(u)$  which contains the semi-arc  $\delta_j$  (by abuse of notation we also denote this component by  $\delta_j$ ). This is a nodal interval one of whose end points is  $y$ . Since  $\mathcal{S}(u) = \mathcal{S}_b(u) = \{y, z\}$ , the other end point is either  $y$  or  $z$ . More precisely, in view of the general properties of nodal sets, we define a map

$$(4.12) \quad \tau_{y,z} : \{\downarrow\} \cup L_{(2k-3)} \rightarrow \{\downarrow\} \cup L_{(2k-3)}$$

as follows (recall that  $L_m = \{1, \dots, m\}$ ).

- (i) There exists a unique element  $a_y^z \in L_{(2k-3)}$  such that starting from  $y$  along  $\delta_{a_y^z}$ , we reach the boundary  $\Gamma$  at  $z$ . We let  $\tau_{y,z}(\downarrow) = a_y^z$  and  $\tau_{y,z}(a_y^z) = \downarrow$ .
- (ii) For  $j \in L_{(2k-3)} \setminus \{a_y^z\}$ , following  $\delta_j$ , we arrive back at  $y$ , along another nodal semi-arc, which we denote by  $\delta_{\tau_{y,z}(j)}$ ; this semi-arc emanates from  $y$  tangentially to the ray  $\omega_{\tau_{y,z}(j)}$ . This defines  $\tau_{y,z}$  on  $L_{(2k-3)} \setminus \{a_y^z\}$ . The local structure theorem implies that for  $j \in L_{(2k-3)} \setminus \{a_y^z\}$ ,  $\tau_{y,z}(j) \in L_{(2k-3)} \setminus \{a_y^z\}$ , and  $\tau_{y,z}(j) \neq j$ .

Doing so, we obtain a uniquely defined map  $\tau_{y,z}$  from  $\{\downarrow\} \cup L_{(2\ell-3)}$  to itself, such that  $(\tau_{y,z})^2 = \text{Id}$ , and  $(\tau_{y,z})(j) \neq j$ .

The pair  $\{\downarrow, a_y^z\}$  corresponds to the nodal interval  $\delta_{a_y^z}$  from  $y$  to  $z$ . For  $j \in L_{(2k-3)} \setminus \{a_y^z\}$ , the pair  $\{j, \tau_{y,z}(j)\}$  corresponds to a loop  $\gamma_{j, \tau_{y,z}(j)}^{y,z}$  at  $y$ . There are  $(\ell - 2)$  such loops. Since  $\mathcal{S}(u) = \{y, z\}$  and  $\rho(u, z) = 1$ , these loops and arc do not intersect away from  $y$ . Since  $\mathcal{Z}(u) \cup \Gamma$  is connected, the nodal set  $\mathcal{Z}(u)$  is actually the union of these  $(\ell - 2)$  loops and arc. Otherwise stated,  $\mathcal{Z}(u)$  is the wedge sum  $\mathcal{B}_{y, (\ell-2)}^z$  of the simple arc  $\delta_{\tau_{y,z}(\downarrow)}$  from  $y$  to  $z$  with an  $(\ell - 2)$ -bouquet of loops at  $y$ .

By analogy with Paragraph 3.1.2.2, we give the following definition.

DEFINITION 4.10. The map  $\tau_{y,z}$  is called the *combinatorial type* of the eigenfunction  $u \in V_{y,z}$  (or of the nodal set  $\mathcal{Z}(u)$ ) with respect to the points  $y$  and  $z$ .

We describe the map  $\tau_{y,z}$  in matrix form as

$$(4.13) \quad \tau_{y,z} = \begin{pmatrix} \downarrow & 1 & \dots & (a_y^z - 1) & a_y^z & (a_y^z + 1) & \dots & (2\ell - 3) \\ a_y^z & \tau_{y,z}(1) & \dots & \tau_{y,z}(a_y^z - 1) & \downarrow & \tau_{y,z}(a_y^z + 1) & \dots & \tau_{y,z}(2\ell - 3) \end{pmatrix}.$$

In the sequel, we shall skip the sub- or super-scripts whenever the context is clear. Figure 4.1 displays some possible nodal patterns (for  $\ell = 5$ ,  $\rho(y) = 7$ , and  $\rho(z) = 1$ ). The corresponding combinatorial types are given respectively by

$$\tau_A = \begin{pmatrix} \downarrow & 1 & 2 & 3 & 4 & 5 & 6 & 7 \\ 1 & \downarrow & 3 & 2 & 5 & 4 & 7 & 6 \end{pmatrix} \quad \tau_B = \begin{pmatrix} \downarrow & 1 & 2 & 3 & 4 & 5 & 6 & 7 \\ 3 & 2 & 1 & \downarrow & 7 & 6 & 5 & 4 \end{pmatrix} \quad \tau_C = \begin{pmatrix} \downarrow & 1 & 2 & 3 & 4 & 5 & 6 & 7 \\ 7 & 6 & 5 & 4 & 3 & 2 & 1 & \downarrow \end{pmatrix}.$$

### 4.2.3. Eigenfunctions with one prescribed boundary singular point.

We use the notation of Subsection 4.1.2, and work under Assumptions 4.6.

For  $y \in \Gamma$ , we introduce the subspaces

$$(4.14) \quad \begin{cases} U_y^1 = \{u \in U \mid \rho(u, y) \geq (2\ell - 2)\}, \\ U_y^2 = \{u \in U \mid \rho(u, y) \geq (2\ell - 3)\}. \end{cases}$$

According to Lemma 2.16,  $U_y^1 \neq \{0\}$ . The purpose of this subsection is to investigate the properties of the functions  $u \in U_y^1$  or  $U_y^2$  – their precise order of vanishing, the structure of their nodal sets – under Assumptions 4.6.

#### 4.2.3.1. Properties of $U_y^1$ and $U_y^2$ .

LEMMA 4.11. *Assume that  $\Omega$  is simply connected. Let  $U$  be a linear subspace of an eigenspace of  $-\Delta + V$  in  $\Omega$ , such that  $\sup\{\kappa(u) \mid 0 \neq u \in U\} \leq \ell$  for some  $\ell \geq 2$ , and  $\dim U = (2\ell - 1)$ . Fix some  $y \in \Gamma$ . The subspaces*

$$\begin{cases} U_y^1 = \{u \in U \mid \rho(u, y) \geq (2\ell - 2)\} \\ U_y^2 = \{u \in U \mid \rho(u, y) \geq (2\ell - 3)\} \end{cases}$$

have the following properties.

- (i)  $\dim U_y^1 = 1$ ,  $\dim U_y^2 = 2$  and,
- (ii) for any  $0 \neq u \in U_y^2$ ,

$$(4.15) \quad \begin{cases} \kappa(u) = \ell \text{ and } \mathcal{Z}(u) \cup \Gamma \text{ is connected,} \\ \mathcal{S}_i(u) = \emptyset, \\ \sum_{z \in \mathcal{S}_b(u)} \rho(u, z) = (2\ell - 2) \text{ and, more precisely,} \\ \quad (a) \text{ either } \rho(u, y) = (2\ell - 2) \text{ and } \mathcal{S}_b(u) = \{y\}, \\ \quad (b) \text{ or } \rho(u, y) = (2\ell - 3), \exists z_u \in \Gamma \setminus \{y\} \text{ with } \rho(u, z_u) = 1, \\ \quad \text{and } \mathcal{S}_b(u) = \{y, z_u\}. \end{cases}$$

*Proof.* Clearly,  $\{0\} \neq U_y^1 \subset U_y^2$ . Take any  $0 \neq u \in U_y^2$ . Euler's formula (4.9) can be rewritten as

$$(4.16) \quad \begin{aligned} 0 \geq \kappa(u) - \ell &= (b_0(\mathcal{Z}(u) \cup \Gamma) - 1) + \frac{1}{2} \sum_{x \in \mathcal{S}_i(u)} (\nu(x) - 2) \\ &\quad + \frac{1}{2} \left( \sum_{x \in \mathcal{S}_b(u)} \rho(x) - 2\ell + 2 \right). \end{aligned}$$

The first two terms in the right-hand side of the equality are nonnegative. Since  $\sum_{x \in \mathcal{S}_b(u)} \rho(x)$  is even, and larger than or equal to  $(2\ell - 3)$ , the last term is nonnegative

too. In view of the first inequality, the three terms must vanish. This proves the relations (4.15).

◇ *Proof that  $\dim U_y^1 = 1$ .* Assume that this is not the case. Then, there exist two linearly independent functions  $u_1, u_2$  in  $U_y^1$  such that  $\rho(u_i, y) = (2\ell - 2)$ . By Lemma 2.17, there would exist a nontrivial linear combination  $u$  such that  $u \in U_y^1$  and  $\rho(u, y) \geq (2\ell - 1)$ , a contradiction with (4.15).

◇ *Proof that  $\dim U_y^2 = 2$ .* Choose some  $0 \neq v_1 \in U_y^1$ . Clearly  $v_1 \in U_y^2$ . On the other hand, given any  $z \in \Gamma \setminus \{y\}$ , Lemma 4.7 provides a function  $v_{y,z}$  belonging to  $U_y^2$ , not to  $U_y^1$ , and hence  $\dim U_y^2 \geq 2$ . Choose  $0 \neq v_2 \in U_y^2$  orthogonal to  $v_1$ . Since  $\dim U_y^1 = 1$ , the function  $v_2$  satisfies  $\rho(v_2, y) = (2\ell - 3)$ , and by Proposition 2.29, there must exist some  $z_2 \in \Gamma$  such that  $\rho(v_2, z_2) \geq 1$ . By Lemma 4.7,  $\rho(v_2, z_2) = 1$  and  $v_2 \in V_{y,z_2}$ . The subspace  $U_y^{1,\perp} := \{u \in U_y^2 \mid u \perp u_1\}$  has dimension at least one. Assume that  $\dim U_y^2 \geq 3$ . Then  $\dim U_y^{1,\perp} \geq 2$ , and we can find two linearly independent functions  $u_1, u_2 \in U_y^{1,\perp}$  such that  $\rho(u_i, y) = (2\ell - 3)$ . By Lemma 2.17, there exists a linear combination  $u \in U_y^{1,\perp}$  such that  $\rho(u, y) \geq (2\ell - 2)$ , a contradiction.  $\square$

REMARK 4.12. Up to scaling, there is a uniquely defined orthogonal basis  $\{v_1, v_2\}$  of  $U_y^2$ , with  $v_1 \in U_y^1$ ,  $v_2 \in U_y^{1,\perp}$ , and a uniquely defined  $z_2 \in \Gamma \setminus \{y\}$  such that  $\rho(v_2, z_2) = 1$ . In view of Lemma 2.19, we can choose  $v_1$  such that  $\check{v}_1 > 0$  on  $\Gamma \setminus \{y\}$ , and  $v_2$  such that  $\check{v}_2 > 0$  on the arc from  $y$  to  $z_2$  moving counter-clockwise on  $\Gamma$ .

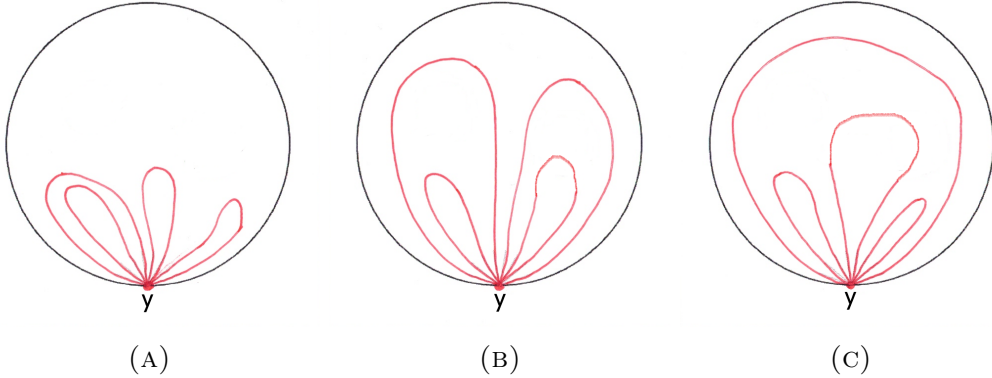


FIGURE 4.2. Some possible nodal patterns for  $0 \neq u \in U_y^1$

4.2.3.2. *Structure and combinatorial type of nodal sets in  $U_y^1$  and  $U_y^2$ .*

◇ Relations (4.15) and an analysis as in Subsection 4.2.2, show that the nodal set of any  $0 \neq u \in U_y^1$  consists of  $(\ell - 1)$  nodal loops at the point  $y$ , and that these loops do not intersect away from  $y$ . The set  $\mathcal{Z}(u)$  is an  $(\ell - 1)$ -bouquet of loops  $\mathcal{B}_{y,(\ell-1)}$  at  $y$ . Adapting the description given in Paragraph 4.2.2.2, for  $0 \neq u \in U_y^1$ , we define the *combinatorial type*  $\tau_y$  of the nodal set  $\mathcal{Z}(u)$  with respect to  $y$  for  $u \in U_y^1$ . This is a map from  $L_{(2\ell-2)}$  to itself.

Some possible nodal patterns for  $u \in U_y^1$  are displayed in Figure 4.2, where  $\ell = 5$ , and  $\rho(y) = 8$ . The corresponding combinatorial types, labeled according to the

figures, are

$$\begin{aligned}\tau_A^{4.2} &= \begin{pmatrix} 1 & 2 & 3 & 4 & 5 & 6 & 7 & 8 \\ 2 & 1 & 4 & 3 & 8 & 7 & 6 & 5 \end{pmatrix}, \\ \tau_B^{4.2} &= \begin{pmatrix} 1 & 2 & 3 & 4 & 5 & 6 & 7 & 8 \\ 4 & 3 & 2 & 1 & 8 & 7 & 6 & 5 \end{pmatrix}, \\ \tau_C^{4.2} &= \begin{pmatrix} 1 & 2 & 3 & 4 & 5 & 6 & 7 & 8 \\ 8 & 3 & 2 & 5 & 4 & 7 & 6 & 1 \end{pmatrix}.\end{aligned}$$

◊ If  $u \in U_y^2$  and  $u \notin U_y^1$ , there exists a unique  $z_u \in \Gamma$ , such that  $z_u \neq y$  and  $\mathcal{S}_b(u) \cap \Gamma = \{y, z_u\}$ , with  $\rho(u, y) = (2\ell - 3)$ ,  $\rho(u, z_u) = 1$ . Furthermore,  $V_{y, z_u} = [u]$ . The nodal set  $\mathcal{Z}(u)$  and its *combinatorial type*  $\tau_{y, z_u}$  are described in Paragraph 4.2.2.2. Then,  $\mathcal{Z}(u)$  is the wedge sum  $\mathcal{B}_{y, (\ell-2)}^{z_u}$  of a simple arc from  $y$  to  $z_u$  with an  $(\ell - 2)$ -bouquet of loops at  $y$ , see Figure 4.1.

#### 4.2.4. Application of the previous analysis.

Fix some  $y \in \Gamma$ . We now apply the analysis of Subsections 4.2.2 and 4.2.3 to investigate the limits of  $v_{y, z} \in U_y^2 \setminus U_y^1$ , when  $z$  tends to  $y$  on  $\Gamma$ , *clockwise* or *counterclockwise*. The notation are the same as in Subsection 4.2.2.

We choose a basis  $\{v_1, v_2\}$  of  $U_y^2$  as described in Remark 4.12. In particular,  $\rho(v_1, y) = (2\ell - 2)$ ,  $v_1 \perp v_2$  in  $L^2(\Omega)$ ,  $\rho(v_2, y) = (2\ell - 3)$ , there exists  $z_2 \in \Gamma \setminus \{y\}$  such that  $\rho(v_2, z_2) = 1$ , and  $\mathcal{S}_b(v_2) = \{y, z_2\}$ . Recall the definition of the functions  $\check{v}_i$  on  $\Gamma$ ,

$$(4.17) \quad \check{v}_i := \begin{cases} \partial_\nu v_i & \text{in the Dirichlet case,} \\ v_i|_\Gamma & \text{in the Robin case.} \end{cases}$$

According to Lemma 2.19, the function  $\check{v}_1$  vanishes only at  $y$  and does not change sign on  $\Gamma$ . The function  $\check{v}_2$  does not vanish on  $\Gamma \setminus \{y, z_2\}$ , and changes sign when crossing  $z_2$  and  $y$  along  $\Gamma$ .

Let  $\gamma : [0, 2\pi] \rightarrow \Gamma$  be a parametrization such that  $\gamma(0) = \gamma(2\pi) = y$ . Given any  $z \in \Gamma \setminus \{y\}$ , there exists a function  $v_{y, z}$  which satisfies (4.15), and this function is uniquely defined up to scaling. In the Dirichlet case, this function is characterized by the fact that  $\check{v}_{y, z} = \partial_\nu v_{y, z}|_\Gamma$  only vanishes at  $y$  and  $z$ . In the Robin case, it is characterized by the fact that  $\check{v}_{y, z} = v_{y, z}|_\Gamma$  only vanishes at  $y$  and  $z$ . Up to scaling, we may choose

$$(4.18) \quad v_{y, z} = a(z) v_1 + b(z) v_2,$$

with

$$(4.19) \quad \begin{cases} a(z) = -\check{v}_2(z) \left( \check{v}_1^2(z) + \check{v}_2^2(z) \right)^{-\frac{1}{2}}, \\ b(z) = \check{v}_1(z) \left( \check{v}_1^2(z) + \check{v}_2^2(z) \right)^{-\frac{1}{2}}, \end{cases}$$

where  $\check{v}_1, \check{v}_2$  are defined in (4.17).

Then, there exists a unique  $\theta(z) \in (0, \pi)$  such that  $\cos(\theta(z)) = a(z)$  and  $\sin(\theta(z)) = b(z)$  (this is because  $\check{v}_1$  is positive on  $\Gamma \setminus \{y\}$ ). Defining the family of functions

$$(4.20) \quad w_\theta = \cos \theta v_1 + \sin \theta v_2,$$

we have  $v_{y, z} = w_{\theta(z)}$ . Conversely, according to the proof of Lemma 4.11, any function  $w_\theta$  has exactly two singular points on  $\Gamma$ , the point  $y$  and some other point  $z_\theta \neq y$ .



Note that the point  $z$  determines the eigenfunction  $v_{y,z}$  uniquely (up to scaling) and vice versa. It follows that we have a continuous, bijective map  $(0, 2\pi) \ni t \mapsto \theta(\gamma(t)) \in (0, \pi)$ . This map is strictly monotone, and provides a diffeomorphism from  $(0, 2\pi)$  to  $(0, \pi)$ , with limits 0 and  $\pi$  respectively. Otherwise stated, the function  $v_{y,\gamma(t)}$  defined in (4.18) tends to  $v_1$  when  $t$  tends to 0 and to  $-v_1$  when  $t$  tends to  $2\pi$ . There exists  $t_2$  such that  $\gamma(t_2) = z_2$ , and hence  $\theta(z_2) = \frac{\pi}{2}$ . We have proved the following property.

**PROPERTY 4.13.** *The function  $v_{y,z}$  defined in (4.18) tends to  $v_1$  when  $z \neq y$  tends to  $y$  counter-clockwise, and to  $-v_1$  when  $z \neq y$  tends to  $y$  clockwise.*

**4.2.5.  $\Omega$  simply connected, proof that  $\text{mult}(\lambda_k) \leq (2k - 2)$  for all  $k \geq 3$ .** In this subsection, we work with the family of functions  $\{w_\theta \mid \theta \in [0, \pi]\}$  introduced in (4.20).

4.2.5.1. *Preparation.* In view of Proposition 4.3, and reasoning by contradiction, we assume that  $\dim U(\lambda_k) = (2k - 1)$ . By Courant's theorem, we have

$$\sup \{\kappa(u) \mid 0 \neq u \in U\} \leq k.$$

We can apply Lemma 4.11 with  $\ell = k$  and  $U := U(\lambda_k)$ .

In the arguments below we keep the notation of Lemma 4.11 and its proof (with  $\ell = k$ ). We fix a basis  $\{v_1, v_2\}$  of  $U_y^2$  as described at the beginning of Subsection 4.2.4, and the direct frame  $\{\vec{e}_1, \vec{e}_2\}$  such that  $\vec{e}_1$  is tangent to  $\Gamma$  at  $y$ , and  $\vec{e}_2$  is normal to  $\Gamma$ , pointing inwards.

4.2.5.2. *Structure and combinatorial types for  $v_1$  and  $v_2$ .* Making a conformal change of coordinates as in Section 2.4, we may assume that  $\Gamma$  is a line segment in some neighborhood of  $y$ . Taking  $r_1$  small enough, in the half-disk  $D_+(y, r_1)$ , the nodal set  $\mathcal{Z}(v_1)$  consists of  $(2k - 2)$  nodal semi-arcs  $\delta_{1,j}$  emanating from  $y$  tangentially to rays  $\omega_{1,j}$ ,  $j \in L_{(2k-2)}$ ; the nodal set  $\mathcal{Z}(v_2)$  consists of  $(2k - 3)$  nodal semi-arcs  $\delta_{2,j}$  emanating from  $y$  tangentially to rays  $\omega_{2,j}$ ,  $j \in L_{(2k-3)}$ .

The combinatorial type of the function  $v_1 \in U_y^1$  with respect to  $y$  is defined in Subsection 4.2.3. This is a map

$$(4.21) \quad \begin{aligned} \tau_y : L_{(2k-2)} &\rightarrow L_{(2k-2)} \text{ such that} \\ \tau_y(j) &\neq j \text{ and } (\tau_y)^2(j) = j, \text{ for all } j \in L_{(2k-2)}. \end{aligned}$$

The nodal set  $\mathcal{Z}(v_1)$  is a  $(k - 1)$ -bouquet of loops at  $y$  described by the map  $\tau_y$ .

The combinatorial type  $\tau_{y,z_2}$  of the function  $v_2 \in U_y^{1,\perp}$ , with respect to  $y$  and  $z_2$ , is defined in Subsection 4.2.3. Recall that it is described as a map

$$(4.22) \quad \begin{cases} \tau_{y,z_2} : \{\downarrow\} \cup L_{(2k-3)} \rightarrow \{\downarrow\} \cup L_{(2k-3)} \text{ such that} \\ \tau_{y,z_2}(\downarrow) =: a \in L_{(2k-3)} \text{ and } \tau_{y,z_2}(a) = \downarrow, \\ \tau_{y,z_2}(j) \neq j \text{ and } (\tau_{y,z_2})^2(j) = j, \text{ for all } j \in L_{(2k-3)} \setminus \{a\}. \end{cases}$$

Here,  $\tau_{y,z_2}(\downarrow)$  is the element  $a \in L_{(2k-3)}$  such that the semi-arc  $\delta_a$  of  $\mathcal{Z}(v_2)$  which emanates from  $y$  tangentially to  $\omega_{2,a}$  eventually hits  $\Gamma$  at the point  $z_2$ . For  $a \neq j \in L_{(2k-3)}$ , the pairs  $(j, \tau_{y,z_2}^{v_2}(j))$  describe the loops of  $\mathcal{Z}(v_2)$  at the point  $y$ , so that  $\mathcal{Z}(v_2)$  is the wedge sum of the nodal interval  $\delta_a$ , where  $a := \tau_{y,z_2}(\downarrow)$ , with a  $(k - 2)$ -bouquet of loops at  $y$ , described by the map  $\tau_{y,z_2}$ .

Since  $\Omega$  is simply connected, the arc  $\delta_a$  separates  $\Omega$  into two components  $\Omega_{a,R}$  (on the right side of  $\delta_a$ ), and  $\Omega_{a,L}$  (on the left side of  $\delta_a$ ). There are three cases to consider,  $a = 1$ ,  $1 < a < (2k - 3)$ , and  $a = (2k - 3)$ . The following properties follow easily from looking at the local structure of  $\mathcal{Z}(v_2)$  at  $y$ .

PROPERTIES 4.14.

- (i) If  $a = 1$ , the component  $\Omega_{a,R}$  does not contain any nodal arc, and the rays  $\omega_{2,j}$ ,  $2 \leq j \leq (2k - 3)$  point inside  $\Omega_{a,L}$ .
- (ii) If  $1 < a < (2k - 3)$ , the rays  $\omega_{2,j}$ ,  $1 \leq j \leq (a - 1)$  point inside  $\Omega_{a,R}$ ; the rays  $\omega_{2,j}$ ,  $(a + 1) \leq j \leq (2k - 3)$  point inside  $\Omega_{a,L}$ .
- (iii) If  $a = (2k - 3)$ , the rays  $\omega_{2,j}$ ,  $1 \leq j \leq (2k - 4)$  point inside  $\Omega_{a,R}$ ; the component  $\Omega_{a,L}$  does not contain any nodal arc.

If the ray  $\omega_{2,j}$  points inside  $\Omega_{a,R}$ , the whole nodal interval  $\delta_j$  of  $\mathcal{Z}(v_2)$  is contained in  $\Omega_{a,R}$ , and so does the corresponding loop  $\gamma_{j,\tau_{y,z_2}(j)}$ . There is an analogous statement for  $\Omega_{a,L}$ .

This means that

$$(4.23) \quad \begin{cases} a = \tau_{y,z_2}(\downarrow) \in L_{(2k-3)} \text{ is odd,} \\ \tau_{y,z_2}(\{1, \dots, (a-1)\}) \subset \{1, \dots, (a-1)\}, \\ \tau_{y,z_2}(\{(a+1), \dots, (2k-3)\}) \subset \{(a+1), \dots, (2k-3)\}. \end{cases}$$

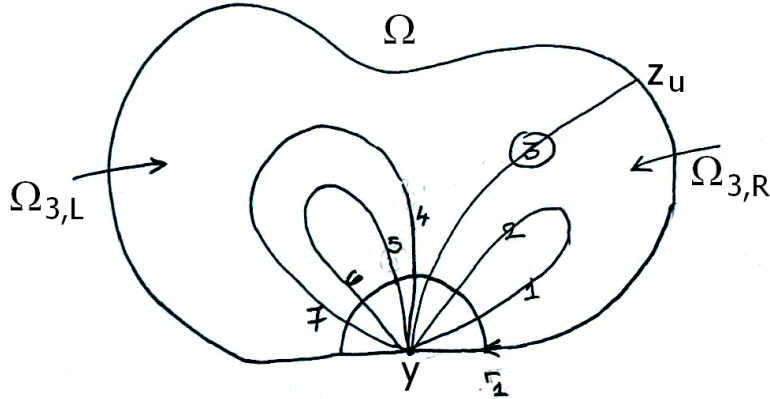


FIGURE 4.3.  $k = 5$ ,  $a = 3$

More precisely, define

$$(4.24) \quad \begin{cases} R := \{1, \dots, (a-1)\}, \text{ with } R = \emptyset \text{ if } a = 1, \\ L := \{(a+1), \dots, (2k-3)\}, \text{ with } L = \emptyset \text{ if } a = (2k-3), \\ n_R := \frac{a-1}{2}. \end{cases}$$

Then, the set  $R$  corresponds to  $n_R$  loops in the component  $\Omega_{a,R}$  of  $\Omega \setminus \delta_a$ , and these loops divide  $\Omega_{a,R}$  into  $(n_R + 1)$  nodal domains of  $v_2$ . The set  $L$  corresponds to  $n_L := (k - 2 - n_R)$  loops in the component  $\Omega_{a,L}$  of  $\Omega \setminus \delta_a$ , and these loops divide  $\Omega_{a,L}$  into  $n_L + 1 = (k - 1 - n_R)$  nodal domains of  $v_2$ , so that we recover the fact that  $v_2$  has  $k$  nodal domains.

Otherwise stated the nodal set  $\mathcal{Z}(v_2)$  consists of the wedge sum of the nodal interval  $\delta_a$  with two bouquets of loops, one  $\mathcal{B}_R$  contained in  $\Omega_{a,R}$ , corresponding to  $\tau_{y,z_2}|_R$ ,

another  $\mathcal{B}_L$  contained in  $\Omega_{a,L}$ , corresponding to  $\tau_{y,z_2}|_L$ . One of these bouquets may be empty (when  $a = 1$  or  $a = (2k - 3)$ ).

For  $\theta \in (0, \pi)$ , let  $w_\theta := \cos \theta v_1 + \sin \theta v_2$ . Then  $\mathcal{S}_b(w_\theta) = \{y, z_\theta\}$ . The nodal set  $\mathcal{Z}(w_\theta)$  has a structure similar to the structure of  $\mathcal{Z}(v_2)$ :

- ◇ one nodal interval  $\delta_{a_\theta, \theta}$  emanating from  $y$  tangentially to some ray  $\omega_{2, a_\theta}$ , and hitting the boundary  $\Gamma$  at the point  $z_\theta \neq y$ ;  $a_\theta$  is odd, and  $a_\theta = \tau_{y, z_\theta}(\downarrow)$ ;
- ◇ loops at  $y$ , on either side of  $\delta_{a_\theta, \theta}$ , described by the restriction of the combinatorial type  $\tau_{y, z_\theta}$  to  $L_{(2k-3)} \setminus \{a_\theta\}$ .

Note: In the above description, the nodal interval is denoted by  $\delta_{a_\theta, \theta}$  because it does not only depend on  $a_\theta$ . This point will be needed later on.

LEMMA 4.15. *Recall the notation  $a = \tau_{y, z_2}(\downarrow)$  and  $a_\theta = \tau_{y, z_\theta}(\downarrow)$ . For all  $\theta \in (0, \pi)$ , we have  $a_\theta = a$ , and  $\tau_{y, z_\theta} = \tau_{y, z_2}$ , i.e., the combinatorial type of the nodal set  $\mathcal{Z}(w_\theta)$  is the same as the combinatorial type of  $\mathcal{Z}(v_2)$ .*

*Proof of Lemma 4.15.* We consider local conformal coordinates as in Section 2.4. The proof of the local structure theorem shows that one can choose the radius  $r_0$  uniformly with respect to  $\theta$ . We use polar coordinates  $(r, \omega)$  associated with  $(\xi_1, \xi_2)$  in  $\mathbb{R}^2$ , and we write  $E(r, \omega)$  for  $E(r \cos \omega, r \sin \omega)$ .

By connectivity, to prove that  $a_\theta$  is constant it suffices to prove that it is locally constant:

*For all  $\theta \in (0, \pi)$  there exists  $\varepsilon_\theta > 0$  such that  $a_{\theta'} = a_\theta$  for  $|\theta' - \theta| < \varepsilon_\theta$ .*

Assume, by contradiction, that this is not the case. Then, there exists  $\theta_0 \in (0, \pi)$  and a sequence  $\theta_n$  with  $|\theta_n - \theta_0| < \frac{1}{n}$  and  $a_{\theta_n} \neq a_{\theta_0} =: a_0$ . Since  $a_\theta$  can only take finitely many values in  $L_{(2k-3)}$ , passing to a subsequence if necessary, we can assume that  $a_{\theta_n} \equiv a_1 \neq a_0$ . By the local structure theorem, there exists a uniform  $r_0 > 0$  (depending on  $\theta_0$ ) such that the nodal arc  $\delta_{a_1, \theta_n}$  intersects the set  $C_+(y, r_0)$  at the point  $z_n := E(r_0, \tilde{\omega}_{a_1}(r_0, \theta_n))$ , where the function  $\tilde{\omega}_{a_1}(r, \theta)$  is smooth in a neighborhood of  $(r_0, \theta_0)$  (with the notation of Section 2.4). The arcs  $\delta_{a_1, \theta_n} \cap \Omega \setminus \mathcal{B}(y, r_0)$  are compact and connected, and we can find a subsequence which converges in the Hausdorff distance to some compact connected set  $\bar{\delta}$  which contains the point  $z_0 = E(r_0, \tilde{\omega}_{a_1}(r_0, \theta_0))$  and the point  $z_{\theta_0} = \lim z_{\theta_n}$  at the boundary. The set  $\bar{\delta}$  is also contained in  $\mathcal{Z}(w_{\theta_0})$  because  $w_{\theta_n}$  tends to  $w_{\theta_0}$  uniformly. Since  $a_1 \neq a_0$ , we have a contradiction.

Since  $a_\theta \equiv a$  in  $(0, \pi)$ , in order to prove that  $\tau_\theta := \tau_{y, z_\theta}$  does not depend on  $\theta$ , it suffices to show that its restrictions to the sets  $R$  and  $L$  are locally constant in  $\theta$ . We give the proof for  $R$  in the case  $a > 1$ . The other cases are similar. Reasoning by contradiction, we assume that there exists  $\theta_0 \in (0, \pi)$  and a sequence  $\theta_n$  such that  $|\theta_n - \theta_0| < \frac{1}{n}$ , and  $j_n \in R$ , such that  $\tau_{\theta_n}(j_n) \neq \tau_{\theta_0}(j_n)$ . Since  $R$  is finite, passing to subsequences if necessary, we may assume that  $j_n \equiv b$  and  $\tau_{\theta_n}(b) \equiv c$  for some  $b, c \in R$  with  $c \neq \tau_{\theta_0}(b)$ . Since  $\theta_n$  is close to  $\theta_0 \in (0, \pi)$  we have a uniform structure theorem, and we can reason as in the proof of Property 3.6 to conclude.  $\square$

Given the basis  $\{v_1, v_2\}$ , we have the associated odd integer  $a := \tau_2(\downarrow) \in L_{(2k-3)}$ , where  $\tau_2 := \tau_{y, z_2}$  is the combinatorial type of  $v_2$ . For all  $\theta \in (0, \pi)$ , the nodal set  $\mathcal{Z}(w_\theta)$  has the same combinatorial type  $\tau_2$ . In particular, it contains a single simple nodal interval  $\delta_{a, \theta}$ , emanating from  $y$  tangentially to the ray  $\omega_{2, a}$ , and hitting the boundary  $\Gamma$  at the point  $z_\theta$ .

Call  $\Omega_{\theta,R}$  the component of  $\Omega \setminus \delta_{a,\theta}$  with semi-tangent at  $y$  the vector  $\vec{e}_1$ , and  $\Omega_{\theta,L}$  the other component, with semi-tangent at  $y$  the vector  $-\vec{e}_1$ . The component  $\Omega_{\theta,R}$  contains the  $n_R$  loops corresponding to the set  $R$ . These loops bound  $(n_R + 1)$  nodal domains of  $w_\theta$  which can be labeled from 1 to  $(n_R + 1)$ . The component  $\Omega_{\theta,L}$  contains the  $n_L = (k - n_R - 2)$  loops corresponding to the set  $L$ . These loops bound  $(k - n_R - 1)$  nodal domains of  $w_\theta$  which can be labeled from  $(n_R + 2)$  to  $k$ .

4.2.5.3. *The rotating function argument.* Look at the simple examples, displayed in Figures 4.4 and 4.5.

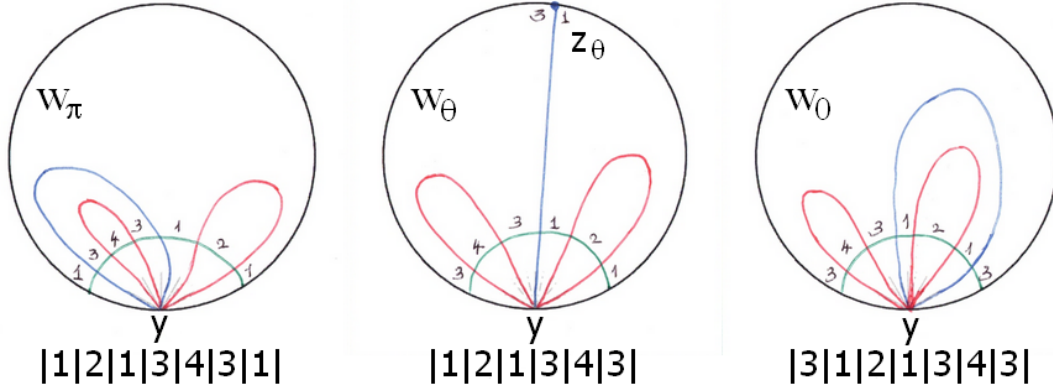


FIGURE 4.4. Example with  $k = 4, a = 3$

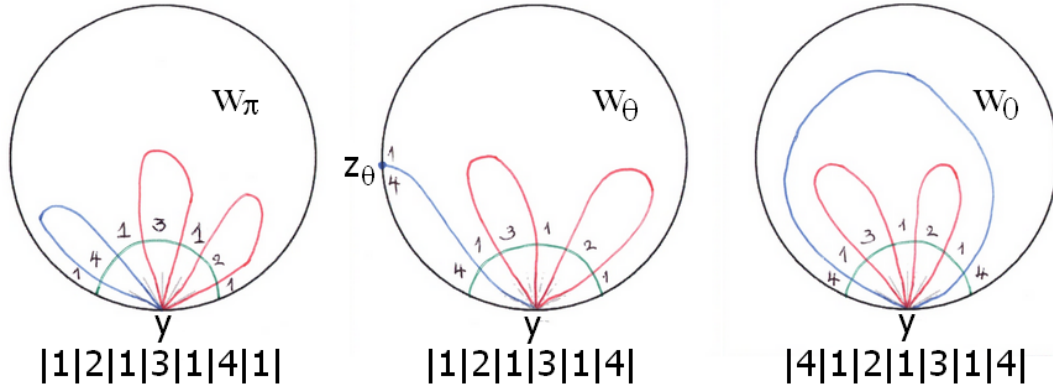


FIGURE 4.5. Example with  $k = 4, a = 5$

When  $\theta$  tends to zero,  $z_\theta$  tends to  $y$  clockwise and the nodal interval  $\delta_{a,\theta}$ , from  $y$  to  $z_\theta$ , tends to a loop in the nodal set of  $w_0 = \lim_{\theta \rightarrow 0} w_\theta$ , whose nodal pattern is displayed in the right sub-figure. When  $\theta$  tends to  $\pi$ ,  $z_\theta$  tends to  $y$  counter-clockwise and the nodal interval  $\delta_{a,\theta}$  tends to a loop in the nodal set of  $w_\pi = \lim_{\theta \rightarrow \pi} w_\theta$ , whose nodal pattern is displayed in the left sub-figure.

The combinatorial types of the functions  $w_0$  and  $w_\pi$  are as follows.

$$\left\{ \begin{array}{l} \text{Nodal patterns in Figure 4.4:} \\ \tau_\pi = \begin{pmatrix} 1 & 2 & 3 & 4 & 5 & 6 \\ 2 & 1 & 6 & 5 & 4 & 3 \end{pmatrix} \quad \tau_\theta = \begin{pmatrix} \downarrow & 1 & 2 & 3 & 4 & 5 \\ 3 & 2 & 1 & \downarrow & 5 & 4 \end{pmatrix} \quad \tau_0 = \begin{pmatrix} 0 & 1 & 2 & 3 & 4 & 5 \\ 3 & 2 & 1 & 0 & 5 & 4 \end{pmatrix} \end{array} \right.$$

$$\left\{ \begin{array}{l} \text{Nodal patterns in Figure 4.5:} \\ \tau_\pi = \begin{pmatrix} 1 & 2 & 3 & 4 & 5 & 6 \\ 2 & 1 & 4 & 3 & 6 & 5 \end{pmatrix} \quad \tau_\theta = \begin{pmatrix} \downarrow & 1 & 2 & 3 & 4 & 5 \\ 5 & 2 & 1 & 4 & 3 & \downarrow \end{pmatrix} \quad \tau_0 = \begin{pmatrix} 0 & 1 & 2 & 3 & 4 & 5 \\ 5 & 2 & 1 & 4 & 3 & 0 \end{pmatrix} \end{array} \right.$$

The above assertions are a consequence of the local structure theorem applied to  $w_0$  or to  $w_\pi$  in a disk  $D_+(y, r)$  with  $r$  small enough. A loop in  $\mathcal{Z}(w_\theta)$  always intersects  $C_+(y, r)$  at two distinct points. For  $\theta$  away from 0 and  $\pi$ , the nodal interval from  $y$  to  $z_\theta$  only intersects  $C_+(y, r)$  at the point  $A_a$ . When  $\theta$  tends to 0, the point  $z_\theta$  enters the disc  $D_+(y, r)$  and the nodal interval from  $y$  to  $z_\theta$  intersects  $C_+(y, r)$  at two points  $A_a$  and  $A_0$ , which lies below the first red arc, see Figure 4.6. This is why  $\tau_0$  is defined on the set  $\{0, \dots, 5\}$ . In the figure, the points  $A_j$  are the intersection points of the nodal set  $\mathcal{Z}(w_\theta)$  with  $C_+(y, r)$ , for  $r$  small enough. Similarly, when  $\theta$  tends to  $\pi$ , the nodal arc from  $y$  to  $z_\theta$  intersects  $C_+(y, r)$  at two points, one of them below the last red arc. This is why  $\tau_\pi$  is defined on the set  $\{1, \dots, 6\}$ . For these arguments, we also refer to Section 5.2, proof of Lemma 5.16.

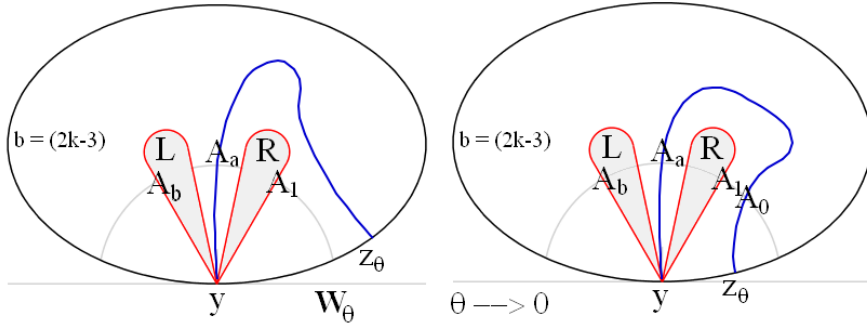


FIGURE 4.6. The behavior of  $w_\theta$  for  $\theta$  close to 0

We label the nodal domains of  $w_\theta$  in the central sub-figures according to the order in which they appear when one moves on  $C_+(y, r)$  counter-clockwise. This order is independent of  $\theta$  because the combinatorial type of  $w_\theta$  is independent of  $\theta$ , see Lemma 4.15. We then follow the deformation of the nodal sets of  $w_\theta$ , when  $\theta$  tends to 0, resp. to  $\pi$ . The order in which the nodal domains appear is encoded in the words  $\mathcal{W}_\theta$  which appear below the images (labels are separated by vertical bars). In Figure 4.4,  $\mathcal{W}_\theta = |1|2|1|3|4|3|$ ,  $\mathcal{W}_\pi = |1|2|1|3|4|3|1|$ ,  $\mathcal{W}_0 = |3|1|2|1|3|4|3|$ . In Figure 4.5,  $\mathcal{W}_\theta = |1|2|1|3|1|4|$ ,  $\mathcal{W}_\pi = |1|2|1|3|1|4|1|$ ,  $\mathcal{W}_0 = |4|1|2|1|3|1|4|$ .

The general procedure for labeling the nodal domains and producing the words is described in Section 5.5.

To see that the nodal patterns are different, and hence that the functions  $w_0$  and  $w_1$  are linearly independent, we look at the invariant  $\sigma(\mathcal{W})$  defined in (5.44):  $\sigma(\mathcal{W})$  is the position at which the first letter of the word  $\mathcal{W}$  reappears. For the nodal patterns in Figure 4.4, we have  $\sigma(\mathcal{W}_0) = 5$  and  $\sigma(\mathcal{W}_\pi) = 3$ . For the nodal patterns in Figure 4.5, we have  $\sigma(\mathcal{W}_0) = 7$  and  $\sigma(\mathcal{W}_\pi) = 3$ .

At least for the above examples, the invariants being different, the functions  $w_0$  and  $w_\pi$  cannot be equal up to scaling, contradicting the fact that  $w_0 = -w_\pi = v_1$ .

The proof in the general case is given in Section 5.5, Section 5.5.7.  $\square$

This completes the proof that the equality  $\dim U(\lambda_k) = (2k - 1)$  for some  $k \geq 3$  leads to a contradiction. Hence we have proved Theorem 4.1 under the additional assumption that  $\Omega$  is *simply connected*.

**PROPOSITION 4.16.** *Let  $\Omega \subset \mathbb{R}^2$  be a simply connected bounded domain with smooth boundary. Let  $\{\lambda_k, k \geq 1\}$  be the eigenvalues of the operator  $-\Delta + V$  in  $\Omega$ , with Dirichlet or Robin boundary condition (where  $V$  is a real valued  $C^\infty$  function). Then,*

$$\text{mult}(\lambda_k) \leq (2k - 2) \text{ for all } k \geq 3.$$

**REMARK 4.17.** The general idea to get rid of the assumption that  $\Omega$  is simply connected is as follows. We decompose the boundary  $\Gamma := \partial\Omega$  into its components,  $\Gamma = \bigcup_{j=1}^q \Gamma_j$ . Then we repeat the arguments in Subsections 4.2.2 and 4.2.3 with the prescribed singular points  $y$  and  $z$  chosen to belong to  $\Gamma_1$ . The main difference with the simply connected case is that an eigenfunction  $u$  with prescribed singular points  $y$  and  $z$  on  $\Gamma_1$  may also have singular points on some other components of  $\Gamma$ . More precisely, using the notation (4.2), the following properties hold:  $\mathcal{Z}(u) \cup \Gamma(u)$  is connected and, for any  $j \in J(u) \setminus \{1\}$ ,  $\sum_{z \in \mathcal{S}_b(u) \cap \Gamma_j} \rho(u, z) = 2$ . It then suffices to work with the projection  $\check{\mathcal{Z}}(u)$  of the nodal set  $\mathcal{Z}(u)$  to the set  $\check{\Omega}$  obtained from  $\Omega$  by identifying each component  $\Gamma_j, j \geq 2$ , to a point, so that the boundary of  $\check{\Omega}$  is  $\Gamma_1$ . The complete proof is given in Section 4.3.

### 4.3. General Case: the Estimate $\text{mult}(\lambda_k) \leq (2k - 2)$ for $k \geq 3$

**4.3.1. An abstract setting.** When the domain  $\Omega \subset \mathbb{R}^2$  is not simply connected, its boundary  $\Gamma := \partial\Omega$  has  $(q + 1)$  components, with  $q \geq 1$ . One of them  $\Gamma_1$ , the ‘‘outer boundary’’, bounds the unbounded component of  $\mathbb{R}^2 \setminus \Gamma$ . The other components,  $\Gamma_j, j \neq 1$ , are contained in the bounded component of  $\mathbb{R}^2 \setminus \Gamma_1$ . We consider the following equivalence relation in  $\bar{\Omega}$ :

$$(4.25) \quad x \sim y \text{ if and only if } x, y \in \Gamma_j \text{ for some } j \in \{2, \dots, (q + 1)\}.$$

**NOTATION 4.18.** Let  $\check{\Omega}$  denote the quotient space  $\bar{\Omega}/\sim$ , where each  $\Gamma_j, j \neq 1$ , is identified to one point  $\xi_j$  in  $\check{\Omega}$  (see [Bona2009]). Define

$$\Xi := \{\xi_2, \dots, \xi_{q+1}\}.$$

Generally speaking,  $\check{A}$  will denote the image of the subset  $A$  of  $\bar{\Omega}$  under the projection map from  $\bar{\Omega}$  to  $\check{\Omega}$ .

We also introduce  $\mathbb{S}_\Omega$ , the quotient space in which each  $\Gamma_j, j \geq 1$ , is identified to a point.

#### 4.3.1.1. $\Omega$ with one hole. Properties of $V_{y,z}$ .

**LEMMA 4.19.** *Assume that  $\Omega$  has one hole, and  $\Gamma = \Gamma_1 \cup \Gamma_2$ , where  $\Gamma_1$  is the outer boundary. Let  $U$  be a linear subspace of an eigenspace of (2.3) in  $\Omega$ , such that  $\sup\{\kappa(u) \mid 0 \neq u \in U\} \leq \ell$  for some  $\ell \geq 2$ , and  $\dim U = (2\ell - 1)$ . Let  $y \neq z \in \Gamma_1$ , and define*

$$V_{y,z} := \{u \in U \mid \rho(u, y) \geq (2\ell - 3) \text{ and } \rho(u, z) \geq 1\}.$$

Then,

- (i)  $\dim V_{y,z} = 1$ .
- (ii) For  $u \neq y, z$ , the following alternative holds,
- ◊ either  $b_0(\mathcal{Z}(u) \cup \Gamma) = 1$ , in which case  $\mathcal{Z}(u)$  hits  $\Gamma_2$ ,  $u$  has precisely two singular points on  $\Gamma_2$  (counting multiplicities),  $\sum_{x \in \mathcal{S}_b(u) \cap \Gamma_2} \rho(u, x) = 2$ ,  $\mathcal{S}_b(u) \cap \Gamma_1 = \{y, z\}$  and  $\mathcal{S}_i(u) = \emptyset$ ;
  - ◊ or  $b_0(\mathcal{Z}(u) \cup \Gamma) = 2$ , in which case  $\mathcal{Z}(u) \cap \Gamma_2 = \emptyset$ ,  $\mathcal{S}_b(u) \cap \Gamma_1 = \{y, z\}$ , and  $\mathcal{S}_i(u) = \emptyset$ ;
- (iii)  $\rho(u, y) = (2\ell - 3)$  and  $\rho(u, z) = 1$ .
- (iv)  $\kappa(u) = \ell$ .

A generator of  $V_{y,z}$  will be denoted by  $v_{y,z}$  (defined up to scaling).

*Proof.* The fact that  $\dim V_{y,z} \geq 1$  follows from Lemma 2.16. Since we now have  $b_0(\Gamma) = 2$ , Euler's formula (4.9) applied to  $u$  gives

$$(4.26) \quad \begin{aligned} 0 \geq \kappa(u) - \ell &= (b_0(\mathcal{Z}(u) \cup \Gamma) - 2) + \frac{1}{2} \sum_{x \in \mathcal{S}_i(u)} (\nu(x) - 2) \\ &\quad + \frac{1}{2} \sum_{x \in \mathcal{S}_b(u) \cap \Gamma_2} \rho(x) \\ &\quad + \frac{1}{2} \sum_{\substack{x \in \mathcal{S}_b(u) \cap \Gamma_1, \\ x \neq y, z}} \rho(x) + \frac{1}{2} (\rho(y) + \rho(z) - 2\ell + 2). \end{aligned}$$

Except for the term  $(b_0(\mathcal{Z}(u) \cup \Gamma) - 2)$ , all the terms in the right-hand side of the equality are nonnegative. This implies that

$$2 \geq b_0(\mathcal{Z}(u) \cup \Gamma) \geq 1,$$

and we have to examine two cases.

◊ If  $b_0(\mathcal{Z}(u) \cup \Gamma) = 1$ , then the nodal set  $\mathcal{Z}(u)$  must hit  $\Gamma_2$ . According to Proposition 2.29, the sum  $\sum_{x \in \mathcal{S}_b(u) \cap \Gamma_2} \rho(x)$  is an even integer, and we deduce from (4.26) that  $\sum_{x \in \mathcal{S}_b(u) \cap \Gamma_2} \rho(x) = 2$ . This equality now implies that the other terms are zero, and hence that  $\kappa(u) = \ell$ .

◊ If  $b_0(\mathcal{Z}(u) \cup \Gamma) = 2$ , then all the terms in the right-hand side of (4.26) vanish, and  $\kappa(u) = \ell$ .

This proves Assertions (ii)–(iv). As in the proof of Lemma 4.7, assuming that there are at least two linearly independent functions  $u_1$  and  $u_2$  in  $V_{y,z}$ , the first assertion follows from Assertion (iii) and Lemma 2.17.  $\square$

4.3.1.2.  $\Omega$  with one hole. *Structure and combinatorial type of nodal sets in  $V_{y,z}$ .* From a geometric point of view, once we have fixed  $y \neq z \in \Gamma_1$  and under the assumptions of Lemma 4.19, either  $\mathcal{Z}(u) \cap \Gamma_2 = \emptyset$  or  $\mathcal{Z}(u) \cap \Gamma_2 = \{y_1, y_2\}$ , possibly with  $y_1 = y_2$ . In the first case, we simply reproduce the description given in Paragraph 4.2.2.2. In the second case, the connectivity of  $\mathcal{Z}(u) \cup \Gamma$  implies that one of the nodal arcs hitting  $\Gamma_2$  also contains  $y$ . The other one contains either  $y$  or  $z$ . More precisely, we choose any  $j \in L_{(2\ell-3)}$  and follow the nodal semi-arc  $\delta_j$  emanating from  $y$  along  $\mathcal{Z}(u)$ , until we meet a singular point  $x$  as described in Paragraph 4.2.2.2. Since  $x \in \mathcal{S}(u) = \{y, z, y_1, y_2\}$ , there are two possibilities. If  $x \in \{y, z\}$  the description is similar to the one in Paragraph 4.2.2.2. If  $x \in \{y_1, y_2\}$ , say  $y_1$ , we continue our path from  $y_1$  to  $y_2$  along  $\Gamma_2$ , and leave  $\Gamma_2$  along the second nodal arc hitting  $\Gamma_2$  at  $y_2$  until we meet a singular point. We then either reach the point  $y$  again or the point  $z$ . It then follows that the nodal set of  $u \in V_{y,z}$  consists of  $(\ell - 2)$  “generalized” nodal loops at  $y$  (one of the loops may comprise some part of  $\Gamma_2$ ), and a “generalized” simple arc from  $y$  to  $z$  (this arc may comprise a sub-arc from  $y_1$  to  $y_2$  on  $\Gamma_2$ ). In the preceding description, the points  $y_1$  and  $y_2$  may coincide.

These “generalized” loops and arc do not intersect away from  $y$ . Then,  $\mathcal{Z}(u)$  is the wedge sum  $\mathcal{B}_{y,(\ell-2)}^z$  of an  $(\ell - 2)$ -bouquet of “generalized” loops at  $y$ , with a simple “generalized” arc from  $y$  to  $z$ . We can then define the *combinatorial type*  $\tau_{y,z}^u$  of  $u$  with respect to the points  $y$  and  $z$  as we did in Paragraph 4.2.2.2, somehow ignoring  $\Gamma_2$ .

Projecting  $\mathcal{Z}(u)$  to  $\check{\Omega}$ , we obtain a set  $\check{\mathcal{Z}}(u) \subset \check{\Omega}$  which is the wedge sum  $\mathcal{B}_{\check{y},(\ell-2)}^{\check{z}}$  of an  $(\ell - 2)$ -bouquet of loops at  $\check{y}$  with a simple arc from  $\check{y}$  to  $\check{z}$ . One of the loops or the arc may contain the point  $\xi_2$ , the image of  $\Gamma_2$  in  $\check{\Omega}$ . Since there are only two semi-arcs at  $\xi_2$ , this point is a regular point of the projected nodal partition  $\check{\mathcal{D}}_u$ . The general picture is then similar to the picture in the simply connected case.

Figures 4.7 and 4.8 display some possible nodal patterns for  $0 \neq u \in V_{y,z}$  when  $\Omega$  has one hole ( $\ell = 5$ ,  $\rho(y) = 7$ , and  $\rho(z) = 1$ ).

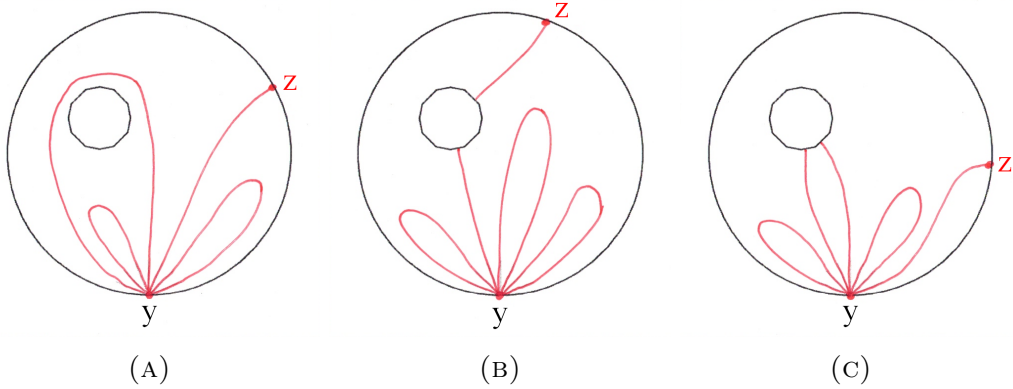


FIGURE 4.7.  $\Omega$  with one hole: some possible nodal patterns for  $v_{y,z}$

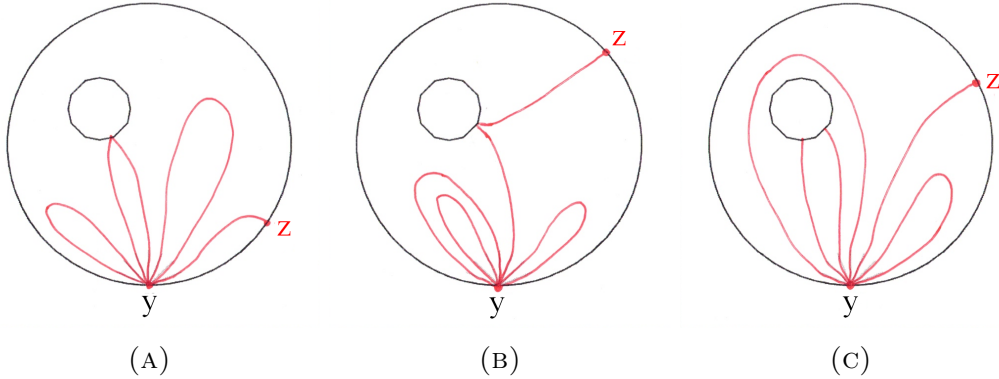


FIGURE 4.8.  $\Omega$  with one hole: some possible nodal patterns for  $v_{y,z}$

For the nodal patterns in Figures 4.7 and 4.8, we have the combinatorial types

$$\begin{aligned} \tau_A^{4.7} = \tau_B^{4.8} = \tau_C^{4.8} &= \begin{pmatrix} \downarrow & 1 & 2 & 3 & 4 & 5 & 6 & 7 \\ 3 & 2 & 1 & \downarrow & 7 & 6 & 5 & 4 \end{pmatrix}, \\ \tau_C^{4.7} = \tau_A^{4.8} &= \begin{pmatrix} \downarrow & 1 & 2 & 3 & 4 & 5 & 6 & 7 \\ 1 & \downarrow & 3 & 2 & 5 & 4 & 7 & 6 \end{pmatrix}, \\ \tau_B^{4.7} &= \begin{pmatrix} \downarrow & 1 & 2 & 3 & 4 & 5 & 6 & 7 \\ 5 & 2 & 1 & 4 & 3 & \downarrow & 7 & 6 \end{pmatrix}. \end{aligned}$$



4.3.1.3.  $\Omega$  with  $k$  holes. *Properties of  $V_{y,z}$ .* In this case,  $\Gamma$  has  $(k+1)$  components,  $\Gamma = \bigcup_{j=1}^{k+1} \Gamma_j$ . Fix  $y \neq z \in \Gamma_1$ . With the notation of Subsection 4.1.2, we have the following lemma.

LEMMA 4.20. *Assume that  $\Omega$  has  $k$  holes, with  $\Gamma = \bigcup_{j=1}^{k+1} \Gamma_j$ . Let  $U$  be an eigenspace of (2.3) in  $\Omega$ , such that, for some  $\ell \geq 2$ ,  $\sup \{\kappa(u) \mid 0 \neq u \in U\} \leq \ell$ , and  $\dim U = (2\ell - 1)$ . Let  $y \neq z \in \Gamma_1$ , and define the subspace*

$$V_{y,z} := \{u \in U \mid \rho(u, y) \geq (2\ell - 3) \text{ and } \rho(u, z) \geq 1\}.$$

Then,  $\dim V_{y,z} = 1$ . Furthermore, for all  $0 \neq u \in V_{y,z}$ :

- (i) The set  $\mathcal{Z}(u) \cup \Gamma(u)$  is connected.
- (ii) If  $J(u) = \{1\}$ , the only singular points of  $u$  are the points  $y$  and  $z$ , with  $\rho(u, y) = (2\ell - 3)$  and  $\rho(u, z) = 1$ .
- (iii) If  $J(u) \neq \{1\}$ , each component  $\Gamma_j, j \in J(u)$ , is hit by exactly two nodal arcs, the function  $u$  has no interior singular point, and its only singular points on  $\Gamma_1$  are  $y$  and  $z$ , with  $\rho(u, y) = (2\ell - 3)$  and  $\rho(u, z) = 1$ .
- (iv) In all cases,  $\kappa(u) = \ell$ .
- (v) In all cases, the nodal set of  $u$  consists of  $(\ell - 2)$  simple non-intersecting ‘‘generalized’’ nodal loops at  $y$  (loops comprising nodal arcs, and possibly arcs contained in some boundary components  $\Gamma_j, j \in J(u) \setminus \{1\}$ ), a simple nodal arc from  $y$  to either  $z$  (when  $J(u) = \{1\}$ ) or to some inner component of  $\Gamma$ , a simple nodal arc from  $y$  to some component  $\Gamma_j, j \in J(u) \setminus \{1\}$ , and possibly some nodal arcs joining components which meet  $\mathcal{Z}(u)$ . These nodal arcs can only intersect at  $y$  or possibly on the components  $\Gamma_j, j \in J(u) \setminus \{1\}$ . In all cases, the point  $y$  is joined to the point  $z$  by a simple arc comprising nodal arcs and possibly sub-arcs of the  $\Gamma_j, j \in J(u) \setminus \{1\}$ .

A generator of  $V_{y,z}$  will be denoted by  $v_{y,z}$  (defined up to scaling).

*Proof of Lemma 4.20.* With the assumptions of the lemma, Euler’s formula (4.9) can be rewritten as,

$$(4.27) \quad \begin{aligned} 0 \geq \kappa(u) - \ell = & (b_0(\mathcal{Z}(u) \cup \Gamma(u)) - 1) + \frac{1}{2} \sum_{x \in \mathcal{S}_i(u)} (\nu(x) - 2) \\ & + \sum_{j \in J(u), j \neq 1} \frac{1}{2} \left( \sum_{x \in \mathcal{S}_b(u) \cap \Gamma_j} \rho(x) - 2 \right) \\ & + \frac{1}{2} \sum_{x \in \mathcal{S}_b(u) \cap \Gamma_1, x \neq y, z} \rho(x) + \frac{1}{2} (\rho(y) + \rho(z) - 2\ell + 2). \end{aligned}$$

In view of our assumptions, and Proposition 2.29, the terms in the right-hand side of (4.27) are all non-negative. In view of the left hand side of the inequality, they must all be zero. We now examine two cases.

◊ If  $J(u) = \{1\}$ , the second line is the right hand side disappears, the nodal set  $\mathcal{Z}(u)$  only meets  $\Gamma_1$ ,  $b_0(\mathcal{Z}(u) \cup \Gamma_1) = 1$ , the only singular points of the function  $u$  are the points  $y$  and  $z$ , and  $\rho(y) = (2\ell - 3)$ ,  $\rho(z) = 1$ .

◊ If  $J(u) \neq \{1\}$ , all the terms in the right hand side must be zero:  $b_0(\mathcal{Z}(u) \cup \Gamma(u)) = 1$ , each component  $\Gamma_j, j \in J(u) \setminus \{1\}$ , is hit by precisely two nodal arcs of  $\mathcal{Z}(u)$ ,  $\rho(y) = (2\ell - 3)$ , and  $\rho(z) = 1$ , and the function  $u$  has no other singular point whether in the interior of  $\Omega$  or on  $\Gamma$ . Furthermore, there is a simple nodal arc from  $y$  to one of the components  $\Gamma_j, j \in J(u)$ , a simple nodal arc from  $z$  to one of the components  $\Gamma_j, j \in J(u)$ , and there is a simple nodal arc, possibly comprising arcs contained in  $\Gamma(u)$  joining  $y$  to  $z$ . Finally,  $\kappa(u) = \ell$ . This proves assertions (i)–(v).

To prove the first assertion, assuming there are at least two linearly independent functions  $u_1$  and  $u_2$  in  $V_{y,z}$ , we can apply Lemma 2.17 as in the previous proofs, and construct yet another function  $0 \neq \tilde{u}$  such that  $\rho(\tilde{u}, y) \geq (2\ell - 3)$  and  $\rho(\tilde{u}, z) \geq 2$ , contradicting Assertions (ii).  $\square$

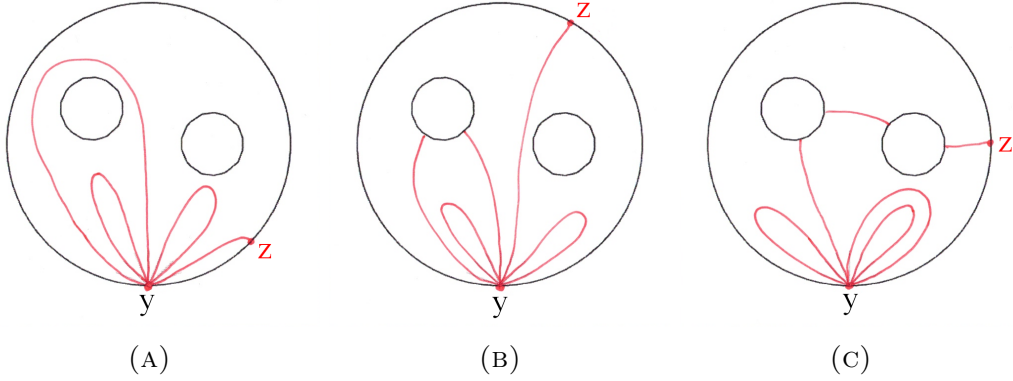


FIGURE 4.9.  $\Omega$  with two holes: some possible nodal patterns for  $v_{y,z}$

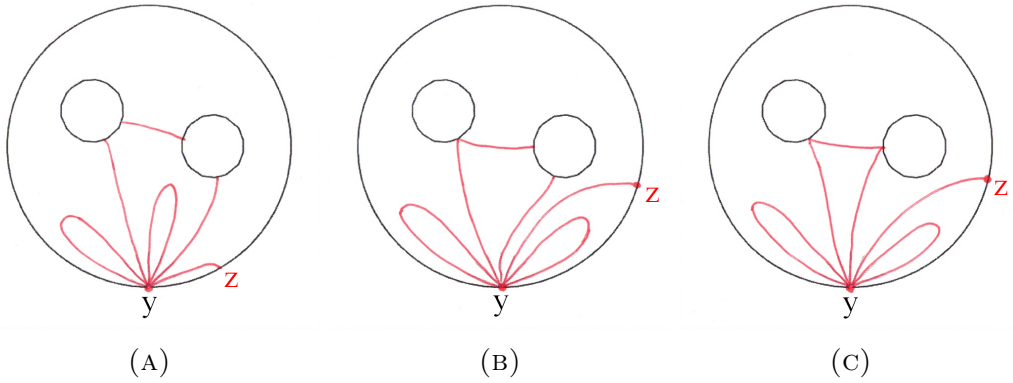


FIGURE 4.10.  $\Omega$  with two holes: some possible nodal patterns for  $v_{y,z}$

4.3.1.4.  $\Omega$  with  $k$  holes. *Structure and combinatorial type of nodal sets in  $V_{y,z}$ .* We can adapt the description of the nodal set  $\mathcal{Z}(u)$ ,  $u \in V_{y,z}$  given in Paragraph 4.3.1.2 to the present case (multiple components of  $\Gamma$ ). The “generalized” loops or arc will then hit one or several components  $\Gamma_j$ ,  $j \in J(u) \setminus \{1\}$ . We can also define the *combinatorial type*  $\tau_{y,z}^u$  of  $u$  with respect to the points  $y$  and  $z$ .

Figures 4.9 and 4.10 display possible nodal patterns for  $0 \neq u \in V_{y,z}$  (in these examples,  $\ell = 5$ ,  $\rho(y) = 7$ , and there are 3 loops). For these nodal patterns, we have the combinatorial types

$$\begin{aligned} \tau_A^{4.9} &= \begin{pmatrix} \downarrow & 1 & 2 & 3 & 4 & 5 & 6 & 7 \\ 1 & \downarrow & 3 & 2 & 7 & 6 & 5 & 4 \end{pmatrix}, \\ \tau_B^{4.9} &= \begin{pmatrix} \downarrow & 1 & 2 & 3 & 4 & 5 & 6 & 7 \\ 3 & 2 & 1 & \downarrow & 7 & 6 & 5 & 4 \end{pmatrix}, \\ \tau_C^{4.9} &= \begin{pmatrix} \downarrow & 1 & 2 & 3 & 4 & 5 & 6 & 7 \\ 5 & 4 & 3 & 2 & 1 & \downarrow & 7 & 6 \end{pmatrix}, \end{aligned}$$

and

$$\begin{aligned} \tau_A^{4.10} &= \begin{pmatrix} \downarrow & 1 & 2 & 3 & 4 & 5 & 6 & 7 \\ 1 & \downarrow & 5 & 4 & 3 & 2 & 7 & 6 \end{pmatrix}, \\ \tau_B^{4.10} = \tau_C^{4.10} &= \begin{pmatrix} \downarrow & 1 & 2 & 3 & 4 & 5 & 6 & 7 \\ 3 & 2 & 1 & \downarrow & 5 & 4 & 7 & 6 \end{pmatrix}. \end{aligned}$$

Lemma 4.20 can be reformulated in the abstract setting of Subsection 4.3.1 as follows. For any  $0 \neq u \in V_{y,z}$ , the projection  $\check{\mathcal{Z}}(u)$  of the nodal set  $\mathcal{Z}(u)$  consists of  $(\ell - 2)$  continuous simple loops at  $\check{y}$  and a continuous simple curve from  $\check{y}$  to  $\check{z}$ . The loops and curve only intersect at  $\check{y}$  and may contain points in  $\Xi$ . If  $\xi_j \in \check{\mathcal{Z}}(u)$ , there are exactly two projected nodal semi-arcs at this point, and the point  $\xi_j$  is a regular point of  $\check{\mathcal{D}}_u$ . The set  $\check{\mathcal{Z}}(u) \subset \check{\Omega}$  is therefore the wedge sum  $\mathcal{B}_{\check{y},(\ell-2)}^{\check{z}}$  of an  $(\ell - 2)$ -bouquet of loops at  $\check{y}$ , with a simple arc from  $\check{y}$  to  $\check{z}$ . The loops or the arc may contain points in  $\Xi$ . This is illustrated in Figure 4.11.

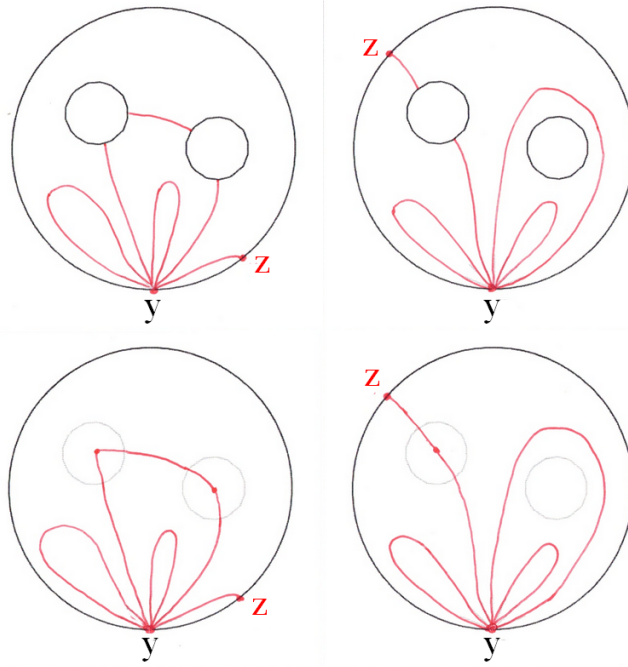


FIGURE 4.11. Nodal patterns in  $\Omega$  and their projections in  $\check{\Omega}$

REMARK 4.21. From the point of view of *partitions*, see [BoHe2017], the points in  $\Xi$  are not singular points of  $\check{\mathcal{D}}_u$ , the projection of the nodal partition  $\mathcal{D}_u$  of  $u$ .

**4.3.2. Analysis of eigenfunctions with one prescribed boundary singular point.** We use the notation of Subsection 4.1.2. In this subsection, we assume that  $U$  is a linear subspace of an eigenspace  $U(\lambda)$  of (2.3), and that for some  $\ell \geq 2$ ,

$$\begin{cases} \sup \{ \kappa(u) \mid 0 \neq u \in U \} \leq \ell \text{ and} \\ \dim U = (2\ell - 1). \end{cases}$$

For  $x \in \Gamma_1$ , we introduce the subspaces

$$(4.28) \quad \begin{cases} U_y^1 = \{ u \in U \mid \rho(u, y) \geq (2\ell - 2) \}, \\ U_y^2 = \{ u \in U \mid \rho(u, y) \geq (2\ell - 3) \}. \end{cases}$$

According to Lemma 2.16,  $U_y^1 \neq \{0\}$ . The purpose of this subsection is to investigate the properties of the functions  $u \in U_y^1$  or  $U_y^2$ —their precise order of vanishing, the structure of their nodal sets—under the above assumptions on  $U$ .

#### 4.3.2.1. Properties of $U_y^1$ and $U_y^2$ .

LEMMA 4.22. *Let  $U$  be a linear subspace of an eigenspace of (2.3) in  $\Omega$ , with*

$$\sup \{ \kappa(u) \mid 0 \neq u \in U \} \leq \ell, \quad \text{and} \quad \dim U = (2\ell - 1).$$

*Fix some  $y \in \Gamma_1$ . For the spaces  $U_y^1$  and  $U_y^2$  defined in (4.28), we have*

$$(4.29) \quad \begin{cases} (i) \dim U_y^1 = 1, \quad \dim U_y^2 = 2 \text{ and,} \\ (ii) \text{ for any } 0 \neq u \in U_y^2, \\ \left\{ \begin{array}{l} \kappa(u) = \ell \text{ and } \mathcal{Z}(u) \cup \Gamma(u) \text{ is connected,} \\ \mathcal{S}_i(u) = \emptyset, \\ \sum_{z \in \mathcal{S}_b(u) \cap \Gamma_j} \rho(u, z) = 2 \text{ for all } j \in J(u) \setminus \{1\}, \\ \sum_{z \in \mathcal{S}_b(u) \cap \Gamma_1} \rho(u, z) = (2\ell - 2) \text{ and, more precisely,} \\ (i) \text{ either } \rho(u, y) = (2\ell - 2) \text{ and } \mathcal{S}_b(u) \cap \Gamma_1 = \{y\}, \\ (ii) \text{ or } \rho(u, y) = (2\ell - 3), \exists z_u \in \Gamma_1 \setminus \{y\} \text{ with } \rho(u, z_u) = 1, \\ \text{and } \mathcal{S}_b(u) \cap \Gamma_1 = \{y, z_u\}. \end{array} \right. \end{cases}$$

*Proof.* Assume that  $\Gamma$  has  $(q + 1)$  components,  $\Gamma_1, \dots, \Gamma_{q+1}$ , with  $x \in \Gamma_1$ .

Clearly,  $\{0\} \neq U_y^1 \subset U_y^2$ . Take any  $0 \neq u \in U_y^2$ . Euler's formula (4.9) can be rewritten as

$$(4.30) \quad \begin{aligned} 0 \geq \kappa(u) - \ell &= (b_0(\mathcal{Z}(u) \cup \Gamma(u)) - 1) + \frac{1}{2} \sum_{z \in \mathcal{S}_i(u)} (\nu(z) - 2) \\ &+ \sum_{i \in J(u), i \neq 1} \frac{1}{2} \left( \sum_{z \in \mathcal{S}_b(u) \cap \Gamma_i} \rho(z) - 2 \right) \\ &+ \frac{1}{2} \left( \sum_{z \in \mathcal{S}_b(u) \cap \Gamma_1} \rho(z) - 2\ell + 2 \right). \end{aligned}$$

The first  $|J(u)| + 2$  terms in the right-hand side of the equality are nonnegative. Since  $\sum_{z \in \mathcal{S}_b(u) \cap \Gamma_1} \rho(z)$  is even, and larger than or equal to  $(2\ell - 3)$ , the last term is nonnegative also. In view of the first inequality, the four terms must vanish. This proves the relations (4.29).

◇ *Proof that  $\dim U_y^1 = 1$ .* Assume that this is not the case. Then, there exist two linearly independent functions  $u_1, u_2$  in  $U_y^1$  such that  $\rho(u_i, y) = (2\ell - 2)$ . By Lemma 2.17, there would exist a nontrivial linear combination  $u$  such that  $u \in U_u^1$  and  $\rho(u, y) \geq (2\ell - 1)$ , a contradiction with (4.29).

◇ *Proof that  $\dim U_y^2 = 2$ .* Choose some  $0 \neq v_1 \in U_y^1$ . Clearly  $v_1 \in U_y^2$ . On the other hand, given any  $y \in \Gamma_1 \setminus \{y\}$ , Lemma 4.7 provides a function  $u_{y,z}$  belonging to  $U_y^2$ , not to  $U_y^1$ , and hence  $\dim U_y^2 \geq 2$ . Choose  $0 \neq v_2 \in U_y^2$  orthogonal to  $v_1$ . Since  $\dim U_y^1 = 1$ , the function  $v_2$  satisfies  $\rho(v_2, y) = (2\ell - 3)$ , and by Proposition 2.29, there must exist some  $y_2 \in \Gamma$  such that  $\rho(v_2, y_2) \geq 1$ . By Lemma 4.20,  $\rho(v_2, y_2) = 1$  and  $v_2 \in V_{y,y_2}$ . The subspace  $U_y^{1,\perp} := \{u \in U_y^2 \mid u \perp u_1\}$  has dimension at least one. Assume that  $\dim U_y^2 \geq 3$ . Then  $\dim U_y^{1,\perp} \geq 2$ , and we can find two linearly independent functions  $u_1, u_2 \in U_y^{1,\perp}$  such that  $\rho(u_i, y) = (2\ell - 3)$ . By Lemma 2.17, there exists a linear combination  $u \in U_y^{1,\perp}$  such that  $\rho(u, y) \geq (2\ell - 2)$ , a contradiction.  $\square$

REMARK 4.23. Up to scaling, there is a uniquely defined orthogonal basis  $\{v_1, v_2\}$  of  $U_y^2$ , with  $v_1 \in U_y^1$ ,  $v_2 \in U_y^{1,\perp}$ , and a uniquely defined  $y_2 \in \Gamma_1 \setminus \{y\}$  such that  $\rho(v_2, y_2) = 1$ . In view of Lemma 2.19, we can choose  $v_1$  such that  $\check{v}_1 > 0$  on  $\Gamma_1 \setminus \{y\}$ , and  $v_2$  such that  $\check{v}_2 > 0$  on the arc from  $y$  to  $y_2$  moving counter-clockwise on  $\Gamma_1$ .

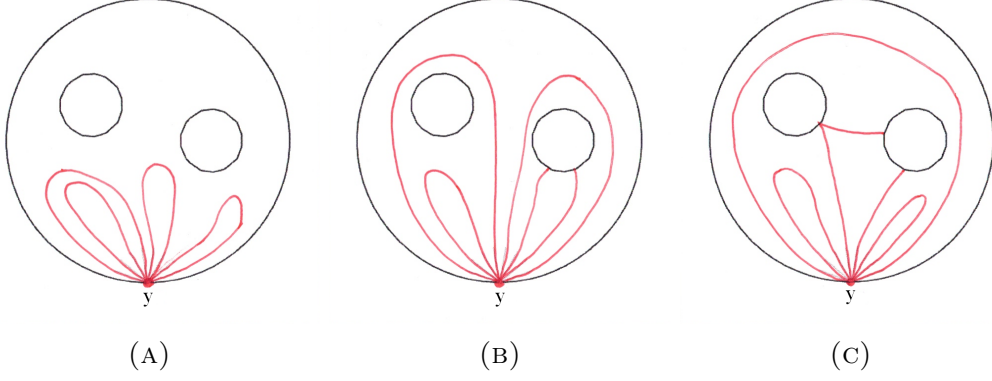


FIGURE 4.12. Some possible nodal patterns for  $0 \neq u \in U_y^1$

#### 4.3.2.2. Structure and combinatorial type of nodal sets in $U_y^1$ and $U_y^2$ .

◇ Relations (4.29) and an analysis as in Subsection 4.2.2, show that the nodal set of any  $0 \neq u \in U_y^1$  consists of  $(\ell - 1)$  “generalized” nodal loops at the point  $y$ , and that these loops do not intersect away from  $y$ . In the abstract setting of Subsection 4.3.1, for any  $0 \neq u \in U_y^1$ , the projection  $\check{Z}(u)$  of the nodal set  $Z(u)$  consists of  $(\ell - 1)$  continuous loops at  $\check{y}$ . The loops only intersect at  $\check{y}$ , and may contain points in  $\Xi$ . If  $\xi_j \in \check{Z}(u)$ , there are exactly two projected nodal semi-arcs at this point. It follows that  $\xi_j$  is a regular point of  $\check{D}_u$ . The set  $\check{Z}(u)$  is an  $(\ell - 1)$ -bouquet of loops  $\mathcal{B}_{\check{y},(2\ell-2)}$  at  $\check{y}$ .

Adapting the description given in Paragraph 4.2.2.2, for  $0 \neq u \in U_y^1$ , we define the *combinatorial type*  $\tau_y^u$  of the nodal set  $Z(u)$  with respect to  $y$ . This is a map from  $L_{(2\ell-2)}$  to itself.

Some possible nodal patterns for  $u \in U_y^1$  are displayed in Figure 4.12, where  $\ell = 5$ , and  $\rho(y) = 8$ . The corresponding combinatorial types are

$$\begin{aligned} \tau_A^{4.12} &= \begin{pmatrix} 1 & 2 & 3 & 4 & 5 & 6 & 7 & 8 \\ 2 & 1 & 4 & 3 & 8 & 7 & 6 & 5 \end{pmatrix}, \\ \tau_B^{4.12} &= \begin{pmatrix} 1 & 2 & 3 & 4 & 5 & 6 & 7 & 8 \\ 4 & 3 & 2 & 1 & 8 & 7 & 6 & 5 \end{pmatrix}, \\ \tau_C^{4.12} &= \begin{pmatrix} 1 & 2 & 3 & 4 & 5 & 6 & 7 & 8 \\ 8 & 3 & 2 & 5 & 4 & 7 & 6 & 1 \end{pmatrix}. \end{aligned}$$

◇ If  $u \in U_y^2$  and  $u \notin U_y^1$ , there exists a unique  $z_u \in \Gamma_1$ , such that  $z_u \neq y$  and  $\mathcal{S}_b(u) \cap \Gamma_1 = \{y, z_u\}$ , with  $\rho(u, y) = (2\ell - 3)$ ,  $\rho(u, z_u) = 1$ . Furthermore,  $V_{y,z_u} = [u]$ . The nodal set  $Z(u)$  and its *combinatorial type*  $\tau_{y,z_u}^u$  are described in Paragraph 4.3.1.3. Projecting  $Z(u)$  to  $\check{\Omega}$ ,  $\check{Z}(u)$  is the wedge sum  $\mathcal{B}_{\check{y},(\ell-2)}^{\check{z}_u}$  of a simple arc from  $\check{y}$  to  $\check{z}_u$  with an  $(\ell - 2)$ -bouquet of loops at  $\check{y}$ .

**4.3.3. Application of the previous analysis.** Fix some  $y \in \Gamma_1$ . We now apply the analysis of Subsections 4.2.2 and 4.2.3 to investigate the limits  $v_{y,z} \in U_y^2 \setminus U_y^1$ , when  $z$  tends to  $y$  on  $\Gamma_1$ , clockwise or anti-clockwise. The notation are the same as in Subsection 4.2.2.

We choose a basis  $\{v_1, v_2\}$  of  $U_x^2$  as described in Remark 4.23. In particular,  $\rho(v_1, y) = (2\ell - 2)$ ,  $v_1 \perp v_2$  in  $L^2(\Omega)$ ,  $\rho(v_2, y) = (2\ell - 3)$ , there exists  $y_2 \in \Gamma_1 \setminus \{y\}$  such that  $\rho(v_2, y_2) = 1$ , and  $\mathcal{S}(v_2) \cap \Gamma_1 = \{y, y_2\}$ . Recall the definition of the functions  $\check{v}_i$  on  $\Gamma$ ,

$$(4.31) \quad \check{v}_i := \begin{cases} \partial_\nu v_i & \text{in the Dirichlet case,} \\ v_i|_\Gamma & \text{in the Robin case.} \end{cases}$$

According to Lemma 2.19, the function  $\check{v}_1$  vanishes only at  $y$  and does not change sign on  $\Gamma_1$ . The function  $\check{v}_2$  does not vanish on  $\Gamma_1 \setminus \{y, y_2\}$ , and changes sign when crossing  $y_2$  and  $y$  along  $\Gamma_1$ .

Let  $\gamma : [0, 2\pi] \rightarrow \Gamma_1$  be a parametrization such that  $\gamma(0) = \gamma(2\pi) = x$ . Given any  $y \in \Gamma_1 \setminus \{y\}$ , there exists a function  $u_{y,z}$  which satisfies (4.29)(ii), and this function is uniquely defined up to multiplication by a nonzero scalar. In the Dirichlet case, this function is characterized by the fact that  $\check{u}_{y,z} = \partial_\nu u_{y,z}|_{\Gamma_1}$  only vanishes at  $y$  and  $z$ . In the Robin case, it is characterized by the fact that  $\check{u}_{y,z} = u_{y,z}|_{\Gamma_1}$  only vanishes at  $y$  and  $z$ . Up to a constant factor, we may choose

$$(4.32) \quad u_{y,z} = a(z)v_1 + b(z)v_2,$$

with

$$(4.33) \quad \begin{cases} a(z) = -\check{v}_2(z) \left( \check{v}_1^2(z) + \check{v}_2^2(z) \right)^{-\frac{1}{2}}, \\ b(z) = \check{v}_1(z) \left( \check{v}_1^2(z) + \check{v}_2^2(z) \right)^{-\frac{1}{2}}, \end{cases}$$

where  $\check{v}_1, \check{v}_2$  are defined in (4.31).

Then, there exists a unique  $\theta(z) \in (0, \pi)$  such that  $\cos(\theta(z)) = a(z)$  and  $\sin(\theta(z)) = b(z)$  (this is because  $\check{v}_1$  is positive on  $\Gamma_1 \setminus \{y\}$ ). Defining

$$(4.34) \quad w_\theta = \cos \theta v_1 + \sin \theta v_2,$$

we have  $u_{y,z} = w_{\theta(z)}$ . Conversely, according to the proof of Lemma 4.22, any function  $w_\theta$  has exactly two singular points on  $\Gamma_1$ , the point  $y$  and some other point  $z_\theta \neq y$ . Note that the point  $z$  determines the eigenfunction  $u_{y,z}$  uniquely (up to scaling) and vice versa. It follows that we have a continuous, bijective map  $(0, 2\pi) \ni t \mapsto \theta(\gamma(t)) \in (0, \pi)$ . This map is strictly monotone (we can assume that it is increasing), and provides a diffeomorphism from  $(0, 2\pi)$  to  $(0, \pi)$ , with limits 0 and  $\pi$  respectively. Otherwise stated, the function  $u_{y,\gamma(t)}$  defined in (4.32) tends to  $v_1$  when  $t$  tends to 0 and to  $-v_1$  when  $t$  tends to  $2\pi$ . There exists  $t_2$  such that  $\gamma(t_2) = y_2$ , and hence  $\theta(y_2) = \frac{\pi}{2}$ . We have proved the following property.

**PROPERTY 4.24.** *The function  $u_{y,z}$  defined in (4.32) tends to  $v_1$  when  $z \neq y$  tends to  $y$  clockwise, and to  $-v_1$  when when  $z \neq y$  tends to  $y$  counter-clockwise.*

4.3.3.1. *Proof that  $\text{mult}(\lambda_k) \leq (2k - 2)$  for  $k \geq 3$ , general case.*

Under the assumption that  $\dim U(\lambda_k) = (2k - 1)$ , the arguments in the simply connected case only use Euler's formula applied to nodal partitions  $\mathcal{D}_u$ , Jordan's separation theorem, the structure of the nodal sets  $\mathcal{Z}(v_1)$  (a bouquet of loops at  $y$ ) and  $\mathcal{Z}(v_2)$  (the wedge sum of an arc from  $y$  to the boundary  $\Gamma_1$  with one or two bouquets of loops at  $y$ ), and the fact that the combinatorial type  $\tau_{y, a_\theta, w_\theta}$  of the nodal sets  $\mathcal{Z}(w_\theta)$  is constant for  $\theta \in (0, \pi)$ .

In the general case, Euler's formula leads to a similar structure for the nodal sets  $\mathcal{Z}(v_1)$ ,  $\mathcal{Z}(v_2)$ , and  $\mathcal{Z}(w_\theta)$ , with "generalized" loops and arcs. We can now look at the projection of these sets to  $\check{\Omega}$  as in Section 4.3.1. As observed in Remark 4.21, the only singular points of the projected sets  $\check{\mathcal{Z}}(u)$  (or partitions  $\check{\mathcal{D}}_u$ ),  $u \in \{v_2, w_\theta\}$ , are the points  $\check{y}$  and  $\check{z}_\theta$ , and the combinatorial type of  $\check{\mathcal{Z}}(w_\theta)$  is constant for  $\theta \in (0, \pi)$ . Since  $\check{\Omega}$  is simply connected, we can now apply the same arguments as in the simply connected case.

This completes the proof of Theorem 4.1 for general  $C^\infty$  bounded domains.





## Simply Connected Plane Domains: the Estimate

$$\text{mult}(\lambda_k) \leq (2k - 3) \text{ for } k \geq 3$$

### 5.1. Introduction

In Section 4.2, we have established that the estimate,  $\text{mult}(\lambda_k) \leq (2k - 2)$  for all  $k \geq 3$ , is valid for any  $C^\infty$  bounded domain  $\Omega$ , see Theorem 4.1. In [HoMN1999, Theorem B, p. 1172], the authors state that this estimate can be improved to  $\text{mult}(\lambda_k) \leq (2k - 3)$  for all  $k \geq 3$ .

The purpose of this chapter is to prove Theorem 1.1, Assertion (ii), namely:

**THEOREM 5.1.** *Let  $\Omega$  be a simply connected  $C^\infty$  bounded domain in  $\mathbb{R}^2$ . The multiplicities of the eigenvalues of the operator  $-\Delta + V$  in  $\Omega$ , with the Dirichlet, Neumann or  $h$ -Robin boundary condition, satisfy the estimate  $\text{mult}(\lambda_k) \leq (2k - 3)$  for any  $k \geq 3$ .*

The proof of the theorem is by contradiction. Introducing the following assumptions, to hold throughout this chapter, we shall reach a contradiction in both cases  $\Gamma_{(2k-2)} = \emptyset$  and  $\Gamma_{(2k-2)} \neq \emptyset$ .

**ASSUMPTIONS 5.2.**

- ◇  $\Omega$  is a simply connected,  $C^\infty$ , bounded domain in  $\mathbb{R}^2$ , and we let  $\Gamma := \partial\Omega$ .
- ◇ For some  $k \geq 3$ , the  $k$ -th eigenvalue  $\lambda_k$  of the eigenvalue problem (2.3)–(2.4) has multiplicity  $(2k - 2)$ , and we let  $U := U(\lambda_k)$  be the corresponding eigenspace.

More precisely, the proof of Theorem 5.1 is organized as follows.

- ◇ In Section 5.2, we prove the existence of certain functions with prescribed singularities. More precisely, given any  $x \in \Omega$  and  $y \in \Gamma$ , we introduce the linear subspaces

$$\begin{cases} W_x & := \{u \in U \mid \nu(u, x) \geq 2k - 2\} \\ U_y & := \{u \in U \mid \rho(u, y) \geq 2k - 3\}. \end{cases}$$

As it turns out, they have dimension 1. Furthermore, for any  $y \in \Gamma$  and  $u \in U_y$ , either  $\rho(u, y) = (2k - 2)$  and  $\mathcal{S}(u) = \{y\}$ , or  $\rho(u, y) = (2k - 3)$  and  $\mathcal{S}(u) = \{y, z(y)\}$  for some  $z(y) \neq y$  on  $\Gamma$  (Lemmas 5.4 and 5.6). We introduce the following subsets of  $\Gamma$ ,

$$\begin{cases} \Gamma_{(2k-3)} & := \{y \in \Gamma \mid \forall 0 \neq u \in U_y, \rho(u, y) = 2k - 3\} \\ \Gamma_{(2k-2)} & := \{y \in \Gamma \mid \forall 0 \neq u \in U_y, \rho(u, y) = 2k - 2\}. \end{cases}$$

We carefully study the properties of the maps  $\Omega \ni x \mapsto [W_x] \in \mathbb{P}(U)$  and  $\Gamma \ni y \mapsto [U_y]$  (the one-dimensional linear subspaces viewed as points in the projective space of  $U$ ), and of the sets  $\Gamma_{(2k-3)}$  and  $\Gamma_{(2k-2)}$ , proving in particular that  $\Gamma_{(2k-3)}$  is open and  $\Gamma_{(2k-2)}$  finite (Lemma 5.10). This subsection contains three key lemmas. In Lemma 5.12, we investigate the global behavior of  $[U_y]$  and its associated singular point when  $y \in \Gamma_{(2k-3)}$ . In Lemma 5.16 we prove that  $[W_x]$  tends to  $[U_y]$  when  $x \in \Omega$

tends to  $y \in \Gamma$ . In Lemma 5.24, we describe the global behavior of the combinatorial types of the  $[U_y]$ ,  $y \in \Gamma$ . As a consequence, we obtain that  $\#(\Gamma_{(2k-2)})$  must be an even integer.

◇ In Section 5.3, analyzing the behavior of  $[W_x]$  when  $x$  is close to some  $y \in \Gamma$ , we conclude that Assumptions 5.2 lead to a contradiction in the case  $\Gamma_{(2k-2)} = \emptyset$  (Lemma 5.31).

◇ In Section 5.4, the analysis of the global behavior of  $[W_x]$  in a neighborhood of  $\Gamma$  shows that the Assumptions 5.2 lead to a contradiction when  $\Gamma_{(2k-2)} \neq \emptyset$  (Lemma 5.41).

◇ We can finally conclude that Assumptions 5.2 lead to a contradiction, and hence that  $\text{mult}(\lambda_k) \leq (2k - 3)$  for  $k \geq 3$ .

◇ Section 5.5 describes the *labeling of nodal domains* of certain eigenfunctions. This notion is closely related to the notion of combinatorial type and used to prove that the combinatorial types of two eigenfunctions are different. This notion also appears in Section 3.2.

◇ In Section 5.6, we give a detailed proof of Lemma 5.8. We also prove other statements which appear in [HoMN1999] but which we do not actually use for our proof of Theorem 5.1.

## 5.2. Properties of $\lambda_k$ -Eigenfunctions under Assumptions 5.2

**5.2.1. Preamble.** This section is devoted to establishing properties of  $\lambda_k$ -eigenfunctions under Assumptions 5.2 (which will systematically be repeated in the lemmas). These properties will be used in Sections 5.3 and 5.4, leading to a contradiction, and showing that  $\text{mult}(\lambda_k)$  cannot be equal to  $(2k - 2)$  for  $k \geq 3$ .

The assumption that the domain  $\Omega$  is simply connected is actually not necessary in this Section 5.2, and only meant to simplify the proofs. For the proofs in the general case, use arguments similar to those given in Section 4.3.

We use the notation of Subsection 4.1.2. For later purposes, we also introduce the following notation.

NOTATION 5.3. Given two points  $y_1 \neq y_2 \in \Gamma$ , we denote by  $\mathcal{A}(y_1, y_2)$  the open arc from  $y_1$  to  $y_2$ , moving counter-clockwise. Given  $y \in \Gamma$  and some number  $a$  smaller than half the length of  $\Gamma$ ,  $\mathcal{A}(y; a)$  denotes the arc centered at  $y$ , with length  $2a$ , taken counter-clockwise. In both cases, we use the mathematical symbols [ and ] to denote the closed or semi-closed arcs.

According to Courant's nodal domain theorem,  $\sup\{\kappa(u) \mid u \in U\} \leq k$ , so that the number  $\ell$  in (4.4) is now  $k$ .

For any  $0 \neq u \in U$ , Euler's formula (4.8) becomes,

$$(5.1) \quad \begin{cases} 0 \geq \kappa(u) - k &= [b_0(\mathcal{Z}(u) \cup \Gamma) - 1] + \frac{1}{2} \sum_{z \in \mathcal{S}_i(u)} (\nu(u, z) - 2) \\ &+ \frac{1}{2} \sum_{z \in \mathcal{S}_b(u)} \rho(u, z) - (k - 1). \end{cases}$$

In the next subsections, we analyze eigenfunctions with prescribed singular points, under Assumptions 5.2.

### 5.2.2. Eigenfunctions with one prescribed interior singular point.

For  $x \in \Omega$ , define the subspace

$$(5.2) \quad W_x := \{u \in U \mid \nu(u, x) \geq 2k - 2\} .$$

In view of Assumptions 5.2, Lemma 2.14 implies that  $W_x \neq \{0\}$ .

#### 5.2.2.1. Properties of $W_x$ .

LEMMA 5.4. *Assume that  $\Omega$  is simply connected; let  $U := U(\lambda_k)$  with  $k \geq 3$ ; assume that  $\dim U = (2k - 2)$  [Assumptions 5.2]. Let  $x \in \Omega$ . Then, the subspace*

$$W_x = \{u \in U \mid \nu(u, x) \geq 2k - 2\}$$

has the following properties.

(i) *The dimension of  $W_x$  is 1.*

(ii) *For all  $0 \neq u \in W_x$ ,*

$$(5.3) \quad \begin{cases} \kappa(u) = k, \\ \mathcal{Z}(u) \text{ is connected,} \\ \mathcal{S}_i(u) = \{x\} \quad \text{and} \quad \nu(u, x) = 2(k - 1), \\ \sum_{z \in \mathcal{S}_b(u)} \rho(u, z) \in \{0, 2\} . \end{cases}$$

(iii) *If  $w_x$  is a generator of  $W_x$ , the map  $\Omega \ni x \mapsto [w_x] \in \mathbb{P}(U)$  is  $C^\infty$ .*

*Proof.* We already know that  $\dim W_x \geq 1$ .

*Proof of Assertion (ii).* The assumptions of the lemma and (5.1) imply that

$$(5.4) \quad \begin{aligned} 0 \geq \kappa(u) - k &= (b_0(\mathcal{Z}(u) \cup \Gamma) - 2) + \frac{1}{2} \sum_{z \in \mathcal{S}_i(u), z \neq x} (\nu(u, z) - 2) \\ &+ \frac{1}{2} (\nu(u, x) - 2k + 2) + \frac{1}{2} \sum_{z \in \mathcal{S}_b(u)} \rho(u, z) . \end{aligned}$$

The terms in the right-hand side are nonnegative, except possibly the first one. The inequality implies that  $b_0(\mathcal{Z}(u) \cup \Gamma) \leq 2$ . We now consider two cases.

◇ If  $b_0(\mathcal{Z}(u) \cup \Gamma) = 2$ , the terms in the right-hand side are nonnegative, with a nonpositive sum. They must all vanish:  $\kappa(u) = k$ ,  $\mathcal{S}_i(u) = \{x\}$ ,  $\mathcal{S}_b(u) = \emptyset$ , and  $\nu(u, x) = 2(k - 1)$ . In this case,  $\mathcal{Z}(u) \cap \Gamma = \emptyset$ . It follows that  $\mathcal{Z}(u)$  is connected. Indeed, since  $\mathcal{Z}(u)$  does not hit  $\Gamma$ , the nodal arcs emanating from  $x$  must form loops at  $x$ . These loops can only intersect each other at  $x$  because  $\mathcal{S}_i(u) = \{x\}$ . The component  $\mathcal{Z}_x(u)$  of  $x$  in  $\mathcal{Z}(u)$  is a  $(k - 1)$ -bouquet of loops at  $x$  whose complement has  $k$  components. Since  $k$  is the maximal possible number of nodal domains, this implies that  $\mathcal{Z}_x(u) = \mathcal{Z}(u)$ .

◇ If  $b_0(\mathcal{Z}(u) \cup \Gamma) = 1$ , the nodal set  $\mathcal{Z}(u)$  must hit  $\Gamma$ , which implies the inequality  $\sum_{z \in \mathcal{S}_b(u)} \rho(z) \geq 2$  (use Proposition 2.29). Re-arranging the inequality (5.4), we conclude that  $\kappa(u) = k$ ,  $\mathcal{S}_i(u) = \{x\}$ ,  $\nu(u, x) = 2(k - 1)$ ,  $\sum_{z \in \mathcal{S}_b(u)} \rho(z) = 2$ , and that  $\mathcal{Z}(u) \cup \Gamma$  is connected. The component  $\mathcal{Z}_x(u)$  of  $x$  in  $\mathcal{Z}(u)$  is either a  $(k - 1)$ -bouquet of loops at  $x$ , or consists of a  $(k - 2)$ -bouquet of loops and two simple arcs from  $x$  to the boundary. Away from  $x$ , the arcs do not intersect the loops and do not intersect each other except possibly on  $\Gamma$ . In the first case, the complement of the bouquet of loops has  $k$  components, and the two points at which  $\mathcal{Z}(u)$  hits  $\Gamma$  would be linked by a simple arc (possibly a loop if these points coincide). We would have too many

nodal domains. This means that the first case does not occur. In the second case, the complement of  $\mathcal{Z}_x(u)$  has  $k$  components, the maximal possible number. As above, this implies that  $Z(u)$  is connected. We have proved Assertion (ii).

*Proof of Assertion (i).* Lemma 2.17 and (5.3) imply that  $\dim W_x \leq 2$ . Assume by contradiction that  $\dim W_x = 2$ . We again use a *rotating function argument* similar to the one used in Subsection 3.1.2, § 3.1.2.3. As in Proposition 3.2, we can choose a basis  $\{v_1, v_2\}$  of  $W_x$  such that, in local polar coordinates centered at  $x$ ,

$$\begin{cases} v_1 = r^{k-1} \sin((k-1)\omega) + \mathcal{O}(r^k), \\ v_2 = r^{k-1} \cos((k-1)\omega) + \mathcal{O}(r^k). \end{cases}$$

Introducing the family of functions

$$w_\theta = \cos((k-1)\theta) v_1 - \sin((k-1)\theta) v_2,$$

and letting  $\theta$  tend to 0 or  $\frac{\pi}{(k-1)}$ , we can follow the arguments given in the proofs of Properties 3.5 and 3.6 to reach a contradiction.

*Proof of Assertion (iii).* Same proof as for Property 3.10.  $\square$

5.2.2.2. *Structure and combinatorial type of nodal sets in  $W_x$ .* In view of Assertion (ii), one can describe the possible nodal patterns for a generator  $w_x$  of  $W_x$ . There are two cases.

- (1) Either  $\mathcal{Z}(w_x)$  consists of  $(k-1)$  loops at  $x$  which do not intersect away from  $x$ , and do not hit  $\Gamma$ .
- (2) Or  $\mathcal{Z}(w_x)$  consists of
  - ◊  $(k-2)$  loops at  $x$  which do not hit the boundary, and
  - ◊ two arcs emanating from  $x$  and hitting  $\Gamma$  at points  $y_1 \neq y_2$ , such that  $\rho(w_x, y_i) = 1$  or, possibly, at one point  $y$ , with  $\rho(w_x, y) = 2$ .

Furthermore, the loops at  $x$  and the arcs from  $x$  to the boundary are pairwise disjoint away from  $x$ , except possibly at the boundary. We then have a “generalized” nodal loop at  $x$  which consists of the two arcs, and a portion of the boundary.

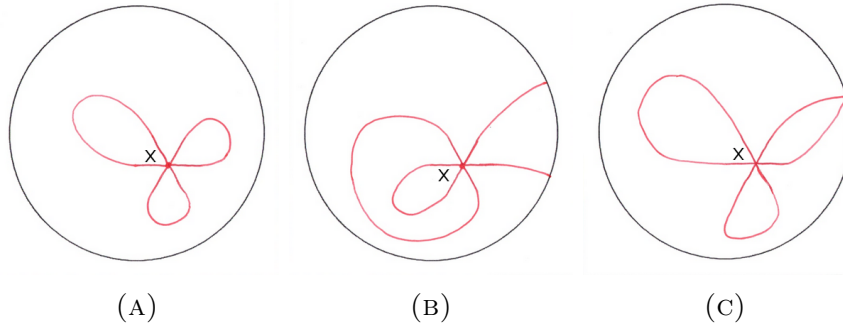


FIGURE 5.1.  $\Omega$  simply connected, nodal patterns for  $w_x \in W_x$  ( $k = 4$ )

Figure 5.1 displays some possible nodal patterns for  $w_x$ .

REMARK 5.5. The *nodal patterns* displayed in Figure 5.1 are valid for both the Dirichlet and Robin boundary conditions. Unless otherwise stated, this remark applies to all figures of this section.

### 5.2.3. Eigenfunctions with one prescribed boundary singular point.

For  $y \in \Gamma$ , we introduce the subspace

$$(5.5) \quad U_y := \{u \in U \mid \rho(u, y) \geq 2k - 3\} .$$

In view of Assumptions 5.2, Lemma 2.15 implies that  $U_y \neq \{0\}$ .

#### 5.2.3.1. Properties of $U_y$ .

LEMMA 5.6. *Assume that  $\Omega$  is simply connected; let  $U := U(\lambda_k)$  with  $k \geq 3$ ; assume that  $\dim U = (2k - 2)$  [Assumptions 5.2]. Let  $y \in \Gamma$ . Then, the subspace*

$$U_y = \{u \in U \mid \rho(u, y) \geq 2k - 3\}$$

has the following properties.

(i) *The dimension of  $U_y$  is 1.*

(ii) *For all  $0 \neq u \in U_y$ ,*

$$(5.6) \quad \begin{cases} \kappa(u) = k \text{ and } \mathcal{Z}(u), \mathcal{Z}(u) \cup \Gamma \text{ are connected,} \\ \mathcal{S}_i(u) = \emptyset, \\ \sum_{z \in \mathcal{S}_b(u)} \rho(u, z) = 2k - 2. \end{cases}$$

Furthermore,

$$(5.7) \quad \begin{cases} \text{either} & \rho(u, y) = 2k - 2 \text{ and } \mathcal{S}_b(u) = \{y\} , \\ \text{or} & \rho(u, y) = 2k - 3 \text{ and } \mathcal{S}_b(u) = \{y, z(y)\} , \\ & \text{for some } z(y) \in \Gamma, z(y) \neq y, \text{ with } \rho(u, z(y)) = 1. \end{cases}$$

(iii) *If  $u_y$  denotes a generator of  $U_y$ , then the map  $\Gamma \ni y \mapsto [u_y] \in \mathbb{P}(U)$  is  $C^\infty$ .*

*Proof.* We already know that  $\dim U_y \geq 1$ .

*Proof of Assertion (ii).* Choose a function  $0 \neq u \in U_y$ , and apply the inequality (5.1) to obtain,

$$(5.8) \quad \begin{aligned} 0 \geq \kappa(u) - k &= (b_0(\mathcal{Z}(u) \cup \Gamma) - 1) + \frac{1}{2} \sum_{z \in \mathcal{S}_i(u)} (\nu(u, z) - 2) \\ &+ \frac{1}{2} \left( \sum_{z \in \mathcal{S}_b(u)} \rho(u, z) - 2k + 2 \right) . \end{aligned}$$

Since  $\rho(u, y) \geq 2k - 3$ , Proposition 2.29 implies that the last term in (5.8) is nonnegative; all the terms in the right-hand side are nonnegative, with nonpositive sum, and hence they must all vanish. This proves (5.6). Looking at the two possible cases,  $\rho(u, y) = (2k - 2)$  or  $(2k - 3)$ , we obtain (5.7). Assertion (ii) is proved.  $\checkmark$

*Proof of Assertion (i).* We already know that  $\dim U_y \geq 1$ . Assume that there exist at least two linearly independent functions  $w_1, w_2$  in  $U_y$ . By (5.6), we have  $2k - 3 \leq \rho(w_i, y) \leq 2k - 2$ . If  $\rho(w_1, y) = \rho(w_2, y) = 2k - 3$ , by Lemma 2.17 there exists some linear combination  $w$  of  $w_1$  and  $w_2$  such that  $\rho(w, y) \geq 2k - 2$ . This function  $w$  must satisfy (5.7) and hence, is uniquely defined (up to scaling). If  $\rho(w_1, y) = (2k - 2)$ , then we must have  $\rho(w_2, y) = (2k - 3)$  since  $w_1$  is uniquely defined. Any other function in  $U_y$  must be a linear combination of  $w_1$  and  $w_2$ . It follows that  $\dim U_y \leq 2$ .

Assume that  $\dim U_y = 2$ , and choose a basis  $\{w_1, w_2\}$  of  $U_y$ , with  $\rho(w_1, y) = (2k - 2)$ ,  $\rho(w_2, y) = (2k - 3)$ , and let  $y_2 = z(y)$  be the unique other singular point of  $w_2$  on

$\Gamma$ . We encountered a similar framework in Subsection 4.2.4 (Proposition 4.13) and in Subsection 4.2.5, and we can use a *rotating function argument* to conclude that  $\dim U_y = 1$ . The claim is proved. This completes the proof of Assertion (i).  $\checkmark$

*Proof of Assertion (iii).* The proof of this assertion is similar to the proof of Property 3.10.  $\square$

Let  $\{\phi_j, 1 \leq j \leq (2k - 2)\}$  be an orthonormal basis of the eigenspace  $U$ . Let  $y_0 \in \Gamma$ . By Lemma 5.6 (iii), there exists some  $\sigma_0 > 0$ , and a  $C^\infty$  map  $\mathcal{A}(y_0; \sigma_0) \ni y \mapsto (a_{y_0,1}(y), \dots, a_{y_0,(2k-2)}(y)) \in \mathbb{S}^{2k-3}$  such that, for all  $y \in \mathcal{A}(y_0; \sigma_0)$ , the eigenfunction

$$(5.9) \quad u_y := \sum_{j=1}^{2k-2} a_{y_0,j}(y) \phi_j \in \mathbb{S}(U)$$

is a generator of  $U_y$  and lies in the unit sphere  $\mathbb{S}(U)$  of the eigenspace  $U$ . (For the notation  $\mathcal{A}(y_0; \sigma_0)$  see Notation 5.3.)

NOTATION 5.7. Define the following subsets of  $\Gamma$ :

$$(5.10) \quad \begin{cases} \Gamma_{(2k-3)} := \{y \in \Gamma \mid \rho(u_y, y) = 2k - 3\} \\ \Gamma_{(2k-2)} := \{y \in \Gamma \mid \rho(u_y, y) = 2k - 2\} . \end{cases}$$

### 5.2.3.2. Structure and combinatorial type of nodal sets in $U_y$ .

Using Lemma 5.6 (ii) one can describe the possible nodal patterns of a generator  $u_y$  of  $U_y$ , as we did in Paragraph 5.2.2.2, see also Subsections 4.2.4 and 4.2.5. If  $\rho(u_y, y) = (2k - 3)$ , the nodal set  $\mathcal{Z}(u_y)$  consists of  $(k - 2)$  simple loops at  $y$ , and a simple arc from  $y$  to some  $z(y) \in \Gamma$ ,  $z(y) \neq y$ ; if  $\rho(u_y, y) = (2k - 2)$ , the nodal set  $\mathcal{Z}(u_y)$  consists of  $(k - 1)$  simple loops at  $y$ . The loops and the arc do not intersect away from  $y$ . Figure 5.2 displays some possible nodal patterns.

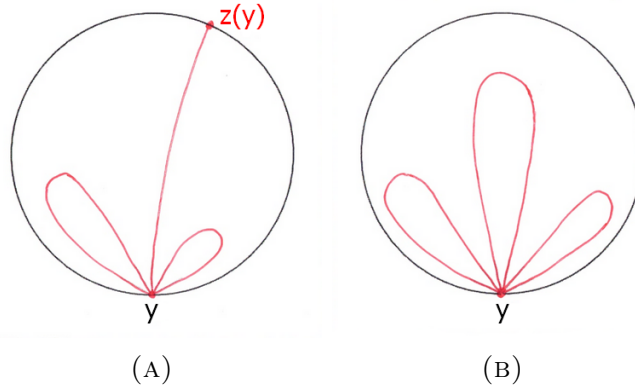


FIGURE 5.2.  $\Omega$  simply connected, nodal patterns for  $u_y \in U_y$  ( $k = 4$ )

For a given  $y \in \Gamma$ , we apply Section 2.4 to a generator  $u_y$  of  $U_y$ . For both Dirichlet or Robin boundary condition, in a neighborhood of  $y$ , the nodal set  $\mathcal{Z}(u_y)$  consists of  $\rho(u_y, y)$  nodal semi-arcs emanating from  $y$ . As in Paragraph 4.2.5.2, for a given  $j \in L_{\rho(u_y, y)} = \{1, \dots, \rho(u_y, y)\}$ , we follow the nodal semi-arc emanating from  $y$  tangentially to the ray  $\omega_j$  along  $\mathcal{Z}(u_y)$ . There are two cases.

- ◇ When  $y \in \Gamma_{(2k-2)}$ , according to Lemma 5.6, we eventually arrive back at  $y$  along a nodal semi-arc emanating from another ray which we denote by  $\omega_{\tau_y^U(j)}$ . This uniquely defines a map  $\tau_y^U : L_{(2k-2)} \rightarrow L_{(2k-2)}$ , such that  $\tau_y^U(j) \neq j$  and  $(\tau_y^U)^2 = \text{Id}$ . In this case, the nodal set  $\mathcal{Z}(u_y)$  consists of a  $(k-1)$ -bouquet of loops  $\gamma_{j, \tau_y^U(j)}^U$  at  $y$ , for  $j \in L_{(2k-2)}$ .
- ◇ When  $y \in \Gamma_{(2k-3)}$ , we define a map  $\tau_y^U$  from  $\{\downarrow\} \cup L_{(2k-3)}$  to itself as follows. According to Lemma 5.6, there exists a unique  $a_y \in L_{(2k-3)}$  (depending on  $y$ ) such that the nodal semi-arc  $\delta_{a_y}$  emanating from  $y$  tangentially to the ray  $\omega_{a_y}$  eventually hits  $\Gamma$  at some  $z(y) \neq y$ . We let  $\tau_y^U(a_y) = \downarrow$  and  $\tau_y^U(\downarrow) = a_y$ . For  $j \neq a_y$ , following the nodal semi-arc  $\delta_j$  emanating from  $y$  tangentially to  $\omega_j$  along  $\mathcal{Z}(u_y)$ , we will eventually reach  $y$  again, along another ray denoted by  $\omega_{\tau_y^U(j)}$ . This uniquely defines a map  $\tau_y^U$  from  $\{\downarrow\} \cup L_{(2k-3)}$  to itself such that  $\tau_y^U(j) \neq j$  and  $(\tau_y^U)^2 = \text{Id}$ . In this case, the nodal set  $\mathcal{Z}(u_y)$  is the wedge sum of the arc  $\delta_{a_y}$  from  $y$  to  $z(y)$  with a  $(k-2)$ -bouquet of loops  $\gamma_{j, \tau_y^U(j)}^U$  at  $y$ .

When  $\Omega$  is simply connected and  $y \in \Gamma_{(2k-3)}$ , the  $(k-2)$ -bouquet of loops actually consists of two bouquets of loops, one in each component of  $\Omega \setminus \delta_{a_y}$ . When  $a_y = 1$  or  $a_y = (2k-3)$ , one of these bouquets of loops is actually empty.

As in Paragraph 4.2.5.2, we define the map  $\tau_y^U$  as the *combinatorial type* of the nodal set  $\mathcal{Z}(u_y)$  at  $y$ , when  $y \in \Gamma_{(2k-2)}$ , resp.  $y \in \Gamma_{(2k-3)}$ . The source-set of  $\tau_y^U$  is  $L_{(2k-2)}$ , resp.  $\{\downarrow\} \cup L_{(2k-3)}$ .

#### 5.2.4. Eigenfunctions with Two Prescribed Boundary Singular Points.

Given  $(y, s) \in \Gamma_{(2k-3)} \times \Gamma$ , with  $y \neq s$ , we define the subspace

$$(5.11) \quad V_{y,s} := \{u \in U \mid \rho(u, y) \geq 2k-4 \text{ and } \rho(u, s) \geq 1\}.$$

In view of Assumptions 5.2, Lemma 2.16 implies that  $V_{y,s} \neq \{0\}$ .

LEMMA 5.8. *Assume that  $\Omega$  is simply connected. Let  $U := U(\lambda_k)$  with  $k \geq 3$ , and assume that  $\dim U = (2k-2)$ . Given  $(y, s) \in \Gamma_{(2k-3)} \times \Gamma$ , with  $y \neq s$ , the subspace*

$$V_{y,s} = \{u \in U \mid \rho(u, y) \geq 2k-4 \text{ and } \rho(u, s) \geq 1\}$$

has the following properties.

- (i) The subspace  $V_{y,s}$  has dimension 1.
- (ii) Any  $0 \neq u \in V_{y,s}$  satisfies

$$(5.12) \quad \left\{ \begin{array}{l} \kappa(u) = k, \\ \mathcal{Z}(u) \cup \Gamma \text{ is connected,} \\ \mathcal{S}_i(u) = \emptyset, \\ \sum_{z \in \mathcal{S}_b(u)} \rho(u, z) = 2k-2, \text{ and} \\ 2k-4 \leq \rho(u, y) \leq 2k-3, \\ 1 \leq \rho(u, s) \leq 2. \end{array} \right.$$

More precisely, there are three distinct possibilities.

**Case A:**  $\rho(u, y) = (2k-3)$  and  $\rho(u, s) = 1$ . In that case,  $u \in U_y$ , with  $\mathcal{S}_b(u) = \{y, s\}$ , and hence  $s = z(y)$ .

**Case B:**  $\rho(u, y) = (2k-4)$  and  $\rho(u, s) = 2$ . In that case,  $\mathcal{S}_b(u) = \{y, s\}$ .

**Case C:**  $\rho(u, y) = (2k - 4)$ ,  $\rho(u, s) = 1$ , and there exists some  $s' \in \Gamma \setminus \{y, s\}$  such that  $\mathcal{S}_b(u) = \{y, s, s'\}$ , with  $\rho(u, s') = 1$ .

(iii) If  $s = z(y)$ , then  $V_{y, z(y)} = U_y$ .

(iv) The map  $\{(y, s) \mid (y, s) \in \Gamma_{(2k-3)} \times \Gamma, s \neq y\} \ni (y, s) \mapsto [V_{y,s}] \in \mathbb{P}(U)$  is  $C^\infty$ .

*Proof.* The proof of Assertion (ii) follows from Euler's formula. Using (5.12), it is easy to prove that  $\dim V_{y,s} \leq 2$ . The proof that  $\dim V_{y,s} = 1$  is easy when  $s \neq z(y)$ . The proof that  $\dim V_{y, z(y)} = 1$  is more involved and follows from a *rotating function argument*. Assertion (iv) is a consequence of Assertion (i), as in the proofs of Lemmas 5.4 and 5.6.  $\square$

In Section 5.6 we provide a detailed proof of Lemma 5.8, as well as further properties of the functions in  $V_{y,s}$ . These results, partially revisit Lemmas 3.4, 3.5 and 3.6 of [HoMN1999, pp. 1180-1183]. In this monograph, we actually only use Lemma 5.8, see the proof of Lemma 5.12.

**5.2.5. Local properties of the map  $\Gamma \ni y \mapsto [U_y] \in \mathbb{P}(U)$ .** Let  $y_0 \in \Gamma$ . For  $y \in \mathcal{A}(y_0; \sigma_0)$  with  $\sigma_0$  small enough (see Notation 5.3), we represent a generator of  $U_y$  as in (5.9),

$$u_y := \sum_{j=1}^{2k-2} a_{y_0, j}(y) \phi_j.$$

Applying Lemma 2.35, we have a conformal mapping  $E_0 : \mathbb{H} \rightarrow \Omega$  such that  $E_0$  extends smoothly to  $\overline{\mathbb{H}}$ ,  $E_0(0) = y_0$  and, when  $y_0 \in \Gamma_{(2k-3)}$ , such that  $E_0(\zeta_0) = z(y_0)$  for some  $\zeta_0 \in \partial\mathbb{H}$ . Since  $E_0|_{\partial\mathbb{H}}$  is a diffeomorphism from  $\partial\mathbb{H}$  onto  $\Gamma \setminus \{y_*\}$ , we can choose some  $r_0 > 0$  such that  $E_0((-r_0, r_0) \times \{0\}) \subset \mathcal{A}(y_0; \sigma_0)$ . We now work in  $\overline{D}_+(0, r_0) \subset \overline{\mathbb{H}}$ , and consider the  $t$ -family of functions  $\xi \mapsto v_t(\xi)$

$$v_t(\xi_1, \xi_2) = \sum_{j=1}^{2k-2} a_{y_0, j}(E_0(t, 0)) \phi_j \circ E_0(\xi_1, \xi_2)$$

which we rewrite as

$$(5.13) \quad v_t(\xi_1, \xi_2) = \sum_{j=1}^{2k-2} a_j(t) \psi_j(\xi_1, \xi_2),$$

with the obvious notation.

The functions  $t \mapsto a_j(t)$  are  $C^\infty$  in  $(-r_0, r_0)$  and the functions  $\psi_j$  satisfy (2.47). Furthermore, for all  $t \in (-r_0, r_0)$ , we have  $\rho(v_t, (t, 0)) = (2k - 2)$  if  $E_0(t, 0) \in \Gamma_{(2k-2)}$ , and  $\rho(v_t, (t, 0)) = (2k - 3)$  if  $E_0(t, 0) \in \Gamma_{(2k-3)}$ . Restricting  $r_0$  if necessary, we may also assume that  $\mathcal{S}_b(v_t) = \{(t, 0), (z(t), 0)\}$  for any  $t \in (-r_0, r_0)$  such that  $E_0(t, 0) \in \Gamma_{(2k-3)}$ , and some  $z(t) \neq t$ .

For convenience, we introduce the notation

$$(5.14) \quad \begin{cases} \Gamma_{0, (2k-2)} := \{(t, 0) \mid t \in (-r_0, r_0) \text{ and } E_0(t, 0) \in \Gamma_{(2k-2)}\} \subset \partial\mathbb{H} \\ \Gamma_{0, (2k-3)} := \{(t, 0) \mid t \in (-r_0, r_0) \text{ and } E_0(t, 0) \in \Gamma_{(2k-3)}\} \subset \partial\mathbb{H}, \end{cases}$$

and

$$(5.15) \quad p := \begin{cases} (2k - 2) & \text{in the Dirichlet case} \\ (2k - 3) & \text{in the Robin case.} \end{cases}$$



Then,

$$\begin{cases} \text{ord}(v_t, (t, 0)) = p & \text{if } (t, 0) \in \Gamma_{0, (2k-3)} \\ \text{ord}(v_t, (t, 0)) = (p+1) & \text{if } (t, 0) \in \Gamma_{0, (2k-2)}. \end{cases}$$

For each  $t$ , write Taylor's formula at order  $(p+1)$  for the function  $\xi \mapsto v_t(\xi)$  in the coordinates  $\xi = (\xi_1, \xi_2)$  of  $\mathbb{H}$ , at the point  $\xi = (t, 0)$ :

$$(5.16) \quad \begin{cases} v_t(\xi_1, \xi_2) = \sum_{|\alpha|=p} \frac{1}{\alpha!} D_\xi^\alpha v_t(t, 0) (\xi_1 - t, \xi_2)^\alpha \\ \quad + \sum_{|\alpha|=p+1} \frac{1}{\alpha!} D_\xi^\alpha v_t(t, 0) (\xi_1 - t, \xi_2)^\alpha \\ \quad + \sum_{|\beta|=p+2} R_\beta(t; \xi_1, \xi_2) (\xi_1 - t, \xi_2)^\beta, \end{cases}$$

where

$$(5.17) \quad R_\beta(t; \xi_1, \xi_2) = \frac{|\beta|}{\beta!} \int_0^1 (1-s)^{|\beta|-1} D_\xi^\beta v_t(t + s(\xi_1 - t), s\xi_2) ds.$$

The first two terms in the Taylor formula (5.16) are *harmonic* homogeneous polynomials of degrees  $p$  and  $(p+1)$  respectively, see Subsection 2.4.6. When  $(t, 0) \in \Gamma_{0, (2k-3)}$ ,  $\text{ord}(v_t, (t, 0)) = p$ , and the first term is nonzero. When  $(t, 0) \in \Gamma_{0, (2k-2)}$ ,  $\text{ord}(v_t, (t, 0)) = (p+1)$ , the first term is identically zero, and the second term is nonzero. In view of (5.13), we can express the coefficients in Taylor's formula as

$$(5.18) \quad D_\xi^\alpha v_t(t, 0) = \sum_{j=1}^{2k-2} a_j(t) D_\xi^\alpha \psi_j(t, 0).$$

Applying the proof of Lemma 2.43 to each function  $\xi \mapsto v_t(\xi)$ , for  $t \in (-r_0, r_0)$ , with a Taylor formula at the boundary point  $(t, 0)$  rather than at  $(0, 0)$ , we obtain the following lemma.

LEMMA 5.9. *The Taylor formula for the function  $\xi \mapsto v_t(\xi)$ , at the point  $\xi = (t, 0)$  and at order  $(p+1)$ , is given by the following identities, depending on the boundary condition (with the notation of Subsection 2.4.6).*

$$(5.19) \quad \begin{cases} \text{Dirichlet case:} \\ v_t(\xi_1, \xi_2) = s_p(t) S_p(\xi_1 - t, \xi_2) + s_{p+1}(t) S_{p+1}(\xi_1 - t, \xi_2) \\ \quad + R_{p+2}(t; \xi_1 - t, \xi_2), \end{cases}$$

$$(5.20) \quad \begin{cases} \text{Neumann case:} \\ v_t(\xi_1, \xi_2) = c_p(t) C_p(\xi_1 - t, \xi_2) + c_{p+1}(t) C_{p+1}(\xi_1 - t, \xi_2) \\ \quad + R_{p+2}(t; \xi_1 - t, \xi_2), \end{cases}$$

$$(5.21) \quad \begin{cases} \text{Robin case:} \\ v_t(\xi_1, \xi_2) = c_p(t) C_p(\xi_1 - t, \xi_2) + c_{p+1}(t) C_{p+1}(\xi_1 - t, \xi_2) \\ \quad + \frac{1}{p+1} c_p(t) h_E(t) S_{p+1}(\xi_1 - t, \xi_2) + R_{p+2}(t; \xi_1 - t, \xi_2), \end{cases}$$

where the remainder term  $R_{p+2}(t; \xi_1 - t, \xi_2) = \sum_{|\beta|=p+2} R_\beta(t; \xi_1, \xi_2) (\xi_1 - t, \xi_2)^\beta$ , vanishes at order at least  $(p+2)$  at  $\xi = (t, 0)$ , with  $R_\beta$  as in (5.17).

We will write these Taylor identities as

$$(5.22) \quad \begin{aligned} v_t(\xi_1, \xi_2) &= A_0(t)P_p(\xi_1 - t, \xi_2) + A_1(t)P_{p+1}(\xi_1 - t, \xi_2) \\ &\quad + \frac{1}{p+1} A_0(t) h_E(t) Q_{p+1}(\xi_1 - t, \xi_2) + R_{p+2}(t; \xi_1 - t, \xi_2), \end{aligned}$$

where, using the notation (2.93),

- ◇  $P_p = S_p$ ,  $P_{p+1} = S_{p+1}$  and  $Q_{p+1} = 0$  in the Dirichlet case,
- ◇  $P_p = C_p$ ,  $P_{p+1} = C_{p+1}$  and  $Q_{p+1} = S_{p+1}$  in the Robin case.

Note that the third term in the right hand side of (5.22) disappears in the Dirichlet and Neumann cases.

The family of functions  $\xi \mapsto v_t(\xi)$  given by (5.13) is  $C^\infty$  with respect to the parameter  $t \in (-r_0, r_0)$ . Its  $t$ -derivative is given by

$$(5.23) \quad w_t := \frac{d}{dt} v_t = \sum_{j=1}^{2k-2} a'_j(t) \psi_j.$$

Let  $w_t^\Omega$  denote the related family

$$(5.24) \quad w_t^\Omega := \sum_{j=1}^{2k-2} a'_j(t) \phi_j,$$

which is a  $C^\infty$  family of eigenfunctions in the eigenspace  $U$ .

Taking the derivative of the identity (5.22) with respect to  $t$ , at  $t = 0$ , we obtain

$$(5.25) \quad \left\{ \begin{aligned} \partial_t v_t|_{t=0}(\xi_1, \xi_2) &= A'_0(0)P_p(\xi_1, \xi_2) - A_0(0) \partial_{\xi_1} P_p(\xi_1, \xi_2) \\ &\quad + A'_1(0) P_{p+1}(\xi_1, \xi_2) - A_1(0) \partial_{\xi_1} P_{p+1}(\xi_1, \xi_2) \\ &\quad + \frac{1}{p+1} (A_0(t)h_E(t))'_{t=0} Q_{p+1}(\xi_1, \xi_2) \\ &\quad - \frac{1}{p+1} A_0(0)h_E(0) \partial_{\xi_1} Q_{p+1}(\xi_1, \xi_2) \\ &\quad + \sum_{|\beta|=p+2} \partial_t R_\beta(0; \xi_1, \xi_2) (\xi_1, \xi_2)^\beta \\ &\quad - \sum_{|\beta|=p+2} \beta_1 R_\beta(0; \xi_1, \xi_2) (\xi_1, \xi_2)^{\beta-(1,0)}. \end{aligned} \right.$$

In view of the relations (2.95) and the definitions of  $P_n$  and  $Q_n$  (depending on the boundary condition, Dirichlet or Robin), we have the relations

$$\partial_{\xi_1} P_n = n P_{n-1} \text{ and } \partial_{\xi_1} Q_n = n Q_{n-1}.$$

It follows that (5.25) reduces to

$$(5.26) \quad \left\{ \begin{aligned} w_0(\xi_1, \xi_2) &= -p A_0(0) P_{p-1}(\xi_1, \xi_2) + [A'_0(0) - (p+1)A_1(0)] P_p(\xi_1, \xi_2) \\ &\quad - A_0(0) h_E(0) Q_p(\xi_1, \xi_2) + \mathcal{O}\left((\xi_1^2 + \xi_2^2)^{\frac{p+1}{2}}\right). \end{aligned} \right.$$

We also consider the function  $\xi_1 \mapsto \check{v}_t(\xi_1)$  as defined in (2.12). In the Dirichlet case, this function is given by  $\check{v}_t(\xi_1) = \partial_{\xi_2} v_t(\xi_1, 0)$ . In the Robin case, it is given by  $\check{v}_t(\xi_1) = v_t(\xi_1, 0)$ . From the definition of  $\check{v}_t(\xi_1)$ , the identity (5.22), the relations in (2.97) and (5.15), we obtain the following relations.

*Dirichlet case:*

$$(5.27a) \quad \check{v}_t(\xi_1) = (2k-2) A_0(t) (\xi_1 - t)^{2k-3} + (2k-1) A_1(t) (\xi_1 - t)^{2k-2} \\ + \mathcal{O}\left((\xi_1 - t)^{2k-1}\right).$$

*Robin case:*

$$(5.27b) \quad \check{v}_t(\xi_1) = A_0(t) (\xi_1 - t)^{2k-3} + A_1(t) (\xi_1 - t)^{2k-2} + \mathcal{O}\left((\xi_1 - t)^{2k-1}\right).$$

#### 5.2.5.1. Properties of $\Gamma_{(2k-3)}$ and $\Gamma_{(2k-2)}$ .

LEMMA 5.10. *Assume that  $\Omega$  is simply connected; let  $U := U(\lambda_k)$  with  $k \geq 3$ ; assume that  $\dim U = (2k-2)$  [Assumptions 5.2]. Then, the following properties hold.*

(i) *The sets  $\Gamma_{(2k-3)}$  and  $\Gamma_{(2k-2)}$  are disjoint and*

$$\Gamma = \Gamma_{(2k-3)} \bigsqcup \Gamma_{(2k-2)}.$$

(ii) *The set  $\Gamma_{(2k-3)}$  is open in  $\Gamma$  and the set  $\Gamma_{(2k-2)}$  is finite.*

*Proof.* Assertion (i) follows from Lemma 5.6, Assertion (i), and (5.7). ✓

*Proof of Assertion (ii).* Let  $y_0 \in \Gamma_{(2k-3)}$ . The generator  $u_{y_0}$  of  $U_{y_0}$  given by (5.9) satisfies  $\mathcal{S}_b(u_{y_0}) = \{y_0, z_0\}$  for some  $z_0 \in \Gamma$ ,  $z_0 \neq y_0$ , with  $\rho(u_{y_0}, y_0) = (2k-3)$ , and  $\rho(u_{y_0}, z_0) = 1$ . This means that the function  $\check{u}_{y_0}$  has precisely two zeros on  $\Gamma$ ,  $y_0$  and  $z_0$ , and changes sign at these points. Given two points  $z_1$  and  $z_2$  on either sides of  $z_0$ , close enough to  $z_0$  and away from  $y_0$ , we have  $\check{u}_{y_0}(z_1) \check{u}_{y_0}(z_2) < 0$ . When  $y \in \mathcal{A}(y_0; \sigma_0)$  is close enough to  $y_0$ , the function  $u_y$  is  $C^1$ -close to the function  $u_{y_0}$  and hence  $\check{u}_y$  is uniformly close to  $\check{u}_{y_0}$ , and satisfies  $\check{u}_y(z_1) \check{u}_y(z_2) < 0$ . In view of Lemma 5.6, this implies that for  $y$  close enough to  $y_0$  in  $\Gamma$ ,  $y \in \Gamma_{(2k-3)}$ , so that  $\Gamma_{(2k-3)}$  is open in  $\Gamma$ .

To prove that the set  $\Gamma_{(2k-2)}$  is finite, it suffices to prove that it is discrete. We work in the setup of Paragraph 5.2.5 with the function  $v_t$  given by (5.13). Assume, by contradiction, that the point  $y_0$  is not isolated in  $\Gamma_{(2k-2)}$ . Then the point  $(0, 0) = E_0^{-1}(y_0)$  is not isolated in  $\Gamma_{0, (2k-2)}$ , and there exists a sequence  $\{t_n\}$  tending to zero, such that  $v_{t_n}$  satisfies  $\rho(v_{t_n}, (t_n, 0)) = (2k-2)$  for all  $n$ .

Writing

$$v_t(\xi_1, \xi_2) = A_0(t) P_p(\xi_1 - t, \xi_2) + A_1(t) P_{p+1}(\xi_1 - t, \xi_2) \\ + \frac{1}{p+1} A_0(t) h_E(t) Q_{p+1}(\xi_1 - t, \xi_2) + R_{p+2}(t; \xi_1 - t, \xi_2),$$

as in (5.22), we have  $A_0(0) = 0$ ,  $A_1(0) \neq 0$ , and since  $A_0(t_n) = 0$  for all  $n$ , we also have  $A_0'(0) = 0$ . Equation (5.26) then reduces to

$$w_0(\xi_1, \xi_2) = -(p+1) A_1(0) P_p(\xi_1, \xi_2) + \mathcal{O}\left(\left(\xi_1^2 + \xi_2^2\right)^{\frac{p+1}{2}}\right).$$

This means that  $\text{ord}(w_0^\Omega, y_0) = \text{ord}(w_0, (0, 0)) = p$ , and hence, using (5.15), that  $\rho(w_0^\Omega, y_0) = (2k-3)$ , and  $w_0^\Omega \in U_{y_0}$ . On the other hand,  $u_{y_0} \in U_{y_0}$ , with  $\rho(u_{y_0}, y_0) = (2k-2)$ . We would have two linearly independent functions in  $U_{y_0}$ , a contradiction with  $\dim U_{y_0} = 1$ . This proves that  $y_0$  is isolated in  $\Gamma$ . It follows that  $\Gamma_{(2k-2)}$  is discrete and hence finite. Assertion (ii) is proved. ✓

The proof of Lemma 5.10 is complete. □

REMARK 5.11. Lemmas 5.4, 5.6, and 5.10 are actually valid when  $\Omega$  is not simply connected: same arguments as in Section 4.3.

### 5.2.6. Global properties of the map $\Gamma \ni y \mapsto [U_y] \in \mathbb{P}(U)$ .

LEMMA 5.12. *Assume that  $\Omega$  is simply connected; let  $U := U(\lambda_k)$  with  $k \geq 3$ ; assume that  $\dim U = (2k - 2)$  [Assumptions 5.2]. Then, the following properties hold.*

- (i) *The map  $\Gamma_{(2k-3)} \ni y \mapsto z(y) \in \Gamma$ , where  $z(y)$  is defined in (5.7) is continuous in  $\Gamma_{(2k-3)}$ . Moreover, if  $\eta \in \Gamma_{(2k-2)}$ , then  $\lim_{y \rightarrow \eta, y \in \Gamma_{(2k-3)}} z(y) = \eta$ , i.e., the map  $y \mapsto z(y)$  extends continuously to  $\Gamma$ , with  $z(\eta) = \eta$  for all  $\eta \in \Gamma_{(2k-2)}$ .*
- (ii) *Let  $C$  be any connected component of  $\Gamma_{(2k-3)}$ . The function  $C \ni y \mapsto z(y) \in \Gamma$  is  $C^\infty$  and monotonic in  $C$  (more precisely, the derivative of  $z$  does not vanish).*
- (iii) *Assume that  $\Gamma_{(2k-2)}$  is not empty, and let  $\eta \in \Gamma_{(2k-2)}$ . When  $y$  is close to  $\eta$ , the points  $y$  and  $z(y)$  lie on either sides of  $\eta$ . More precisely, let  $E : \overline{\mathbb{H}} \rightarrow \overline{\Omega}$  is a conformal map such that  $E(0,0) = \eta$ . For  $t \neq 0$  small enough, let  $\mathcal{S}_b(u_{E(t,0)}) = \{E(t,0), z(E(t,0))\}$  and define  $z(t) := z(E(t,0))$ . Then,*

$$z(t) = -(2k - 3)t + o(t).$$

- (iv) *Assume that  $\Gamma_{(2k-2)}$  is not empty. When the point  $y$  moves clockwise in a connected component  $C$  of  $\Gamma_{(2k-3)}$  the point  $z(y)$  moves counter-clockwise in  $\Gamma$ .*
- (v) *Assume that  $\Gamma_{(2k-2)}$  is not empty. The set  $\Gamma_{(2k-2)}$  cannot be reduced to one point. Each component  $C$  of  $\Gamma_{(2k-3)}$  has two distinct boundary points  $\eta_1, \eta_2 \in \Gamma_{(2k-2)}$ , and its image  $z(C)$  is equal to  $\Gamma \setminus \overline{C}$ . In particular, if  $y \in C$ ,  $z(y) \notin C$ .*

*Proof of Lemma 5.12.*

*Proof of Assertion (i).* Consider a component  $C$  of  $\Gamma_{(2k-3)}$ . Recall that

$$(5.28) \quad \check{u}_y := \begin{cases} \partial_\nu u_y & \text{in the Dirichlet case} \\ u_y|_\Gamma & \text{in the Robin case.} \end{cases}$$

Let  $y \in C$ , and let  $\{y_n\} \subset C$  be a sequence such that  $y_n$  converges to  $y$ , so that  $u_n := u_{y_n}$  converges to  $u := u_y$  (uniformly in the  $C^m$  topology for any fixed  $m$ , see Lemma 5.6). Recall that  $\check{u}$  and  $\check{u}_n$  have precisely two distinct zeros  $y, z(y)$  and  $y_n, z(y_n)$  respectively. Since  $\check{u}_n$  converges uniformly to  $\check{u}$ , and since  $\check{u}$  changes sign at  $z(y)$ , it follows that  $z(y_n)$  belongs to some neighborhood of  $z(y)$ , and that  $z(y_n)$  tends to  $z(y)$ . This proves that  $y \rightarrow z(y)$  is continuous in  $C$ . We now investigate the behavior of  $z(y)$  when  $y$  tends to  $\partial C$  (assuming that  $C \neq \Gamma$ ). Assume that  $\{y_n\} \subset C$ , with  $y_n$  tending to some  $\eta \in \partial C \subset \Gamma_{(2k-2)}$ . Choose a subsequence of  $\{z(y_n)\}$  which converges to some  $z$ . Since  $u_n$  tends to  $u_\eta$ , we conclude that  $\check{u}_\eta(z) = 0$ , and hence that  $z = \eta$  since  $\eta$  is the unique zero of  $\check{u}_\eta$  in  $\Gamma$ .  $\checkmark$

*Assertion (ii).* The properties to be established are local. We work in a neighborhood of some  $y_0 \in \Gamma_{(2k-3)}$ . Taking a suitable conformal mapping as in Paragraph 5.2.5.1, we consider the family of functions  $v_t$  defined in (5.13), near the point  $0 \in \partial \mathbb{H}$  corresponding to  $y_0$ . Since  $\Gamma_{(2k-3)}$  is open in  $\Gamma$ , so does  $\Gamma_{0,(2k-3)}$  in  $\partial \mathbb{H}$ . Hence, there exists  $r_0$  such that  $(-r_0, r_0) \times \{0\} \subset \Gamma_{0,(2k-3)}$ , i.e., for all  $t \in (-r_0, r_0)$ ,  $\rho(v_t, (t, 0)) = (2k - 3)$ . As a consequence, the following properties hold.

$\diamond$  For all  $t \in (-r_0, r_0)$ , the first term  $A_0(t)$  in the Taylor expansion (5.22) is nonzero, so that

$$(5.29) \quad v_t(\xi_1, \xi_2) = A_0(t) P_p(\xi_1 - t, \xi_2) + R_{p+1}(t; \xi_1 - t, \xi_2),$$

where  $P_p = S_p$  in the Dirichlet case,  $P_p = C_p$  in the Robin case, and the remainder term is given by

$$R_{p+1}(t; \xi_1 - t, \xi_2) = \sum_{|\beta|=p+1} R_\beta(t; \xi_1, \xi_2) (\xi_1 - t, \xi_2)^\beta,$$

with  $R_\beta$  as in (5.17).

Taking the derivative of  $v_t$  with respect to  $t$ , and using (2.95), we infer that

$$(5.30) \quad w_t(\xi_1, \xi_2) = -p A_0(t) P_{p-1}(\xi_1 - t, \xi_2) + R_{w,p}(t; \xi_1 - t, \xi_2)$$

where the remainder term  $R_{w,p}(t; \xi_1, \xi_2)$  vanishes at order at least  $p$  at  $\xi = (t, 0)$ . This implies that

$$(5.31) \quad \rho(w_t^\Omega, E_0(t, 0)) = \rho(w_t, (t, 0)) = (2k - 4).$$

◇ We now look at the associated family of maps  $\check{v}_t$  on the boundary  $\partial\mathbb{H}$ .

$$\check{v}_t(\xi_1) = \sum a_j(t) \check{\psi}_j(\xi_1).$$

For convenience, we write the families  $v_t$  and  $\check{v}_t$  as

$$v(t; \xi_1, \xi_2) := \sum a_j(t) \psi_j(\xi_1, \xi_2) \text{ for } (\xi_1, \xi_2) \in \mathbb{H}, \quad t \in (-r_0, r_0),$$

and

$$\check{v}(t; \xi_1) := \sum a_j(t) \check{\psi}_j(\xi_1) \text{ for } (\xi_1, 0) \in \partial\mathbb{H}, \quad t \in (-r_0, r_0).$$

Similarly, for the derivatives with respect to the parameter  $t$ , we write

$$w(t; \xi_1, \xi_2) := \partial_t v(t; \xi_1, \xi_2) = \sum a'_j(t) \psi_j(\xi_1, \xi_2) \text{ for } (\xi_1, \xi_2) \in \mathbb{H}, \quad t \in (-r_0, r_0),$$

and

$$(5.32) \quad \check{w}(t; \xi_1) := \sum a'_j(t) \check{\psi}_j(\xi_1) \text{ for } (\xi_1, 0) \in \partial\mathbb{H}, \quad t \in (-r_0, r_0).$$

◇ The map  $(-r_0, r_0) \ni t \mapsto z(t)$  is such that  $\mathcal{S}_b(v(t; \cdot)) = \{t, z(t)\}$ , where  $z(t) \neq t$ . According to Lemmas 5.6 and 2.19, for all  $t$ , the function  $\check{v}(t; \cdot)$  has a zero of order 1 at the point  $z(t)$ , i.e.  $\check{v}(t; z(t)) = 0$  and  $\partial_{\xi_1} \check{v}(t; z(t)) \neq 0$ . The implicit function theorem implies that  $t \mapsto z(t)$  is  $C^\infty$ . This proves the first half of Assertion (ii).

◇ Since  $\check{v}(t; z(t)) \equiv 0$ , taking the derivative with respect to  $t$ , we obtain

$$\partial_t \check{v}(t; z(t)) + z'(t) \partial_{\xi_1} \check{v}(t; z(t)) \equiv 0.$$

Assuming by contradiction that  $z'(t_0) = 0$  for some  $t_0 \in (-r_0, r_0)$ , we conclude that  $\partial_t \check{v}(t_0; z(t_0)) = 0$ , i.e.,  $\check{w}(t_0; z(t_0)) = 0$ , and hence

$$(5.33) \quad \rho(w(t_0; z(t_0))) \geq 1.$$

From Equations (5.31) and (5.33) we obtain that

$$\rho(w_{t_0}^\Omega, E_0(t_0, 0)) = (2k - 4) \text{ and } \rho(w_{t_0}^\Omega, z(t_0)) \geq 1$$

which imply that the function  $w_{t_0}^\Omega$  belongs to the subspace  $V_{E_0(t_0, 0), z(t_0)}$ . According to Lemma 5.8, this subspace is  $U_{E_0(t_0, 0)}$  so that  $\rho(w_{t_0}^\Omega, E_0(t_0, 0)) = (2k - 3)$  contradicting Equation (5.31). We have proved that the assumption  $z'(t_0) = 0$  yields a contradiction. Hence  $z'(t) \neq 0$  for all  $t \in (-r_0, r_0)$  and Assertion (ii) follows.  $\checkmark$

*Assertion (iii).* As above, we work in the framework described in Paragraph 5.2.5, with  $t$  in an interval  $(-r_0, r_0)$  such that  $\rho(v_t, (t, 0)) = (2k - 3)$  for  $t \neq 0$ , and  $\rho(v_0, 0) = (2k - 2)$ . According to (5.22), we have

$$\begin{aligned} v_t(\xi_1, \xi_2) &= A_0(t)P_p(\xi_1 - t, \xi_2) + A_1(t)P_{p+1}(\xi_1 - t, \xi_2) \\ &\quad + A_0(t)\frac{1}{p+1}h_E(t)Q_{p+1}(\xi_1 - t, \xi_2) + R_{p+2}(t; \xi_1 - t, \xi_2), \end{aligned}$$

with  $A_0(0) = 0$ ,  $A_1(0) \neq 0$ , and  $A_0(t) \neq 0$  for  $t \neq 0$ . (Recall that  $P_p = S_p$ ,  $P_{p+1} = S_{p+1}$  and  $Q_{p+1} = 0$  in the Dirichlet case;  $P_p = C_p$ ,  $P_{p+1} = C_{p+1}$  and  $Q_{p+1} = S_{p+1}$  in the Robin case.)

Using (5.26), we obtain

$$w_0(\xi_1, \xi_2) = [A'_0(0) - (p+1)A_1(0)] P_p(\xi_1, \xi_2) + \mathcal{O}\left((\xi_1^2 + \xi_2^2)^{\frac{p+1}{2}}\right).$$

CLAIM 5.13. *Assume that  $A_0(0) = 0$ ,  $A_1(0) \neq 0$ , and  $A_0(t) \neq 0$  when  $t \neq 0$ . Then,  $A'_0(0) = (p+1)A_1(0)$ .*

*Proof.* Otherwise, we would have  $\text{ord}(w_0, 0) = p$ , and hence  $\rho(w_0, 0) = (2k - 3)$  so that  $w_0^\Omega \in U_{y_0}$ , contradicting the fact that  $\dim U_{y_0} = 1$  since  $u_{y_0} \in U_{y_0}$  with  $\rho(u_{y_0}, y_0) = (2k - 2)$ . The claim is proved.  $\checkmark$

We now use the relations (5.27a) and (5.27b), respectively in the Dirichlet and the Robin case,

$$\left\{ \begin{array}{l} \text{Dirichlet case:} \\ \check{v}_t(\xi_1) = (2k - 2)A_0(t)(\xi_1 - t)^{2k-3} + (2k - 1)A_1(t)(\xi_1 - t)^{2k-2} \\ \quad + \mathcal{O}\left((\xi_1 - t)^{2k-1}\right). \end{array} \right.$$

$$\left\{ \begin{array}{l} \text{Robin case:} \\ \check{v}_t(\xi_1) = A_0(t)(\xi_1 - t)^{2k-3} + A_1(t)(\xi_1 - t)^{2k-2} \\ \quad + \mathcal{O}\left((\xi_1 - t)^{2k-1}\right). \end{array} \right.$$

Choosing  $\xi_1 = z(t)$ , and recalling that  $z(t)$  tends to 0 as  $t$  tends to zero (Assertion (i)), we obtain

$$\left\{ \begin{array}{l} \text{Dirichlet case:} \\ 0 \equiv (2k - 2)A_0(t)(z(t) - t)^{2k-3} + (2k - 1)A_1(t)(z(t) - t)^{2k-2} \\ \quad + \mathcal{O}\left((z(t) - t)^{2k-1}\right). \end{array} \right.$$

$$\left\{ \begin{array}{l} \text{Robin case:} \\ 0 \equiv A_0(t)(z(t) - t)^{2k-3} + A_1(t)(z(t) - t)^{2k-2} \\ \quad + \mathcal{O}\left((z(t) - t)^{2k-1}\right). \end{array} \right.$$

Writing  $A_0(t) = A'_0(0)t + o(t)$ ,  $A_1(t) = A_1(0) + O(t)$  with  $A_1(0) \neq 0$ , and taking into account the fact that  $A'_0(0) = (p+1)A_1(0)$ , we conclude that

$$(5.34) \quad z(t) = -(2k - 3)t + o(t) \text{ as } t \text{ tends to } 0$$

in both the Dirichlet and the Robin case.

For  $t \neq 0$  small enough, Equation (5.34) implies that  $t$  and  $z(t)$  are on either sides of 0. This means that for  $y$  close enough to  $\eta \in \Gamma_{(2k-2)}$ , the points  $y$  and  $z(y)$  are located on either sides of  $\eta$ . Assertion (iii) is proved.  $\checkmark$

*Assertion (iv).* Assume that  $0 \in \Gamma_{0,(2k-2)}$  and  $t \in \Gamma_{0,(2k-3)}$  for  $t \neq 0$ , small enough. Then,  $t^{-1}[z(2t) - z(t)] = z'(\theta_t) = -(2k-3) + o(1)$  for some  $\theta_t$  between  $t$  and  $2t$ . This implies that  $z'(\theta_t) < 0$  for  $t$  small enough. According to Assertion (ii),  $z'(t) < 0$  in the connected components of  $\Gamma_{0,(2k-3)}$  which have 0 as boundary point.

Note that Equation (5.34) also implies that  $z$  is differentiable everywhere on  $\Gamma$ , with derivative equal to  $-(2k-3)$  at the points in  $\Gamma_{(2k-2)}$ . It is not clear though that  $z'$  is continuous everywhere.

*Assertion (v).* Assume that  $\Gamma_{(2k-2)} = \{\eta\}$ . For  $y_0$  close to  $\eta$  and on the right of  $\eta$ , the point  $z(y_0)$  is close to  $\eta$  and on the left of  $\eta$ . When  $y$  moves counter-clockwise from  $y_0$ , the point  $z(y)$  moves clockwise from  $z(y_0)$  and we would eventually find some  $y_1$  with  $z(y_1) = y_1$ , a contradiction. If  $\Gamma_{(2k-2)}$  is not empty, then  $\#(\Gamma_{(2k-2)}) \geq 2$ , and the boundary of a connected component  $C$  of  $\Gamma_{(2k-3)}$  consists of two distinct points  $\eta_1, \eta_2$  belonging to  $\Gamma_{(2k-2)}$ . Since  $z(y)$  tends to  $z(\eta_i)$  when  $y$  tends to  $\eta_i$ , the last assertion follows.  $\checkmark$

Lemma 5.12 is now proved.  $\square$

REMARK 5.14. Under Assumptions 5.2, the Taylor identity (5.22) for the function  $v_t$  yields the Taylor identity (5.26) for its derivative  $w_0$  at  $t = 0$ . Since 0 is an isolated point in  $\Gamma_{0,(2k-2)}$ , we have  $\rho(v_0, 0) = (2k-2)$ , i.e.,  $A_0(0) = 0$ , and Claim 5.13 tells us that  $A'_0(0) = (p+1)A_1(0) \neq 0$ . From (5.26), we deduce that  $\rho(w_0, 0) \geq (2k-2)$ . Since  $w_0$  is orthogonal<sup>1</sup> to  $v_0$ , this implies that  $w_0 = 0$  because  $\dim U_0 = 1$ . The second derivative of  $v_t$  at  $t = 0$  does not vanish, more precisely,

$$\frac{d^2 v_t}{dt^2} \Big|_{t=0}(\xi_1, \xi_2) = -p(p+1)A_1(0)P_{p-1}(\xi_1, \xi_2) + \mathcal{O}\left((\xi_1^2 + \xi_2^2)^{\frac{p}{2}}\right).$$

Since  $v_t$  has norm 1,  $w_t$  is orthogonal to  $v_t$ , and since  $w_0 = 0$ , it follows that  $\frac{d^2 v_t}{dt^2} \Big|_{t=0}$  is orthogonal to  $v_0$ .

REMARKS 5.15.

- 1) In Lemma 5.24, we shall prove that  $\#(\Gamma_{(2k-2)})$  is an even integer.
- 2) In Section 5.3, using a global argument, we shall prove that  $\Gamma_{(2k-2)} \neq \emptyset$ .
- 3) For the time being, note that if  $\Gamma_{(2k-2)}$  were empty, we would have  $z'(t) > 0$ . The function  $z'$  has indeed a constant sign and if  $z'(t)$  were negative, we would reach a contradiction by finding a point  $y_1$  such that  $z(y_1) = y_1$  as in the proof of Assertion (iv).

### 5.2.7. Boundary behavior of the map $\Omega \ni x \mapsto [w_x] \in \mathbb{P}(U)$ .

The assumption that  $\Omega$  is simply connected in this subsection might be necessary. It is motivated by Remark 1.2 and also makes the proofs of the following lemmas simpler. It would be worthwhile determining where the assumption that  $\Omega$  is simply connected is actually necessary.

The proof of the next lemma relies very much on Section 2.4, in particular Subsection 2.4.5.

LEMMA 5.16. *Assume that  $\Omega$  is simply connected; let  $U := U(\lambda_k)$  with  $k \geq 3$ ; assume that  $\dim U = (2k-2)$  [Assumptions 5.2]. Let  $\{x_n\} \subset \Omega$  be a sequence*

<sup>1</sup>Recall that orthogonality is meant with respect to the inner product induced by the  $L^2$ -inner product of eigenfunctions.

converging to some  $y \in \Gamma$ . Let  $\{w_n\}$  be a corresponding sequence of eigenfunctions, with  $w_n := w_{x_n} \in W_{x_n} \cap \mathbb{S}(U)$ .

(i) If  $w$  is a limit point of  $\{w_n\}$ , then  $w \in U_y$ . In particular, the continuous maps

$$\Omega \ni x \mapsto [w_x] \text{ of Lemma 5.4,}$$

and

$$\Gamma \ni y \mapsto [u_y] \text{ of Lemma 5.6,}$$

give rise to a continuous map  $x \mapsto [\bar{w}_x]$  from  $\bar{\Omega}$  into  $\mathbb{P}(U)$ .

- (ii) The point  $y$  belongs to  $\Gamma_{(2k-3)}$  if and only if, for  $n$  large enough,  $\mathcal{S}_b(w_n) = \{y_n, z_n\}$  with  $y_n \rightarrow y$ , and  $z_n \rightarrow z(y) \neq y$ , where  $\mathcal{S}_b(u_y) = \{y, z(y)\}$ .
- (iii) The point  $y$  belongs to  $\Gamma_{(2k-2)}$  if and only if there exists an infinite subsequence  $\{w_{s(n)}\}$  such that  $\mathcal{S}_b(w_{s(n)}) = \emptyset$ , or an infinite subsequence  $\{w_{s(n)}\}$  such that  $\mathcal{S}_b(w_{s(n)}) \neq \emptyset$ , and the points in  $\mathcal{S}_b(w_{s(n)})$  converge to  $y$ .
- (iv) There exists a continuous map  $x \mapsto \bar{w}_x$ , from  $\bar{\Omega}$  to  $\mathbb{S}(U)$ , whose restrictions to  $\Omega$  and to  $\Gamma$  are  $C^\infty$ , and such that  $\bar{w}_x \in W_x$  whenever  $x \in \Omega$  and  $\bar{w}_x \in U_x$  whenever  $x \in \Gamma$ .

For the proof of Lemma 5.16, it suffices to reason locally near a point  $y \in \Gamma$ . Using a conformal map  $E : \mathbb{H} \rightarrow \Omega$  as in Section 2.4, we work with the functions  $v_n := w_n \circ E$  and  $v := w \circ E$  in  $D_+(0, r_0)$ . Let  $\xi_n \in \mathbb{H}$  be the points such that  $E(\xi_n) = x_n$ . In the sequel, we use the notation of Paragraph 2.4.3.2:  $J_E$  is the Jacobian of the conformal map, and

$$V_E := J_E(V \circ E), \quad h_E := \sqrt{J_E}(h \circ E).$$

At some point in the proof of Lemma 5.16, we will need the following *energy argument*.

LEMMA 5.17 (Energy argument). *Working with the eigenvalue problem (2.47)-(2.48),*

$$\begin{cases} (-\Delta + J_E V_E)v = \lambda J_E v & \text{in } \mathbb{H} \\ B_E(v) = 0 & \text{on } \partial\mathbb{H}, \end{cases}$$

there exists  $r_E > 0$  such that

$$(5.35) \quad \mu_1(D_+(0, r)) > \lambda_k$$

for any  $r \leq r_E$ . Here  $\lambda_k$  is the eigenvalue associated with  $U$ , and  $\mu_1(D_+(0, r))$  denotes the lowest eigenvalue of  $(-\Delta + J_E V_E)v = \lambda J_E v$  in the domain  $D_+(0, r)$  with the following mixed boundary conditions: Dirichlet on the subset  $C_+(0, r) = \partial D_+(0, r) \cap \mathbb{H}$ , and the current boundary condition  $B_E(u) = 0$  (Dirichlet or Robin) on the subset  $(-r, r) \times \{0\} = \partial D_+(0, r) \cap \partial\mathbb{H}$ .

*Proof of Lemma 5.17.* We give the proof of the lemma when the boundary condition (2.48) on  $\partial\mathbb{H}$  is the  $h$ -Robin condition (the Dirichlet or Neumann cases are simpler to deal with). We have to consider the Rayleigh quotient  $R(u)$  for  $u \in \mathcal{H}_r$  where

$$\mathcal{H}_r := \left\{ u \in H^1(D_+(0, r)) \mid u = 0 \text{ on } C_+(0, r) \right\},$$

and

$$R(u) := \left( \int_{D_+(0, r)} (|du|^2 + V_E u^2) d\xi + \int_{-r}^r h_E u^2(t, 0) dt \right) \left( \int_{D_+(0, r)} J_E u^2 d\xi \right)^{-1}.$$



On  $\overline{D}_+(0, r_0)$ , the functions  $V_E$  and  $h_E$  are bounded from below, and  $J_E$  is bounded from above and below by positive constants. Since  $\int_{-r}^r u^2(t, 0) dt \leq r \int_{D_+(0, r)} |du|^2 d\xi$ , it follows that

$$R(u) \geq (1 - c_1 r) \left( \sup_{D_+(0, r_0)} J_E \right)^{-1} R_0(u) - c_2,$$

where  $c_1$  and  $c_2$  are positive constants depending only on  $(V, h, E, r_0)$ , and  $R_0(u) := \left( \int_{D_+(0, r)} |du|^2 d\xi \right) \left( \int_{D_+(0, r)} u^2 d\xi \right)^{-1}$ . The quotient  $R_0(u)$  is bounded from below by the least eigenvalue of the Laplacian with mixed boundary conditions, Dirichlet on  $C_+(0, r)$  and Neumann on  $(-r, r)$ . Hence,  $R_0(u) \geq \frac{\pi j_{0,1}^2}{r^2}$ , the least Dirichlet eigenvalue of  $D(0, r)$ , the disk of center 0 and radius  $r$ . The lemma follows.  $\square$

**REMARKS 5.18.** The proof of Lemma 5.17 shows that a similar result holds if we fix the current boundary condition (2.48) on a given interval  $(a, b) \subset (-r, r)$ , and the Dirichlet boundary condition on  $\partial D_+(0, r) \setminus ((a, b) \times \{0\})$ .

*Proof of Lemma 5.16.* We divide the proof of Lemma 5.16 into several steps labeled **(A)**, **(B)**,  $\dots$ .

**(A)** To the sequence of interior points  $\{x_n\} \subset \Omega$  we associate a sequence  $\{w_n := w_{x_n}\}$  in the sphere  $\mathbb{S}(U)$  (Lemma 5.4). Taking a subsequence if necessary, we may assume that  $\{w_n\}$  converges to some  $w \in \mathbb{S}(U)$ . Then, the convergence is uniform in  $C^m$  for any fixed  $m \geq 0$ . Since  $\nu(w_n, x_n) = 2(k-1)$ , or equivalently  $\text{ord}(w_n, x_n) = (k-1)$ , with  $k \geq 3$ , and since the convergence is uniform, we have  $\text{ord}(w, y) \geq (k-1) \geq 2$ , so that  $y$  is a boundary singular point of the  $\lambda_k$ -eigenfunction  $w$ .

Define  $p := \text{ord}(w, y)$ ,  $q := \rho(w, y)$ . Recall that  $p = (q+1)$  in the Dirichlet case, and  $p = q$  in the Robin case.

By Lemma 2.20, the (sub)sequence  $\{\mathcal{Z}(w_n)\}$  converges to  $\mathcal{Z}(w)$  in the Hausdorff distance. This in particular implies that the set  $\mathcal{Z}(w)$  is connected.

**(B)** The singular points of the nodal set  $\mathcal{Z}(w)$  are isolated. We can choose some point  $y_0 \in \Gamma$  with  $y_0 \notin \mathcal{S}_b(w)$ . According to Section 2.4, there is a conformal map  $E : \mathbb{H} \rightarrow \Omega$  which extends smoothly to  $\overline{\mathbb{H}}$ , sends 0 to  $y$ , and the point at infinity on  $\partial\mathbb{H}$  to  $y_0$ . Fix the map  $E$ , and choose some  $r_0 > 0$  such that the nodal set  $\mathcal{Z}(w \circ E)$  is contained in  $D_+(0, r_0) \cup (-r_0, r_0) \times \{0\}$ . For  $n$  large enough, the nodal sets  $\mathcal{Z}(w_n \circ E)$  will also be contained in  $D_+(0, r_0) \cup (-r_0, r_0) \times \{0\}$ .

To prove Assertion (i) in Lemma 5.16, we apply Subsection 2.4.5, to the function  $v$ . Let  $(\rho, \omega)$  be the polar coordinates at  $0 \in \overline{\mathbb{H}}$ ,  $\xi = (\rho \cos \omega, \rho \sin \omega)$ . We use the following notation,

$$\begin{cases} [r, \omega] := (r \cos \omega, r \sin \omega), \\ C_+(0, r) := \{[r, \omega] \mid \omega \in (0, \pi)\}, \\ \text{and we fix } \alpha_1 \in (0, \frac{\pi}{8}), \alpha_p := \frac{\alpha_1}{p}. \end{cases}$$

We consider the Dirichlet and Robin boundary conditions separately.

$\diamond$  In the Dirichlet case,  $v([r, \omega]) = a_v \rho^p \sin(p\omega) + \mathcal{O}(\rho^{p+1})$ , for some  $a_v \neq 0$ . Define the rays

$$\{\omega = \omega_j \mid 1 \leq j \leq p-1\},$$

where  $\omega_j := j\frac{\pi}{p}$ . As in (2.80), consider the following arcs.

$$(5.36) \quad \begin{cases} \mathcal{G}_d(r, j) := \{[r, \omega] \mid \omega \in (\omega_j - \alpha_p, \omega_j + \alpha_p)\}, \text{ for } 1 \leq j \leq (p-1), \\ \mathcal{R}_d(r, j) := \{[r, \omega] \mid \omega \in [\omega_j + \alpha_p, \omega_{j+1} - \alpha_p]\}, \text{ for } 0 \leq j \leq (p-1), \\ \mathcal{B}_d(r, 0) := \{[r, \omega] \mid \omega \in (0, \alpha_p)\}, \\ \mathcal{B}_d(r, p) := \{[r, \omega] \mid \omega \in [\pi - \alpha_p, \pi)\}. \end{cases}$$

These ‘‘colored arcs’’ are displayed in Figure 5.3 (left picture, here  $p := \text{ord}(v, 0) = 8$ ,  $q := \rho(v, 0) = 7$ ).

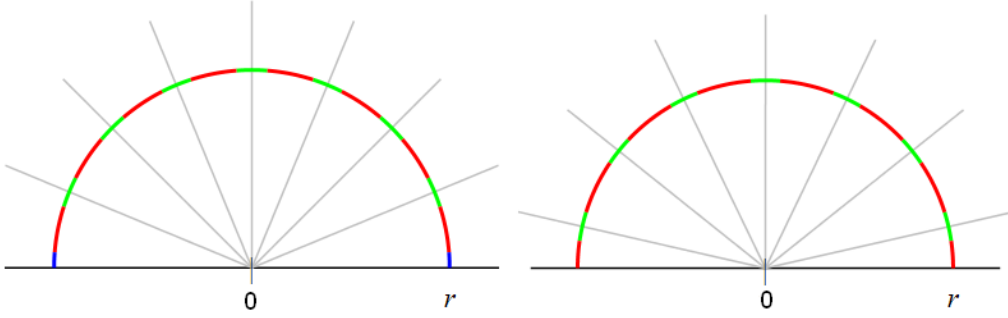


FIGURE 5.3. ‘‘Colored arcs’’ for  $v$  with  $\rho(v, 0) = 7$  (Dirichlet/Robin)

According to Proposition 2.40, there exists some  $r_1$ ,  $0 < r_1 \leq \frac{r_0}{2}$ , such that the following properties hold for any  $r \leq r_1$ , see Equation (2.81).

$$(5.37) \quad \begin{cases} \pm (-1)^j \text{sgn}(a_v) v([r, \omega_j \pm \alpha_p]) \geq \frac{1}{2} |a_v| \sin(\alpha_1) r^p. \\ |\partial_\omega v([r, \omega])| \geq \frac{p}{2} |a_v| \cos(\alpha_1) r^p \text{ in each } \mathcal{G}_d(r, j), 1 \leq j \leq (p-1), \\ \text{and } v([r, \omega]) \text{ vanishes precisely once in each arc.} \\ |\partial_\omega v([r, \omega])| \geq \frac{p}{2} |a_v| \cos(\alpha_1) r^p \text{ in } \mathcal{B}_r(r, 0) \cup \mathcal{B}_d(r, p), \\ \text{and } v(r, \omega) \text{ does not vanish in these arcs.} \\ |v([r, \omega])| \geq \frac{1}{2} |a_v| \sin(\alpha_1) r^p \text{ in } \mathcal{R}_d(r, j), 0 \leq j \leq (p-1), \\ \text{and } v(r, \omega) \text{ does not vanish in these arcs.} \end{cases}$$

◇ In the Robin case,  $v([\rho, \omega]) = a_v \rho^p \cos(p\omega) + \mathcal{O}(\rho^{p+1})$ . Define the rays

$$\{\omega = \omega'_j \mid 1 \leq j \leq p\},$$

where  $\omega'_j := (j - \frac{1}{2})\frac{\pi}{p}$ . As in (2.88), consider the following arcs.

$$(5.38) \quad \begin{cases} \mathcal{G}_n(r, j) := \{[r, \omega] \mid \omega \in (\omega'_j - \alpha_p, \omega'_j + \alpha_p)\}, \text{ for } 1 \leq j \leq p, \\ \mathcal{R}_n(r, j) := \{[r, \omega] \mid \omega \in [\omega'_j + \alpha_p, \omega'_{j+1} - \alpha_p]\}, \text{ for } 1 \leq j \leq (p-1), \\ \mathcal{R}_n(r, 0) := \{[r, \omega] \mid \omega \in (0, \omega'_1 - \alpha_p)\}, \\ \mathcal{R}_n(r, p) := \{[r, \omega] \mid \omega \in [\omega'_p + \alpha_p, \pi)\}. \end{cases}$$

These ‘‘colored arcs’’ are displayed in Figure 5.3 (right picture, here  $p := \text{ord}(v, 0) = 7$ ,  $q := \rho(v, 0) = 7$ ). According to Proposition 2.41, there exists some  $r_1$ ,  $0 < r_1 \leq \frac{r_0}{2}$ ,

such that the following properties hold for any  $r \leq r_1$ , see Equation (2.89).

$$(5.39) \quad \left\{ \begin{array}{l} \mp (-1)^j \operatorname{sgn}(a_v) v([r, \omega'_j \pm \alpha_p]) \geq \frac{1}{2} |a_v| \sin(\alpha_1) r^p. \\ |\partial_\omega v([r, \omega])| \geq \frac{p}{2} |a_v| \cos(\alpha_1) r^p \text{ in each } \mathcal{G}_n(r, j), 1 \leq j \leq p, \\ \text{and } v([r, \omega]) \text{ vanishes precisely once in each arc.} \\ |v([r, \omega])| \geq \frac{1}{2} |a_v| \sin(\alpha_1) r^p \text{ in } \mathcal{R}_n(r, 0) \cup \mathcal{R}_n(r, p), \\ \text{and hence } v([r, \omega]) \text{ does not vanish in these arcs.} \\ |v([r, \omega])| \geq \frac{1}{2} |a_v| \sin(\alpha_1) r^p \text{ in } \mathcal{R}_n(r, j), 1 \leq j \leq (p-1), \\ \text{and } v(r, \omega) \text{ does not vanish in these arcs.} \end{array} \right.$$

The arcs  $\mathcal{G}(r, j)$  appear in “green” in Figure 5.3. In both cases,  $\mathcal{Z}(v) \cap D_+(0, r_1)$  consists of  $q$  nodal arcs emanating from 0,  $r \mapsto \delta_j(r) := [r, \tilde{\omega}_j(r)]$ ,  $1 \leq j \leq q$ , where the functions  $\tilde{\omega}_j(r)$  are smooth for  $0 < r < r_1$ . These arcs are transverse to the half circles  $C_+(0, r)$ .

Fix  $r_2$  such that  $0 < r_2 < r_1$ . When  $x_n$  tends to  $y$  in  $\bar{\Omega}$ , the sequence  $\{w_n\}$  tends to  $w$  uniformly in the  $C^m$  topology for any fixed  $m$ . Similarly, when the sequence  $\{\xi_n\}$  tends to 0 in  $\bar{\mathbb{H}}$ , the sequence  $\{v_n\}$  tends to  $v$  uniformly in the  $C^m$  topology in  $D_+(0, r_0)$ . This implies that the properties (5.37) (Dirichlet case) and (5.39) (Robin case) are satisfied by the functions  $v_n$  provided that  $r_2 < r < r_1$ , provided we relax the constant  $|a_v|$  to  $\frac{|a_v|}{2}$  in the right hand sides of the above inequalities, and provided we choose  $n$  large enough implying that  $v_n$  is  $C^1$ -close to  $v$ . This proves the following claim.

**CLAIM 5.19.** *Fix any  $r_2$  such that  $0 < r_2 < r_1$ . Then, for  $n$  large enough, depending on  $r_2$ , and for any  $r$  such that  $r_2 \leq r \leq r_1$ ,*

$$(5.40) \quad \left\{ \begin{array}{l} \mathcal{Z}(v_n) \cap C_+(0, r) \subset \bigcup_{j=1}^q \mathcal{G}(r, j), \\ \text{and} \\ \mathcal{Z}(v_n) \text{ crosses each } \mathcal{G}(r, j) \text{ precisely once.} \end{array} \right.$$

From now on, we assume that:

- ◇  $r_1 < r_E$  and we fix  $r_2$ ,  $0 < r_2 < r_1$ ,
- ◇  $n$  is large enough so that both (5.35) and (5.40) are satisfied for any  $r_2 < r < r_1$ , with  $\{\xi_n\} \subset D_+(0, r_2/2)$  close enough to 0.

(C) Recall that  $v_n = w_n \circ E$ ,  $v = w \circ E$ , and  $x_n = E(\xi_n)$ . We now study the sequence  $\{v_n\}$ , with  $\{\xi_n\} \subset D_+(0, r_2/2)$ . Taking Lemma 5.4 into account, there are two possible cases.

**Case C1.** *There exists an infinite subsequence  $\{v_{s(n)}\}$  of the sequence  $\{v_n\}$  such that, for all  $n$ ,  $\mathcal{S}_b(v_{s(n)}) = \emptyset$ .*

In this case, according to the proof of Lemma 5.4, the nodal set  $\mathcal{Z}(v_{s(n)})$  consists of  $(k-1)$  simple loops at  $\xi_{s(n)}$ . These loops do not intersect away from  $\xi_{s(n)}$ , and do not hit  $\partial\mathbb{H}$ . Choose  $\gamma$ , any of these loops. Since  $\xi_{s(n)} \in D_+(0, r_2/2)$ , either the loop  $\gamma$  crosses  $C_+(0, r_2)$  at (at least) two distinct points  $z_{\gamma,1}$  and  $z_{\gamma,2}$ , or it is entirely contained in  $D_+(0, r_2)$ . In the latter case, the function  $v_{s(n)}$  would have a nodal domain contained in  $D_+(0, r_2)$ . Taking into account our choice for  $r_2$  and

Lemma 5.17 (Energy argument), this would contradict (5.35), see Figure 5.4 (right)<sup>2</sup>. For each  $n$ , the set  $\mathcal{Z}(v_{s(n)})$  consists of  $(k - 1)$  loops which do not intersect away from  $\xi_{s(n)}$ . It follows that we have at least  $(2k - 2)$  distinct points  $z_{s(n),j}$  in  $C_+(0, r_2) \cap \mathcal{Z}(v_{s(n)})$ , for  $1 \leq j \leq (2k - 2)$ .

By Claim 5.19,  $\mathcal{Z}(v_{s(n)})$  can only intersect  $C_+(0, r_2)$  in the arcs  $\mathcal{G}(r_2, j)$ , and at only one point for each  $j$ . This means that  $q \geq (2k - 2)$ , i.e.,  $\rho(w, y) = \rho(v, 0) \geq (2k - 2)$ . From Lemma 5.6 we infer that  $w \in U_y$ , and  $\rho(w, y) = (2k - 2)$ , so that  $y \in \Gamma_{(2k-2)}$ .

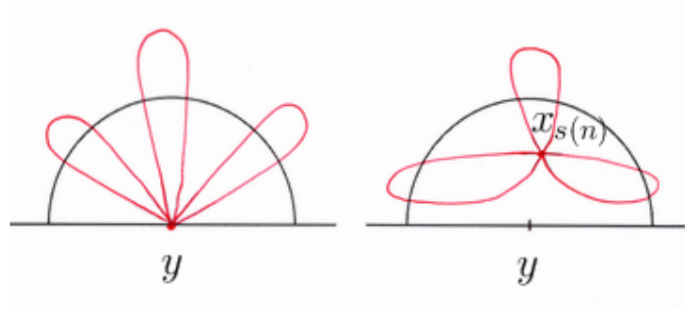


FIGURE 5.4. Lemma 5.16, Case C1: nodal patterns for  $w$  and  $w_{s(n)}$

Figure 5.5 displays forbidden configurations for the nodal sets  $\mathcal{Z}(w_{s(n)})$ .

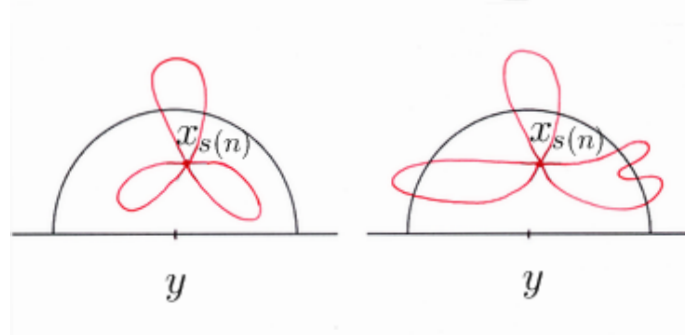


FIGURE 5.5. Lemma 5.16, Case C1: forbidden configurations for  $w_{s(n)}$

**Case C2.** *There exists an infinite subsequence  $\{v_{s(n)}\}$  such that, for each  $n$ , we have  $\mathcal{S}_b(v_{s(n)}) \neq \emptyset$ .*

In this case, according to the proof of Lemma 5.6, the nodal set  $\mathcal{Z}(v_{s(n)})$  consists of  $(k - 2)$  simple loops at  $\xi_{s(n)}$ , and two simple nodal intervals from  $\xi_{s(n)}$  to the boundary  $\partial\mathbb{H}$ . The loops do not intersect away from  $\xi_{s(n)}$ , and do not hit  $\partial\mathbb{H}$ . The nodal intervals do not intersect each other, except at  $\xi_{s(n)}$ , and possibly on  $\partial\mathbb{H}$  if they hit  $\partial\mathbb{H}$  at the same point; they do not intersect the loops away from  $\xi_{s(n)}$ . The energy argument (Lemma 5.17) used in Case C1, shows that each loop in  $\mathcal{Z}(v_{s(n)})$  intersects  $C_+(0, r_2)$  at (at least) two distinct points. A similar energy argument for mixed boundary conditions (Dirichlet on the nodal intervals, and the given boundary condition, Dirichlet or Robin, on  $\partial\mathbb{H}$ ) shows that the nodal intervals cannot both be contained in  $D_+(0, r_2)$ , and at least one of them crosses  $C_+(0, r_2)$ , see Figure 5.7.

<sup>2</sup>We draw the following pictures in a domain  $\Omega$  whose boundary  $\Gamma$  is a segment around  $y$ .

Indeed, there would otherwise exist a nodal domain  $\Omega_1$  of  $v_{s(n)}$  with  $\Omega_1 \subset D_+(0, r)$  as in Figure 5.6 (such a domain appears in Figure 5.8 (right), with  $y_{s(n),2} = y_{s(n),1}$ , and in Figure 5.9 (left)). The function  $v_{s(n)}|_{\Omega_1}$  would be a first eigenfunction of  $(-\Delta + J_E V \circ E) u = \lambda J_E u$  in  $\Omega_1$ , with the Dirichlet boundary condition on the nodal arcs from  $\xi_{s(n)}$  to the boundary, and the given boundary condition (2.48) on the interval between  $y_{s(n),1}$  and  $y_{s(n),2}$ , with associated first eigenvalue  $\lambda_k$ . Consider the function defined by

$$f(x) := \begin{cases} v_{s(n)}(x) & \text{if } x \in \Omega_1 \\ 0 & \text{if } x \in D_+(0, r) \setminus \Omega_1. \end{cases}$$

The function  $f$  satisfies the  $B_E$  boundary condition (Dirichlet or Robin) on the segment  $(y_{s(n),1}, y_{s(n),2})$ , vanishes on the nodal arcs from  $x_{s(n)}$  to  $y_{s(n),1}$  and  $y_{s(n),2}$ , and is 0 outside  $\Omega_1$ .

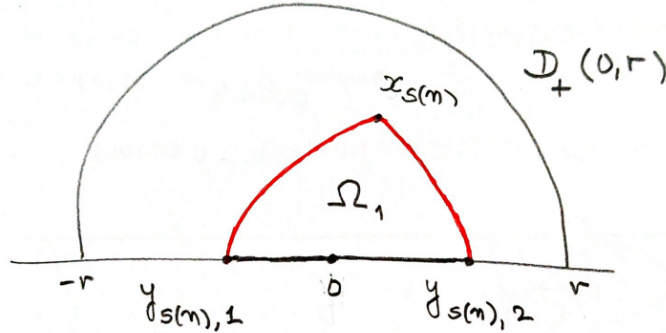


FIGURE 5.6. Proof of Lemma 5.16: the domain  $\Omega_1$

Then,  $f \in H^1(D_+(0, r))$  and vanishes on  $\partial D_+(0, r)$ , except possibly on the segment  $(y_{s(n),1}, y_{s(n),2})$ . Looking at the quadratic forms, and using Lemma 5.17 and Remark 5.18, we conclude that

$$\lambda_k = \mu_1(\Omega_1) > \mu_1(D_+(0, r)) > \lambda_k,$$

a contradiction.

Finally, for each  $n$ , we have at least  $(2k - 3)$  distinct points in  $C_+(0, r_2) \cap \mathcal{Z}(v_{s(n)})$ , for  $1 \leq j \leq (2k - 3)$ . As in Case C1, we conclude that  $q \geq (2k - 3)$ , i.e., that  $\rho(w, y) = \rho(v, 0) \geq (2k - 3)$  so that  $w \in U_y$ , and we have two possible cases, either  $\rho(w, y) = (2k - 3)$  and  $y \in \Gamma_{(2k-3)}$ , or  $\rho(w, y) = (2k - 2)$  and  $y \in \Gamma_{(2k-2)}$

Claim 5.19 also implies that, for  $n$  large enough,  $Z(v_{s(n)})$  meets  $C_+(0, r_2)$  at precisely  $(2k - 3)$  or  $(2k - 2)$  points.

At this stage we have proved that the only possible limit points of a sequence  $\{w_n\}$  are in  $U_y$ , see Figure 5.4 (left). Since  $\dim U_y = 1$ , this proves Assertion (i) of the lemma. ✓

According to Lemma 5.6, we have  $\mathcal{S}_b(v_{s(n)}) = \{\eta_{s(n),1}, \eta_{s(n),2}\}$  possibly with  $\eta_{s(n),1} = \eta_{s(n),2}$ . Recalling that  $y = E(0)$ , the only possible limit points of these sequences are

$$\begin{cases} 0 & \text{if } \rho(v, 0) = (2k - 2), \\ 0 \text{ and } \zeta & \text{if } \rho(v, 0) = (2k - 3), \end{cases}$$

where  $v = u_y \circ E$ ,  $\mathcal{S}_b(v) = \{0, \zeta\}$ , with  $\zeta \neq 0$ . When  $\rho(v, 0) = (2k - 3)$ ,  $\rho(v, \zeta) = 1$ , and the function  $\check{v}$  vanishes and changes sign at 0 and  $\zeta$ . Since  $\{v_{s(n)}\}$  converges to  $v$   $C^1$ -uniformly, this implies that, for  $n$  large enough, the function  $\check{v}_{s(n)}$  changes sign near 0 and near  $\zeta$ , and hence that one sequence, say  $\{\eta_{s(n),2}\}$  tends to  $\zeta$ , and the other  $\{\eta_{s(n),1}\}$  tends to 0. Note that they cannot both tend to  $\zeta$  since  $\rho(v, \zeta) = 1$ . When  $\rho(v, 0) = (2k - 2)$ , the sequences  $\{\eta_{s(n),1}\}$  and  $\{\eta_{s(n),2}\}$  must both converge to 0.

Applying Claim 5.19, we find that there are three sub-cases.

**C2 (i):** There exists a subsequence  $\{v_{s(n)}\}$  such that the sequences  $\{\eta_{s(n),1}\}$  and  $\{\eta_{s(n),2}\}$  coincide and tend to 0. For energy reasons ( $r_1 < r_E$ ), the arcs from  $\xi_{s(n)}$  to  $\eta_{s(n),1}$  and  $\eta_{s(n),2}$  cannot both be contained in  $D_+(0, r_2)$ . One of these arcs, and actually only one for  $n$  large enough, has to meet  $C_+(0, r_2)$  at two distinct points, see Figure 5.7 (left).

**C2 (ii):** There exists a subsequence  $\{v_{s(n)}\}$  such that  $\eta_{s(n),1} \neq \eta_{s(n),2}$ , and both tend to 0. For energy reasons ( $r_1 < r_E$ ), the arcs from  $\xi_{s(n)}$  to  $\eta_{s(n),1}$  and  $\eta_{s(n),2}$  cannot both be contained in  $D_+(0, r_2)$ . One of these arcs, and actually only one for  $n$  large enough, has to meet  $C_+(0, r_2)$  at two distinct points. See Figure 5.7 (center).

**C2 (iii):** There exists a subsequence  $\{v_{s(n)}\}$  such that  $\eta_{s(n),1} \neq \eta_{s(n),2}$ , with  $\eta_{s(n),1}$  tending to 0 and  $\eta_{s(n),2}$  tending to some  $\zeta \neq 0$ . For  $n$  large enough, the arc from  $\xi_{s(n)}$  to  $\eta_{s(n),2}$  intersects  $C_+(0, r_2)$  at one point, and the arc from  $\xi_{s(n)}$  to  $\eta_{s(n),1}$  stays inside  $D_+(0, r_2)$ . See Figure 5.7 (right).

In subcases C2 (i) and C2 (ii), we have  $\rho(w, y) = \rho(v, 0) = (2k - 2)$ , so that  $y \in \Gamma_{(2k-2)}$ . In subcase C2 (iii), we have  $\rho(w, y) = \rho(v, 0) = (2k - 3)$ , so that  $y \in \Gamma_{(2k-3)}$  with  $z(y) = E(\zeta)$ , the limit of  $\{E(\eta_{s(n),2})\}$ .

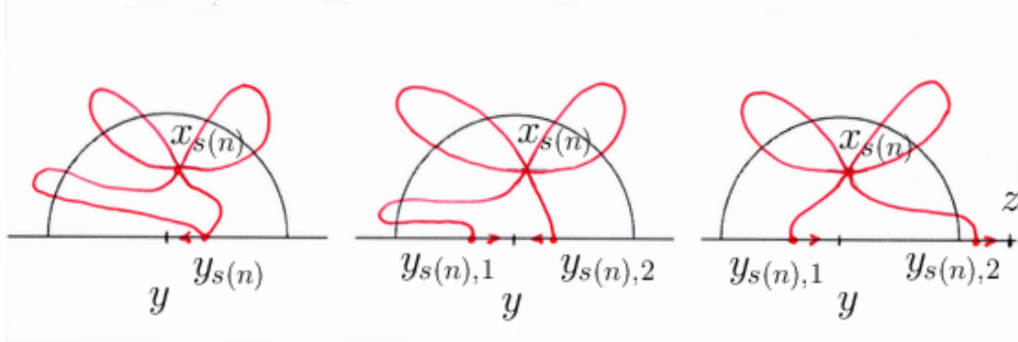


FIGURE 5.7. Lemma 5.16, Case C2: nodal patterns for  $w_{s(n)}$

Figures 5.8 and 5.9 display forbidden configurations for the nodal sets  $\mathcal{Z}(w_{s(n)})$  when  $\mathcal{S}_b(w_{s(n)}) \neq \emptyset$ .

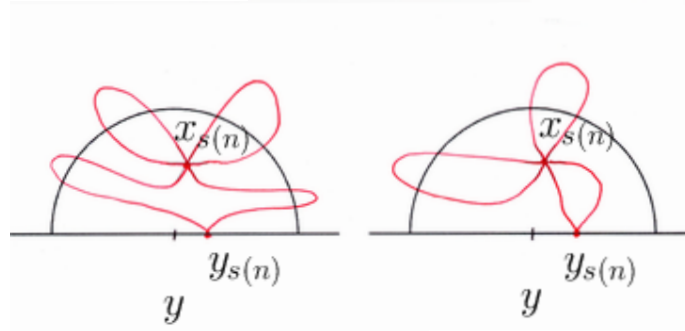


FIGURE 5.8. Lemma 5.16, Case C2(i): forbidden configurations for  $w_{s(n)}$

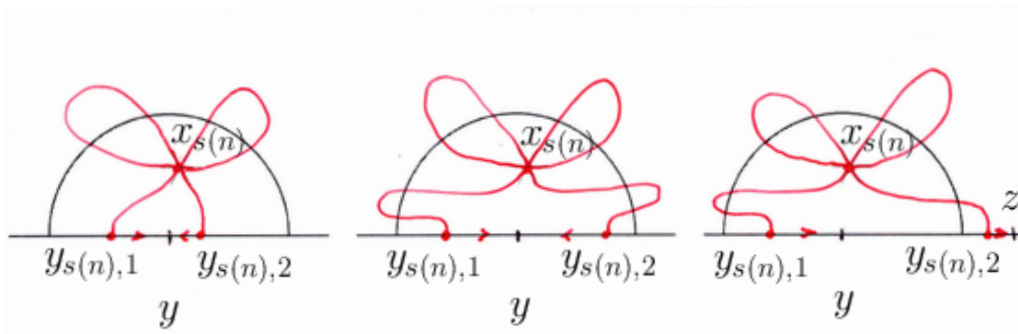


FIGURE 5.9. Lemma 5.16, Case C2(ii)/(iii): forbidden configurations for  $w_{s(n)}$

This proves Assertions (ii) and (iii). ✓

*Assertion (iv).* Since  $\bar{\Omega}$  and  $\mathbb{S}(U)$  are simply connected, the map from  $\bar{\Omega}$  to  $\mathbb{P}(U)$  given by Assertion (i) can be lifted to the  $\mathbb{S}(U)$  with the desired properties. ✓

The proof of Lemma 5.16 is complete. □

REMARK 5.20. As a byproduct of the proof of Lemma 5.16, we obtain the configurations of the nodal sets  $\mathcal{Z}(w_x)$  when  $x \in \Omega$  is close to some  $y \in \Gamma$ . When  $y \in \Gamma_{(2k-3)}$ ,  $\mathcal{S}_b(u_y) = \{y, z(y)\}$  with  $z(y) \neq y$ . For  $x$  close enough to  $y$ ,  $\mathcal{S}_b(w_x) = \{y(x), z(x)\}$  with  $y(x) \neq z(x)$ ,  $y(x)$  close to  $y$  and  $z(x)$  close to  $z(y)$ . When  $y \in \Gamma_{(2k-2)}$ ,  $\mathcal{S}_b(u_y) = \{y\}$ . For  $x$  close enough to  $y$ ,  $\mathcal{S}_b(w_x)$  might be empty or consist of one or two points close to  $y$ .

Figures 5.4 and 5.7 display typical configurations for  $\mathcal{Z}(w_n)$  when  $r_1 < r_E$  is small enough and  $n$  large: the loops intersect  $E(C_+(0, r_2))$  at two distinct points; one arc exits  $E(D_+(0, r_0))$ .

Figures 5.5, 5.8 and 5.9 display forbidden configurations for  $\mathcal{Z}(w_n)$  when  $r_2$  is small enough and  $n$  large: a loop cannot be contained in  $E(D_+(0, r_2))$ ; the arcs cannot both be contained in  $E(D_+(0, r_2))$ ; the arcs cannot both meet  $E(C_+(0, r_2))$ .

REMARK 5.21. The *nodal patterns* displayed in the above figures hold for both the Dirichlet and Robin boundary conditions. Unless otherwise stated this remark applies to all figures of this section.

REMARK 5.22. For  $x \in \Omega$ , let  $h_{x,(k-1)}(\bar{w}_x)$  be the first nonzero term in the Taylor expansion of  $\bar{w}_x$  at the point  $x$  (this is a harmonic polynomial of degree  $(k - 1)$ ). Then, the map  $x \rightarrow h_{x,(k-1)}(\bar{w}_x)$  is continuous, and extends continuously to  $\bar{\Omega}$ . Unfortunately, this extension is not so interesting because  $\lim_{x \rightarrow y \in \Gamma} h_{x,(k-1)}(\bar{w}_x) = 0$  since  $\bar{w}_x$  tends to  $\bar{w}_y \in U_y$ , so that  $h_{y,(k-1)}(\bar{w}_y) = 0$ . See also the final comment in [BeNP2016]. We will mainly use Assertions (ii) and (iii).

REMARK 5.23. In this Subsection 5.2.7, we considered the behavior of  $\mathcal{Z}(w_x)$  when  $x$  tends to some fixed  $y \in \Gamma$ . The radii  $r_0, r_E, r_1$  which appear in the proofs depend on  $y$  and  $E$ . In the next sections we will need to take care of these constants for varying  $y$ 's.

### 5.2.8. Behavior of the combinatorial types of the functions $u_y$ .

LEMMA 5.24. *Assume that  $\Omega$  is simply connected; let  $U := U(\lambda_k)$  with  $k \geq 3$ ; assume that  $\dim U = (2k - 2)$  [Assumptions 5.2]. Then, the following properties hold.*

- (i) *The combinatorial type of a generator  $u_y$  of  $U_y$  is constant in any component of  $\Gamma_{(2k-3)}$  in the sense that the maps  $y \mapsto \tau_y^U(\downarrow)$  and  $y \mapsto \tau_y^U$  are constant in each component of  $\Gamma_{(2k-3)}$ .*
- (ii) *Assume that  $\Gamma_{(2k-2)}$  is not empty, and let  $\eta \in \Gamma_{(2k-2)}$ . The eigenfunctions  $u_\eta$  have different combinatorial types on either sides of  $\eta$ . Then,  $\#(\Gamma_{(2k-2)}) \geq 2$ .*
- (iii) *Assume that  $\Gamma_{(2k-2)}$  is not empty. Let  $\eta_1 \neq \eta_2$  be two points of  $\Gamma_{(2k-2)}$  such that the open arc  $\mathcal{A}(\eta_1, \eta_2)$  is contained in  $\Gamma_{(2k-3)}$ . The combinatorial types  $\tau_{\eta_1}$  and  $\tau_{\eta_2}$  are different.*
- (iv) *Assume that  $\Gamma_{(2k-2)}$  is not empty, then  $\#(\Gamma_{(2k-2)})$  is an even positive integer.*

*Proof of Lemma 5.24.*

*Assertion (i).* Let  $C$  be a component of  $\Gamma_{(2k-3)}$ . For  $y \in C$ , define the number  $\alpha(y) = \tau_y^U(\downarrow) \in L_{(2k-3)}$ . Assume that the map  $y \mapsto \alpha(y)$  is not locally constant. Then, there exists  $y \in C$  and a sequence  $y_n$  tending to  $y$  in  $C$  such that  $\alpha(y_n) \neq \alpha(y) := a$ . Since the map  $\alpha$  takes finitely many values, after taking a subsequence if necessary, we may assume that  $\alpha(y_n) = b \neq a$ . Let  $u_n := u_{y_n}$ . The nodal interval of  $\mathcal{Z}(u_n)$  which emanates from  $y_n$  tangentially to the ray  $\omega_b$  hits the boundary at the point  $z_n := z(y_n)$ . Since the sequence  $\{u_n\}$  converges to  $u_y$  in the  $C^m$  topology for any fixed  $m$ , taking subsequences if necessary, we may assume that  $\mathcal{Z}(u_n)$  converges to  $\mathcal{Z}(u_y)$  in the Hausdorff distance, and that  $\{z_n\}$  converges to  $z(y)$ . On the other hand, we can apply the local structure theorem to the functions  $u_n$  in a neighborhood of  $y$ : the arcs emanating from  $y_n$  intersect a circle of radius  $\varepsilon$  (with  $\varepsilon$  independent of  $n$ ), at points  $x_{n,j}, 1 \leq j \leq 2k - 3$  and these points converge to the corresponding points  $x_j, 1 \leq j \leq 2k - 3$ , for the function  $u_y$ . To prove that  $\varepsilon$  can be taken independent of  $n$  we use the fact that, for any fixed  $m$ , the derivatives of  $u_n$  of order less than or equal to  $m$  converge uniformly to the corresponding derivatives of  $u_y$  so that the remainder term in Taylor's formula can be controlled independently of  $n$ , see the proof of the local structure theorem in Section 2.4. The arc in  $\mathcal{Z}(u_n)$  between  $x_{n,b}$  and  $z_n$  must tend in the Hausdorff distance to the arc in  $\mathcal{Z}(u_y)$  between  $x_b$  and  $y$ , and we get a contradiction since  $b \neq a$ . It follows that the map  $\alpha$  is locally constant, hence constant, on the component  $C$ . Since the map  $y \mapsto \tau_y^U(\downarrow)$  is constant on  $C$ , the set  $L_{(2k-3)} \setminus \{\tau_y^U(\downarrow)\}$  is constant, and it suffices to look at the restriction of  $\tau_y^U$  to this set. To prove that the map  $y \mapsto \tau_y^U$  is locally constant on  $C$  we can



reproduce the arguments in the proof of Property 3.6 or Lemma 4.15. This proves Assertion (i).  $\checkmark$

*Assertion (ii).* Since  $\eta$  is isolated in  $\Gamma_{(2k-2)}$ , it suffices to work locally near  $\eta$ . Assume by contradiction, that the combinatorial type of  $u_y$  is the same on either sides of  $\eta$  for  $y$  close to  $\eta$ .

$\diamond$  In the framework of Paragraph 5.2.5, let  $E_\eta$  be a conformal mapping from  $\mathbb{H}$  to  $\Omega$  whose extension to the boundary sends 0 to  $\eta$ . Let  $r_0$  be small enough so that  $E_\eta((-r_0, r_0) \times \{0\})$  is a neighborhood of  $\eta$  in  $\Gamma$  whose intersection with  $\Gamma_{(2k-2)}$  is reduced to  $\{\eta\}$ . Let  $\{v_t\}$  be the associated family of functions given by (5.6).

According to our assumption, for  $t \neq 0$  small enough, the combinatorial type of  $v_t$  is constant. For  $t \neq 0$ , let  $\mathcal{S}_b(v_t) = \{t, z(t)\}$ . According to Lemma 5.12, when  $t$  tends to 0, the point  $z(t)$  tends to 0, with  $z(t) < 0$  when  $t > 0$ , and  $z(t) > 0$  when  $t < 0$ .

$\diamond$  We first consider the simple case  $k = 4$  and  $a = 3$  displayed in Figure 5.10. The numbers between brackets are the labels of the rays. The numbers between braces are the labels of the nodal domains according to their order of appearance along a small half-circle centered at  $t$ , moving counter-clockwise. The labeling word for the nodal domains of  $v_t$  is  $\mathcal{W}_t = |1|2|1|3|4|3|$ . From our assumption, it is constant for  $t$  small. The nodal interval from  $t$  to  $z(t)$  separates the domain  $\Omega$  into two connected components and bounds the nodal domains labeled  $\{1\}$  and  $\{3\}$ .

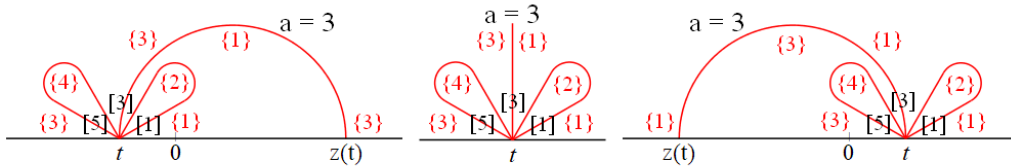


FIGURE 5.10. Example with  $k = 4$  and  $a = 3$

The combinatorial type of  $v_t$  is given by

$$\tau = \begin{pmatrix} \downarrow & 1 & 2 & 3 & 4 & 5 \\ 3 & 2 & 1 & \downarrow & 5 & 4 \end{pmatrix}.$$

The arguments in the proof of Lemma 5.16 show that the combinatorial type of  $v_{0,L}$ , the limit of  $v_t$  when  $t$  tends to 0 from the left, is determined by the combinatorial type of  $v_t$ . When  $t$  tends to 0 from the left,  $z(t)$  tends to 0 from the right, and the nodal interval from  $t$  to  $z(t)$  closes up to form a loop  $\gamma_{0,a}$  in the nodal set of  $v_{0,L}$ . We write the combinatorial type of  $v_{0,L}$  as

$$\tau_L = \begin{pmatrix} 0 & 1 & 2 & 3 & 4 & 5 \\ 3 & 2 & 1 & 0 & 5 & 4 \end{pmatrix},$$

so that the ray previously labeled  $a$  (here 3) keeps the same label. Following the deformation of the nodal domains, when  $t$  tends to zero from the left, we see that the nodal word  $\mathcal{W}_t$  yields the word  $\mathcal{W}_L = |3|1|2|1|3|4|3|$  for  $v_{0,L}$ .

Similarly, when  $t$  tends to 0 from the right, we obtain a function  $v_{0,R}$  whose combinatorial type is given by

$$\tau_R = \begin{pmatrix} 1 & 2 & 3 & 4 & 5 & 6 \\ 2 & 1 & 6 & 5 & 4 & 3 \end{pmatrix}$$

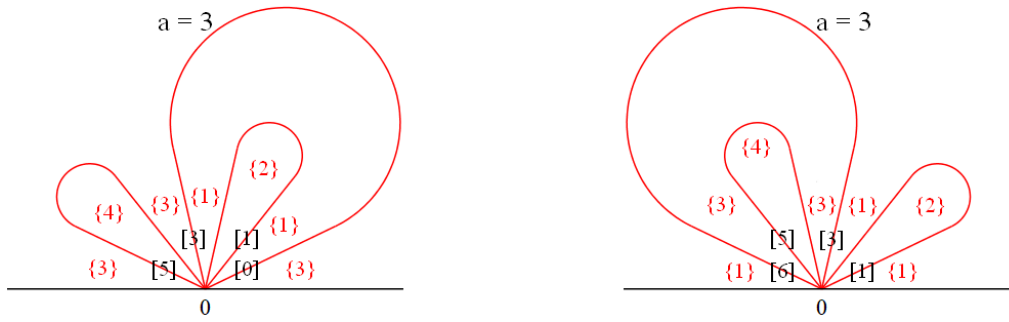


FIGURE 5.11.  $k = 4$  and  $a = 3$ :  $\mathcal{Z}(v_{0,L})$  and  $\mathcal{Z}(v_{0,R})$

and whose nodal set contains a loop  $\gamma_{a,6}$  (the ray previously labeled  $a$ , here  $a = 3$ , keeps the same label). Following the deformation of the nodal domains, when  $t$  tends to zero from the right, we see that the nodal word  $\mathcal{W}_t$  yields the word  $\mathcal{W}_R = |1|2|1|3|4|3|1|$  for  $v_{0,R}$ . This is illustrated in Figure 5.11.

The *signature*  $\sigma(\mathcal{W})$  of a word  $\mathcal{W}$  is the least rank, greater than or equal to 2 at which the first letter of the word reappears (see Section 5.5 for more details). We obtain

$$\mathcal{W}_L = |3|1|2|1|3|4|3|, \quad \sigma(\mathcal{W}_L) = 5 \quad \text{and} \quad \mathcal{W}_R = |1|2|1|3|4|3|1|, \quad \sigma(\mathcal{W}_R) = 3$$

respectively. This shows that the combinatorial types  $\tau_L$  and  $\tau_R$  are different, contradicting the fact that  $v_{0,L} = v_{0,R}$  according to Lemma 5.6.

The general case follows similar lines. It is detailed in Subsection 5.5.8. In particular, this excludes the case  $\#(\Gamma_{(2k-2)}) = 1$ . We have proved Assertion (ii).  $\checkmark$

*Assertion (iii).* We give the proof on an example.

Assuming that  $\Gamma_{(2k-2)}$  is not empty, we have  $\#(\Gamma_{(2k-2)}) \geq 2$ . Consider two consecutive points  $\eta_1$  and  $\eta_2$  in  $\Gamma_{(2k-2)}$ , i.e.,  $\mathcal{A}(\eta_1, \eta_2)$  is a connected component of  $\Gamma_{(2k-3)}$ . From Assertion (i), we know that the combinatorial type of  $u_y$  is constant in  $\mathcal{A}(\eta_1, \eta_2)$ . For  $y \in \mathcal{A}(\eta_1, \eta_2)$ , Lemma 5.12 and Lemma 5.16 imply that the combinatorial types of  $u_{\eta_1}$ ,  $u_y$  and  $u_{\eta_2}$  are determined once one of them is known.

We work out the following example:  $k = 10$  and the combinatorial type  $\tau_y$  of  $u_y$  is given by

$$\tau_y = \left( \begin{array}{cccccccccccccccccccc} \downarrow & 1 & 2 & 3 & 4 & 5 & 6 & 7 & 8 & 9 & 10 & 11 & 12 & 13 & 14 & 15 & 16 & 17 \\ 11 & 6 & 3 & 2 & 5 & 4 & 1 & 10 & 9 & 8 & 7 & \downarrow & 15 & 14 & 13 & 12 & 17 & 16 \end{array} \right).$$

The nodal set  $\mathcal{Z}(u_y)$  is displayed in Figure 5.12, middle sub-figure. The labels between brackets are the labels of the rays at  $y$ . Recall that  $\mathcal{S}_b(u_y) = \{y, z(y)\}$  with  $z(y) \in \Gamma$  and  $z(y) \neq y$ .

We have chosen  $k = 10$ , i.e.,  $\rho(u_y, y) = 17$ , so that the example looks as general as possible, see Section 5.5. To draw a readable figure and accommodate the seventeen rays tangent to  $\mathcal{Z}(u_y)$  at  $y$  and the various labels, we have opened the half-plane like a fan.

According to Lemma 5.12, when  $y \in \mathcal{A}(\eta_1, \eta_2)$  moves clockwise to  $\eta_1$ , the point  $z(y)$  moves counter-clockwise to  $\eta_1$ , and  $u_y$  tends to some  $u_{\eta_1} \in U_{\eta_1}$ . The proof of Lemma 5.16 shows that the loops in  $\mathcal{Z}(u_y)$  move continuously as  $y$  moves, that the

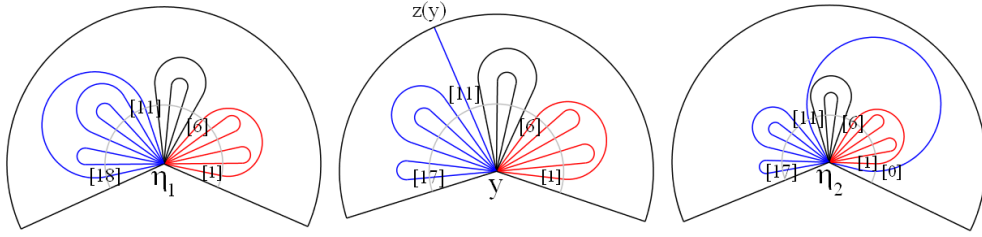


FIGURE 5.12. Transition from  $u_{\eta_1}$  to  $u_{\eta_2}$  (here  $k = 10$ )

nodal interval  $\delta_y^{z(y)} \subset \mathcal{Z}(u_y)$  from  $y$  to  $z(y)$  tends to a loop  $\gamma_{11,18}^{u_{\eta_1}} \subset \mathcal{Z}(u_{\eta_1})$ , and that the combinatorial type of  $u_{\eta_1}$  is

$$\tau_{\eta_1} = \begin{pmatrix} 1 & 2 & 3 & 4 & 5 & 6 & 7 & 8 & 9 & 10 & 11 & 12 & 13 & 14 & 15 & 16 & 17 & 18 \\ 6 & 3 & 2 & 5 & 4 & 1 & 10 & 9 & 8 & 7 & 18 & 15 & 14 & 13 & 12 & 17 & 16 & 11 \end{pmatrix}.$$

This is illustrated in the left sub-figure of Figure 5.12. The sets of loops in  $\mathcal{Z}(u_y) \setminus \delta_y^{z(y)}$  and in  $\mathcal{Z}(u_{\eta_1}) \setminus \gamma_{11,18}^{u_{\eta_1}}$  have the same combinatorics and look very much alike.

When  $y$  moves counter-clockwise to  $\eta_2$ ,  $z(u)$  moves clockwise to  $\eta_2$ , and the proof of Lemma 5.16 shows that the nodal interval  $\delta_y^{z(y)}$  in  $\mathcal{Z}(u_y)$  closes up as a loop  $\gamma_{0,11}^{u_{\eta_2}}$  in  $\mathcal{Z}(u_{\eta_2})$  tangent to a ray labeled  $[0]$ . This is illustrated in the right sub-figure (upon arriving at  $\eta_2$  a new ray pops up and we label it  $\omega_0$  so that the labels of the other rays do no change, and we retain the counter-clockwise labeling of rays). This is a consequence of the local structure theorem applied to  $u_{\eta_2}$ , the limit of  $u_y$  when  $y$  tends to  $\eta_2$  from the left. Then,

$$\tau_{\eta_2} = \begin{pmatrix} 0 & 1 & 2 & 3 & 4 & 5 & 6 & 7 & 8 & 9 & 10 & 11 & 12 & 13 & 14 & 15 & 16 & 17 \\ 11 & 6 & 3 & 2 & 5 & 4 & 1 & 10 & 9 & 8 & 7 & 18 & 15 & 14 & 13 & 12 & 17 & 16 \end{pmatrix}.$$

The combinatorial types  $\tau_{\eta_1}$  and  $\tau_{\eta_2}$  look different. In order to prove that they are indeed different, we look at how the nodal domains of  $u_y$  deform when  $y$  moves in  $\mathcal{A}(\eta_1, \eta_2)$ . We first choose  $r$  small enough so that the local structure theorem holds (for the eigenfunctions we are interested in). Then, we label the nodal domains of  $u_y$  according to their order of appearance while moving counter-clockwise along  $C_+(y, r)$ , taking into account that the intersection of a given nodal domain with  $C_+(y, r)$  may consist of several disjoint intervals. This labeling of the nodal domains of  $u_y$  is displayed in the top sub-figure of Figure 5.13. One can view the labeling as a map from the set of intervals determined by  $\mathcal{Z}(u_y)$  on  $C_+(y, r)$ ,  $\{1, \dots, 18\}$ , to the set of nodal domains of  $u_y$  which has 10 elements. Equivalently, one can view the labeling as a word of length 18 in the 10 letters  $1, \dots, 10$ , the labels of the nodal domains, separated by a vertical bar  $|$ . The labeling word  $\mathcal{W}_y$  corresponding to  $u_y$  in the example appears at the bottom of the top sub-figure in Figure 5.13

$$\mathcal{W}_y = |1|2|3|2|4|2|1|5|6|5|1|7|8|9|8|7|1|0|7|.$$

The nodal interval  $\delta_y^{z(y)}$  divides  $\Omega$  into two components, one component on the right of the nodal interval which contains 5 loops and hence 6 nodal domains, labeled from 1 to 6; and another component on the left of the nodal interval which contains

3 loops and hence 4 nodal domains labeled from 7 to 10. The nodal interval  $\delta_y^{z(y)}$  is the common boundary of the nodal domains labeled 1 and 7.

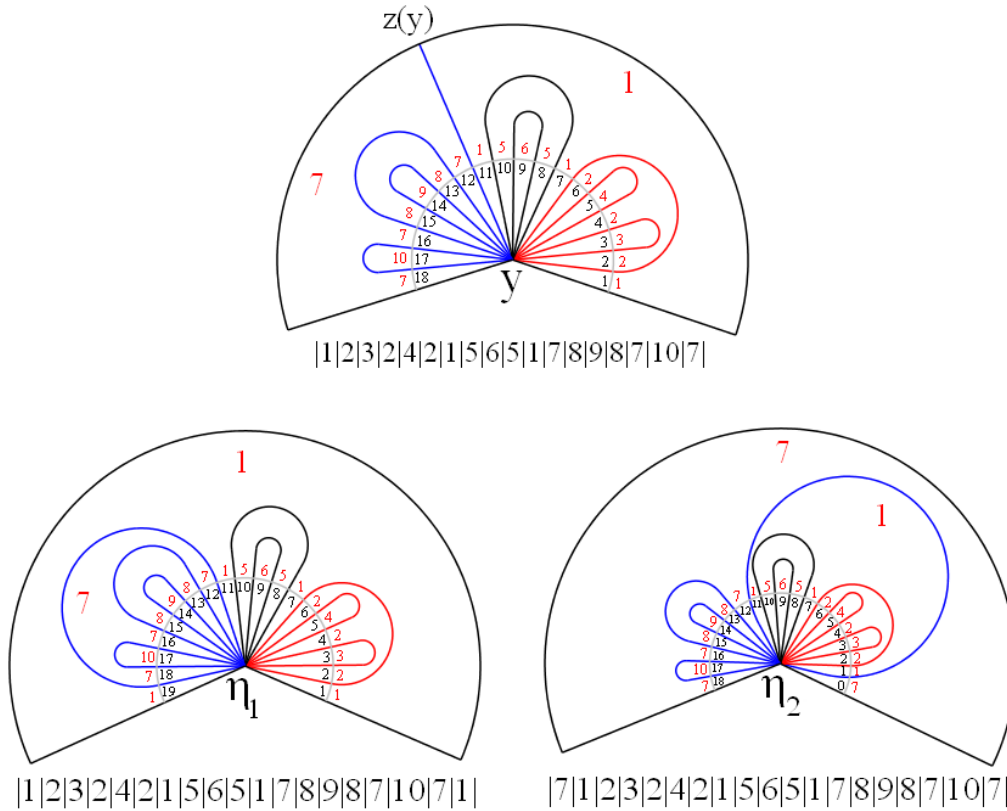


FIGURE 5.13. Words for  $u_{\eta_1}$  and  $u_{\eta_2}$  deduced from the word for  $u_y$

When  $y$  moves, the nodal domains of  $u_y$  deform but the corresponding labeling word does not change. When  $y$  reaches  $\eta_1$ , the nodal interval  $\delta_y^{z(y)}$  closes up to form the loop  $\gamma_{11,18}^{u_{\eta_1}}$  in  $\mathcal{Z}(u_{\eta_1})$  and the nodal domain labeled 1 contains  $\Gamma$  in its boundary. When  $y$  reaches  $\eta_2$ , the nodal interval  $\delta_y^{z(y)}$  closes up to form the loop  $\gamma_{0,11}^{u_{\eta_2}}$  in  $\mathcal{Z}(u_{\eta_2})$  and the nodal domain labeled 7 contains  $\Gamma$  in its boundary. The corresponding words appear at the bottom of the bottom sub-figures in Figure 5.13,

$$\mathcal{W}_{\eta_1} = |1|2|3|2|4|2|1|5|6|5|1|7|8|9|8|7|1|0|7|1| = \mathcal{W}_y|1|$$

$$\mathcal{W}_{\eta_2} = |7|1|2|3|2|4|2|1|5|6|5|1|7|8|9|8|7|1|0|7| = |7|\mathcal{W}_y.$$

The word  $\mathcal{W}_{\eta_1}$  is obtained from the word  $\mathcal{W}_y$  by adding the letter 1 at the end; the word  $\mathcal{W}_{\eta_2}$  by adding the letter 7 at the beginning. In  $\mathcal{W}_{\eta_1}$ , the first letter of the word is 1 and it first reappears as the 7th letter. In  $\mathcal{W}_{\eta_2}$ , the first letter is 7 and it first reappears as the 13th letter, so that for the signatures,  $\sigma(\mathcal{W}_{\eta_1}) \neq \sigma(\mathcal{W}_{\eta_2})$ . This shows that the functions  $u_{\eta_1}$  and  $u_{\eta_2}$  have different combinatorial types. This proves Assertion (iv) for the above example. ✓

The general case follows similar lines, see Subsection 5.5.9.

*Assertion (iv).* Look at the example in Figure 5.13. The function  $u_y$  changes sign across the nodal interval  $\delta_y^{z(y)}$ , i.e., it has different signs in the nodal domains

labeled 1 and 7. For  $i = 1, 2$ , the function  $\check{u}_{\eta_i}$  only vanishes at  $\eta_i$  and has a constant sign on  $\Gamma \setminus \{\eta_i\}$ . Letting  $y$  tend to  $\eta_1$ , resp.  $\eta_2$ , in the above argument, we infer that  $\check{u}_{\eta_1} \cdot \check{u}_{\eta_2} < 0$  on  $\Gamma \setminus \{\eta_1, \eta_2\}$ . This property is general and does not depend on the particular example. According to Lemma 5.16 (iv), we have a globally defined continuous function  $\Gamma \ni y \mapsto u_y \in \mathbb{S}(U)$ . In view of the previous property, this implies that the number of point in  $\Gamma_{(2k-2)}$  is even.  $\checkmark$

The proof of Lemma 5.24 is complete.  $\square$

### 5.3. Nodal Sets of $\lambda_k$ -Eigenfunctions under Assumptions 5.2

In this section, we continue to work under Assumptions 5.2.

**5.3.1.  $\mathcal{Z}(w_x)$  for  $x$  close to  $y \in \Gamma_{(2k-3)}$ , local picture.** In order to describe the combinatorial type of the eigenfunction  $w_x$  when  $x \in \Omega$  is close to some boundary point  $y \in \Gamma_{(2k-3)}$ , we first review the description of  $\mathcal{Z}(u_y)$ .

[1] Fix some  $y \in \Gamma_{(2k-3)}$ . The nodal set  $\mathcal{Z}(u_y)$  only hits  $\Gamma$  at  $y$  and some  $z(y) \neq y$ . Fix a conformal mapping  $E$  from  $\mathbb{H}$  to  $\Omega$  such that  $E(0) = y$ ,  $E(\zeta) = z(y)$ , and  $\mathcal{Z}(u_y) \subset E(D_+(0, r_0))$ , for some  $r_0 > 0$ , see the proof of Lemma 5.16 and Section 2.4. We now work locally in  $\mathbb{H}$  rather than in  $\Omega$ , using the conformal mapping  $E$ . For the sake of simplicity, we identify the function  $u_y \circ E$  with the function  $u_y$  and, for  $x \in \Omega$ , the function  $w_x \circ E$  with  $w_x$ . We use the same notation  $D_+(y, r)$ , resp.  $C_+(y, r)$ , to denote  $D_+(0, r)$ , resp.  $C_+(0, r)$ , and their images under  $E$ . With these identifications, we write  $\mathcal{Z}(u_y) \subset D_+(y, r_0)$ . Then, for  $x$  close enough to  $y$ , we also have  $\mathcal{Z}(w_x) \subset D_+(y, r_0)$ .

[2] Recall from Subsection 5.2.3, that the nodal set  $\mathcal{Z}(u_y)$  can be described in terms of the combinatorial type of the eigenfunction  $u_y$ ,

$$(5.41) \quad \tau := \tau_{u_y} = \begin{pmatrix} 1 & \dots & (a-1) & a & (a+1) & \dots & (2k-3) \\ \tau(1) & \dots & \tau(a-1) & \downarrow & \tau(a+1) & \dots & \tau(2k-3) \end{pmatrix}.$$

We can add to  $\tau$  a last, resp. first, column  $\begin{pmatrix} \downarrow \\ a \end{pmatrix}$  to take into account the fact that

$$\tau_{\eta_1} = \begin{pmatrix} 1 & \dots & (a-1) & a & (a+1) & \dots & (2k-3) & (2k-2) \\ \tau(1) & \dots & \tau(a-1) & (2k-2) & \tau(a+1) & \dots & \tau(2k-3) & a \end{pmatrix}$$

$$\tau_{\eta_2} = \begin{pmatrix} 0 & 1 & \dots & (a-1) & a & (a+1) & \dots & (2k-3) \\ a & \tau(1) & \dots & \tau(a-1) & 0 & \tau(a+1) & \dots & \tau(2k-3) \end{pmatrix}$$

when  $y \in \mathcal{A}(\eta_1, \eta_2)$ , with  $\eta_1 \neq \eta_2$  two consecutive points in  $\Gamma_{(2k-2)}$ , so that the initial rays keep their labels while

$$\tau_{\eta_1}(a) = (2k-2) \text{ and } \tau_{\eta_1}(2k-2) = a, \text{ resp. } \tau_{\eta_2}(a) = 0 \text{ and } \tau_{\eta_2}(0) = a.$$

The nodal set  $\mathcal{Z}(u_y)$  contains a nodal interval  $\delta_{y,a}$  which emanates from  $y$  tangentially to the ray  $\omega_{y,a}$  at  $y$ , for some  $a \in J := \{1, \dots, (2k-3)\}$ , and hits the boundary  $\Gamma$  at the point  $z(y) \neq y$ . The nodal interval  $\delta_{y,a}$  separates  $\Omega$  into two components  $\Omega_{y,-}$  on the right of  $\delta_{y,a}$ , and  $\Omega_{y,+}$  on the left. The rays  $\omega_{y,j}$ ,  $1 \leq j \leq (a-1)$ , point inside  $\Omega_{y,-}$ . The rays  $\omega_{y,j}$ ,  $(a+1) \leq j \leq (2k-3)$ , point inside  $\Omega_{y,+}$ . The map  $\tau$  leaves the subsets  $J_{a,-} := \{1, \dots, (a-1)\}$  and  $J_{a,+} := \{(a+1), \dots, (2k-3)\}$  globally invariant. Its restrictions  $\tau_{\pm}$  to  $J_{a,\pm}$  describe two bouquets of nodal loops  $\mathcal{B}_{y,\pm} := \left\{ \gamma_{j,\tau(j)}^y \right\}_{j \in J_{a,\pm}}$  at the point  $y$ , contained respectively in  $\Omega_{y,\pm}$ . The nodal

set  $\mathcal{Z}(u_y)$  is the wedge sum of the bouquets of loops  $\mathcal{B}_{y,\pm}$  with the nodal interval  $\delta_{y,a}$ . There are  $n_{y,-} := (a + 1)/2$  nodal domains of  $u_y$  contained in  $\Omega_{y,-}$  and  $n_{y,+} := [k - (a + 1)/2]$  nodal domains contained in  $\Omega_{y,+}$ . The nodal interval  $\delta_{y,a}$  is a partial common boundary to the nodal domains  $D_1$  and  $D_{1+n_{y,-}}$ .

We now apply the structure theorem of Section 2.4 to the function  $u_y$  at the point  $y$ . More precisely, we apply Propositions 2.40 (Dirichlet case) and 2.41 (Robin case). We also retain the definitions and notation of this section. In particular, we use the notation  $\mathcal{G}_{y,j}(r)$  for the ‘‘colored arcs’’, defined by Equations (2.80) (Dirichlet case) and (2.88) (Robin case). Similar arguments can be found in the proof of Lemma 5.16.

We are given some angle  $\alpha_1 \in (0, \frac{\pi}{8})$ , and we have a radius  $r_{1,d}$  or  $r_{1,n}$ , given by (2.78) or (2.86). We now work in  $D_+(y, r_1)$ , with the radius  $r_1$  satisfying

$$(5.42) \quad \begin{cases} r_1 \leq r_{1,d} \text{ or } r_{1,n} \text{ (Dirichlet or Robin)} \\ r_1 \leq r_E \text{ (the energy radius given by Lemma 5.17)} \\ z(y) \notin D_+(y, 2r_1). \end{cases}$$

This choice of  $r_1$  implies that the half disk  $D_+(y, r)$  satisfies the energy inequality (5.35) of Lemma 5.17, for any  $r \leq r_1$ . Fix some  $r_2$ , such that  $0 < r_2 < r_1$ .

- ◊ In the Dirichlet case, we have the ‘‘colored arcs’’ (2.80) associated with the rays (2.74), and the inequalities (2.81) satisfied by  $u_y$  (alias  $u_y \circ E = v$ ).
- ◊ In the Robin case, we have the ‘‘colored arcs’’ (2.88) associated with the rays (2.82), and the inequalities (2.89) satisfied by  $u_y$ .

The ‘‘colored’’ arcs appear in Figure 5.14, left image for the Dirichlet boundary condition, right image for the Robin boundary condition<sup>3</sup>.

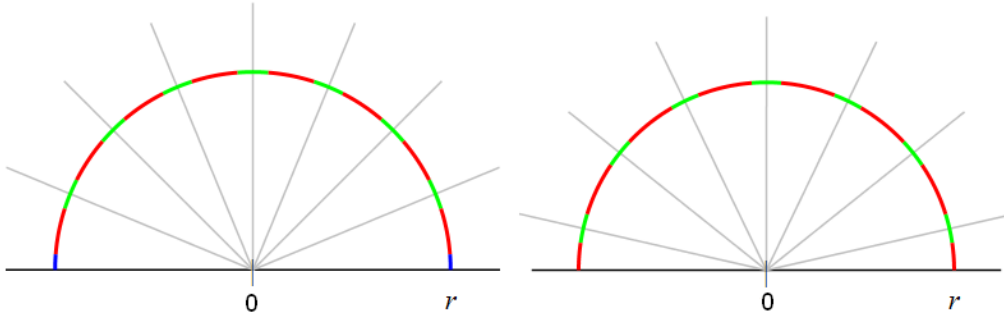


FIGURE 5.14. Colored intervals for  $u_y$ , here  $k = 5$ ,  $\rho(u_y, y) = 7$

According to Propositions 2.40 and 2.41, for  $0 < r < r_1$ , the nodal arc  $\delta_{y,j}$  emanating from  $y$  tangentially to the ray  $\omega_{y,j}$  intersects the curve  $C_+(y, r)$  at a unique point  $A_{y,j}(r) := [r, \tilde{\omega}_{y,j}(r)] \in \mathcal{G}_{y,j}(r)$  in polar coordinates, with  $\omega_j - \alpha < \tilde{\omega}_{y,j}(r) < \omega_j + \alpha$ , and the nodal set  $\mathcal{Z}(u_y)$  does not intersect  $C_+(y, r)$  elsewhere. Here,  $\alpha = \alpha_1 / \text{ord}(u_y, y)$  with  $\alpha_1 \in (0, \frac{\pi}{8})$ , see Subsection 2.4.5.

<sup>3</sup>The rays which appear in the other figures of this section are for the Dirichlet boundary condition. Except for the rays, the figures for the Neumann or Robin boundary condition are similar to the figures for the Dirichlet boundary condition.

*Sketch of the proof of the above properties.* Using the Taylor expansion of  $u_y$ , the fact that the arcs  $\delta_{y,j}$  meet the arcs  $\mathcal{G}_{y,j}(r)$  (in green in the figure) follows from the intermediate value theorem and the choice of  $r_1$ . The fact that there is precisely one crossing point in each arc  $\mathcal{G}_{y,j}(r)$  follows from the fact that the derivative of  $u_y$  along the circle is nonzero in these arcs. The fact that the nodal set  $\mathcal{Z}(u_y)$  does not meet the arcs  $\mathcal{R}_{y,j}(r)$  and  $\mathcal{B}_{y,k}(r)$  contained in  $C_+(y, r) \setminus (\cup \mathcal{G}_{y,j}(r))$  (in red and blue in the figure) follows from the choice of  $r_1$  and the fact that either  $u_y$  or its derivative along the circle are controlled away from 0 in these arcs (the details are given in Section 2.4 and in the proof of Lemma 5.16).  $\checkmark$

The nodal set  $\mathcal{Z}(u_y)$  (viewed in  $\mathbb{H}$ ) appears in red in Figure 5.15, in which

$$k = 5, a = 3, \text{ and } \tau = \begin{pmatrix} 1 & 2 & 3 & 4 & 5 & 6 & 7 \\ 2 & 1 & \downarrow & 5 & 4 & 7 & 6 \end{pmatrix}.$$

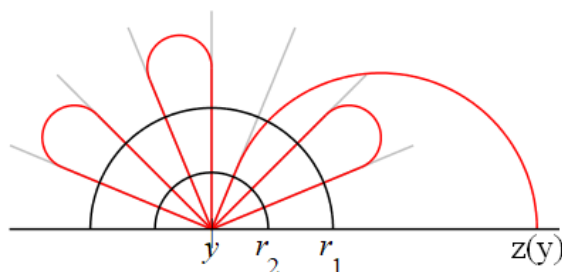


FIGURE 5.15. The nodal sets  $\mathcal{Z}(u_y)$  (here  $k = 5, a = 3$ )

Look at  $D_+^c(y, r_1)$ , the complement of  $D_+(y, r_1)$ . The nodal arcs in  $\mathcal{Z}(u_y) \cap D_+^c(y, r_1)$  are pairwise disjoint and compact, so that they have disjoint neighborhoods of size  $\varepsilon$ , for some  $\varepsilon > 0$ ,  $\mathcal{U}_{y,a}^\varepsilon, \mathcal{U}^\varepsilon(\tau_-) := \cup_{j=1}^{a-1} \mathcal{U}_{y,j}^\varepsilon$ , and  $\mathcal{U}^\varepsilon(\tau_+) := \cup_{j=a+1}^{2k-3} \mathcal{U}_{y,j}^\varepsilon$ . This is illustrated in Figure 5.16.

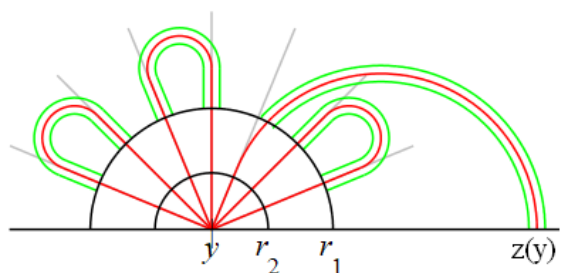
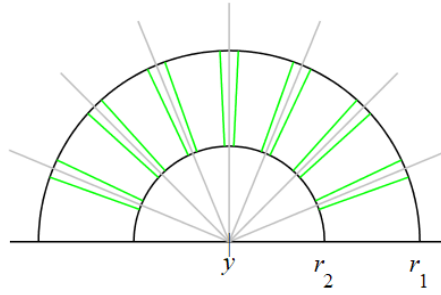
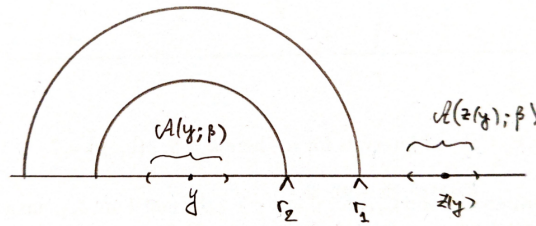


FIGURE 5.16. Neighborhoods of  $\mathcal{Z}(u_y)$  outside  $D_+(y, r_1)$

In the annulus  $D_+(y, r_1) \setminus D_+(y, r_2)$ , we consider sectors containing the rays, as illustrated in Figure 5.17. According to the local structure theorem for  $u_y$ , the intersection  $\mathcal{Z}(u_y) \cap (D_+(y, r_1) \setminus D_+(y, r_2))$  is contained in these sectors.

At the boundary, we consider the function  $\check{u}_y$  which vanishes precisely at the points  $y$  and  $z(y)$ , and changes sign at both points. Fix some  $\beta, 0 < \beta < r_2$ , such that  $\mathcal{A}(y; \beta) \subset \mathcal{A}(y; r_2)$  and  $\mathcal{A}(z(y); \beta) \cap \mathcal{A}(y; r_1) = \emptyset$ , see Figure 5.18.

FIGURE 5.17. Sectors in  $D_+(y, r_1) \setminus D_+(y, r_2)$ FIGURE 5.18. The setting at  $y$ 

[3] We now look at the nodal sets  $\mathcal{Z}(w_x)$  when  $x$  is close to  $y$ , making use of the description of  $\mathcal{Z}(u_y)$  in [2].

Since  $w_x$  tends to  $u_y$   $C^1$ -uniformly when  $x$  tends to  $y$ , for  $x$  close enough to  $y$ , the function  $\check{w}_x$  vanishes precisely once in both arcs  $\mathcal{A}(y; \beta)$  and  $\mathcal{A}(z(y); \beta)$ , and only there, so that  $\mathcal{S}_b(w_x) = \{y(x), z(x)\}$ . According to Lemma 5.4, the nodal set  $\mathcal{Z}(w_x)$  is the wedge sum of two nodal intervals,  $\delta_x^{y(x)}$  from  $x$  to  $y(x)$  and  $\delta_x^{z(x)}$  from  $x$  to  $z(x)$ , and a  $(k - 2)$ -bouquet of loops at  $x$ .

Since  $w_x$  tends to  $u_y$   $C^1$ -uniformly when  $x$  tends to  $y$ , for  $r_2 < r < r_1$ , and for  $x$  close enough to  $y$ , the function  $w_x$  satisfies inequalities similar to the inequalities (5.37) or (5.39) satisfied by  $u_y$  (see the proof of Lemma 5.16). It follows that  $\mathcal{Z}(w_x) \cap C_+(y, r) \subset \bigcup_{j=1}^q \mathcal{G}_{y,j}(r)$  and  $\mathcal{Z}(w_x)$  crosses each  $\mathcal{G}_{y,j}(r)$  precisely once, at a point denoted by  $A_{x,j}(r)$ . Since  $z(x)$  lies outside  $D_+(y, r_1)$ , the nodal interval  $\delta_x^{z(x)}$  must cross  $C_+(y, r)$  precisely once. For energy reasons (choice of  $r_1$ ), each nodal loop in  $\mathcal{Z}(w_x)$  intersects  $C_+(y, r)$  precisely twice. Counting the points in  $\mathcal{Z}(w_x) \cap C_+(y, r)$ , it follows that the nodal interval  $\delta_x^{y(x)}$ , from  $x$  to  $y(x)$ , does not cross  $C_+(y, r)$  for  $r_2 < r < r_1$ , and hence is contained in  $D_+(y, r_2)$ .

Given any  $x \in \Omega$ , there is a priori no natural labeling of the star<sup>4</sup> of  $w_x$  at the point  $x$ . Assuming that  $x$  is close enough to some  $y \in \Gamma_{(2k-3)}$ , the situation is different. We have indeed identified the nodal interval  $\delta_x^{z(x)}$  which crosses  $C_+(y, r)$  in  $\mathcal{G}_{y,a}(r)$ , and we label  $\omega_{x,a}$  the corresponding ray at  $x$  accordingly. This gives us a natural labeling of the rays at  $x$ : we label the rays  $\omega_{x,(a-1)}$  to  $\omega_{x,1}$  counter-clockwise starting from  $\omega_{x,a}$ , and  $\omega_{x,(a+1)}$  to  $\omega_{x,(2k-2)}$  clockwise starting from  $\omega_{x,a}$ . In this labeling, we denote by  $\omega_{x,b}$  the ray tangent to  $\delta_x^{y(x)}$ , for some  $b \in \{1, \dots, (2k - 2)\} \setminus \{a\}$ .

<sup>4</sup>Recall that the star at  $x$  is the collection of rays tangent to  $\mathcal{Z}(w_x)$  at the point  $x$ .



Since  $w_x$  tends to  $u_y$  in the  $C^1$  topology, for  $x$  close enough to  $y$ ,  $\mathcal{Z}(w_x) \cap D_+^c(y, r_1)$  is contained in the neighborhood  $\mathcal{U}^\varepsilon(u_y) = \cup_{j=1}^{(2k-3)} \mathcal{U}_{y,j}^\varepsilon$ .

Properties 5.25 summarize the above statements.

PROPERTIES 5.25. *Under Assumptions 5.2, let  $y \in \Gamma_{(2k-3)}$  and let  $\omega_{y,a}$ ,  $1 \leq a \leq (2k-3)$  be the ray at  $y$  tangent to the nodal interval  $\delta_y^{z(y)}$  in  $\mathcal{Z}(u_y)$  going from  $y$  to  $z(y)$ . For  $x$  close enough to  $y$ , the nodal set  $\mathcal{Z}(w_x)$  has the following properties.*

- (i) *There is one nodal interval, denoted by  $\delta_x^{z(x)}$ , going from  $x$  to a point  $z(x) \in \Gamma$  close to  $z(y)$ . We denote the ray at  $x$  tangent to this nodal interval by  $\omega_{x,a}$ , so that  $\delta_x^{z(x)} = \delta_{x,a}$ , the nodal interval in  $\mathcal{Z}(w_x)$  emanating from  $x$  tangentially to  $\omega_{x,a}$ . For each  $r_2 \leq r \leq r_1$ ,  $\delta_{x,a}$  crosses  $C_+(y, r)$  at exactly one point  $A_{x,a}(r)$  in  $\mathcal{G}_{y,a}(r)$ . In  $D_+^c(y, r_2)$ ,  $\delta_{x,a}$  is “close” to  $\delta_{y,a}$ , in the sense that it is contained in  $\mathcal{U}_{y,a}^\varepsilon$ .*
- (ii) *The ray  $\omega_{x,a}$  induces a natural labeling of the rays at  $x$ .*
- (iii) *There is one nodal interval, denoted by  $\delta_x^{y(x)} = \delta_{x,b}$ , from  $x$  to a point  $y(x) \in \Gamma$  close to  $y$ . This nodal interval emanates from  $x$  tangentially to a ray, denoted by  $\omega_{x,b}$ , for some  $b \neq a$ . This nodal interval is entirely contained in  $D_+(y, r_2)$ .*
- (iv) *There are  $(k-2)$  loops  $\gamma_{j, \tau_x(j)}^x$  for some map  $\tau_x$  on the set of rays at  $x$ , minus the pair  $\{\omega_{x,a}, \omega_{x,b}\}$ . Each loop crosses  $C_+(y, r)$  at exactly two points,  $A_{x,j}(r)$  in  $\mathcal{G}_{y,j}(r)$  and  $A_{x, \tau(j)}(r)$  in  $\mathcal{G}_{y, \tau(j)}(r)$ .*

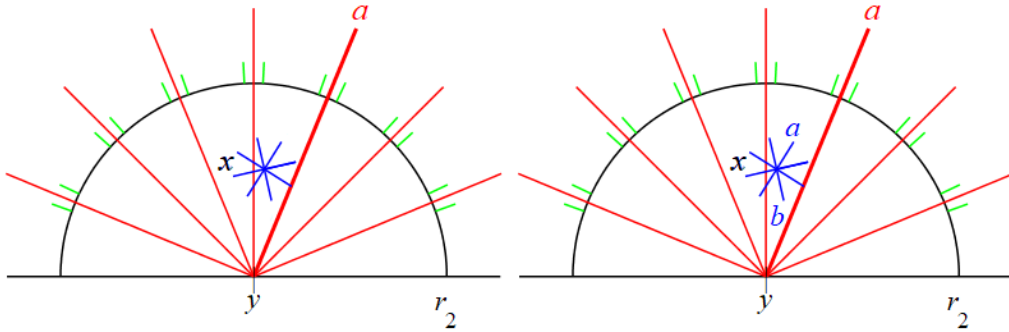


FIGURE 5.19.  $k = 5$ : the star at  $x$  and the rays  $\omega_{x,a}$  and  $\omega_{x,b}$

LEMMA 5.26. *Let  $y \in \Gamma_{(2k-3)}$ . Under Assumptions 5.2, the combinatorial type of  $u_y$  determines the combinatorial type of  $w_x$  when  $x$  is close enough to  $y$ .*

*Proof.* We use Properties 5.25. For  $x$  close enough to  $y$ , we follow the nodal interval  $\delta_{x,b}^{-1} \subset \mathcal{Z}(w_x)$  from  $y(x)$  to  $x$ , and then the nodal interval  $\delta_{x,a} \subset \mathcal{Z}(w_x)$  from  $x$  to  $z(x)$ . The corresponding arc  $\delta_{x,a} \circ \delta_{x,b}^{-1}$  from  $y(x)$  to  $z(x)$ , through  $x$ , divides the simply connected domain  $\overline{D}_+(y, r)$  into two connected components, say  $\Omega_{x,\mp}$  respectively on the right/left of the arc  $\delta_{x,a} \circ \delta_{x,b}^{-1}$ . Since the nodal interval  $\delta_{x,b}$  is contained in  $D_+(y, r_2)$ , the domain  $\Omega_{x,-}$  contains the points  $A_{x,j}(r)$  for  $1 \leq j \leq (a-1)$ , and the domain  $\Omega_{x,+}$  contains the points  $A_{x,j}(r)$  for  $(a+1) \leq j \leq (2k-3)$ .

CLAIM 5.27. *In the natural labeling of the rays at  $x$ ,  $b = (2k-2)$  and, for all  $j \in \{1, \dots, (2k-3)\} \setminus \{a\}$ , the nodal arc  $\delta_{x,j} \subset \mathcal{Z}(w_x)$  intersects  $C_+(y, r)$  at the point  $A_{x,j}(r)$ .*

*Proof.* If  $b \neq (2k - 2)$  there would exist some  $j \in \{1, \dots, (2k - 2)\} \setminus \{a, b\}$  such that the nodal arc  $\delta_{x,j}$  intersects  $\delta_{x,a} \circ \delta_{x,b}^{-1}$  inside  $D_+(y, r)$ , away from  $x$ , a contradiction with the fact that  $\mathcal{S}_i(w_x) = \{x\}$ .

Assume that  $\delta_{x,(a-1)}$  intersects  $C_+(y, r)$  at the point  $A_{x,j}(r)$ , with  $j \leq (a - 2)$ . Then the point  $A_{x,(a-1)}(r)$  would be on  $\delta_{x,k}$  for some  $k \leq (a - 2)$ . The arcs  $\delta_{x,(a-1)}$  and  $\delta_{x,k}$  would therefore intersect which is not possible because  $x$  is the only interior singular point of  $w_x$ , see Figure 5.20. We can then reason recursively with  $(a - 2)$ ,  $(a - 3) \dots 1$ . The proof is similar for  $(a + 1) \leq j \leq (2k - 3)$ .  $\checkmark$

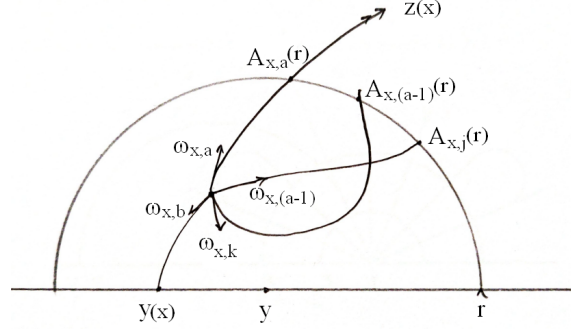


FIGURE 5.20. Claim 5.27: prohibited situation

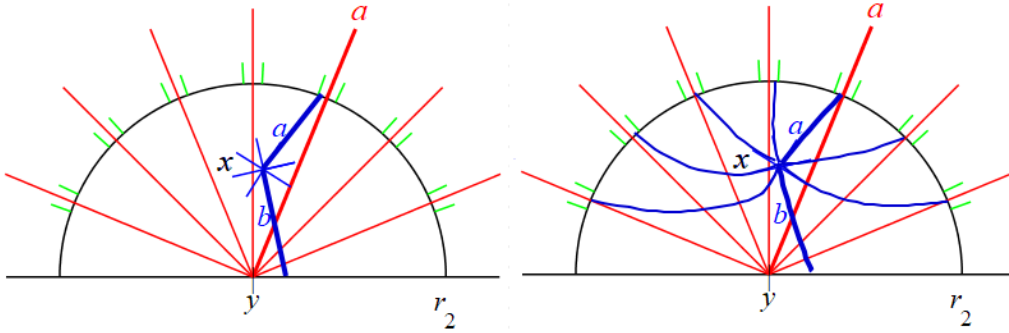


FIGURE 5.21.  $k = 5$ : star at  $x$  with  $\delta_{x,b}^{-1} \circ \delta_{x,a}$ , and  $\mathcal{Z}(w_x)$  near  $x$

Outside  $D_+(y, r_1)$ ,  $\mathcal{Z}(w_x) \cap D_+^c(y, r_1) \subset \mathcal{U}^\varepsilon(u_y)$ , and we conclude that the combinatorial type of  $w_x$ , in the above labeling of rays at  $x$ , is given by

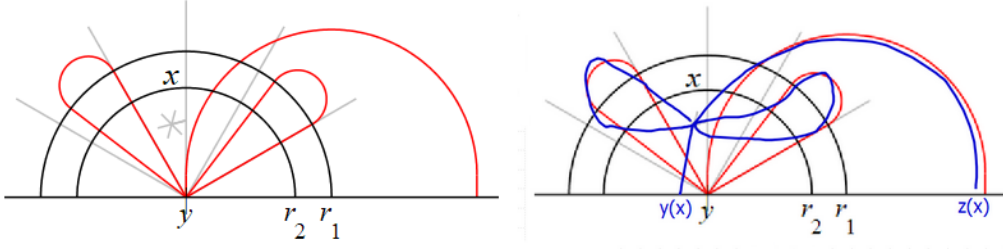
$$(5.43) \quad \tau_{w_x} = \begin{pmatrix} 1 & \dots & (a - 1) & a & (a + 1) & \dots & (2k - 3) & b \\ \tau(1) & \dots & \tau(a - 1) & \downarrow_{z(x)} & \tau(a + 1) & \dots & \tau(2k - 3) & \downarrow_{y(x)} \end{pmatrix}$$

where  $b = (2k - 2)$ , and

$$\begin{cases} \tau_{w_x} = \tau_{u_y} = \tau \text{ in } \{1, \dots, (a - 1)\} \cup \{(a + 1), \dots, (2k - 3)\} \\ \tau_{w_x}(a) = \downarrow_{z(x)} \text{ and } \tau_{w_x}(b) = \downarrow_{y(x)} . \end{cases}$$

This is illustrated in Figure 5.22 in which the  $\mathcal{Z}(u_y)$  appears in red, and  $\mathcal{Z}(w_x)$  in blue.

The proof of Lemma 5.26 is complete.  $\square$


 FIGURE 5.22.  $k = 4, a = 3$ : nodal sets  $\mathcal{Z}(u_y)$  and  $\mathcal{Z}(w_x)$ 

REMARK 5.28. Note that for  $x$  close to  $y \in \Gamma_{(2k-3)}$ , the map  $x \mapsto \omega_{x,a}$  is continuous. This is because there are finitely many rays.

REMARK 5.29. If  $y \in \mathcal{A}_0 \subset \Gamma_{(2k-3)}$  where  $\mathcal{A}_0$  is some compact arc, the numbers  $r_1, r_2, \dots$  in the proof of Lemma 5.26 can be chosen uniformly with respect to  $y \in \mathcal{A}_0$ . This is in particular the case when we assume  $\Gamma_{(2k-3)} = \Gamma$  and consider  $\mathcal{A}_0 = \Gamma$ .

**5.3.2.  $\mathcal{Z}(w_x)$  for  $x$  close to  $y \in \Gamma_{(2k-3)}$ , global picture when  $\Gamma_{(2k-2)} = \emptyset$ .** We now describe the global picture for  $\mathcal{Z}(u_y)$  and  $\mathcal{Z}(w_x)$  when  $x$  is close to  $y$ , under the additional assumption that  $\Gamma_{(2k-2)} = \emptyset$ . Let  $\gamma : [0, L] \rightarrow \Gamma$  be a parametrization by arc length. Let  $\gamma(s, t) = \gamma(t) + s\nu(t)$  for  $s$  small enough, with  $\nu$  the unit normal pointing inwards.

LEMMA 5.30. *Under Assumptions 5.2 and the further assumption that  $\Gamma_{(2k-2)}$  is empty, the following properties hold.*

- (i) *The infimum  $\delta := \inf \{d(y, z(y)) \mid y \in \Gamma\}$  is positive. ( $d$  is the distance on  $\Gamma$ .)*
- (ii) *For all  $\beta \leq \frac{\delta}{4}$ , there exists some positive  $\varepsilon$  such that for all  $s, 0 < s \leq \varepsilon$ , for all  $t \in [0, L]$ ,*

$$\mathcal{S}_b(w_{\gamma(s,t)}) \cap \mathcal{A}(\gamma(t); \beta) \neq \emptyset \text{ and } \mathcal{S}_b(w_{\gamma(s,t)}) \cap \mathcal{A}(z(t); \beta) \neq \emptyset,$$

where  $z(t) := z(\gamma(t))$  is such that  $\mathcal{S}_b(u_{\gamma(t)}) = \{\gamma(t), z(t)\}$ .

*Proof.*

*Assertion (i).* Assume that  $\delta = 0$ . Then there exists a sequence  $\{y_n\} \subset \Gamma$  such that  $\delta(y_n, z(y_n)) \leq \frac{1}{n}$ . We may assume that  $y_n$  tends to some  $y \in \Gamma$ . Then,  $z(y_n)$  tends to  $y$  as well. Choose  $u_y, u_{y_n} \in \mathbb{S}(U)$  given by Lemma 5.6. We may assume that  $u_{y_n}$  tends to  $u_y$   $C^1$ -uniformly, implying that  $\check{u}_{y_n}$  tends to  $\check{u}$  uniformly. Since  $\Gamma_{(2k-3)} = \Gamma$ ,  $\mathcal{S}_b(u) = \{y, z(y)\}$  with  $z(y) \neq y$ . The properties of  $\check{u}_y$  imply that  $\check{u}_{y_n}$  vanishes near  $y$  and  $z(y)$ , a contradiction with the fact that  $z(y_n)$  tends to  $y \neq z(y)$ .  $\checkmark$

*Assertion (ii).* Assume that the assertion is false. Then, there exists some  $\beta \leq \frac{\delta}{4}$ , a sequence  $\{s_n\}$  tending to 0, a sequence  $\{t_n\}$  tending to some  $\bar{t}$ , such that the sequence  $\{w_n := w_{\gamma(s_n, t_n)}\}$  tends to  $u_{\gamma(\bar{t})}$ , with the property that  $\mathcal{S}_b(w_n) \cap \mathcal{A}(\gamma(t_n); \beta) = \emptyset$  or  $\mathcal{S}_b(w_n) \cap \mathcal{A}(z(t_n); \beta) = \emptyset$ . Since  $\bar{t} \in \Gamma_{(2k-3)}$ ,  $\mathcal{S}_b(u_{\gamma(\bar{t})}) = \{\gamma(\bar{t}), z(\bar{t})\}$ . We may also assume that  $\mp \check{u}_{\bar{t}}(\gamma(\bar{t}) \pm \frac{\beta}{4}) > 0$  and  $\pm \check{u}_{\bar{t}}(z(\bar{t}) \pm \frac{\beta}{4}) > 0$ . For  $n$  large enough, we will have that  $|\gamma(t_n) - \gamma(\bar{t})| < \frac{\beta}{4}$ ,  $|z(t_n) - z(\bar{t})| < \frac{\beta}{4}$ ,  $\mp \check{w}_n(\gamma(\bar{t}) \pm \frac{\beta}{4}) > 0$ , and  $\pm \check{w}_n(z(\bar{t}) \pm \frac{\beta}{4}) > 0$ . This implies that  $\check{w}_n$  vanishes in both  $(\gamma(t_n) - \frac{\beta}{2}, \gamma(t_n) + \frac{\beta}{2})$  and  $(z(t_n) - \frac{\beta}{2}, z(t_n) + \frac{\beta}{2})$ , a contradiction with our assumption.  $\checkmark$

The lemma is proved.  $\square$

LEMMA 5.31. *Under Assumptions 5.2, the set  $\Gamma_{(2k-2)}$  is not empty.*

*Proof.* Assuming that  $\Gamma_{(2k-2)} = \emptyset$ , the arguments in the proof of Lemma 5.26 can be globalized because the radii  $r_1$  and  $r_2$  can be chosen uniformly with respect to  $y \in \Gamma = \Gamma_{(2k-3)}$ . There exists  $\varepsilon > 0$  such that, for all  $(s, t) \in (0, \varepsilon] \times [0, 2\pi]$ , the combinatorial type of  $w_{\gamma(s,t)}$  is determined by the combinatorial type of  $u_{\gamma(t)}$  which is constant on  $\Gamma$  (see Lemma 5.24). Taking  $\varepsilon$  small enough in Lemma 5.30, we can apply Lemma 5.26 to the pair  $y = \gamma(t)$  and  $x(s, t) = \gamma(s, t)$  for all  $(s, t) \in (0, \varepsilon] \times [0, 2\pi]$ . Fix some  $s_0, s_1, 0 < s_1 < s_0 \leq \varepsilon$ . According to Lemma 5.26, for each  $t \in [0, 2\pi]$  the star at  $\gamma(s_0, t)$  inherits a natural labeling from the labeling of the star at  $\gamma(t)$ , with the same index  $a$  corresponding to the nodal interval emanating from  $\gamma(s_0, t)$  and hitting  $\Gamma$  at  $z(\gamma(s_0, t))$  close to  $z(\gamma(t))$ . Since the curve  $t \mapsto \gamma(s_0, t)$  bounds a simply connected domain  $\Omega_{s_0}$ , using the continuity of  $x \mapsto \omega_{x,a}$ , we can extend this labeling from the curve  $\gamma(s_0, \cdot)$  continuously into  $\Omega_{s_0}$ .

Fix  $s_1, 0 < s_1 < s_0$ . Along  $s \mapsto \gamma(s, t)$ , we can deform the labeled star at  $\gamma(s_0, t)$  continuously into the labeled “star”  $\{\omega_{y,1}, \dots, \omega_{y,(2k-3)}, \omega_{y,\nu}\}$  at  $\gamma(s_1, t)$ , with  $\omega_{\gamma(s_0,t),(2k-2)}$  deforming to  $\omega_{y,\nu}$ . Here,  $\omega_{y,\nu}$  is the direction of the normal to  $\Gamma$  at  $y$ , pointing outwards (this can be visualized on Figure 5.21, right image).

We have constructed a continuous nonzero vector field in  $\Omega_{s_1}$  which is transverse to the boundary  $\Gamma_{s_1}$ , pointing outwards. This is impossible by the Poincaré-Hopf theorem for manifold with boundary, see [Miln1997], Chap. 6, p. 35. The assumption that  $\Gamma_{(2k-2)}$  is empty yields a contradiction, therefore,  $\Gamma_{(2k-2)}$  cannot be empty.  $\square$

For later purposes (see Remark 5.40), we introduce the following generalization of the Poincaré-Hopf theorem, see [Gott1990, GoSa1995] and the recent paper [BaPP2024].

THEOREM 5.32. *Let  $X$  be a compact manifold with boundary. Let  $V$  be a  $C^\infty$  vector-field on  $X$  with isolated zeros  $x_i$  in  $X$  and no zero on  $\partial X$ . Then,*

$$(5.44) \quad \sum_i \text{ind}_{x_i} V = \chi(X) - \sum_{\xi \in \partial X, V^{tg}(\xi)=0, \langle V, \nu \rangle < 0} \text{ind}_\xi V^{tg},$$

where  $V^{tg} = V - \langle V, \nu \rangle \nu$  is the tangential component of  $V$  at the boundary and  $\nu$  is the outward pointing normal.

When  $V$  points outwards, the sum on the right hand side is empty.

#### 5.4. Behavior of $\lambda_k$ -Eigenfunctions near $\Gamma$ under Assumptions 5.2

In this section, we work under Assumptions 5.2.

Let  $\gamma : [0, L] \rightarrow \Gamma$  be an arc-length parametrization of  $\Gamma$ , compatible with the orientation, and such that the unit normal vector  $\nu(t)$  points inwards. Assume that  $\gamma(0) = \gamma(L) \notin \Gamma_{(2k-2)}$ . Let  $\gamma(s, t) = \gamma(t) + s\nu(t)$  where  $0 < s < s_0$ , with  $s_0$  small enough so that the map  $(0, s_0) \times [0, L] \rightarrow \Omega$  is a diffeomorphism onto a neighborhood of  $\Gamma$  in  $\Omega$ . We also use the notation  $\gamma_s(t)$  for  $\gamma(s, t)$ .

**5.4.1. Analysis near  $\eta \in \Gamma_{(2k-2)}$ .**

Under Assumptions 5.2, according to Lemmas 5.10 and 5.24, the subset  $\Gamma_{(2k-2)}$  is finite, with an even number of points. According to Section 5.3, this set has at least two points. Fix a radius  $r_1$  such that for all  $\eta \in \Gamma_{(2k-2)}$  the local structure theorem (see Section 2.4) and the energy argument (Lemma 5.17) apply to the function  $u_\eta$  in the disk  $D_+(\eta, 2r_1)$ . This is possible because the set  $\Gamma_{(2k-2)}$  is finite. Fix  $\beta = \frac{r_1}{10}$ .

LEMMA 5.33. *There exists  $r_2$ ,  $0 < 2r_2 < \beta$ , such that for all  $\eta \in \Gamma_{(2k-2)}$ , and for all  $x \in D_+(\eta, 2r_2)$ ,  $\mathcal{S}_b(w_x) \subset \mathcal{A}(\eta; \beta)$ , including the possibility that  $\mathcal{S}_b(w_x) = \emptyset$ .*

*Proof.* Assume that this is not the case. Then, there exists a sequence  $\{x_n\}$  tending to some  $\eta \in \Gamma_{(2k-2)}$  such that  $\mathcal{S}_b(w_n) \not\subset \mathcal{A}(\eta; \beta)$ , with  $w_n := w_{x_n} \in \mathbb{S}(U) \cap W_x$ , i.e., there exists  $z_n \in \mathcal{S}_b(w_n)$ ,  $z_n \notin \mathcal{A}(\eta; \beta)$ . We may assume that the sequence  $\{z_n\}$  converges to some  $z \neq \eta$ . Since  $w_n$  tends to  $u_\eta$   $C^1$ -uniformly and since  $\check{w}_n(z_n) = 0$ , we have  $\check{u}_\eta(z) = 0$ , a contradiction since  $\check{u}_\eta$  vanishes only at  $\eta$ .  $\square$

$\diamond$  A general combinatorial type  $\tau_\eta$  for  $u_\eta$ ,  $\eta \in \Gamma_{(2k-2)}$  is given by

$$(5.45) \quad \tau_\eta = \begin{pmatrix} 1 & R & a & C & b & L & f \\ a & \tau_\eta(R) & 1 & \tau_\eta(C) & f & \tau_\eta(L) & b \end{pmatrix}$$

where  $f := (2k-2)$ ,  $g := (2k-3)$ ,  $R := \{2, \dots, (a-1)\}$ ,  $C := \{(a+1), \dots, (b-1)\}$ , and  $L = \{(b+1), \dots, g\}$ , with  $R, C$  and  $L$  globally invariant under  $\tau_\eta$ . Here, we only consider the case  $2 \leq a < b \leq (2k-3)$ . The case in which  $\tau_\eta(1) = (2k-2)$  can be treated similarly, see Section 5.5.

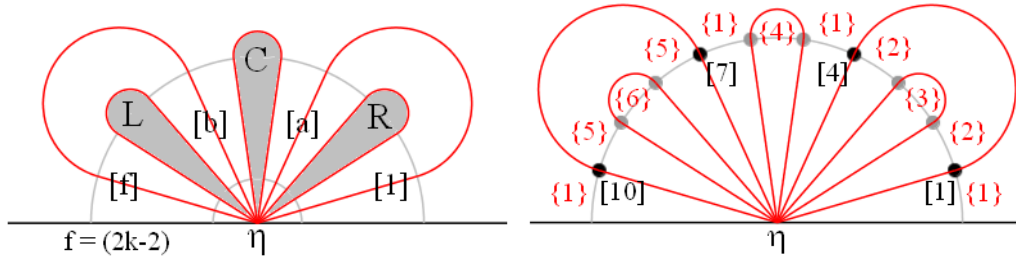


FIGURE 5.23. Rays and nodal domains for  $u_\eta$

The nodal set  $\mathcal{Z}(u_\eta)$  is a  $(k-1)$ -bouquet of loops  $\gamma_{j, \tau_\eta(j)}^\eta$ . Call  $A_{\eta, j}(r_1)$  the intersection points of  $\mathcal{Z}(u_\eta)$  with  $C_+(\eta, r_1)$ , labeled counter-clockwise along  $C_+(\eta, r_1)$ . By the local structure theorem and the energy argument, there are precisely  $(2k-2)$  such points, and there exists some  $\alpha_0 > 0$  such that the  $(2k-2)$  sub-arcs  $\mathcal{A}(A_{\eta, j}(r_1); \alpha_0)$  on  $C_+(\eta, r_1)$  are pairwise disjoint. Let  $D_+^c(\eta, r_1) = \Omega \setminus D_+(\eta, r_1)$  denote the complement of  $D_+(\eta, r_1)$ . The set  $\mathcal{Z}(u_\eta) \cap D_+^c(\eta, r_1)$  consists of  $(k-1)$  pairwise disjoint nodal arcs  $\gamma_{j, \tau_\eta(j)}^\eta \cap D_+^c(\eta, r_1)$ . By compactness, these arcs have pairwise disjoint  $\varepsilon_0$ -tubular neighborhoods  $\mathcal{U}_{j, r_1, \varepsilon_0}^\varepsilon$ , for some  $\varepsilon_0 < \alpha_0$  small enough. Fix the values  $\alpha_0$  and  $\varepsilon_0$  for the rest of this subsection.

We label the nodal domains of  $u_\eta$  according to their order of appearance when moving along  $C_+(\eta, r_1)$  counter-clockwise, encountering the point  $A_{\eta, 1}(r_1)$ ,  $A_{\eta, 2}(r_1)$ , etc. In the right part of Figure 5.23,  $k = 6$ ,  $a = 4$  and  $b = 7$ . The numbers between brackets are the labels of the rays at  $\eta$ . The numbers between braces are the labels of the nodal domains. The big dots stand for the intervals around the points  $A_{\eta, j}(r_1)$

(in grey, the dots corresponding to the bouquets of loops associated with the subsets  $R, C$  and  $L$ ) which might occur in the general case.

◇ To study  $\mathcal{Z}(w_x)$ , we now choose  $r_2$  such that:

- (i)  $r_2$  satisfies Lemma 5.33
- (ii)  $\forall \eta \in \Gamma_{(2k-2)}, \forall x \in D_+(\eta, 2r_2), \forall j, 1 \leq j \leq (2k - 2)$ , the set  $\mathcal{Z}(w_x) \cap \mathcal{A}(A_{\eta,j}(r_1), \alpha_0)$  contains exactly one point  $A_{x,j}(r_1)$
- (iii)  $\forall \eta \in \Gamma_{(2k-2)}, \forall x \in D_+(\eta, 2r_2), \mathcal{Z}(w_x) \cap D_+^c(\eta, r_1) \subset \bigcup \mathcal{U}_{\eta,j}^{\varepsilon_0}$ .

For  $x \in D_+(\eta, r_2)$ , there are two possibilities:

- a) either  $\mathcal{S}_b(w_x) = \emptyset$  and  $\mathcal{Z}(w_x)$  is a  $(k - 1)$ -bouquet of loops
- b) or  $\mathcal{S}_b(w_x) \neq \emptyset$  and  $\mathcal{Z}(w_x)$  is the wedge sum at  $x$  of a  $(k - 2)$ -bouquet of loops with two nodal intervals from  $x$  to the boundary points in  $\mathcal{S}_b(w_x) \subset \mathcal{A}(\eta; \beta)$ .

The choice of  $r_1$  and the energy argument imply that any nodal loop in  $\mathcal{Z}(w_x)$  intersects  $C_+(\eta, r_1)$  at precisely two points located in different intervals  $\mathcal{A}(A_{\eta,j}(r_1); \alpha_0)$ . Furthermore, when  $\mathcal{S}_b(w_x) \neq \emptyset$ , the nodal intervals from  $x$  to the boundary cannot both be contained in  $D_+(\eta, r_1)$ . Since  $\mathcal{S}_b(w_x) \subset \mathcal{A}(\eta; \beta)$ , one of the nodal intervals has to exit  $D_+(\eta, r_1)$  and re-enter. Call  $\delta_x^{z(x)}$  this nodal interval and  $z(x) \in \mathcal{S}_b(w_x)$  its end point. The interval  $\delta_x^{z(x)}$  actually intersects  $C_+(\eta, r_1)$  at precisely two points. Counting the points in  $\mathcal{Z}(w_x) \cap C_+(\eta, r_1)$ , we infer that the other nodal interval does not exit  $D_+(\eta, r_1)$ . Call  $\delta_x^{y(x)}$  this nodal interval and  $y(x) \in \mathcal{S}_b(w_x)$  its end point. Note that it may happen that  $y(x) = z(x)$ . The points  $A_{\eta,j}(r_1), 1 \leq j \leq (2k - 2)$ , are in natural bijection with the rays  $\omega_{\eta,j}$  at  $\eta$ . We will now show that, for  $x \in D_+(\eta, r_2)$ , the points  $A_{x,j}(r_1) \in \mathcal{A}(A_{\eta,j}, \alpha_0)$  define a labeling of the rays of the star at  $x$ .

*Case a)*  $\mathcal{S}_b(w_x) = \emptyset$ . Call  $\omega_{x,j}$  the unique ray at  $x$  such that the nodal arc  $\delta_{x,\omega_{x,j}}$  emanating from  $x$  tangentially to  $\omega_{x,j}$  exits  $C_+(\eta, r_1)$  at  $A_{x,j}(r_1)$ . Because these nodal arcs are pairwise disjoint away from  $x$ , Jordan's theorem implies that the  $\omega_{x,j}$  are ordered counter-clockwise as the points  $A_{x,j}(r_1)$ , i.e.  $\mathcal{R}_{\frac{\pi}{k-1}}(\omega_{x,j}) = \omega_{x,j+1}$ , where  $\mathcal{R}_{\frac{\pi}{k-1}}$  is the rotation with center  $x$  and angle  $\frac{\pi}{k-1}$ . Looking at  $\mathcal{Z}(w_x) \cap D_+^c(\eta, r_1)$ , we infer that the combinatorial types satisfy  $\tau_{w_x} = \tau_\eta$  with the above labeling of the star at  $x$ .

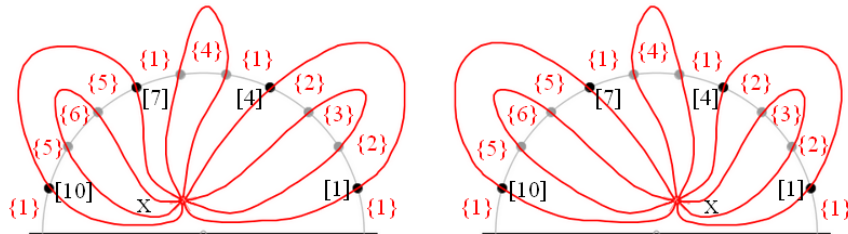


FIGURE 5.24.  $k = 6, \mathcal{Z}(w_x)$  with no boundary singular point

*Case b)*  $\mathcal{S}_b(w_x) \neq \emptyset$ . The  $(2k - 2)$  points  $A_{x,j}(r_1)$  can be partitioned into two subsets, the subset  $\mathcal{L}(x)$  which consists of the  $(2k - 4)$  points which belong to a nodal loop in  $\mathcal{Z}(w_x)$  and the subset  $\mathcal{L}'(x)$  which consists of the two points in

$\delta_x^{z(x)} \cap C_+(\eta, r_1)$ ; call  $A_{x,e}(r_1)$  the point at which  $\delta_x^{z(x)}$  exits  $D_+(\eta, r_1)$  and  $A_{x,e_z}(r_1)$  the point at which  $\delta_x^{z(x)}$  re-enters  $D_+(\eta, r_1)$ .

CLAIM 5.34. *With the above notation,  $e \neq e_z$  and  $e_z \in \{1, (2k - 2)\}$ .*

*Proof.* The first assertion is obvious.

Assume that  $e = 1$  and that  $e_z \neq (2k - 2)$ . Follow the nodal arc from  $A_{x,(2k-2)}(r_1)$  to  $x$  and then to  $A_{x,1}(r_1)$ . In  $D_+(\eta, r_1)$ , the point  $A_{x,e_z}(r_1)$  lies above this arc and the point  $z(x)$  below this arc, a contradiction since nodal arcs cannot intersect away from  $x$ . This is illustrated in Figure 5.25, left picture. The proof in the other cases,  $e = (2k - 2)$  and  $e, e_z \notin \{1, (2k - 2)\}$ , is similar.  $\square$

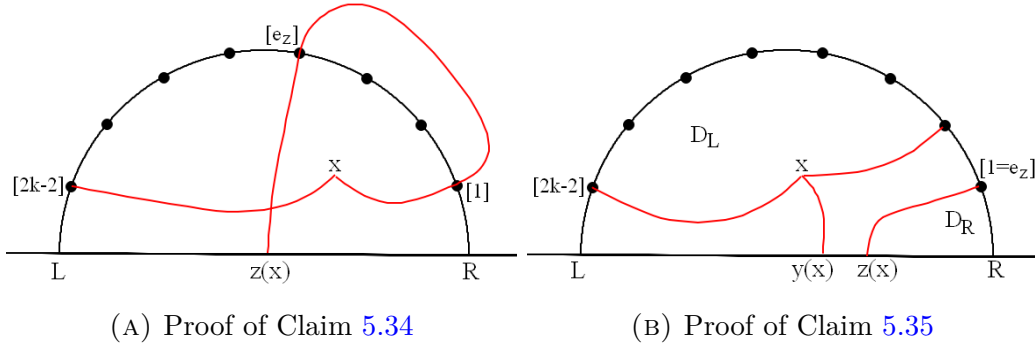


FIGURE 5.25. Proofs of Claims

Look at the rays at  $x$ . Call  $\omega_{x,j}$  the ray such that the nodal arc  $\delta_{x,\omega_{x,j}}$ , emanating from  $x$  tangentially to the ray  $\omega_{x,j}$ , first exits  $C_+(\eta, r_1)$  at the point  $A_{x,j}(r_1)$ . Doing so, we label the  $(2k - 4)$  rays corresponding to the  $(k - 2)$  loops in  $\mathcal{Z}(w_x)$ , as well as the ray corresponding to the nodal interval  $\delta_x^{z(x)}$ . One ray has not yet been labeled, namely the ray which corresponds to the nodal interval  $\delta_x^{y(x)}$ . This must be the ray  $\omega_{x,e_z}$ , so that  $\delta_x^{y(x)} = \delta_{x,\omega_{x,1}}$  or  $\delta_x^{y(x)} = \delta_{x,\omega_{x,(2k-2)}}$  according to Claim 5.34.

CLAIM 5.35. *In Case b), with the above notation,*

$$(5.46) \quad \begin{cases} e_z = 1 \Rightarrow y(x) \leq z(x) & \text{and } y(x) < z(x) \Rightarrow e_z = 1 \\ e_z = (2k - 2) \Rightarrow y(x) \geq z(x) & \text{and } y(x) > z(x) \Rightarrow e_z = (2k - 2). \end{cases}$$

*Proof.* Assume that  $e_z = 1$  and consider the nodal arc inside  $D_+(\eta, r_1)$ , between  $A_{x,1}(r_1)$  and  $z(x)$ . This arc divides  $D_+(\eta, r_1)$  into two connected components,  $D_R$  and  $D_L$ , with  $D_R$  containing the arc of  $C_+(\eta, r_1)$  from  $A_{x,1}(r_1)$  to the boundary point  $R$  on the right of  $z(x)$  and  $D_L$  containing the arc of  $C_+(\eta, r_1)$  from  $A_{x,(2k-2)}(r_1)$  to the boundary point  $L$  on the left of  $z(x)$ . Because the nodal arcs cannot intersect away from  $x$ , the point  $x$  must belong to  $D_L$  and  $y(x) \leq z(x)$ . Similarly, if  $e_z = (2k - 2)$ , then  $z(x) \leq y(x)$ . These statements imply the remaining statements. The proof is illustrated in Figure 5.25, right picture.  $\square$

REMARK 5.36. Let  $x \in \Omega$  be such that  $y(x) = z(x)$ . Then, there exists a neighborhood  $\mathcal{U}_x$  of  $x$  such that there do not exist  $x_1, x_2 \in \mathcal{U}_x$  with  $y(x_1) < z(x_1)$  and  $y(x_2) > z(x_2)$ . Otherwise stated, for any  $x_1 \in \mathcal{U}_x$ , with  $\mathcal{S}_b(w_{x_1}) \neq \emptyset$ , either  $y(x_1) \leq z(x_1)$  or  $y(x_1) \geq z(x_1)$ . This is a consequence of Claim 5.35.

The possible combinatorial types of  $w_x$ , depending on whether  $y(x) < z(x)$  or  $z(x) < y(x)$  are as follows.

$$(5.47) \quad \tau_{y(x) < z(x)} = \begin{pmatrix} 1 & R & a & C & b & L & f \\ \downarrow_{y(x)} & \tau_\eta(R) & \downarrow_{z(x)} & \tau_\eta(C) & f & \tau_\eta(L) & b \end{pmatrix}$$

$$(5.48) \quad \tau_{z(x) < y(x)} = \begin{pmatrix} 1 & R & a & C & b & L & f \\ a & \tau_\eta(R) & 1 & \tau_\eta(C) & \downarrow_{z(x)} & \tau_\eta(L) & \downarrow_{y(x)} \end{pmatrix}.$$

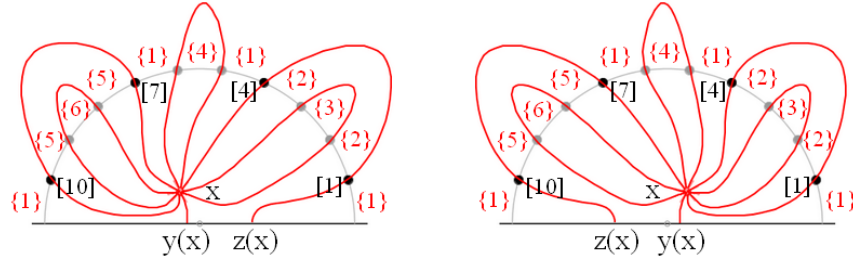


FIGURE 5.26.  $k = 6$ ,  $\mathcal{Z}(w_x)$  with two boundary singular points

Joining the extremities  $y(x)$  and  $z(x)$  of the nodal intervals  $\delta_x^{y(x)}$  and  $\delta_x^{z(x)}$  with the interval  $[y(x), z(x)]$ , we obtain a loop at  $x$ . The combinatorial types  $\tau_{z(x) < y(x)}$  and  $\tau_{y(x) < z(x)}$  then correspond to  $\tau_\eta$ . Labeling the nodal domains of  $u_\eta$  as usual, and following the nodal domains of  $w_x$  by deformation, the words describing the nodal domains on  $C_+(\eta, r_1)$  are the same.

Note that both cases  $y(x) < z(x)$  and  $y(x) > z(x)$  actually occur. Indeed, choose some  $y \in \Gamma_{(2k-3)}$  close to  $\eta$ , on its left. Then  $\mathcal{S}_b(u_y) = \{y, z(y)\}$  with  $z(y)$  on the right of  $\eta$ . Choosing  $x$  above  $y$  and close enough, we will have  $\mathcal{S}_b(w_x) = \{y(x), z(x)\}$  with  $y(x) < z(x)$ . If we choose  $y$  to the right of  $\eta$ , we will similarly obtain  $z(x) < y(x)$ .

Figure 5.26 illustrates the two possible cases. In this figure, the numbers in brackets represent the labels of the points  $A_{x,j}(r_1)$ . Label the rays at  $x$  so that the nodal arc emanating from  $x$  tangentially to  $\omega_{x,a}$  exits  $C_+(\eta, r_1)$  at  $A_{x,a}(r_1)$  and hits the boundary at  $z(x)$ . Then, when  $y(x) < z(x)$ , the ray tangent to  $\delta_x^{y(x)}$  at  $x$  is  $\omega_{x,1}$ ; when  $z(x) < y(x)$ , the ray tangent to  $\delta_x^{y(x)}$  at  $x$  is  $\omega_{x,(2k-2)}$ .

Figure 5.27 displays a simple transition. When  $x$  moves on a line parallel to the boundary  $\Gamma$ , the rays corresponding to  $\delta_x^{z(x)}$  are labeled either [4], when  $y(x) < z(x)$ , or [7], when  $z(x) < y(x)$ .

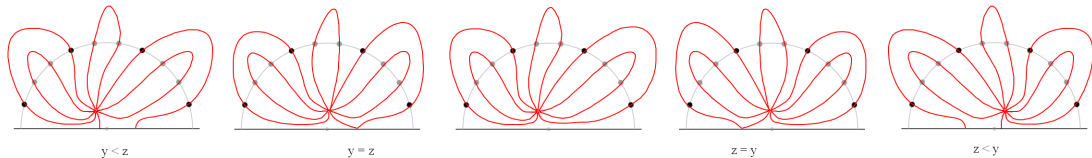


FIGURE 5.27. Simple transition in  $D_+(\eta, r_2)$

Move from left to right on a parallel to  $\Gamma$ . Start from  $x_1$  above  $y_1$  on the left of  $\eta$  with  $y(x_1) < z(x_1)$ . Arrive at  $x_2$  such that  $y(x_2) = z(x_2)$ . When  $x$  moves from  $x_2$  to



the right, the broken loop  $\gamma_{1,4}^{w_{x_2}}$  lifts off, and  $\mathcal{Z}(w_x)$  does not hit  $\Gamma$  (middle picture). When  $x$  reaches some  $x_3$  such that  $y(x_3) = z(x_3)$ , a loop in  $\mathcal{Z}(w_x)$  touches down as the broken loop  $\gamma_{7,10}^{w_{x_3}}$ . When  $x$  moves on from  $x_3$  to  $x_4$  on the right, we have  $z(x) < y(x)$ . During this transition, we can glue the interval between  $y(x)$  and  $z(x)$  on the boundary with the nodal intervals  $\delta_x^{y(x)}$  and  $\delta_x^{z(x)}$  in order to make a loop. Following the nodal domains continuously, their labeling does not change and the combinatorial type of  $w_x$  does not change either. There has been some shift from the ray  $\omega_{x_1,4}$  to the ray  $\omega_{x_4,7}$ .

REMARK 5.37. The simple transition displayed in Figure 5.27 might not be what happens in general. When  $x$  moves on  $\gamma_{s_0}$ , from above  $\eta_1$  to above  $\eta_2$ , there might be several points  $x$  for which  $y(x) = z(x)$ . Although we do not need this information in the reasoning below, it would be interesting to investigate what actually occurs.

We can continuously deform the nodal arcs inside  $D_+(\eta, r_1)$  into the rays from  $x$  to the points  $A_{\eta,j}(r_1)$ . For  $r_2$  small enough and for  $x \in D_+(\eta, r_2)$ , the star at  $x$  can be continuously deformed to the constant set  $\{A_{\eta,1}(r_1), \dots, A_{\eta,(2k-2)}(r_1)\}$ .

**5.4.2. Analysis inside the arc  $\mathcal{A}(\eta_1, \eta_2)$ .** Let  $\eta_1, \eta_2$  be two points in  $\Gamma_{(2k-2)}$ , such that  $\mathcal{A}(\eta_1, \eta_2) \subset \Gamma_{(2k-3)}$ . Call  $t'_1, t'_2$  the parameters such that  $\gamma(t'_i) = \eta_i$ .

For the sake of simplicity, we assume that the combinatorial type of a generator  $u_y$  of  $U_y$  for  $y \in \mathcal{A}(\eta_1, \eta_2)$  is given by Figure 5.28. More precisely, we assume that  $1 < a < (2k - 3)$ ,

$$R = \{2, \dots, (a - 1)\} \quad \text{and} \quad L = \{(a + 1), \dots, (2k - 3)\},$$

and that, for  $y \in \mathcal{A}(\eta_1, \eta_2)$ , the combinatorial type  $\tau$  of  $u_y$  is given by

$$(5.49) \quad \tau_+ = \begin{pmatrix} \downarrow & R & a & L \\ a & \tau(R) & \downarrow & \tau(L) \end{pmatrix} \quad \text{or} \quad \tau_- = \begin{pmatrix} R & a & L & \downarrow \\ \tau(R) & \downarrow & \tau(L) & a \end{pmatrix}.$$

The cases in which  $a \in \{1, (2k - 3)\}$  can be dealt with similarly.

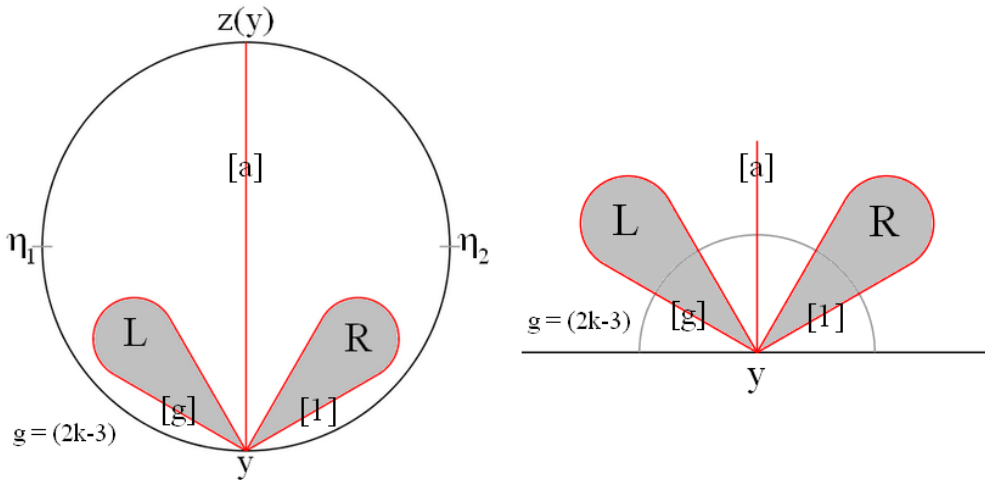


FIGURE 5.28. The global and local pictures for  $\mathcal{Z}(u_y)$

The nodal interval  $\delta := \delta_{y,a} = \delta_y^{z(y)}$  from  $y$  to  $z(y)$  separates the domain  $\Omega$  into two connected components  $\Omega_{a,R}$  and  $\Omega_{a,L}$ . To label nodal domains, we use Procedure 5.49.

The domain  $\Omega_{a,R}$  contains the bouquet of loops  $\mathcal{B}_R$  and  $(n_R + 1)$  nodal domains of  $u_y$ , where  $n_R = (a - 1)/2$  is the number of loops in  $\mathcal{B}_R$ . We call  $D_1$  the nodal domain exterior to  $\mathcal{B}_R$  in  $\Omega_{a,R}$ , its boundary contains the nodal interval  $\delta$ . The interior nodal domains of  $\mathcal{B}_R$  are labeled  $D_2$  to  $D_{n_R+1}$ . The word which describes the nodal domains of  $u_y$  inside  $\Omega_{a,R}$  is

$$(5.50) \quad \mathcal{W}_{a,R} = |1|\mathcal{W}_R|1| \quad \text{with} \quad \|\mathcal{W}_{a,R}\| = 2 + \|\mathcal{W}_R\| = (2n_R + 1).$$

The “letters” of the words are labels of the nodal domains, and separated by vertical bars, as in Paragraph 4.2.5.3.

Here, the word  $\mathcal{W}_R$  describes the nodal domains related to  $\mathcal{B}_R$ . This is a word in the letters  $2, \dots, (n_R + 1)$ , and possibly the letter 1 (this occurs if  $\mathcal{B}_R$  contains consecutive loops as in Figure 5.53, left sub-figure).

The domain  $\Omega_{a,L}$  contains the bouquet of loops  $\mathcal{B}_L$  and  $(n_L + 1)$  nodal domains of  $u_y$ , where  $n_L = (2k - a - 3)/2$  is the number of loops in  $\mathcal{B}_L$ . We call  $D_{n_R+2}$  the nodal domain exterior to  $\mathcal{B}_L$  in  $\Omega_{a,L}$ , its boundary contains the nodal interval  $\delta$ . The interior nodal domains of  $\mathcal{B}_L$  are labeled  $D_{n_R+3}$  to  $D_k$ , and we have  $k = n_R + n_L + 2$ . Letting  $m := (n_R + 2)$ , the word which describes the nodal domains of  $u_y$  inside  $\Omega_{a,L}$  is

$$(5.51) \quad \mathcal{W}_{a,L} = |m|\mathcal{W}_L|m| \quad \text{with} \quad \|\mathcal{W}_{a,L}\| = 2 + \|\mathcal{W}_L\| = 2n_L + 1.$$

Here,  $\mathcal{W}_L$  describes the nodal domains related to  $\mathcal{B}_L$ . This is a word in the letters  $(n_R + 3), \dots, k$ , and possibly  $m = (n_R + 2)$ .

Finally, the word which describes how the nodal domains of  $u_y$  hit  $C_+(y, r)$  for  $r$  small enough is given by

$$(5.52) \quad \mathcal{W}_y = |1|\mathcal{W}_R|1|m|\mathcal{W}_L|m| \quad \text{with} \quad \|\mathcal{W}_y\| = (2n_R + 2n_L + 2) = (2k - 2).$$

The important fact is that the nodal domains  $D_1$  and  $D_m$  (with  $m = (n_R + 2)$ ) share a common boundary line, the nodal interval  $\delta$ .

In the following figures, the letters or numbers between brackets are the labels of the rays; the numbers between braces are the labels of the nodal domains. The labeling of the nodal domains in the central sub-figure of Figure 5.29 follows Procedure 5.49.

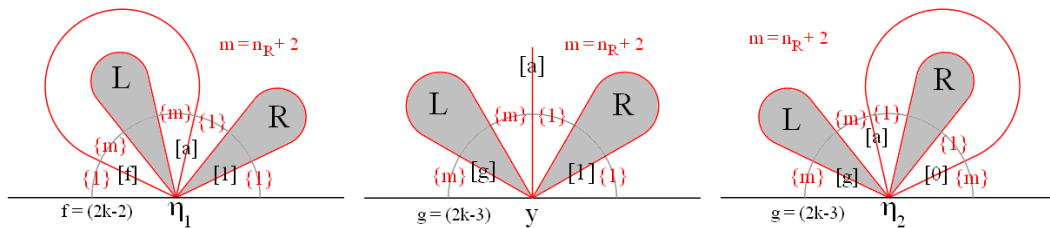
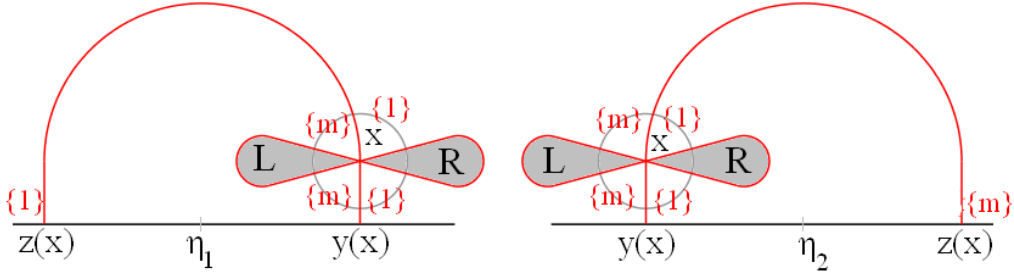
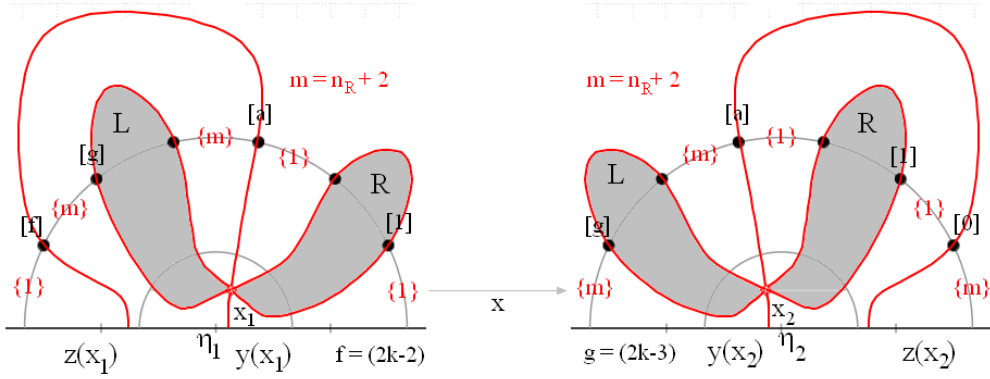


FIGURE 5.29. Limits when  $y$  tends to  $\eta_2$  from the left or to  $\eta_1$  from the right



FIGURE 5.31. Nodal patterns for  $x$  above  $y$ , and close to  $y$ FIGURE 5.32. The transition from above  $y_1$  to above  $y_2$ 

More precisely, let  $t_1$  and  $t_2$  be such that  $\gamma(t_i) = y_i$ . As in Lemma 5.30, there exists some  $s_1 > 0$  such that for all  $t \in [t_1, t_2]$ , and  $0 < s \leq s_1$ , the function  $w_{\gamma(s,t)}$  satisfies  $\mathcal{S}_b(w_{\gamma(s,t)}) = \{y(s,t), z(s,t)\}$  with  $y(s,t)$  close to  $\gamma(t)$ , and  $z(s,t)$  close to  $z(\gamma(t))$ .

#### 5.4.3. Under Assumption 5.2 and the further assumption $\Gamma_{(2k-2)} \neq \emptyset$ .

Let  $\gamma_0 : [0, L] \rightarrow \Gamma$  be an arc-length ‘counter-clockwise’ parametrization of  $\Gamma$ , such that  $\gamma_0(0) = \gamma_0(L) \notin \Gamma_{(2k-2)}$ . Let  $m = \#(\Gamma_{(2k-2)}) \geq 2$ , an even integer. Let  $0 < t_1 < \dots < t_m < L$  be such that  $\Gamma_{(2k-2)} = \{\eta_1, \dots, \eta_m\}$ , with  $\eta_i = \gamma_0(t_i)$ . Let  $\gamma(s, t) := \gamma_0(t) + s\nu(t)$ , where  $\nu(t)$  is the unit normal to  $\gamma_0$  at  $\gamma_0(t)$ , pointing inwards. For  $s$  small enough, we have a diffeomorphism from  $[0, s] \times [0, L]$  onto a neighborhood of  $\Gamma$ . We also write  $\gamma_s(t)$  for  $\gamma(s, t)$  and view this map as  $L$ -periodic in  $t$ . Denote by  $\Omega_{s_0}$  the simply connected domain contained in  $\Omega$ , and bounded by  $\Gamma_{s_0}$ , with  $\Gamma_{s_0} := \partial\Omega_{s_0} = \gamma_{s_0}([0, L])$ .

We now choose  $r_1, r_2, r_3$ , and  $s_0$  small enough so that the following properties hold.

- i) The number  $r_1, r_2$  are chosen according to Subsection 5.4.1, which describes the behaviour of  $\mathcal{Z}(w_x)$  in  $D_+(\eta, r_1)$  for any  $x \in D_+(\eta, r_2)$ , and any  $\eta \in \Gamma_{(2k-2)}$ .
- ii) For  $j \in \{1, \dots, m\}$ , define the points  $t_j^\pm := t_j \pm \frac{1}{2}r_2$ , and first choose  $s_0$  so that  $\gamma(s_0, t_j^\pm) \in D_+(\eta_j, r_2)$ . According to Remark 5.29, there exists some  $r_3 > 0$  such that, choosing  $s_0$  small enough, Subsection 5.4.2 applies to the behavior of  $\mathcal{Z}(w_{\gamma(s_0,t)})$  in  $D_+(\gamma(t), r_3)$ , for  $t \in [t_j^+, t_{j+1}^-]$ ,  $y(\gamma(s_0, t)) \neq z(\gamma(s_0, t))$ , and we can follow these points by continuity.

Figure 5.33 displays the nodal sets  $\mathcal{Z}(w_{\gamma(s_0,t)})$  for  $t = t_1^+, t \in (t_1^+, t_2^-), t = t_2^-, t = t_2^+$  (here  $k = 6$ ).

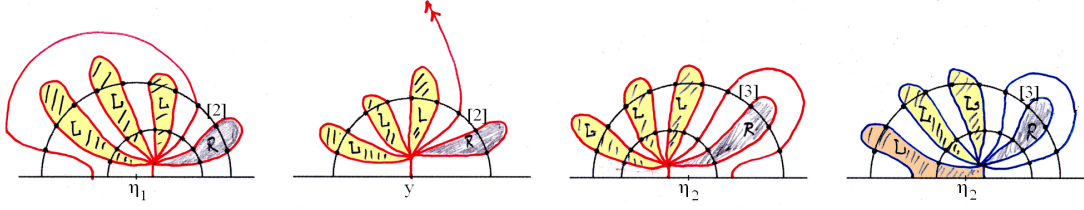


FIGURE 5.33.  $\mathcal{Z}(w_{\gamma(s_0,t)})$  for  $t = t_1^+, t \in (t_1^+, t_2^-), t = t_2^-, t = t_2^+$

The  $C^\infty$  family  $\Omega \ni x \mapsto w_x \in U(\lambda_k)$  has the property that the function  $w_x$  vanishes precisely at order  $(k - 1)$  at the point  $x$ , and that the leading term  $h_x$  in the Taylor expansion of  $w_x$  at the point  $x$  is a nonzero harmonic homogeneous polynomial of degree  $(k - 1)$  in  $T_x\Omega$ .

We fix a reference orthonormal direct frame in  $\mathbb{R}^2$ , with coordinates  $(\xi_1, \xi_2) = [\rho, \theta]$ . We use  $C, S$  as the basis for the two dimensional space of harmonic homogenous polynomials of degree  $(k - 1)$  in  $\mathbb{R}^2$ , where

$$C(\rho \cos \theta, \rho \sin \theta) = \rho^{k-1} \cos((k - 1)\theta); \quad S(\rho \cos \theta, \rho \sin \theta) = \rho^{k-1} \sin((k - 1)\theta).$$

We represent  $h_x$  in this basis as

$$h_x = a_x C + b_x S$$

with  $a_x^2 + b_x^2 > 0$ . Since  $x \mapsto h_x$  is  $C^\infty$ , it follows that we have a  $C^\infty$  map

$$(5.55) \quad \tilde{h} : \Omega_{s_0} \ni x \mapsto \tilde{h}_x := \left( a_x (a_x^2 + b_x^2)^{-\frac{1}{2}}, b_x (a_x^2 + b_x^2)^{-\frac{1}{2}} \right) \in \mathbb{S}^1.$$

Since  $\Omega_{s_0}$  is simply connected, the restriction  $\tilde{h}|_{\Gamma_{s_0}}$  of this map to  $\Gamma_{s_0}$  must have degree 0.

CLAIM 5.38. *The map  $\tilde{h}|_{\Gamma_{s_0}}$  has nonzero degree.*

*Proof.* Define the angle  $\phi_{\gamma(s_0,t)}$  by continuity along  $\gamma_{s_0}(\mathbb{R})$  so that

$$\tilde{h}_{\gamma(s_0,t)} = \left( \cos(\phi_{\gamma(s_0,t)}), \sin(\phi_{\gamma(s_0,t)}) \right).$$

Consider the map  $x \mapsto h_x$ . The zero set of the polynomial  $h_x$  consists of the  $(2k - 2)$  equi-angular rays tangent to the nodal set of  $w_x$  at the point  $x$ , the so-called *star*  $\Sigma_x$  at this point. These rays  $\omega_{x,j}$  are the zeros of the equation  $\cos((k - 1)\theta - \phi_x) = 0$ , so that

$$\omega_{x,j} = \frac{1}{k - 1} \left( \frac{\pi}{2} + \phi_x \right) + j \frac{\pi}{k - 1}, \quad j \in \{0, \dots, (2k - 3)\}.$$

When  $t$  varies, we can follow one ray in  $\Sigma_{\gamma(s_0,t)}$  by continuity. If this ray turns by an angle  $\omega$ , then the previous equation shows that  $\tilde{h}_{\gamma(s_0,t)}$  turns by the angle  $(k - 1)\omega$ . To compute the degree of  $\tilde{h}|_{\Gamma_{s_0}}$  it suffices to follow one ray of  $\Sigma_{\gamma(s_0,t)}$ .

Fix some  $j, 1 \leq j \leq m$  (with the convention that  $t_{m+1} = t_1$ ). Call  $e^{(j)}(s_0)$  the unit vector at  $\gamma(s_0, t_j^+)$  which is tangent to the nodal arc emanating from  $\gamma(s_0, t_j^+)$  which intersects  $C_+(\eta_j, r_1)$  at  $A_{\gamma(s_0, t_j^+), 2}(r_1)$  near the point  $A_{\eta_j, 2}(r_1)$ . Viewing  $\gamma$  as an  $L$ -periodic function in  $t$ , call  $e^{(j)}(\gamma(s_0, t))$  the continuous unit vector field along

$\gamma(s_0, [t_j, t_j + L))$  which takes the value  $e^{(j)}(s_0)$  at  $t_j^+$  and such that  $e^{(j)}(\gamma(s_0, t))$  belongs to the star  $\Sigma_{\gamma(s_0, t)}$ .

According to Subsection 5.4.2, for  $t \in [t_j^+, t_{j+1}^-]$ , the vector  $e^{(j)}(\gamma(s_0, t))$  is tangent at the point  $\gamma(s_0, t)$  to the nodal arc from  $\gamma(s_0, t)$  to  $A_{\gamma(s_0, t), 2}(r_1)$ .

When  $t$  varies from  $t_j^+$  to  $t_{j+1}^-$ , the nodal interval  $\delta_{\gamma(s_0, t)}^{z(\gamma(s_0, t))}$  changes continuously and we have the following phenomenon:

- ◇ For  $t := t_j^+$ ,  $\delta_{\gamma(s_0, t)}^{z(\gamma(s_0, t))}$  exits  $D_+(\eta_j, r_1)$  near the point  $A_{\eta_j, a_j}(r_1)$  for some integer  $a_j$ , and re-enters  $D_+(\eta_j, r_1)$  near the point  $A_{\eta_j, (2k-2)}(r_1)$ .
- ◇ For  $t := t_{j+1}^-$ ,  $\delta_{\gamma(s_0, t)}^{z(\gamma(s_0, t))}$  exits  $D_+(\eta_{j+1}, r_1)$  near the point  $A_{\eta_{j+1}, a_{j+1}}(r_1)$ , and re-enters  $D_+(\eta_{j+1}, r_1)$  near the point  $A_{\eta_{j+1}, 1}(r_1)$ . This is illustrated in Figure 5.32, right picture, in which the points  $A_{\eta_{j+1}, i}(r_1)$  are labeled  $i = 0, 1, \dots, (2k - 3)$  where as we use the labeling  $i = 1, \dots, (2k - 2)$  in the previous statement. The important fact is the shift from  $a_j$  to  $a_j + 1$ .
- ◇ Furthermore, for  $t \in (t_j^+, t_{j+1}^-)$  the nodal interval  $\delta_{\gamma(s_0, t), e^{(j)}(\gamma(s_0, t))}$  exits  $D_+(\eta_{j+1}, r_1)$  near the point  $A_{\eta_{j+1}, a_{j+1}}(r_1)$ , and re-enters  $D_+(\eta_{j+1}, r_1)$  near the point  $A_{\eta_{j+1}, 1}(r_1)$ .

This behavior is illustrated in Figure 5.34. Figure 5.35 gives a more global view.

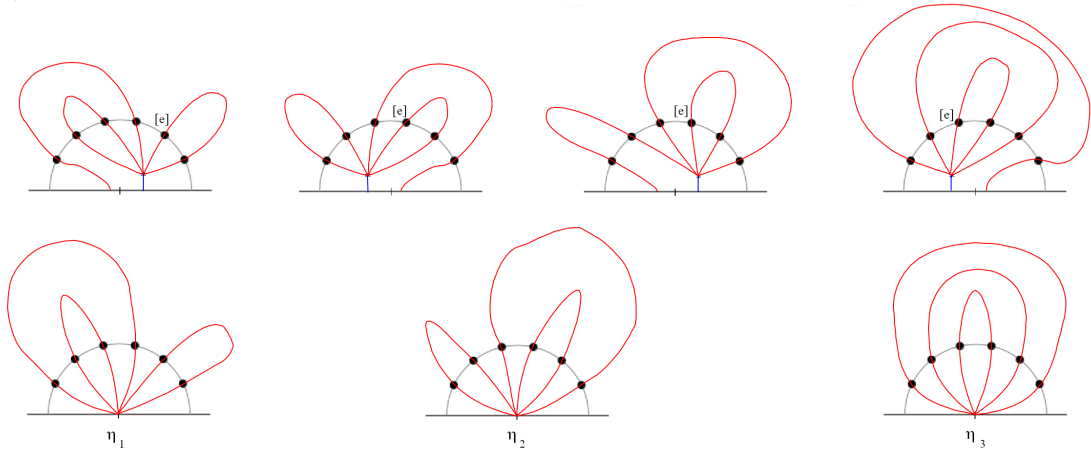


FIGURE 5.34.  $e^{(1)}$  is in positions 2-3-3-4 on  $C_+$

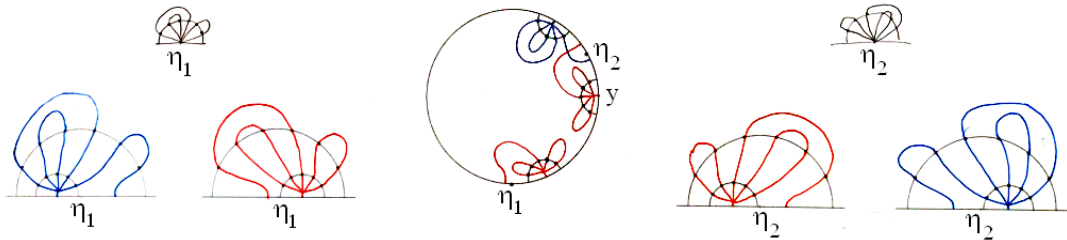


FIGURE 5.35. From  $t_1^+$  to  $t_2^+$ , local and global views

We interpret this phenomenon by saying that the angle of the vector  $e^{(j)}(\gamma(s_0, t))$  with respect to the  $t$ -derivative  $\gamma'(s_0, t)$  has increased by  $\frac{\pi}{k-1}$  when passing from  $t_j^+$  to  $t_{j+1}^+$ . Otherwise stated, in the reference frame, the vector  $\tilde{h}_{\gamma(s_0, t)}$  has turned by  $\pi + (k - 1)\angle(\gamma'(s_0, t_j^+), \gamma'(s_0, t_{j+1}^+))$ , where  $\angle$  denotes the angle between two vectors.

Moving along  $\Gamma_{s_0}$ , the vector  $\tilde{h}$  has turned by  $m\pi + 2(k-1)\pi$  in the reference frame. It follows that the degree of  $\tilde{h}$  is  $\frac{m}{2} + (k-1)$ , a positive integer since  $m$  is even and positive. Claim 5.38 is proved.  $\checkmark$

REMARK 5.39. One could also give a “degree proof” of Lemma 5.31. In the framework of this lemma, the star along  $\gamma_s$ , turning counter-clockwise, follows the moving frame. When  $\Gamma_{(2k-2)} \neq \emptyset$ , the same occurs with extra counter-clockwise rotations due to the presence of the points  $\eta_j \in \Gamma_{(2k-2)}$ .

REMARK 5.40. An alternative approach to reach a contradiction is to construct a non-zero continuous vector-field, and to apply the Poincaré-Hopf theorem with boundary, Theorem 5.32.

We can summarize the previous analysis in the following lemma.

LEMMA 5.41. *Under Assumptions 5.2, the set  $\Gamma_{(2k-2)}$  cannot be non-empty.*

**5.4.4. Overall conclusion.** Putting Subsection 5.4.2 (Lemma 5.31) and Subsection 5.4.3 (Lemma 5.41) together, we see that Assumptions 5.2, lead to a contradiction. Therefore,  $\text{mult}(\lambda_k) \leq (2k - 3)$  for all  $k \geq 3$ .

**5.4.5. Examples.**

In this subsection, we look at simple examples which shed some more light on the approach in Subsection 5.4.3. Indeed moving along  $\Gamma$  counter-clockwise starting from  $\eta_1$ , the combinatorial type of  $u_y$  changes on crossing a point  $\eta_j$  (Lemma 5.24). In some cases, arriving back at  $\eta_1$ , the combinatorial type is different from the original one, a contradiction since  $\dim U_y = 1$  for all  $y \in \Gamma$ .

Let  $m := \#(\Gamma_{(2k-2)})$ . As we already know,  $m$  is positive (see Lemma 5.31) and even (see Lemma 5.24).

Let us consider the simple case in which  $m = 2$ , with  $\Gamma_{(2k-2)} = \{\eta_1, \eta_2\}$ . Figure 5.36, left picture, exhibits an impossible configuration. Indeed, when the base point  $y$  moves away from  $\eta_1$  towards  $\eta_2$ , and continues moving to reach  $\eta_1$  again, the combinatorial type of  $u_y$  changes according to the figure. The words associated with the corresponding functions are  $\mathcal{W}_{\eta_1} = |1|2|1|3|4|3|1|$ ,  $\mathcal{W}_{\eta_2} = |1|2|3|2|1|4|1|$  and  $\mathcal{W}_{\eta_1} = |1|2|3|4|3|2|1|$ . The first and third words have different signatures, a contradiction.

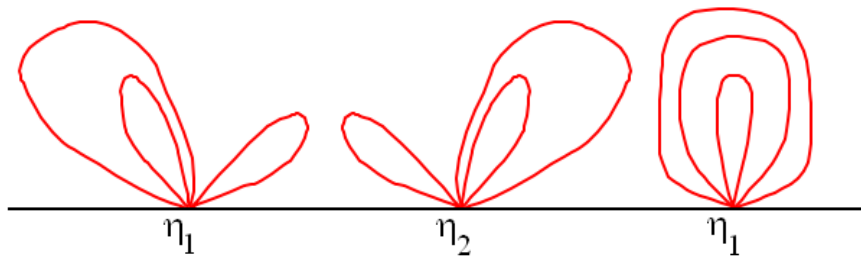


FIGURE 5.36. Case  $m = 2$ ,  $k = 4$ , impossible configuration

Figure 5.37 displays a case in which no such contradiction is reached by this argument. In this example,  $y$  moves counter-clockwise (i.e. from left to right) from  $\eta_1$  to

$\eta_2$ , and then to  $\eta_1$  again. To visualize the changes better, we change the color of the loop which opens up, first from black to red at  $\eta_1$ , then from black to blue at  $\eta_2$ . The red loop  $\gamma_{1,6}^{\eta_1}$  in the left figure opens up on the left of  $\eta_1$ , the end point  $z(y)$  moves from  $\eta_1$  to  $\eta_2$  clockwise, and the loop closes up again on the right of  $\eta_2$  to become the red loop  $\gamma_{1,2}^{\eta_2}$  (middle figure). When  $y$  continues moving counter-clockwise, from  $\eta_2$  to  $\eta_1$ , the blue loop at  $\gamma_{5,6}^{\eta_2}$  opens up on the left of  $\eta_2$ , its end point  $z(y)$  moves clockwise from  $\eta_2$  to  $\eta_1$ , and closes up again on the right of  $\eta_1$  to become the blue loop  $\gamma_{1,6}^{\eta_1}$  (right figure). The colors show that although the combinatorial types of  $u_{\eta_1}$  and  $u_{\eta_2}$  are identical, there is some change in the colored loop, hinting at some kind of rotation.

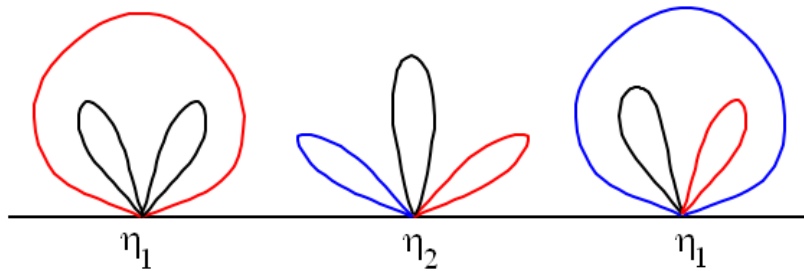


FIGURE 5.37. Case  $m = 2, k = 4$

This rotation can be visualized as follows. Label the nodal domains in the left figure. When  $y$  moves counter-clockwise from  $\eta_1$  to  $\eta_2$  and then to  $\eta_1$  again, follow the nodal domains under deformation. The labels are indicated by the numbers between braces in Figure 5.38. The corresponding words are respectively given by

$$|1|2|3|2|4|2|1| \quad |2|1|2|3|2|4|2| \quad |4|2|1|2|3|2|4|.$$

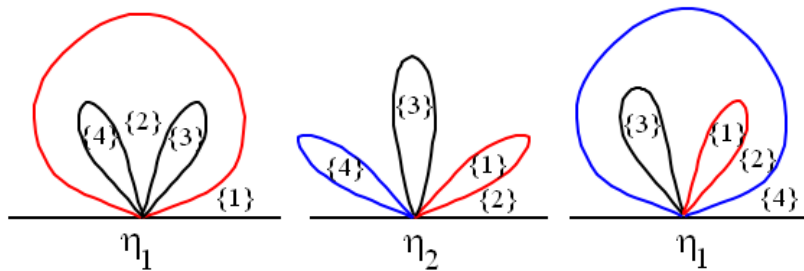


FIGURE 5.38. Case  $m = 2, k = 4$ , with nodal labeling

Since the first and last letter are always the same, it turns out to be more appropriate to look at these words as written on a circle (so that the last letter is suppressed). This is indicated by the symbol  $\circ$  at the end of the words. With this convention, the words in Figure 5.38 are now given by

$$|1|2|3|2|4|2|\circ \quad |2|1|2|3|2|4|\circ \quad |4|2|1|2|3|2|\circ$$

as illustrated in Figure 5.39 which indicates a positive rotation by  $\frac{2\pi}{3}$ .

The previous situation always occurs when  $m = 2$  and  $k = 3$ , as we now show.



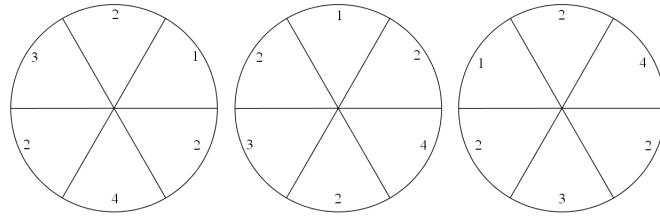


FIGURE 5.39. Nodal words seen on the circle

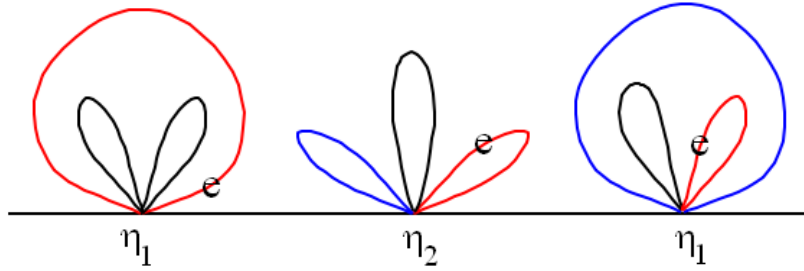


FIGURE 5.40. Case  $m = 2, k = 4$ , with the vector  $e^{(1)}$

Case  $m := \#(\Gamma_{(2k-2)}) = 2, k = 3$ . In this case, there are two possible combinatorial types at  $\eta \in \Gamma_{(2k-2)}$ , namely

$$\tau_1 = \begin{pmatrix} 1 & 2 & 3 & 4 \\ 4 & 3 & 2 & 1 \end{pmatrix} \quad \text{and} \quad \tau_2 = \begin{pmatrix} 1 & 2 & 3 & 4 \\ 2 & 1 & 4 & 3 \end{pmatrix}.$$

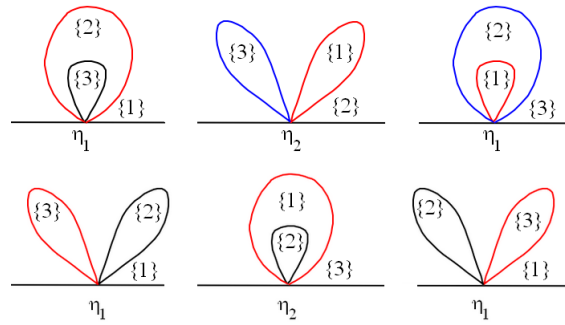


FIGURE 5.41. Evolution of the nodal domains ( $m = 2, k = 3$ )

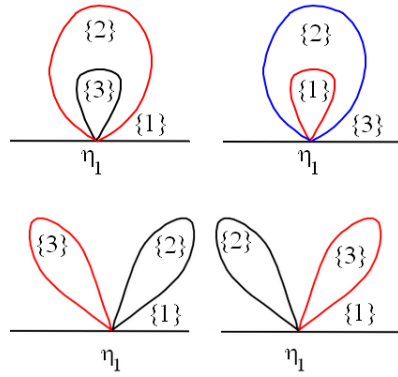


FIGURE 5.42.  $\mathcal{Z}(u_{\eta_1})$ : initial (left) – after returning to  $\eta_1$  (right)

Figure 5.41 describes the evolution of  $\mathcal{Z}(u_y)$  when  $y$  moves counter-clockwise from  $\eta_1$  to  $\eta_2$ , and then to  $\eta_1$ . The nodal domains of  $u_{\eta_1}$  are indicated in the pictures on the left; the other pictures then indicate how the nodal domains deform. The initial and final words (seen on the circle as above) are then given by

$$\begin{array}{ll} \text{Row 1:} & |1|2|3|2| \circ \quad |3|2|1|2| \circ \\ \text{Row 2:} & |1|2|1|3| \circ \quad |1|3|1|2| \circ \end{array}$$

and they differ by a circular permutation which indicates a rotation by  $\pi$ . The initial and final patterns are best compared in Figure 5.42.

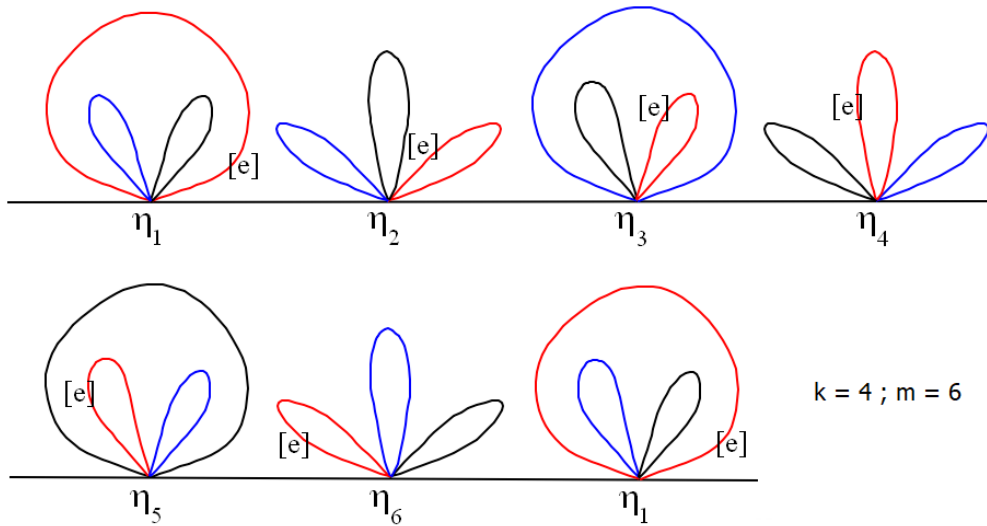


FIGURE 5.43. The case  $k = 4, m = 6$ , with the vector  $e$

Figures 5.45 and 5.46 describe the behavior of  $\mathcal{Z}(w_x)$  when  $x$  is near  $\eta_1$  or  $\eta_2$  moving on a parallel curve close enough to  $\Gamma$ , on the left, resp. on the right. The end point  $y(x)$  of the blue arc and the end point  $z(x)$  of the red arc satisfy  $y(x) < z(x)$ , resp.  $z(x) < y(x)$ . When  $x$  moves, the points may coincide or disappear (the nodal set  $\mathcal{Z}(w_x)$  does not touch the boundary). In any case, the intersection points of  $\mathcal{Z}(w_x)$

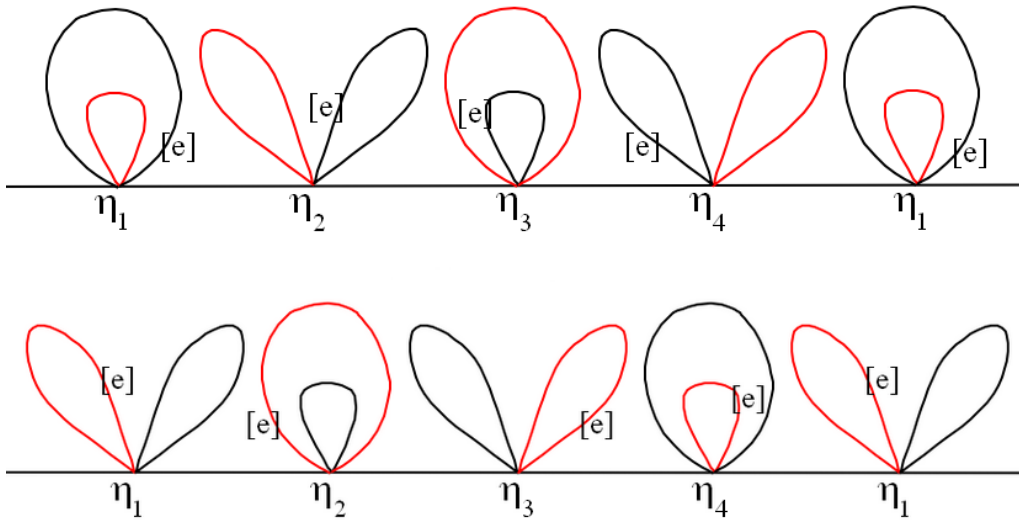


FIGURE 5.44. The case  $k = 3, m = 4$ , with the vector  $e$

with the curve  $C_+(\eta_i, r)$ ,  $i = 1, 2$  remain in small pairwise disjoint intervals (the black dots) around the points in  $\mathcal{Z}(u_{\eta_i}) \cap C_+(\eta_i, r)$ ,  $i = 1, 2$ .

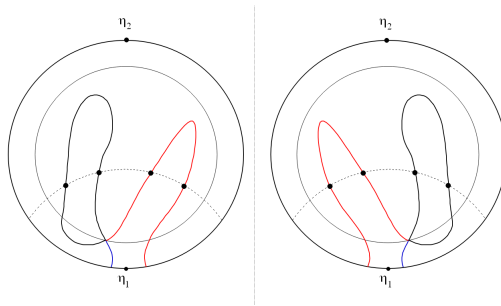


FIGURE 5.45.  $m = 2, k = 3$ ,  $x$  near  $\eta_1$

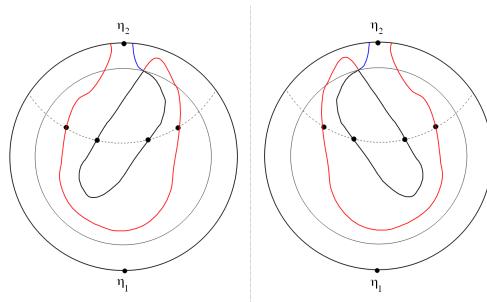


FIGURE 5.46.  $m = 2, k = 3$ ,  $x$  near  $\eta_2$

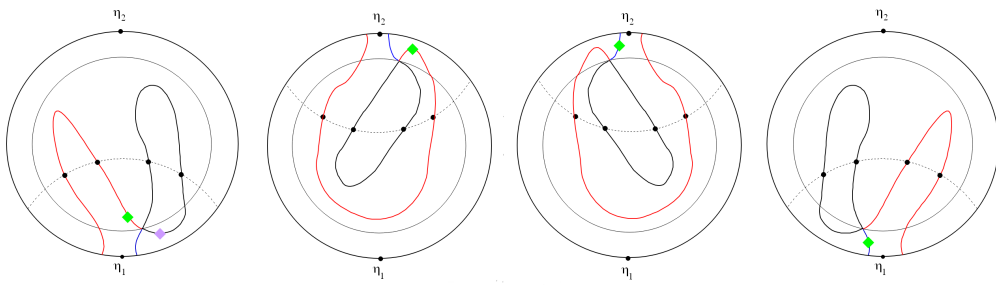


FIGURE 5.47.  $m = 2, e^{(1)}$

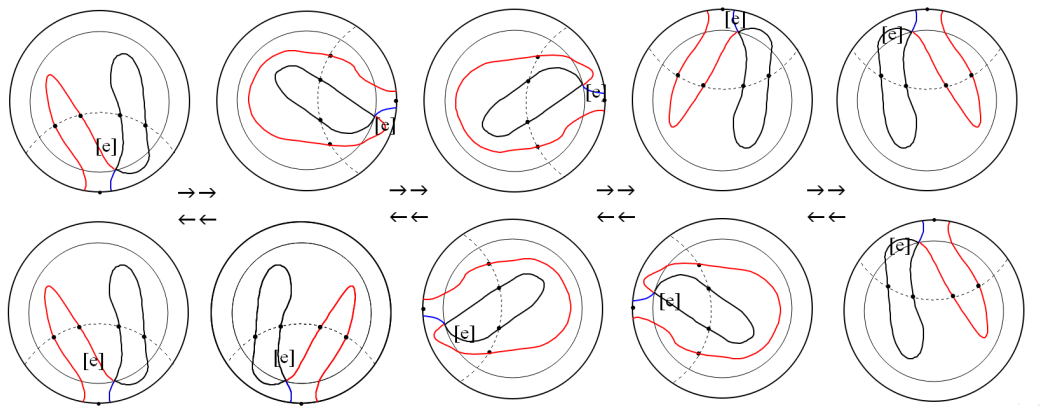


FIGURE 5.48.  $m = 4, e^{(1)}$

## 5.5. Labeling Nodal Domains

### 5.5.1. Preliminaries.

Let  $y \in \Gamma$  and let  $u$  be an eigenfunction such that  $\rho(u, y) = q$ .

We will either work in  $\Omega$  (global picture), or in a neighborhood of  $y$  (local picture) of the form  $E(D_+(0, r))$  where  $E$  is a conformal map as in Section 2.4. By abuse of notation, we shall denote such a neighborhood by  $D_+(y, r)$  without mentioning  $E$ , and work there as if we were actually working in  $\mathbb{H}$ .

Let  $\{\omega_1, \dots, \omega_q\}$  be the rays tangent to the nodal set  $\mathcal{Z}(u)$  at the point  $y$ . In the Dirichlet case, the rays are given by  $\omega_j = j\frac{\pi}{q}$ , for  $1 \leq j \leq q$ . In the Robin case, they are given by  $\omega_j = (j - \frac{1}{2})\frac{\pi}{q}$ .

Let  $r > 0$  be small enough so that the local structure theorem applies to  $u$  in  $D_+(y, 2r)$ . For  $1 \leq j \leq q$ , the nodal arc of  $u$  emanating from  $y$  tangentially to the ray  $\omega_j$  intersects  $C_+(y, r)$  at a unique point  $A_j^u(r)$  close to the intersection point  $\omega_j \cap C_+(y, r)$ . Call  $A_+(r)$ , resp.  $A_-(r)$ , the intersection points of  $C_+(y, r)$  with  $\Gamma$  (these points do not belong to  $\mathcal{Z}(u)$ ). The points  $A_j^u(r)$  determine  $(q + 1)$  intervals on  $C_+(y, r)$ , denoted  $I_j^u(r)$  for  $1 \leq j \leq (q + 1)$ :  $I_1^u(r)$  is the arc of  $C_+(y, r)$  from  $A_+(r)$  to  $A_1^u(r)$  (moving on  $\Gamma$  counter-clockwise),  $\dots$ ,  $I_{q+1}^u(r)$  is the arc from  $A_q^u(r)$  to  $A_-(r)$ . We shall skip the superscripts when the context is clear.

Throughout this section, we fix some  $k \geq 3$ , and we consider eigenfunctions  $u$  satisfying the following assumptions.

ASSUMPTIONS 5.42.

- (i) The function  $u$  satisfies  $\rho(u, y) = q$ , for some  $y \in \Gamma$ ,  $q \in \{(2k - 3), (2k - 2)\}$ .
- (ii) When  $q = (2k - 2)$ , the point  $y$  is the only singular point of  $u$  and  $\mathcal{Z}(u)$  is a  $(k - 1)$ -bouquet of loops at  $y$ .
- (iii) When  $q = (2k - 3)$ ,  $u$  has two singular points  $y$  and  $z \neq y$ , both in  $\Gamma$ , and there is a nodal interval  $\delta = \delta_{y,z}^u$  which emanates from  $y$  tangentially to the ray  $\omega_b$  and hits  $\Gamma$  at  $z$ . The nodal set  $\mathcal{Z}(u)$  is the wedge sum of the nodal interval  $\delta$  with a  $(k - 2)$ -bouquet of loops at  $y$ .
- (iv) The function  $u$  has  $k$  nodal domains, i.e.,  $\kappa(u) = k$ .
- (v) For  $r$  small enough, all the nodal domains of  $u$  intersect  $C_+(y, r)$ .

Eigenfunctions satisfying the above assumptions occur in Section 5.2, Lemma 5.6 and Figure 5.2. They also occurred in Section 4.2, Lemmas 4.7 and 4.11, Figures 4.1 and 4.2).

Examples are displayed in Figures 5.49 and 5.50. To differentiate the two cases, we will denote by  $u_0$  or  $v_0$  a function for which  $q = (2k - 2)$ , and  $u_1$  a function for which  $q = (2k - 3)$ .

The purpose of this section is to give a simple criterion to establish that the functions  $u_0$  and  $v_0$ , whose nodal patterns are displayed in Figure 5.50, are different in  $\mathbb{P}(U)$ , i.e.,  $[u_0] \neq [v_0]$ . This criterion is used in Paragraph 4.2.5.3, in Section 5.2, and in Section 5.6.

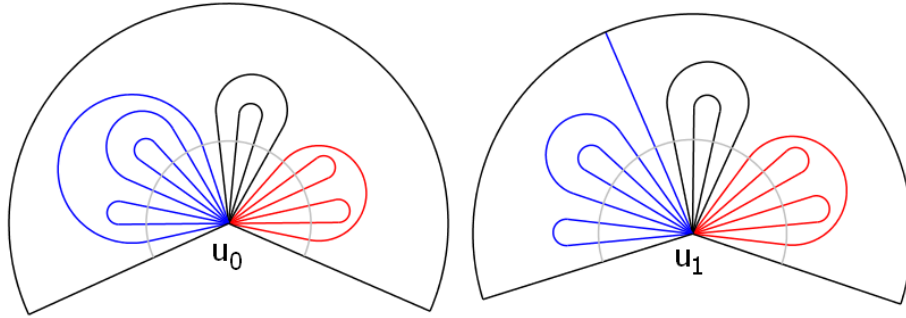


FIGURE 5.49.  $\rho(u_0, y) = (2k - 2)$ ,  $\rho(u_1, y) = (2k - 3)$  [here  $k = 10$ ]

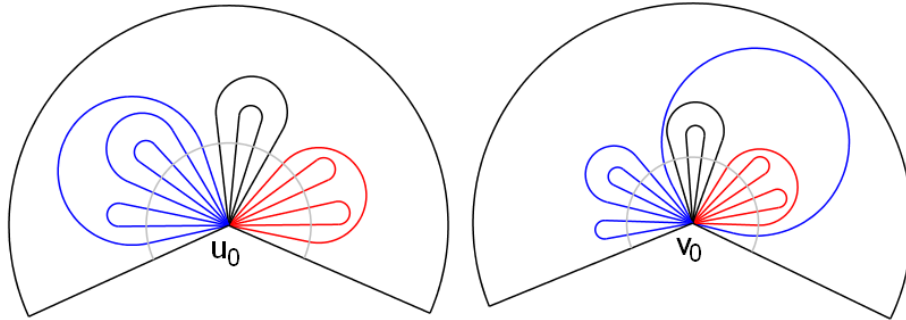


FIGURE 5.50.  $\rho(u_0, y) = \rho(v_0, y) = (2k - 2)$  [here  $k = 10$ ]

### 5.5.2. Labeling nodal domains and the signature of nodal patterns.

DEFINITION 5.43. A *labeling of the nodal domains* of an eigenfunction  $u$  with  $\kappa(u) = k$  is a set of pairwise distinct labels  $\mathcal{D} := \{d_1, \dots, d_k\}$  in bijection with the set of nodal domains of  $u$ , so that they can be listed as  $D_{d_1}, \dots, D_{d_k}$ .

Let  $\mathcal{D} = \{d_1, \dots, d_k\}$  be a labeling of the nodal domains of  $u$ . Given  $r$  small enough, let  $\{I_i^u(r)\}_{i=1}^{q+1}$  be the intervals determined by the points  $\mathcal{Z}(u) \cap C_+(y, r)$  on  $C_+(y, r)$ . We attach labels to these intervals as follows: for  $1 \leq j \leq k$ , the label  $d_j$  is attached to the intervals  $I_i^u(r)$  which are contained in the nodal domain  $D_{d_j}$ .

Note that the same label  $d_j$  may be given to several intervals.

We now encode this information into a word  $\mathcal{W}_{u, \mathcal{D}}$ , of length  $\|\mathcal{W}_{u, \mathcal{D}}\| = (q + 1)$ ,

$$\mathcal{W}_{u, \mathcal{D}} = \ell_{u, \mathcal{D}, 1} \cdots \ell_{u, \mathcal{D}, (q+1)},$$

whose letters  $\ell_{u, \mathcal{D}, i}$ ,  $1 \leq i \leq (q + 1)$ , belong to the labeling set  $\mathcal{D}$ .

Note that the word does not depend on  $r$  provided that  $r$  is small enough (this is a consequence of the local structure theorem, Section 2.4). Since an eigenfunction changes sign across a nodal line, two consecutive letters in the word  $\mathcal{W}_{u, \mathcal{D}}$  are different. Different label sets  $\mathcal{D}_1$  and  $\mathcal{D}_2$  give rise to a priori different words.

DEFINITION 5.44. Let  $\mathcal{I}_{u,\mathcal{D}} := \{i, 1 \leq i \leq (q+1) \mid \ell_{u,\mathcal{D},i} = \ell_{u,\mathcal{D},1}\}$ . The signature  $\sigma(\mathcal{W}_{u,\mathcal{D}})$  of the word  $\mathcal{W}_{u,\mathcal{D}}$  is defined as

$$(5.56) \quad \sigma(\mathcal{W}_{u,\mathcal{D}}) := \begin{cases} 1 & \text{if } \mathcal{I}_{u,\mathcal{D}} = \{1\}, \\ \min((\mathcal{I}_{u,\mathcal{D}} \setminus \{1\})) & \text{if } \mathcal{I}_{u,\mathcal{D}} \neq \{1\}. \end{cases}$$

PROPERTIES 5.45. The signature  $\sigma$  is well defined for eigenfunctions satisfying Assumptions 5.42, and does not depend on the labeling set  $\mathcal{D}$ .

Indeed, let  $D$  be the nodal domain of  $u$  which contains the interval  $I_1^u(r)$  and let  $\mathcal{I}_u := \{j \mid I_j^u(r) \subset D\}$ . Then,  $\mathcal{I}_{u,\mathcal{D}} = \mathcal{I}_u$ , and

$$\sigma(\mathcal{W}_{u,\mathcal{D}}) = \begin{cases} 1 & \text{if } \mathcal{I}_u = \{1\} \\ \min(\mathcal{I}_u \setminus \{1\}) & \text{if } \mathcal{I}_u \neq \{1\}, \end{cases}$$

and the right hand side is clearly independent of the choice of the labeling set. Figure 5.51 illustrates this fact (here on the coloring scheme). Figure 5.52 illustrates the fact that the signature provides a criterion to distinguish different nodal patterns. As we shall see below, a labeling of the nodal domains of an eigenfunction satisfying Assumptions 5.42 can be deduced from the combinatorial type  $\tau_u$  of  $u$ .

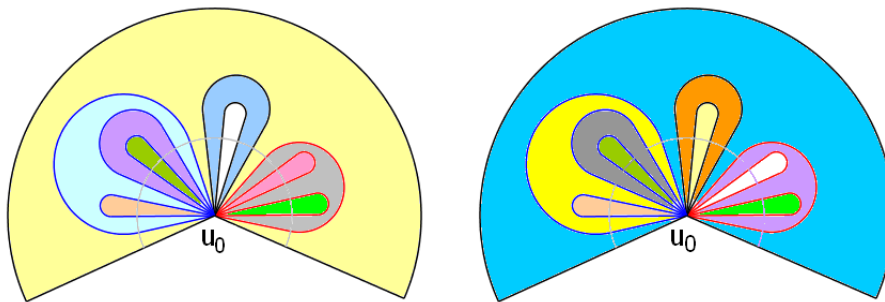


FIGURE 5.51. Same nodal pattern, different labeling sets,  $\sigma = 7$

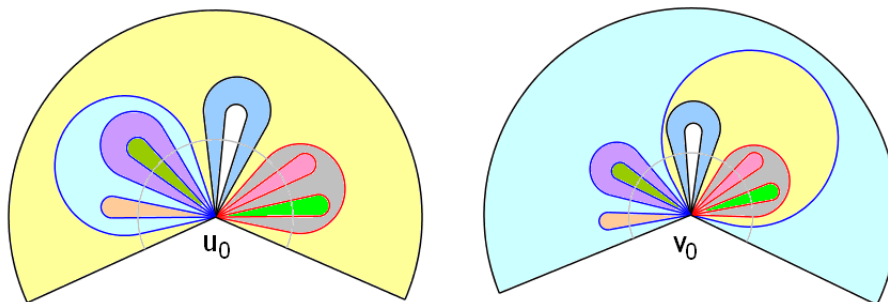


FIGURE 5.52.  $\sigma(\mathcal{W}_{u_0, \mathcal{D}_1}) = 7$  (left),  $\sigma(\mathcal{W}_{v_0, \mathcal{D}_2}) = 13$  (right)

### 5.5.3. A general description of nodal patterns.

Let  $u$  be an eigenfunction satisfying Assumptions 5.42. Let  $\tau$  be its combinatorial type.

**[A]** *Sub-bouquets.* Given a subset  $F \subset \{1, \dots, q\}$ , define  $b_F := \min F$  and  $e_F := \max F$ . In the sequel, we only consider subsets  $F$  with the following property:

$$(5.57) \quad F = \{j \mid b_F \leq j \leq e_F\} \text{ and } \tau(F) = F,$$

i.e.,  $F$  is an interval in  $\{1, \dots, q\}$ , and  $\tau$  leaves  $F$  globally invariant. If  $q = (2k - 3)$  and  $\tau(a) = \downarrow$  for some  $a \in \{1, \dots, q\}$ , we also assume that  $a \notin F$ .

With such a subset  $F$  we associate the bouquet of loops  $\mathcal{B}_F^u$ ,

$$\mathcal{B}_F^u = \bigcup_{j \in F} \gamma_{j, \tau(j)}^u,$$

more precisely, the wedge sum at  $y$  of the loops in  $\mathcal{Z}(u)$  associated with  $F$ .

DEFINITIONS 5.46.

- (i) A loop  $\gamma$  in  $\mathcal{Z}(u)$ , at the point  $y$ , taken individually, divides  $\Omega$  into two connected components. The *interior* of  $\gamma$  is the component which only touches the boundary  $\Gamma$  at  $y$ . The other component is called the *exterior* of  $\gamma$ .
- (ii) Given  $\mathcal{B}_F^u$ , the bouquet of loops associated with  $u$  and  $F$ , we call *interior domain* of  $\mathcal{B}_F^u$  a nodal domain of  $u$  contained in the interior of some loop  $\gamma_{j, \tau(j)}$ ,  $j \in F$ . We call *exterior* of  $\mathcal{B}_F^u$  the set of points of  $\Omega$  which belong neither to  $\mathcal{B}_F^u$ , nor to an interior domain of  $\mathcal{B}_F^u$ .
- (iii) We denote by  $n_F^u$  the number of loops in  $\mathcal{B}_F^u$ .

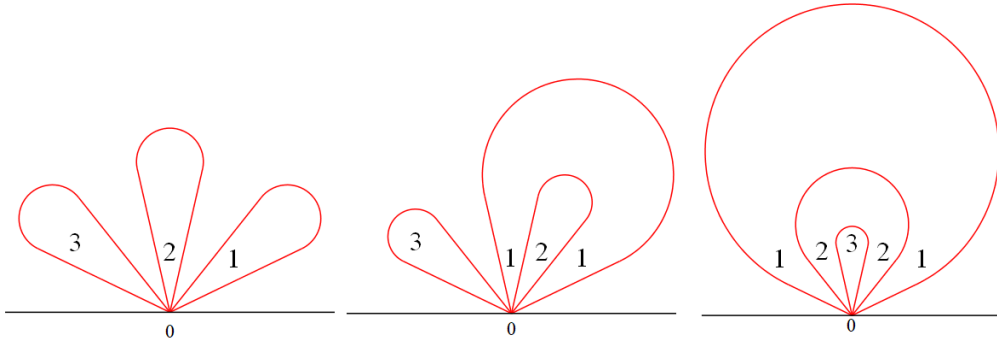


FIGURE 5.53. Examples of bouquets

Figure 5.53 displays bouquets with 3 loops:

- The numbers are labels for the interior nodal domains.
- The unlabeled domain is the exterior of the bouquet.

The following relations hold.

$$(5.58) \quad \begin{cases} \#(F) = e_F - b_F + 1. \\ \|F\| := e_F - b_F = \# \{ i \mid I_i(r) \subset \mathcal{A}(A_{b_F}^u(r), A_{e_F}^u(r)) \}. \\ n_F = \# \{ \text{interior nodal domains of } \mathcal{B}_F^u \}. \\ 2n_F = \#(F) = \|F\| + 1. \end{cases}$$



Here,  $\mathcal{A}(A_{b_F}^u(r), A_{e_F}^u(r))$  denotes the arc from  $A_{b_F}^u(r)$  to  $A_{e_F}^u(r)$ , moving counter-clockwise along  $C_+(y, r)$ . The intervals contained in this arc are  $I_{b_F+1}^u, \dots, I_{e_F}^u$ . Since  $\tau(F) = F$ , the number  $\#(F)$  is even. Note that  $n_F$  depends on  $\tau$ , not on  $u$  itself.

**[B]** *The case  $q = (2k - 3)$ .* Let  $u_1$  be an eigenfunction satisfying Assumptions 5.42, with  $\rho(u_1, y) = (2k - 3)$ . Let  $\tau_1$  denote its combinatorial type. Let  $b := \tau_1(\downarrow)$ . Let  $\delta = \delta_{b,y,z}^{u_1}$  be the nodal interval which emanates from  $y$  tangentially to the ray  $\omega_b$  and hits  $\Gamma$  at a point  $z \neq y$ . It divides  $\Omega$  into two connected (and simply-connected) components  $\Omega_{b,R}$  and  $\Omega_{b,L}$ , resp. on the right and on the left of  $\delta$ . A nodal domain  $D$  of  $u_1$  must be contained in either  $\Omega_{b,R}$  or  $\Omega_{b,L}$ . Define the subsets  $R := \{1, \dots, (b - 1)\}$  and  $L := \{(b + 1), \dots, (2k - 3)\}$ . Assumptions 5.42 and Jordan's theorem imply that  $\tau_1(R) = R$  and  $\tau_1(L) = L$ . It follows that  $\#(R)$  and  $\#(L)$  are even, and that  $b$  is odd. The corresponding bouquets of loops  $\mathcal{B}_R^{u_1}$  and  $\mathcal{B}_L^{u_1}$  are contained respectively in  $\{y\} \cup \Omega_{b,R}$ , resp.  $\{y\} \cup \Omega_{b,L}$ . It follows that  $\Omega_{b,R}$  contains  $k_R := n_R + 1$  nodal domains of  $u_1$ , and that  $\Omega_{b,L}$  contains  $k_L := n_L + 1$  nodal domains of  $u_1$ . Here,  $n_R := \frac{b-1}{2}$  and  $n_L = \frac{2k-b-3}{2}$ , so that  $k_R + k_L = k$ . Figure 5.49 (right) displays an example with  $k = 10, b = 11, R = \{1, \dots, 10\}$  and  $L = \{12, \dots, 17\}$ . The bouquet  $\mathcal{B}_R^{u_1}$  consists of the two black and three red loops; the bouquet  $\mathcal{B}_L^{u_1}$  of the three blue loops.

To label the  $k$  nodal domains of  $u_1$ , it suffices to first label the nodal domains contained in  $\Omega_{b,R}$ , from  $d_1$  to  $d_{k_R}$ , and then the nodal domains contained in  $\Omega_{b,L}$ , from  $d_{k_R+1}$  to  $d_k$ .

Since both  $\Omega_{b,R}$  and  $\Omega_{b,L}$  are simply connected and only contain loops, we are reduced to labeling nodal domains for functions such that  $\rho(u, y)$  is even.

**[C]** *The case  $q = (2k - 2)$ . An example with  $k = 10, q = 18$ .* Decompose the nodal set  $\mathcal{Z}(u_0)$  displayed in Figure 5.49 (left), into a large (red) loop  $\gamma_{1,6}^{u_0}$  which contains the (red) bouquet  $\mathcal{B}_R^{u_0}$ , a large (blue) loop  $\gamma_{11,18}^{u_0}$  which contains the (blue) bouquet  $\mathcal{B}_L^{u_0}$ , and a (black) bouquet  $\mathcal{B}_C^{u_0}$ . More precisely, for this example,

$$(5.59) \quad \begin{cases} a = 6, \tau_{u_0}(1) = 6, & b = 11, \tau_{u_0}(11) = 18, \\ R = \{2, 3, 4, 5\}, \quad C = \{7, 8, 9, 10\}, \quad L = \{12, 13, 14, 15, 16, 17\}. \end{cases}$$

Similarly, in Figure 5.50 (right),  $k = 10$  and  $q = 18$ , and we decompose the nodal set into a large (blue) loop  $\gamma_{1,12}^{v_0}$  whose interior contains the (red) bouquet  $\mathcal{B}_{R'}^{v_0}$  and the (black) bouquet  $\mathcal{B}_{N'}^{v_0}$ , and the (blue) bouquet  $\mathcal{B}_{L'}^{v_0}$  contained in the exterior of  $\gamma_{1,12}^{v_0}$ . More precisely, for this example,

$$(5.60) \quad \begin{cases} \tau_{v_0}(1) = 12, \\ R' = \{2, 3, \dots, 6, 7\}, \quad N' = \{8, 9, 10, 11\}, \quad L' = \{13, 14, \dots, 17, 18\}. \end{cases}$$

REMARK 5.47. In the example  $u_0$ , we pay a special attention to the loops one of whose semi-tangents is  $\omega_1$  or  $\omega_{(2k-2)}$ . The reason is explained in Section 5.2.

**[D]** *The general case  $k \geq 3, q = (2k - 2)$ .* Let  $u_0$  be an eigenfunction satisfying Assumptions 5.42, with  $\rho(u_0, y) = (2k - 2)$  and combinatorial type  $\tau_0$ . Define  $a = \tau_0(1)$  and  $b = \tau_0(2k - 2)$ . We observe that  $a$  is even and  $b$  odd.

◇ When  $a = (2k - 2), b = 1$ . The nodal set  $\mathcal{Z}(u_0)$  decomposes into the loop  $\gamma_{1,(2k-2)}$  and the bouquet  $\mathcal{B}_R^{u_0}$  with  $R = \{2, \dots, (2k - 3)\}$ . The exterior of  $\gamma_{1,(2k-2)}$  is a nodal

domain of  $u_0$ . The bouquet  $\mathcal{B}_R^{u_0}$  is contained in the interior of  $\gamma_{1,(2k-2)}$  which contains  $(n_R + 1)$  nodal domains, with  $n_R = (k - 2)$ .

◇ If  $a \neq (2k - 2)$ , then  $2 \leq a \leq (2k - 4)$  and  $(a + 1) \leq b \leq (2k - 3)$ . In this case,  $\mathcal{Z}(u_0)$  consists of two loops  $\gamma_{1,a}^{u_0}, \gamma_{b,(2k-2)}^{u_0}$ , and three bouquets of loops  $\mathcal{B}_R^{u_0}, \mathcal{B}_C^{u_0}$  and  $\mathcal{B}_L^{u_0}$ . The subsets  $R, C$  and  $L$  are given by

$$(5.61) \quad \begin{cases} R = \{2, \dots, (a - 1)\}, & C = \{(a + 1), \dots, (b - 1)\}, \\ L = \{(b + 1), \dots, (2k - 3)\}. \end{cases}$$

The combinatorial type  $\tau_{u_0}$  is given by

$$(5.62) \quad \tau_{u_0} = \begin{pmatrix} 1 & R & a & C & b & L & q \\ a & \tau_{u_0}(R) & 1 & \tau_{u_0}(C) & q & \tau_{u_0}(L) & b \end{pmatrix}.$$

REMARK 5.48. With the same subsets  $R, C, L$ , the combinatorial type of the function  $u_1$ , whose nodal pattern is displayed in Figure 5.49, is

$$(5.63) \quad \tau_{u_1} = \begin{pmatrix} 1 & R & a & C & b & L & \downarrow \\ a & \tau_{u_1}(R) & 1 & \tau_{u_1}(C) & \downarrow & \tau_{u_1}(L) & b \end{pmatrix}$$

where the symbol  $\downarrow$  indicates that the nodal interval  $\delta_{b,y,z}^{u_1}$  emanating from  $y$  tangentially to the ray  $\omega_b$  hits the boundary at  $z \neq y$ . In Figure 5.49, the maps  $\tau_{u_0}$  and  $\tau_{u_1}$  coincide on the sets  $R, C$  and  $L$ .

#### 5.5.4. A labeling procedure and the word associated with it.

We now explain a procedure to label the nodal domains of a function  $u$  satisfying Assumptions 5.42 in the case  $q = (2k - 2)$ , see Figure 5.49.

Let  $\mathcal{D} = \{d_1, \dots, d_k\}$  be a set of labels with  $k = \kappa(u)$ . Since every nodal domain of  $u$ , intersects  $C_+(y, r)$ , we label the nodal domains from  $d_1$  to  $d_k$  according to their order of appearance in the intervals  $I_i^u(r)$ ,  $1 \leq i \leq (2k - 1)$ , working counter-clockwise along  $C_+(y, r)$ .

PROCEDURE 5.49. *The following procedure attributes a unique label  $d_j, 1 \leq j \leq \kappa(u) = k$  to each nodal domain of the eigenfunction  $u_0$ , and a well defined label to each interval  $I_i^u(r)$  determined by  $\mathcal{Z}(u) \cap C_+(y, r)$ ,  $1 \leq i \leq (q + 1)$  on  $C_+(y, r)$ . The labeling is independent of  $r$  provided that  $r$  is small enough for the local structure theorem to apply to the function  $u$  at  $y$ .*

Step 1 Let  $D_{d_1}$  be the nodal domain which contains the interval  $I_1^u(r)$ . Attach the label  $d_1$  to all the intervals  $I_i^u(r)$  contained in  $D_{d_1}$ .

Step 2 Because an eigenfunction changes sign across a nodal arc, the interval  $I_2^u(r)$  is not contained in  $D_{d_1}$ . Call  $D_{d_2}$  the nodal domain which contains  $I_2^u(r)$ . Attach the label  $d_2$  to all the intervals contained in  $D_{d_2}$ .

Step 3 For the same reason as in the previous item, the label  $d_2$  is not attached to the interval  $I_3^u(r)$ . If  $I_3^u(r) \subset D_{d_1}$ , then the label  $d_1$  is already attached to  $I_3^u(r)$  by step 1. If  $I_3^u(r) \not\subset D_{d_1}$ , let  $D_{d_3}$  be the nodal domain which contains  $I_3^u(r)$ , and attach the label  $d_3$  to all the intervals  $I_i^u(r)$  contained in  $D_{d_3}$ .

Step 4 Assume that the intervals  $I_i^u(r)$ ,  $1 \leq i \leq (j - 1)$ , have been labeled, using the labels  $d_1, \dots, d_p$  for some  $p \geq 2$ .

◇ If  $p = k$ , all the nodal domains have been labeled, and all the intervals have received a label as well.

◇ If  $p < k$  then,

- either  $I_j^u(r)$  has already been labeled because it is contained in an already labeled nodal domain and we proceed to  $I_{j+1}^u(r)$ ,
- or  $I_j^u(r)$  has no label attach to it yet. Then, call  $D_{d_{p+1}}$  the nodal domain which contains  $I_j^u(r)$ , and attach the label  $d_{p+1}$  to all the intervals  $I_i^u(r)$  which are contained in  $D_{d_{p+1}}$ .

After at most  $q$  steps all nodal domains and all intervals will be labeled.

The labeling of the  $(q+1)$  intervals  $I_1^u(r), \dots, I_{(q+1)}^u(r)$  produces a word  $\mathcal{W}_u$  of length  $\|\mathcal{W}_u\| = (q+1)$  (the number of intervals), in the  $\kappa(u)$  letters  $d_1, \dots, d_k$ . Equivalently, we can view the labeling as a map  $\Lambda_u : \{1, \dots, (q+1)\} \rightarrow \mathcal{D}$ .

REMARK 5.50. The above procedure applies to both types of functions,  $u_0$  with  $q = (2k - 2)$ , or  $u_1$  with  $q = (2k - 3)$ . There are two differences in the output words. The word  $\mathcal{W}_{u_0}$  has length  $(2k - 1)$ , it begins and ends with the letter  $d_1$ . The word  $\mathcal{W}_{u_1}$  has length  $(2k - 2)$ , and consists of two words with no common letter. This is due to the fact that the nodal interval  $\delta_{b,y,z}^{u_1}$  divides the domain  $\Omega$  into two components,  $\Omega_{b,R}$ ,  $\Omega_{b,L}$ , so that the nodal domains of  $u$  are divided into two distinct families. The Procedure 5.49 will first label the  $(n_R + 1)$  nodal domains contained in  $\Omega_{b,R}$ , from 1 to  $(n_R + 1)$ , and then label the  $(n_L + 1)$  nodal domains contained in  $\Omega_{b,L}$ , from  $(n_R + 2)$  to  $k$ .

### 5.5.5. Examples.

5.5.5.1. *Examples with  $k = 4$ , and  $a = 3$  or 5, in Paragraph 4.2.5.3.* The labeling of nodal domains in Figures 4.4 and 4.5, left and middle sub-figures, follows Procedure 5.49. The labeling in the right sub-figures follows the deformation of the nodal domains when  $\theta$  tends to 0. In the first figure, the signatures are  $\sigma(\text{left}) = 3$ ,  $\sigma(\text{right}) = 5$ ; in the second figure,  $\sigma(\text{left}) = 3$ ,  $\sigma(\text{right}) = 7$ .

5.5.5.2. *An example with  $k = 4$  and  $a = 3$  in the proof of Lemma 5.24 (ii).* The labeling of nodal domains in Figure 5.11 is deduced by deformation from the labeling of the nodal domains in the middle subfigure of Figure 5.10 which follows Procedure 5.49. We have  $\sigma(v_{0,R}) = 3$  and  $\sigma(v_{0,L}) = 5$ .

5.5.5.3. *Examples with  $k = 10$  in the proof of Lemma 5.24 (iv).*

A Example (5.59),  $k = 10, q = 18$ , Figure 5.49, function  $u_0$ .

- (1) The interval  $I_1^{u_0}(r)$  is contained in the exterior domain of  $\mathcal{Z}(u_0)$ . We call  $D_{d_1}$  the exterior domain of  $\mathcal{Z}(u_0)$ , and we label  $d_1$  the intervals  $I_j^{u_0}(r)$ ,  $j \in \{1, 7, 11, 19\}$ .
- (2) The interval  $I_2^{u_0}(r)$  is contained in the interior of the loop  $\gamma_{1,6}^{u_0}$ . We call  $D_{d_2}$ , the nodal domain in the interior  $\gamma_{1,6}^{u_0}$ , which contains points close to the loop, and we label  $d_2$  the intervals  $I_j^{u_0}(r)$ ,  $j \in \{2, 4, 6\}$ .
- (3) The interval  $I_3^{u_0}(r)$  is contained in the interior of the loop  $\gamma_{2,3}^{u_0}$ . We label both  $d_3$ .
- (4) The interval  $I_4^{u_0}(r)$  is already labeled  $d_2$ . The interval  $I_5^{u_0}(r)$  is contained in the interior of the loop  $\gamma_{4,5}^{u_0}$ . We label both  $d_4$ .
- (5) The intervals  $I_6^{u_0}(r)$  and  $I_7^{u_0}(r)$  are already labeled, respectively  $d_2$  and  $d_1$ . The interval  $I_8^{u_0}(r)$  is contained in the interior of the loop  $\gamma_{7,10}^{u_0}$ . We label both  $d_5$ , as well as  $I_{10}^{u_0}(r)$ .
- (6) The interval  $I_9^{u_0}(r)$  is contained in the interior of the loop  $\gamma_{8,9}^{u_0}$ . We label both  $d_6$ .

(7) Continuing the procedure, we obtain

$$\mathcal{W}_{u_0} = d_1 d_2 d_3 d_2 d_4 d_2 d_1 d_5 d_6 d_5 d_1 d_7 d_8 d_9 d_8 d_7 d_{10} d_7 d_1 .$$

For simplicity, we use the alternative notation

$$\mathcal{W}_{u_0} = |1|2|3|2|4|2|1|5|6|5|1|7|8|9|8|7|10|7|1|$$

in which we have only written the indices of the labels, separated by a vertical bar.

For this example, we have

$$(5.64) \quad \mathcal{W}_{u_0} = |1|2|3|2|4|2|1|5|6|5|1|7|8|9|8|7|10|7|1| \quad \text{with } \sigma(\mathcal{W}_{u_0}) = 7 .$$

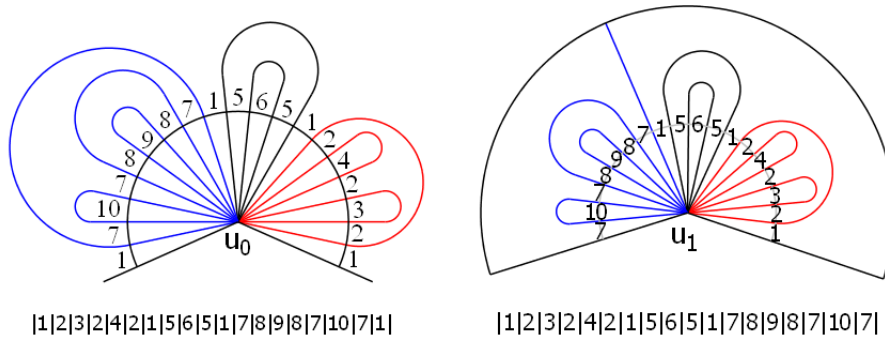


FIGURE 5.54. The words  $\mathcal{W}_{u_0}$  and  $\mathcal{W}_{u_1}$  [here  $k = 10$ ]

[B] Example (5.59),  $k = 10, q = 17$ , Figure 5.49, function  $u_1$ . Applying Procedure 5.49, we obtain

$$(5.65) \quad \mathcal{W}_{u_1} = |1|2|3|2|4|2|1|5|6|5|1|7|8|9|8|7|10|7| .$$

Note that  $\mathcal{W}_{u_1} = \mathcal{W}_{1,R}\mathcal{W}_{1,L}$  is the juxtaposition of two disjoint words,  $\mathcal{W}_{1,R} = |1|2|3|2|4|2|1|5|6|5|1|$  and  $\mathcal{W}_{1,L} = |7|8|9|8|7|10|7|$  which correspond respectively to the nodal sets contained in  $\Omega_{11,R}$  and  $\Omega_{11,L}$ .

[C] Example (5.60),  $k = 10, q = 18$ , Figure 5.50, function  $v_0$ . Applying Procedure 5.49, we obtain

$$(5.66) \quad \mathcal{W}_{v_0} = |1|2|3|4|3|5|3|2|6|7|6|2|1|8|9|8|1|10|1| \quad \text{with } \sigma(\mathcal{W}_{v_0}) = 13 .$$

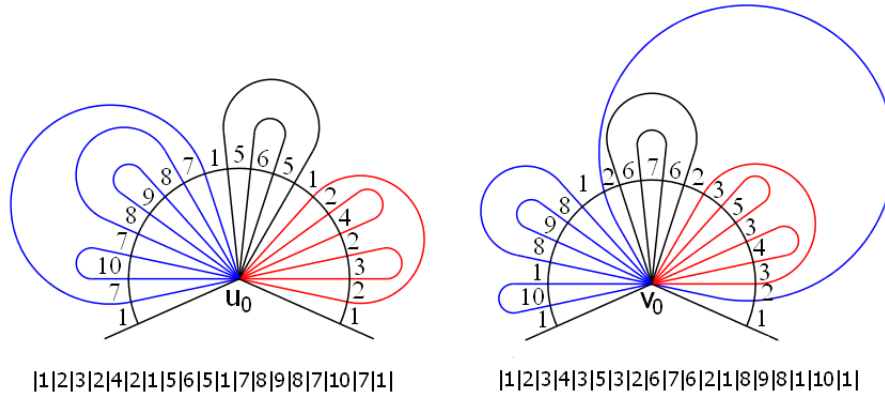


FIGURE 5.55. Words  $\mathcal{W}_{u_0}$  and  $\mathcal{W}_{v_0}$ , with 7 and 13 [ $k = 10$ ]

**5.5.6. Applying the labeling procedure in the general case.**

The nodal set  $\mathcal{Z}(u_0)$  of an eigenfunction  $u_0$  such that  $\rho(u_0, y) = (2k - 2)$  is a  $(k - 1)$  bouquet of loops at  $y$ . Let  $\tau_0$  be the combinatorial type of  $u_0$ .

◊ If  $\tau_0(1) = (2k - 2)$ , we decompose  $\mathcal{Z}(u_0)$  into the loop  $\gamma_{1, (2k-2)}^{u_0}$  and the bouquet of loops  $\mathcal{B}_R$  which is contained in the interior of  $\gamma_{1, (2k-2)}^{u_0}$ , where  $R := \{2, \dots, (2k - 3)\}$ , see paragraph A below.

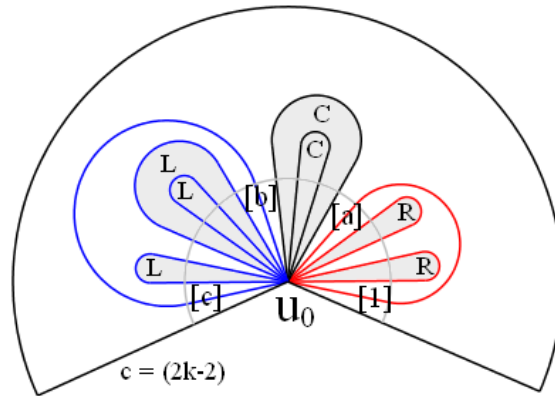


FIGURE 5.56. The decomposition of  $\mathcal{Z}(u_0)$  when  $\tau_0(1) \neq (2k - 2)$

◊ If  $a := \tau_0(1) \neq (2k - 2)$ , then we define  $b := \tau_0(2k - 2)$ , and we decompose  $\mathcal{Z}(u_0)$  into the loops  $\gamma_{1,a}^{u_0}$ ,  $\gamma_{b, (2k-2)}^{u_0}$ , and the bouquets of loops associated with the subsets  $R, C, L$  given in (5.61). This decomposition is illustrated in Figure 5.56, with the bouquets  $R, C$  and  $L$  represented in grey shade. Recall that this decomposition implies that  $a$  is even and  $b$  odd. Using Definitions 5.46 and Equation (5.58), we have that  $(n_R + n_C + n_L + 3) = k$ , the number of nodal domains of  $u_0$ . The labeling of nodal domains for this decomposition is given in paragraph B below.

**A** *The case  $\tau_0(1) := a = (2k - 2)$ .* Call  $w_0$  a corresponding eigenfunction. The exterior of the loop  $\gamma_{1,(2k-2)}$  is a nodal domain of  $w_0$ , which we call  $D_{d_1}$  and we label  $d_1$  the intervals  $I_1^{w_0}(r)$  and  $I_{(2k-1)}^{w_0}(r)$ . No other interval has the label  $d_1$ . The nodal domain  $D_{d_2}$  contains the intervals  $I_2^{w_0}(r)$  and  $I_{(2k-2)}^{w_0}(r)$  and, possibly, other intervals. This nodal domain is the intersection of the interior of  $\gamma_{1,(2k-2)}$  with the exterior of the bouquet  $\mathcal{B}_R^{w_0}$  associated with  $R = \{2, \dots, (2k - 3)\}$ . There are  $(k - 2)$  interior domains of  $\mathcal{B}_R^{w_0}$ , labeled  $D_{d_3}, \dots, D_{d_k}$ . The associated word is  $\mathcal{W}_{w_0} = d_1 d_2 \mathcal{W}_R d_2 d_1$  where  $\mathcal{W}_R$  is the word associated with  $R$ , with length  $\|\mathcal{W}_R\| = (2k - 5)$ , in the letters  $d_3, \dots, d_k$ , and possibly the letter  $d_2$ . The word  $\mathcal{W}_R$  does not contain the letter  $d_1$ . It follows that the signature of the nodal pattern of  $w_0$  is  $(2k - 1)$ .

**B** *The case  $2 \leq \tau_0(1) := a \leq (2k - 4)$ .* Call  $u_0$  a corresponding function, with combinatorial type  $\tau_0$ . In this case,  $(a + 1) \leq b \leq (2k - 3)$ .

1) The nodal domains of  $u_0$  are split into four disjoint families. The following description takes Procedure 5.49 and the relation  $k = (n_R + n_C + n_L + 3)$  into account.

- ◇ The exterior of  $\mathcal{Z}(u_0)$ . It is called  $D_{d_1}$ .
- ◇ The  $(n_R + 1)$  nodal domains contained in the interior of  $\gamma_{1,a}^{u_0}$ . This family consists of the  $n_R$  interior domains of  $\mathcal{B}_R^{u_0}$ ,  $D_{d_3}$  to  $D_{d_{(n_R+2)}}$ , and the domain  $D_{d_2}$  which is the complement of  $D_{d_3} \cup \dots \cup D_{d_{(n_R+2)}}$  in the interior of  $\gamma_{1,a}^{u_0}$ . The domain  $D_{d_2}$  contains the interval  $I_2^{u_0}(r)$ , and its boundary contains the loop  $\gamma_{1,a}^{u_0}$  itself.
- ◇ The  $n_C$  interior domains of  $\mathcal{B}_C^{u_0}$ . They are labeled from  $d_{(n_R+3)}$  to  $d_{(n_R+n_C+2)}$ .
- ◇ The  $(n_L + 1)$  nodal domains contained in the interior of  $\gamma_{b,(2k-2)}^{u_0}$ . This family consists of the  $n_L$  interior domains of  $\mathcal{B}_L^{u_0}$ , labeled from  $d_{(n_R+n_C+4)}$  to  $d_k$ , and the domain  $D_{d_{(n_R+n_C+3)}}$  which is the complement of  $D_{d_{n_R+n_C+4}} \cup \dots \cup D_{d_k}$  in the interior of  $\gamma_{b,(2k-2)}^{u_0}$ . The domain  $D_{d_{(n_R+n_C+3)}}$  contains the interval  $I_{b+1}^{u_0}(r)$ , and its boundary contains the loop  $\gamma_{b,(2k-2)}^{u_0}$  itself.

2) The  $(2k - 1)$  intervals  $I_j^{u_0}(r)$  determined by  $\mathcal{Z}(u_0) \cap C_+(\eta, r)$  are as follows.

- ◇ The exterior domain  $D_{d_1}$  contains four intervals  $I_j^{u_0}(r)$ , with  $j$  in the set  $\{1, (a + 1), b, (2k - 1)\}$ .
- ◇ The interior of the loop  $\gamma_{1,a}^{u_0}$  contains  $(a - 1)$  intervals  $I_j^{u_0}(r)$ ,  $j \in \{2, \dots, a\}$ . The bouquet  $\mathcal{B}_R^{u_0}$  determines  $(a - 3)$  intervals, and there are two intervals touching the loop  $\gamma_{1,a}^{u_0}$ .
- ◇ The bouquet  $\mathcal{B}_C^{u_0}$  determines  $(b - a - 2)$  intervals  $I_j^{u_0}(r)$ , with  $j$  in the set  $\{(a + 2), \dots, (b - 1)\}$ .
- ◇ The interior of the loop  $\gamma_{b,(2k-2)}^{u_0}$  contains  $(2k - b - 2)$  intervals  $I_j^{u_0}(r)$ , with the index  $j$  in the set  $\{(b + 1), \dots, (2k - 2)\}$ . The bouquet  $\mathcal{B}_L^{u_0}$  determines  $(2k - b - 4)$  intervals, and there are two intervals touching the loop  $\gamma_{b,(2k-2)}^{u_0}$ .

3) Applying Procedure 5.49, the nodal domains of  $u_0$  are described by the word

$$(5.67) \quad \mathcal{W}_{u_0} = |1|2|\mathcal{W}_R^{u_0}|2|1|\mathcal{W}_C^{u_0}|1|\hat{b}|\mathcal{W}_L^{u_0}|\hat{b}|1|.$$

Here  $\hat{b} := (n_R + n_C + 3)$ , and  $d_{\hat{b}}$  is the label of the nodal domain contained in the interior of the loop  $\gamma_{b,(2k-2)}^{u_0}$  and whose boundary contains the loop itself; the words  $\mathcal{W}_R^{u_0}$ , resp.  $\mathcal{W}_C^{u_0}$  and  $\mathcal{W}_L^{u_0}$ , describe the nodal domains containing the intervals determined by  $\mathcal{B}_R^{u_0}$ , resp.  $\mathcal{B}_C^{u_0}$  and  $\mathcal{B}_L^{u_0}$ . More precisely,

- ◇  $\mathcal{W}_R^{u_0}$  is a word of length  $\|\mathcal{W}_R^{u_0}\| = (a - 3)$ , in the letters  $d_3, \dots, d_{(n_R+2)}$  and, possibly the letter  $d_2$
- ◇  $\mathcal{W}_C^{u_0}$  is a word of length  $\|\mathcal{W}_C^{u_0}\| = (b - a - 2)$ , in the letters  $d_{(n_R+3)}, \dots, d_{(n_R+n_C+2)}$  and, possibly the letter  $d_1$
- ◇  $\mathcal{W}_L^{u_0}$  is a word of length  $\|\mathcal{W}_L^{u_0}\| = (2k - b - 4)$ , in the letters  $d_{(n_R+n_C+4)}, \dots, d_k$  and, possibly the letter  $d_b$ .

We recover the fact that  $\|\mathcal{W}^{u_0}\| = (2k - 1) = 8 + \|\mathcal{W}_R^{u_0}\| + \|\mathcal{W}_C^{u_0}\| + \|\mathcal{W}_L^{u_0}\|$ .

In view of (5.67), and the description of the words  $\mathcal{W}_R^{u_0}$ ,  $\mathcal{W}_C^{u_0}$  and  $\mathcal{W}_L^{u_0}$ , we have

$$(5.68) \quad \sigma(\mathcal{W}_{u_0}) = 4 + \|\mathcal{W}_R^{u_0}\| = (a + 1).$$

C *Another example with  $q = (2k - 2)$ .* Call  $v_0$  an eigenfunction such that  $\rho(v_0, y) = (2k - 2)$  with combinatorial type  $\tau_{v_0}$  given by

$$\tau_{v_0} = \begin{pmatrix} 0 & 1 & R & a & C & b & L \\ b & a & \tau_{v_0}(R) & 1 & \tau_{v_0}(C) & 0 & \tau_{v_0}(L) \end{pmatrix}$$

where the sets  $R, C, L$  are as in (5.61) (the same subsets as in the previous example) and the corresponding bouquets are shaded in grey in the picture. The nodal set  $\mathcal{Z}(v_0)$  is partitioned as follows, see Figure 5.57.

- ◇ The loop  $\gamma_{0,b}$ .
- ◇ The bouquet  $\mathcal{B}_{R'} := \gamma_{1,a} \cup \mathcal{B}_R \cup \mathcal{B}_C$  contained in the interior of the loop  $\gamma_{0,b}$ .
- ◇ The bouquet  $\mathcal{B}_L$  contained in the exterior of  $\gamma_{0,b}$ .

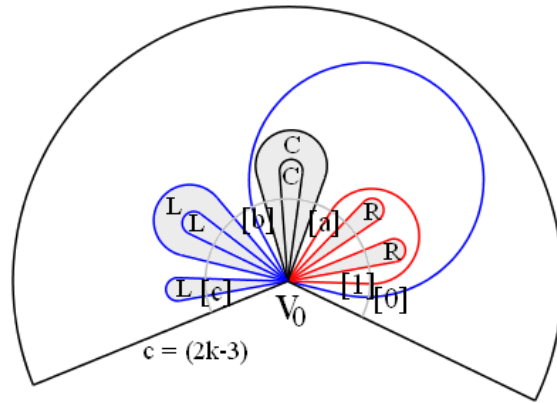


FIGURE 5.57. The decomposition of the nodal set  $\mathcal{Z}(v_0)$

The intervals are ordered from  $I_1(r)$  to  $I_{(2k-2)}(r)$  as usual. The exterior of  $\mathcal{Z}(v_0)$  is called  $D_{d_1}$ . The nodal domain  $D_{d_2}$  contains the interval  $I_2(r)$ . It also contains an inner neighborhood of  $\gamma_{0,b}$  and the interval  $I_{(b+1)}(r)$ . The interior of  $\gamma_{0,b}$  contains the  $1 + n_R + n_C$  interior domains of the bouquet  $\mathcal{B}_{R'}$ . The word  $\mathcal{W}_{v_0}$  is given by

$$\mathcal{W}_{v_0} = |1|2|\mathcal{W}_{R'}|2|1|\mathcal{W}_L$$

where the word  $\mathcal{W}_{R'}$  is associated with  $\mathcal{B}_{R'}$ . By (5.58),  $\|\mathcal{W}_{R'} = (b - 2)\|$  and  $\mathcal{W}_{R'}$  is a word in the letters  $d_3, \dots, d_{n_R+n_C+2}$  and, possibly,  $d_2$ . It follows that

$$(5.69) \quad \sigma(\mathcal{W}_{v_0}) = (b + 2).$$

Note that  $(b + 2) \geq (a + 3) > (a + 1)$ , so that  $[v_0] \neq [u_0]$ .

### 5.5.7. The rotating function argument of § 4.2.5.3 in the general case.

In Section 4.2, under Assumption 4.6, we studied functions  $u_{y,z}$  such that  $\rho(u_{y,z}, y) = (2k - 3)$  and  $\rho(u_{y,z}, z) = 1$ , and we looked at the limits when  $z$  tends to  $y$  clockwise or counter-clockwise.

The general combinatorial type  $\tau$  is as follows.

$$\tau = \begin{pmatrix} \downarrow & R & a & L \\ a & \tau(A) & \downarrow & \tau(B) \end{pmatrix}$$

where  $R = \{1, \dots, (a - 1)\}$  and  $L = \{(a + 1), \dots, (2k - 3)\}$ .

Letting  $z$  tend to  $y$  clockwise or counter-clockwise, we obtain the combinatorial types  $\tau_R$  and  $\tau_L$  given by

$$\tau_R = \begin{pmatrix} 0 & R & a & L \\ a & \tau(R) & 0 & \tau(L) \end{pmatrix}$$

and

$$\tau_L = \begin{pmatrix} R & a & L & (2k - 2) \\ \tau(R) & (2k - 2) & \tau(L) & a \end{pmatrix}.$$

Using Procedure 5.49, it is easy to show that

$$\sigma_L = 4 + \|\mathcal{W}_R\| \quad \text{and} \quad \sigma_R \leq 2 + \|\mathcal{W}_R\|,$$

where  $\mathcal{W}_R$  is the word describing  $\mathcal{B}_R$ . It follows that the combinatorial types  $\tau_R$  and  $\tau_L$  are different.

This proves that the rotating function argument in Paragraph 4.2.5.3 yields a contradiction in the general case. This finishes the proof of Proposition 4.16.

### 5.5.8. Proof of Lemma 5.24, Assertion (ii), general case.

Let  $\eta \in \Gamma_{(2k-2)}$  (assuming this set is not empty). Assume, by contradiction, that the functions  $u_y$  have the same combinatorial type  $\tau$  for  $y$  close enough to  $\eta$ , on either sides of  $\eta$ .

Working in  $\mathbb{H}$ , according to Lemma 5.12, the general combinatorial type is given by

$$\tau = \begin{pmatrix} \downarrow & R & a & L \\ a & \tau(R) & \downarrow & \tau(L) \end{pmatrix},$$

where  $R = \{1, \dots, (a - 1)\}$  and  $L = \{(a + 1), \dots, (2k - 3)\}$ , and the nodal patterns are as follows depending on whether  $t$  is on the right or on the left of 0.

When  $t$  tends to zero, the limit functions have the following combinatorial types

$$\tau_L = \begin{pmatrix} 0 & R & a & L \\ a & \tau(R) & 0 & \tau(L) \end{pmatrix}$$

and

$$\tau_R = \begin{pmatrix} R & a & L & (2k - 2) \\ \tau(R) & (2k - 2) & \tau(L) & a \end{pmatrix}.$$



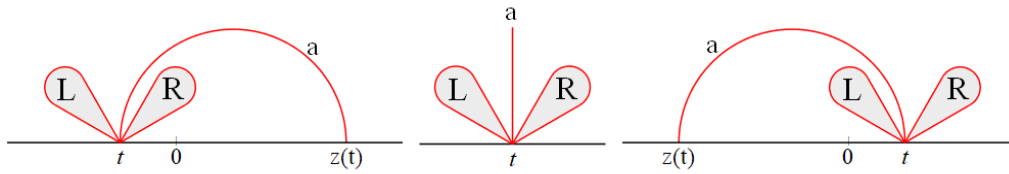


FIGURE 5.58. Nodal patterns with the same  $\tau$

and nodal patterns

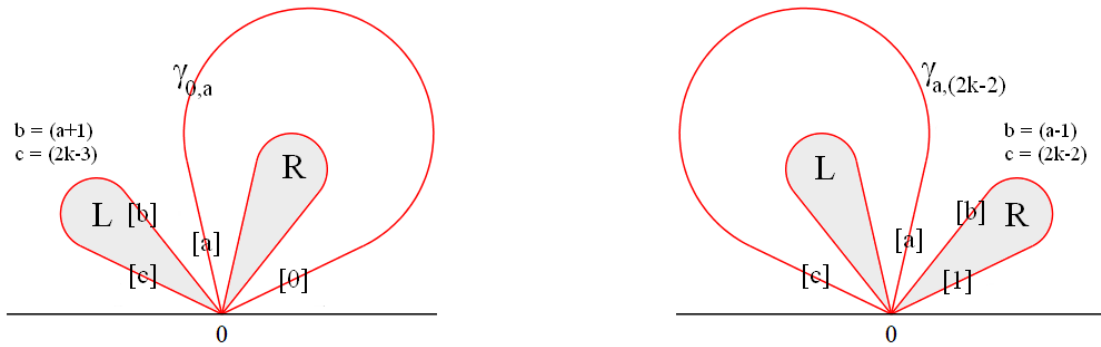


FIGURE 5.59. Nodal patterns for  $u_L$  and  $u_R$

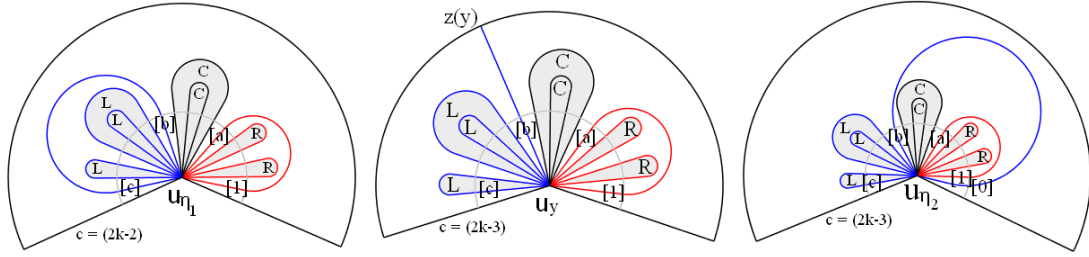
Using Procedure 5.49, it is easy to show that

$$\sigma_L = 4 + \|\mathcal{W}_R\| \quad \text{and} \quad \sigma_R \leq 2 + \|\mathcal{W}_R\|,$$

where  $\mathcal{W}_R$  is the word describing  $\mathcal{B}_R$ . It follows that the combinatorial types  $\tau_R$  and  $\tau_L$  belong to different eigenfunctions.  $\square$

**5.5.9. Proof of Lemma 5.24, Assertion (iv), general case.**

Assuming it is not empty, let  $\eta_1, \eta_2$  be two successive points of  $\Gamma_{(2k-2)}$ , i.e., points such that the arc  $\mathcal{A}(\eta_1, \eta_2)$  is contained in  $\Gamma_{(2k-3)}$ . We want to prove that the combinatorial types of  $u_{\eta_1}$  and  $u_{\eta_2}$  are different. For this purpose, we choose the general pattern described in Subsection 5.5.6, part [B], see Figure 5.56. In view of Lemma 5.12, when the point  $y$  moves off  $\eta_1$  to the right (i.e., counter-clockwise on  $\Gamma$ ), the loop  $\gamma_{b,(2k-2)}^{u_{\eta_1}}$  opens up to become a nodal interval from  $y$  to  $z(y)$ , emanating from  $y$  tangentially to the ray  $\omega_b$ . When  $y$  approaches  $\eta_2$  from the left, this nodal interval closes in into the loop  $\gamma_{0,b}^{u_{\eta_2}}$  and  $u_{\eta_2}$  has the nodal pattern of  $v_0$  (as in Figure 4.6), see Subsection 5.5.6, part [C]. The transition from  $\mathcal{Z}(u_{\eta_1})$  to  $\mathcal{Z}(u_{\eta_2})$  is illustrated in Figure 5.60. According to (5.68) and (5.69), we have  $\sigma(\mathcal{W}_{\eta_1}) \neq \sigma(\mathcal{W}_{\eta_2})$ , showing that the nodal patterns are different. This proves Lemma 5.24, Assertion (iv), in the general case.  $\square$

FIGURE 5.60. Nodal patterns for  $u_{\eta_1}$ ,  $u_y$  and  $u_{\eta_2}$ 

## 5.6. Eigenfunctions with Two Prescribed Boundary Singular Points: proof of Lemma 5.8 and further results

### 5.6.1. Introduction.

The main purpose of this section is provide a detailed proof of Lemma 5.8. We also derive further properties of  $V_{y,s}$  which appear in [HoMN1999, pp. 1180-1183], see Table 5.1. We do not use these properties for our proof of Theorem 5.1.

We retain the notation of Section 5.2, in particular Notation 5.3.

We work under Assumptions 5.2, i.e. assuming that

$$(5.70) \quad \begin{cases} \Omega \text{ is simply connected, } \Gamma := \partial\Omega, \\ k \geq 3 \text{ and } \dim U(\lambda_k) = (2k - 2). \end{cases}$$

The sets  $\Gamma_{(2k-3)}$  and  $\Gamma_{(2k-2)}$  are defined in (5.10).

REMARK 5.51. The assumption  $\Omega$  simply connected is motivated by Remark 1.2, and makes the proofs of the following lemmas simpler. It would be interesting to know whether it is actually necessary.

Recall that for  $(y, s) \in \Gamma_{(2k-3)} \times \Gamma$ , with  $y \neq s$ ,

$$V_{y,s} := \{u \in U \mid \rho(u, y) \geq 2k - 4 \text{ and } \rho(u, s) \geq 1\}.$$

In view of the Equation (5.70), Lemma 2.16 implies that  $V_{y,s} \neq \{0\}$ .

### 5.6.2. Proof of Lemma 5.8. For convenience, we reproduce the lemma.

LEMMA 5.52 (Restatement of Lemma 5.8). *Assume that  $\Omega$  is simply connected. Let  $U := U(\lambda_k)$  with  $k \geq 3$ , and assume that  $\dim U = (2k-2)$ . Given  $(y, s) \in \Gamma_{(2k-3)} \times \Gamma$ , with  $y \neq s$ , the subspace*

$$V_{y,s} = \{u \in U \mid \rho(u, y) \geq 2k - 4 \text{ and } \rho(u, s) \geq 1\}$$

has the following properties.

- (i) The subspace  $V_{y,s}$  has dimension 1.

(ii) Any  $0 \neq u \in V_{y,s}$  satisfies

$$(5.71) \quad \begin{cases} \kappa(u) = k, \\ \mathcal{Z}(u) \cup \Gamma \text{ is connected,} \\ \mathcal{S}_i(u) = \emptyset, \\ \sum_{z \in \mathcal{S}_b(u)} \rho(u, z) = 2k - 2, \text{ and} \\ 2k - 4 \leq \rho(u, y) \leq 2k - 3, \\ 1 \leq \rho(u, s) \leq 2. \end{cases}$$

More precisely, there are three distinct possibilities.

**Case A:**  $\rho(u, y) = (2k - 3)$  and  $\rho(u, s) = 1$ . In that case,  $u \in U_y$ , with  $\mathcal{S}_b(u) = \{y, s\}$ , and hence  $s = z(y)$ .

**Case B:**  $\rho(u, y) = (2k - 4)$  and  $\rho(u, s) = 2$ . In that case,  $\mathcal{S}_b(u) = \{y, s\}$ .

**Case C:**  $\rho(u, y) = (2k - 4)$ ,  $\rho(u, s) = 1$ , and there exists some  $s' \in \Gamma \setminus \{y, s\}$  such that  $\mathcal{S}_b(u) = \{y, s, s'\}$ , with  $\rho(u, s') = 1$ .

(iii) If  $s = z(y)$ , then  $V_{y,z(y)} = U_y$ .

(iv) The map  $\{(y, s) \mid (y, s) \in \Gamma_{(2k-3)} \times \Gamma, s \neq y\} \ni (y, s) \mapsto [V_{y,s}] \in \mathbb{P}(U)$  is  $C^\infty$ .

*Proof.* We already know that  $\dim V_{y,s} \geq 1$ .

We retain the notation of Lemma 5.6. In particular, for  $y \in \Gamma_{(2k-3)}$ , we have  $U_y = [u_y]$  with  $0 \neq u_y \in U$  satisfying  $\mathcal{S}_b(u_y) = \{y, z(y)\}$  with  $z(y) \neq y$ , and  $\rho(u_y, y) = (2k - 3)$ ,  $\rho(u_y, z(y)) = 1$ .

◇ *Proof of Assertion (ii).* From Euler's formula (5.1) we obtain,

$$(5.72) \quad \begin{aligned} 0 \geq \kappa(u) - k &= (b_0(\mathcal{Z}(u) \cup \Gamma) - 1) + \frac{1}{2} \sum_{z \in \mathcal{S}_i(u)} (\nu(u, z) - 2) \\ &+ \frac{1}{2} \left( \sum_{z \in \mathcal{S}_b(u)} \rho(u, z) - 2k + 2 \right). \end{aligned}$$

If  $0 \neq u \in V_{y,s}$ , we have  $\sum_{z \in \mathcal{S}_b(u)} \rho(u, z) \geq 2k - 3$ , and hence  $\sum_{z \in \mathcal{S}_b(u)} \rho(u, z) \geq 2k - 2$  since the sum is an even integer, by Corollary 2.13. All the terms in the right hand side of (5.72) must vanish; this proves (5.71). Assertion (ii) then follows from (5.71) and the assumptions that  $\rho(u, y) \geq (2k - 4)$  and  $\rho(u, s) \geq 1$ .

◇ *Proof of Assertion (i).*

[1] We first assume that  $s \neq z(y)$ . Assume that there are at least two linearly independent functions  $u_1, u_2 \in V_{y,s}$ , then  $\rho(u_i, y) = (2k - 4)$  and  $\rho(u_i, s) \geq 1$ . According to Lemma 2.17, there exists a nontrivial linear combination  $u$  of  $u_1$  and  $u_2$  such that  $\rho(u, y) \geq (2k - 3)$  and  $\rho(u, s) \geq 1$ . Euler's formula implies that  $u$  pertains to Assertion (ii), Case (1), contradicting the fact that  $s \neq z(y)$ .

[2] We now assume that  $s = z(y)$ . In this case, a generator  $u_y$  of  $U_y$  belongs to  $V_{y,z(y)}$ . Assume that  $\dim V_{y,z(y)} \geq 2$ . Define  $V'_{y,z(y)} = V_{y,z(y)} \ominus U_y$ , which has dimension at least 1. If  $\dim V_{y,z(y)} \geq 3$ , we can find two linearly independent  $u_1, u_2 \in V'_{y,z(y)}$ , such that  $\rho(u_i, y) = (2k - 4)$ , and  $\rho(u_i, s) \geq 1$ . By Lemma 2.17, there exists a nontrivial linear combination  $u \in V'_{y,z(y)}$  such that  $\rho(u, y) \geq (2k - 3)$  and  $\rho(u, s) \geq 1$ . Hence,  $u \in U_y$ , a contradiction. Assuming that  $\dim V_{y,z(y)} = 2$ , we can choose a basis  $\{u_y, v_y\}$  such that  $v_y \notin U_y$ . Then,  $\rho(v_y, y) = (2k - 4)$ , and there are two cases,

**Case a:**  $\rho(v_y, z(y)) = 2$ ,

**Case b:**  $\rho(v_y, z(y)) = 1$ , and there exists some  $z_1(y) \in \Gamma$ ,  $z_1(y) \neq z(y)$ , such that  $\mathcal{S}_b(v_y) = \{y, z(y), z_1(y)\}$  and  $\rho(v_y, z_1(y)) = 1$ .

Without loss of generality, making use of Lemma 2.19, we may choose the functions  $u_y$  and  $v_y$  as follows (we consider open arcs). First we choose  $u_y$  so that  $\check{u}_y > 0$  on the arc  $\mathcal{A}(y, z(y))$ , and  $\check{u}_y < 0$  on the arc  $\mathcal{A}(z(y), y)$ .

◦ In Case a, we choose  $v_y$  such that  $\check{v}_y > 0$  on  $\mathcal{A}(y, z(y)) \cup \mathcal{A}(z(y), y)$ .

◦ In Case b, assuming that  $z_1(y) \in \mathcal{A}(y, z(y))$ , we choose  $v_y$  such that  $\check{v}_y > 0$  on  $\mathcal{A}(z(y), y) \cup \mathcal{A}(y, z_1(y))$ , and  $\check{v}_y < 0$  on  $\mathcal{A}(z_1(y), z(y))$ .

Figure 5.61 displays the signs of  $\check{u}_y$  and of  $\check{v}_y$  in both cases.

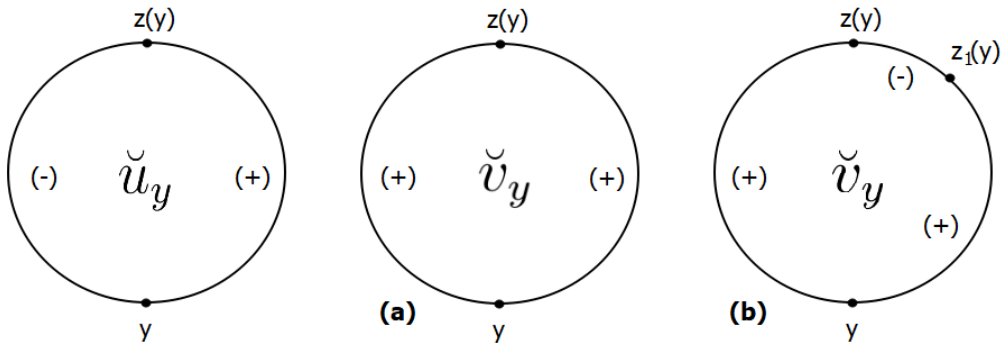


FIGURE 5.61. Signs of  $\check{u}_y$  and of  $\check{v}_y$ , Cases a and b

*Claim 1.* Under the assumption that  $\dim V_{y,z(y)} = 2$ , there exists some function  $v \in V_{y,z(y)}$  such that  $\rho(v, y) = (2k - 4)$  and  $\rho(v, z(y)) = 2$ .

*Proof of Claim 1.* If  $v_y$  satisfies Claim 1, there is nothing to prove. If not,  $v_y$  falls into Case b above.

Given  $t \in \Gamma \setminus \{y, z(y)\}$ ,  $\check{u}_y(t) \neq 0$ , and we can define the function

$$(5.73) \quad \xi_t := a(t)u_y - b(t)v_y \in V_{y,z(y)},$$

where

$$(5.74) \quad \begin{cases} a(t) = \check{v}_y(t) (\check{v}_y^2(t) + \check{u}_y^2(t))^{-\frac{1}{2}}, \\ b(t) = \check{u}_y(t) (\check{v}_y^2(t) + \check{u}_y^2(t))^{-\frac{1}{2}}. \end{cases}$$

For  $t \notin \{y, z(y)\}$ ,  $b(t) \neq 0$ , and hence  $\rho(\xi_t, y) = 2k - 4$ ,  $\rho(\xi_t, z(y)) \geq 1$ ,  $\rho(\xi_t, t) \geq 1$ . Euler's formula applied to  $\xi_t$  implies that  $\rho(\xi_t, z(y)) = \rho(\xi_t, t) = 1$ , and  $\mathcal{S}_b(\xi_t) = \{y, z(y), t\}$ . According to Lemma 2.19, the function  $\check{\xi}_t$  has precisely three zeros at  $y, z(y)$  and  $t$ , changes sign at  $z(y)$  and  $t$ , and does not change sign at  $y$ . For  $t \in \mathcal{A}(z_1(y), z(y))$ ,  $\check{\xi}_t(z_1(y)) < 0$ , and we conclude that

$$(5.75) \quad \text{for } t \in \mathcal{A}(z_1(y), z(y)), \quad \begin{cases} \check{\xi}_t > 0 \text{ in } \mathcal{A}(t, z(y)), \text{ and} \\ \check{\xi}_t < 0 \text{ in } \mathcal{A}(z(y), y) \cup \mathcal{A}(y, t). \end{cases}$$

where  $y, z(y)$  and  $z_1(y)$  are as in Figure 5.61 (b).

Choose a sequence  $\{t_n\} \subset \mathcal{A}(z_1(y), z(y))$ , with  $t_n \rightarrow z(y)$ . Taking a subsequence if necessary, we may assume that the sequence  $\{(a(t_n), b(t_n))\}$  converges to some

$(a, b) \in \mathbb{S}^1$ , so that the sequence  $\{\xi_{t_n}\}$  converges uniformly to the function  $\xi := au_y - bv_y$ . From (5.75), we conclude that  $\check{\xi} \leq 0$  on  $\Gamma$ . Since  $\xi \in V_{y,z(y)}$  we have three possibilities,

- (i)  $\rho(\xi, y) = (2k - 3)$  and  $\rho(\xi, z(y)) = 1$ ,
- (ii)  $\rho(\xi, y) = (2k - 4)$ ,  $\rho(\xi, z(y)) = 1$ , and  $\rho(\xi, z_2)$  for some  $z_2 \neq y, z(y)$ ,
- (iii)  $\rho(\xi, y) = (2k - 4)$  and  $\rho(\xi, z(y)) = 2$ .

Since (i) and (ii) are incompatible with  $\check{\xi} \leq 0$  on  $\Gamma$ , we conclude that  $\rho(\xi, y) = (2k - 4)$  and  $\rho(\xi, z(y)) = 2$ . This proves Claim 1.  $\checkmark$

We now continue with part [2] in the proof of Assertion (i). In view of Claim 1, assuming that  $\dim V_{y,z(y)} = 2$ , we may choose a basis  $\{u_y, v_y\}$  of  $V_{y,z(y)}$  such that

$$(5.76) \quad \begin{cases} \rho(u_y, y) = 2k - 3, \\ \rho(u_y, z(y)) = 1, \\ \check{u}_y|_{\mathcal{A}(y,z(y))} > 0 \text{ and } \check{u}_y|_{\mathcal{A}(z(y),y)} < 0, \end{cases} \quad \text{and} \quad \begin{cases} \rho(v_y, y) = 2k - 4, \\ \rho(v_y, z(y)) = 2, \\ \check{v}_y|_{\Gamma\{y,z(y)\}} > 0. \end{cases}$$

Examples of nodal sets of these functions are displayed in Figure 5.62: on the left  $\mathcal{Z}(u_y)$ , on the right  $\mathcal{Z}(v_y)$ , with two possible cases.

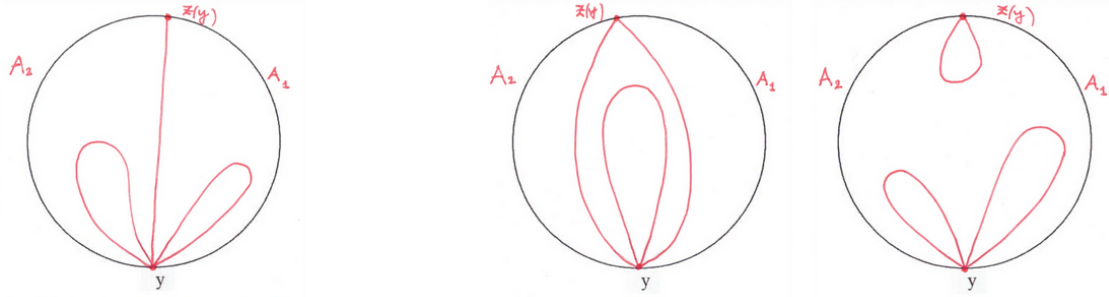


FIGURE 5.62. Nodal sets of  $u_y$  (left) and  $v_y$  (right), with  $k = 4$ .

From now on, to simplify the notation in the proof, we denote the arc  $\mathcal{A}(y, z(y))$  by  $A_1$ , and the arc  $\mathcal{A}(z(y), y)$  by  $A_2$ . We now use another “rotating function argument”.

For  $s \notin \{y, z(y)\}$ , we consider the function

$$(5.77) \quad \xi_s = a(s)u_y - b(s)v_y,$$

where  $u_y$  and  $v_y$  satisfy (5.76), and  $a(s)$ ,  $b(s)$  are given by

$$(5.78) \quad \begin{cases} a(s) = \check{v}_y(s) \left( \check{v}_y^2(s) + \check{u}_y^2(s) \right)^{-\frac{1}{2}}, \\ b(s) = \check{u}_y(s) \left( \check{v}_y^2(s) + \check{u}_y^2(s) \right)^{-\frac{1}{2}}. \end{cases}$$

In particular,  $a(s) > 0$  in  $A_1 \cup A_2$ ,  $b(s) > 0$  in  $A_1$  and  $b(s) < 0$  on  $A_2$ . Since  $a(s)$  and  $b(s)$  are different from 0,  $\rho(\xi_s, y) = (2k - 4)$  and  $\rho(\xi_s, z(y)) = 1$ . Since  $\check{\xi}_s(s) = 0$ ,  $\rho(\xi_s, s) \geq 1$ . Since  $\xi_s \in V_{y,z(y)}$ , Equation (5.12) implies that  $\rho(\xi_s, s) = 1$ ,  $\mathcal{S}_b(\xi_s) = \{y, z(y), s\}$ , and  $\check{\xi}_s$  changes sign at  $z(y)$  and  $s$  (use Lemma 2.19 again).

Taking  $s_2 \in A_2$  and  $s \in A_1$ , we find that  $\check{\xi}_s(s_2) < 0$  and hence,

$$(5.79) \quad \text{for } s \in A_1, \quad \begin{cases} \check{\xi}_s > 0 & \text{in } \mathcal{A}(s, z(y)), \\ \check{\xi}_s < 0 & \text{in } A_2 \cup \mathcal{A}(y, s). \end{cases}$$

Similarly, taking  $s_1 \in A_1$  and  $s \in A_2$ , we find that  $\check{\xi}_s(s_1) > 0$  and hence,

$$(5.80) \quad \text{for } s \in A_2, \quad \begin{cases} \check{\xi}_s < 0 & \text{in } \mathcal{A}(z(y), s), \\ \check{\xi}_s > 0 & \text{in } \mathcal{A}(s, y) \cup A_1. \end{cases}$$

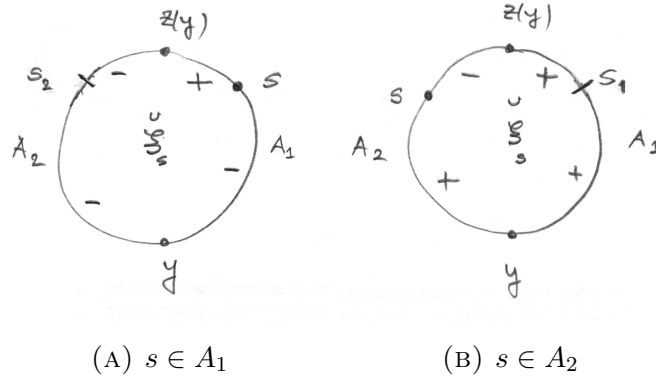


FIGURE 5.63. Signs of the function  $\check{\xi}_s$

There exists a unique  $\theta(s) \in (-\frac{\pi}{2}, \frac{\pi}{2})$  such that  $a(s) = \cos(\theta(s))$  and  $b(s) = \sin(\theta(s))$ , so that  $\xi_s = \cos(\theta(s))u_y - \sin(\theta(s))v_y$ . Then,  $\theta(s) \in (0, \frac{\pi}{2})$  when  $b(s) > 0$  or equivalently when  $s \in A_1$ ;  $\theta(s) \in (-\frac{\pi}{2}, 0)$  when  $b(s) < 0$  or equivalently when  $s \in A_2$ . Furthermore, the map  $s \mapsto \theta(s)$  is injective because  $\mathcal{S}_b(\xi_s) = \{y, z(y), s\}$ .

For  $s_1, s_2 \in A_1$  or  $A_2$ , we have

$$(5.81) \quad \begin{cases} \xi_{s_1} - \xi_{s_2} = (\cos(\theta(s_1)) - \cos(\theta(s_2)))u_y - (\sin(\theta(s_1)) - \sin(\theta(s_2)))v_y \\ = -2 \sin \frac{\theta(s_1) - \theta(s_2)}{2} \left( \sin \frac{\theta(s_1) + \theta(s_2)}{2} u_y + \cos \frac{\theta(s_1) + \theta(s_2)}{2} v_y \right). \end{cases}$$

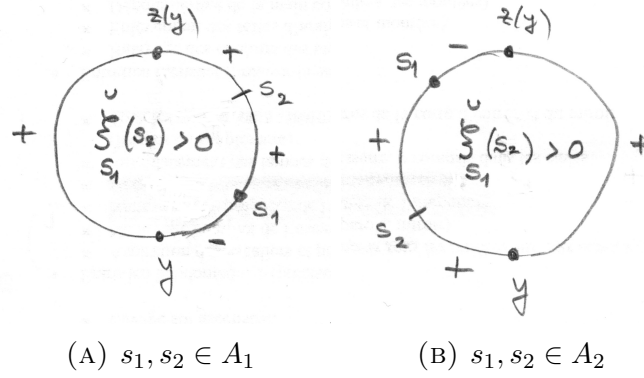
If  $s_1, s_2 \in A_1$ ,  $\theta(s_1), \theta(s_2) \in (0, \frac{\pi}{2})$ , and the second factor in the second line of Equation (5.81) is positive in  $A_1$ . If  $s_1, s_2 \in A_2$ ,  $\theta(s_1), \theta(s_2) \in (-\frac{\pi}{2}, 0)$ , and the second factor in the second line of Equation (5.81) is positive in  $A_2$ .

Since  $\check{\xi}_{s_1}(s_2) - \check{\xi}_{s_2}(s_2) = \check{\xi}_{s_1}(s_2)$ , using Equations (5.79) and (5.80) we conclude that,

$$(5.82) \quad \begin{cases} s_1 \in A_1 \text{ and } s_2 \in \mathcal{A}(s_1, z(y)) \Rightarrow \check{\xi}_{s_1}(s_2) > 0 \\ \Rightarrow \sin \frac{\theta(s_1) - \theta(s_2)}{2} < 0 \Rightarrow \theta(s_2) > \theta(s_1) \text{ in } (0, \frac{\pi}{2}), \\ s_1 \in A_2 \text{ and } s_2 \in \mathcal{A}(s_1, y) \Rightarrow \check{\xi}_{s_1}(s_2) > 0 \\ \Rightarrow \sin \frac{\theta(s_1) - \theta(s_2)}{2} < 0 \Rightarrow \theta(s_2) > \theta(s_1) \text{ in } (-\frac{\pi}{2}, 0), \end{cases}$$

otherwise stated, when  $s$  moves counter-clockwise on  $A_1$ , resp.  $A_2$ , the function  $\theta(s)$  increases from 0 to  $\frac{\pi}{2}$ , resp. from  $-\frac{\pi}{2}$  to 0, see Figure 5.64.

Under the assumption that  $\dim V_{y,z(y)} = 2$ , we are in a framework similar to that of Subsection 4.2.5, with  $V_{y,z(y)}$  replacing  $U_x^2$ . We use a rotating function argument


 FIGURE 5.64. Sign of  $\check{\xi}_{s_1}(s_2)$ 

similar to the one used in Paragraph 4.2.5.3. For this purpose, we first investigate the limits of  $\xi_s$  and  $\theta(s)$  when  $s$  tends to  $z(y)$  or to  $y$ .

Let  $\gamma_z$  (resp.  $\gamma_y$ ) denote a local parametrization of  $\Gamma$  in a neighborhood of  $z(y)$  (resp.  $y$ ), such that  $\gamma_z(0) = z(y)$ ,  $\gamma_z(-\varepsilon) \in A_2$ , and  $\gamma_z(\varepsilon) \in A_1$  (resp.  $\gamma_y(0) = y$ ,  $\gamma_y(-\varepsilon) \in A_2$ , and  $\gamma_y(\varepsilon) \in A_1$ ). Using our choice of sign for  $\check{u}_y$  and  $\check{v}_y$ , the vanishing properties of these functions, and Lemma 2.19, we find that, in a pointed neighborhood of  $z(y)$ ,

$$\begin{cases} \check{u}_y(\gamma_z(t)) = \alpha_u t + o(t), \text{ with } \alpha_u > 0, \\ \check{v}_y(\gamma_z(t)) = \alpha_v t^2 + o(t^2), \text{ with } \alpha_v > 0, \\ a(\gamma_z(t)) = \frac{\alpha_v}{\alpha_u} |t| + o(t), \\ b(\gamma_z(t)) = \text{sgn}(t) + o(1). \end{cases}$$

Similarly, in a neighborhood of  $y$ ,

$$\begin{cases} \check{u}_y(\gamma_y(t)) = \beta_u t^{2k-3} + o(t^{2k-3}), \text{ with } \beta_u > 0, \\ \check{v}_y(\gamma_y(t)) = \beta_v t^{2k-4} + o(t^{2k-4}), \text{ with } \beta_v > 0, \\ a(\gamma_y(t)) = 1 + o(1), \\ b(\gamma_y(t)) = \frac{\beta_u}{\beta_v} t + o(t). \end{cases}$$

This gives us the limits of  $\xi_s$  and  $\theta(s)$  when  $s$  tends to  $z(y)$  in  $A_1$  or  $A_2$  (resp. when  $s$  tends to  $y$  in  $A_1$  and  $A_2$ ),

$$(5.83) \quad \begin{cases} \lim_{\substack{s \rightarrow z(y) \\ s \in A_1}} \xi_s = -v_y, & \lim_{\substack{s \rightarrow z(y) \\ s \in A_1}} \theta(s) = \frac{\pi}{2}, \\ \lim_{\substack{s \rightarrow y \\ s \in A_1}} \xi_s = u_y, & \lim_{\substack{s \rightarrow y \\ s \in A_1}} \theta(s) = 0, \\ \lim_{\substack{s \rightarrow z(y) \\ s \in A_2}} \xi_s = v_y, & \lim_{\substack{s \rightarrow z(y) \\ s \in A_2}} \theta(s) = 0, \\ \lim_{\substack{s \rightarrow y \\ s \in A_2}} \xi_s = u_y, & \lim_{\substack{s \rightarrow y \\ s \in A_2}} \theta(s) = -\frac{\pi}{2}. \end{cases}$$

When  $s$  moves counter-clockwise from  $y$  to  $z(y)$  on  $A_1$ ,  $\theta(s)$  increases from 0 to  $\frac{\pi}{2}$ ; when  $s$  moves counter-clockwise from  $z(y)$  to  $y$  on  $A_2$ ,  $\theta(s)$  increases from  $-\frac{\pi}{2}$  to 0.

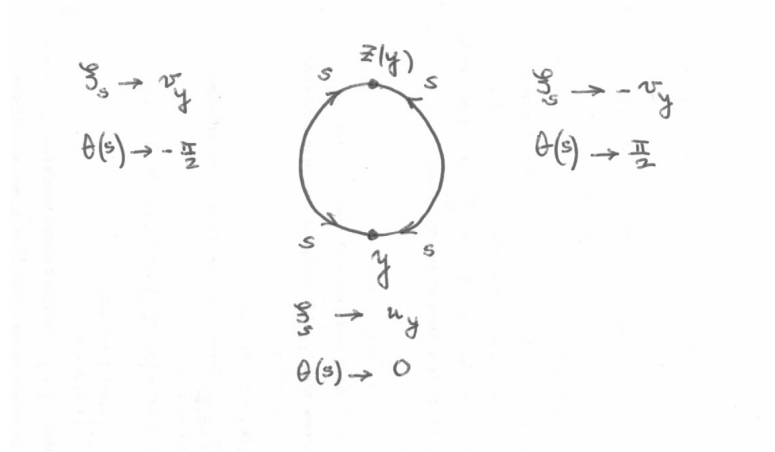


FIGURE 5.65. Lemma 5.52: limits of  $\xi_s$  when  $s$  tends to  $y$  or  $z(y)$

Let  $[-\frac{\pi}{2}, \frac{\pi}{2}] \ni \sigma \mapsto \Gamma(\sigma)$  be a parametrization of  $\Gamma$  such that  $\gamma_1(-\frac{\pi}{2}) = \gamma_1(\frac{\pi}{2}) = z(y)$ ,  $\gamma_1(0) = y$ ,  $\gamma_1((-\frac{\pi}{2}, 0)) = A_2$ , and  $\gamma_1((0, \frac{\pi}{2})) = A_1$ .

Consider the map

$$\theta_1 : (-\frac{\pi}{2}, 0) \cup (0, \frac{\pi}{2}) \ni \sigma \mapsto \theta(\gamma_1(\sigma)) \in (-\frac{\pi}{2}, \frac{\pi}{2}).$$

Then,  $\theta_1$  extends to a continuous, increasing map from  $(-\frac{\pi}{2}, \frac{\pi}{2})$  to  $(-\frac{\pi}{2}, \frac{\pi}{2})$  such that  $\lim_{\sigma \rightarrow \pm \frac{\pi}{2}} \theta_1(\sigma) = \pm \frac{\pi}{2}$  and  $\lim_{\sigma \rightarrow 0} \theta_1(\sigma) = 0$ .

For  $t \in [-\frac{\pi}{2}, \frac{\pi}{2}]$ , introduce the functions

$$(5.84) \quad \zeta_t := \cos t u_y - \sin t v_y,$$

$\zeta_{-\frac{\pi}{2}} = v_y$ ,  $\zeta_0 = u_y$ , and  $\zeta_{\frac{\pi}{2}} = -v_y$ . If  $t \notin \{-\frac{\pi}{2}, 0, \frac{\pi}{2}\}$  there exists a unique  $s(t) \in \Gamma \setminus \{y, z(y)\}$  such that

$$(5.85) \quad \begin{cases} \rho(\zeta_t, y) = (2k - 4), \quad \rho(\zeta_t, z(y)) = 1, \quad \rho(\zeta_t, s(t)) = 1, \\ \mathcal{S}_b(\zeta_t) = \{y, z(y), s(t)\}, \\ s(t) \in A_1 \text{ if } t \in (0, \frac{\pi}{2}), \text{ and } s(t) \in A_2 \text{ if } t \in (-\frac{\pi}{2}, 0). \end{cases}$$

Indeed, near  $z(y)$ ,  $\cos t > 0$  implies that  $\zeta_t$  has the sign of  $u_y$ . In a small pointed arc  $J_y$  around  $y$ ,  $\zeta_t \sim -\sin t v_y$  which has the sign of  $(-t)$ .

We now apply the “rotating function argument”, see Paragraph 4.2.5.3, to the family of nodal sets  $\mathcal{Z}(\zeta_t)$ . We have  $\mathcal{Z}(\zeta_{-\frac{\pi}{2}}) = \mathcal{Z}(\zeta_{\frac{\pi}{2}}) = \mathcal{Z}(v_y)$ ; when  $t \in (0, \frac{\pi}{2})$ ,  $\mathcal{S}_b(\zeta_t) = \{y, z(y), s(t)\}$  with  $s(t) \in A_1$ ; when  $t \in (-\frac{\pi}{2}, 0)$ ,  $s(t) \in A_2$ .

Figure 5.66 (resp. Figure 5.67) illustrates the deformation of the nodal set  $\mathcal{Z}(v_y)$  given in Subfigure (A) in a particular case with  $k = 4$ .

In Figure 5.66 the nodal set  $\mathcal{Z}(v_y)$  is connected. When  $t$  decreases from  $\frac{\pi}{2}$  to 0 (top line), the nodal set  $\mathcal{Z}(\zeta_t)$  deforms from  $\mathcal{Z}(v_y)$  in Subfigure (A) to  $\mathcal{Z}(u_y)$  in Subfigure (L). When  $t$  increases from  $-\frac{\pi}{2}$  to 0 (bottom line), the nodal set  $\mathcal{Z}(\zeta_t)$  deforms from  $\mathcal{Z}(v_y)$  in Subfigure (A) to  $\mathcal{Z}(u_y)$  in Subfigure (R). In Figure 5.67 the nodal set  $\mathcal{Z}(\zeta_t)$  has two components and deforms to (R) or (L).



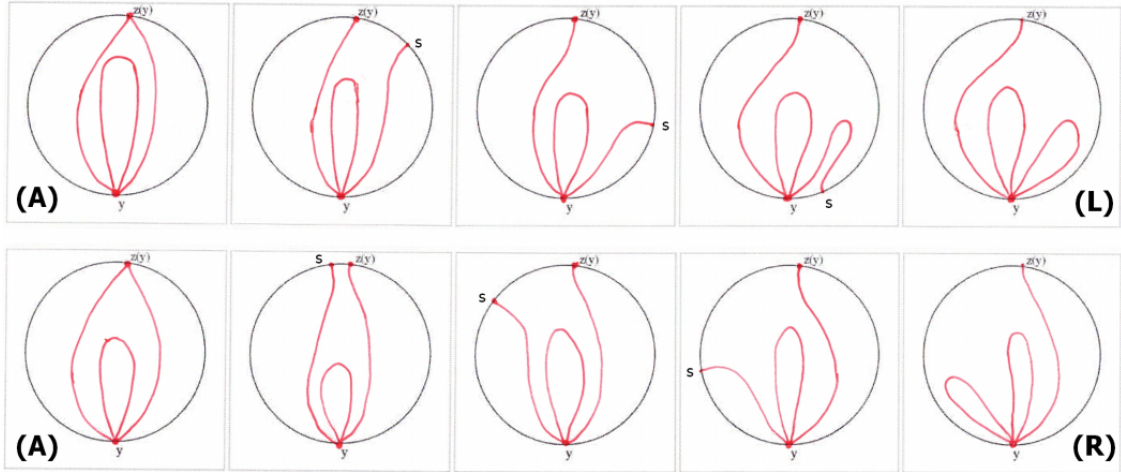


FIGURE 5.66. The point  $s$  tends to  $y$  clockwise (top) or counter-clockwise (bottom), here  $k = 4$

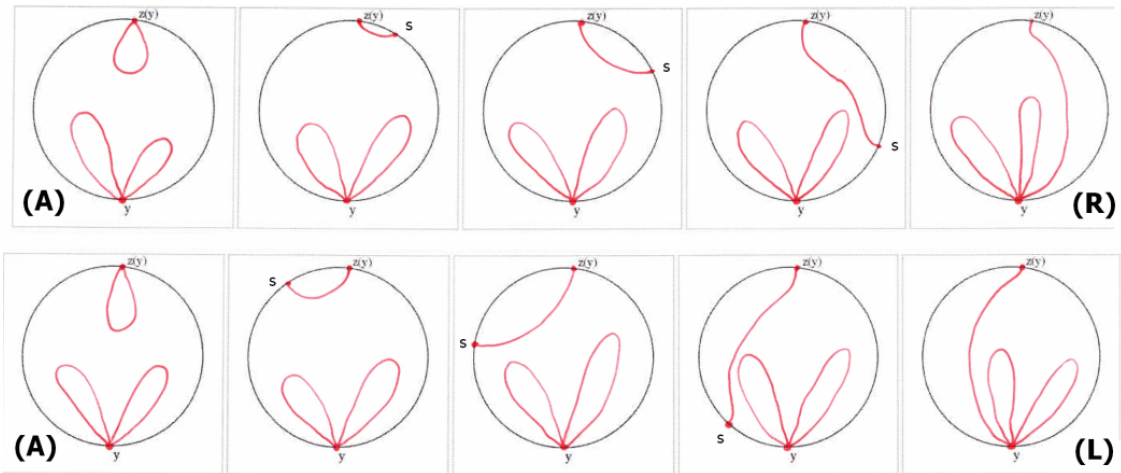


FIGURE 5.67. The point  $s$  tends to  $y$  clockwise (top) or counter-clockwise (bottom), here  $k = 4$

The nodal patterns  $(L)$  and  $(R)$  belong to a function  $u_y$ . We claim that they are different. For this purpose, we label the loops as in Paragraph 4.2.5.2, and we use the combinatorial type of the function  $u_y$ , see Paragraph 5.2.3.2.

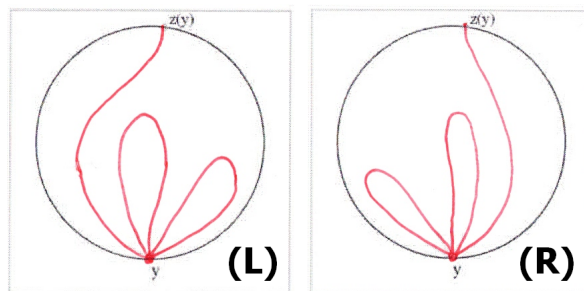


FIGURE 5.68. The nodal patterns  $(L)$  and  $(R)$  are different

The maps  $\tau$  describing the combinatorial types of the nodal patterns  $(L)$  and  $(R)$  of Figure 5.68 are given by

$$\tau_L = \begin{pmatrix} \downarrow & 1 & 2 & 3 & 4 & 5 \\ 5 & 2 & 1 & 4 & 3 & \downarrow \end{pmatrix} \quad \text{and} \quad \tau_R = \begin{pmatrix} \downarrow & 1 & 2 & 3 & 4 & 5 \\ 1 & \downarrow & 3 & 2 & 5 & 4 \end{pmatrix},$$

where  $\downarrow$  corresponds to the arc hitting the boundary. Correspondingly, we label the nodal domains as in Section 5.5, and we find the words,

$$\mathcal{W}_L = |1|2|1|3|1|4| \quad \text{and} \quad \mathcal{W}_R = |1|2|3|2|4|2|.$$

The nodal patterns  $(L)$  and  $(R)$  having different signatures (see Definition 5.44), they are different, although they should both be the nodal pattern of  $u_y$ , a contradiction. Recall that we already proved that  $\dim V_{y,s} \leq 2$ . Since the assumption  $\dim V_{y,s} = 2$  leads to a contradiction, at least in the example at hand, we conclude that  $\dim V_{y,s} = 1$ . The proof in the general case follows the same lines, as in Subsection 4.2.5. This proves Assertion (i).  $\checkmark$

**REMARK 5.53.** When  $t$  varies in  $(-\frac{\pi}{2}, \frac{\pi}{2})$ , the nodal sets  $\mathcal{Z}(\zeta_t)$  vary continuously with respect to the Hausdorff distance, see Lemma 2.20. It follows that they are either all connected, or that they all have two components, so that their type in Figure 5.69 is either (b) & (c) or (d) & (e).

$\diamond$  *Proof of Assertion (iii).* This is a consequence of Assertion (i) and its proof.  $\checkmark$

$\diamond$  *Proof of Assertion (iv).* Let  $v_{y,s}$  denote a generator of  $V_{y,s}$ . Then, the linear system which defines  $v_{y,s}$  up to scaling has constant rank, so that it has a solution which depends smoothly on the parameters  $y, s$  locally.  $\checkmark$

Lemma 5.52 (aka Lemma 5.8) is proved.  $\square$

**5.6.3. Structure and combinatorial type of nodal sets in  $V_{y,s}$ .** The last two lines in (5.12) give rise to three cases for  $0 \neq u \in V_{y,s}$ .

**Case 1.**  $\rho(u, y) = (2k - 3)$ ,  $\rho(u, s) = 1$ , and  $\mathcal{S}_b(u) = \{y, s\}$ . This means that  $u \in U_y$ , and this case only occurs when  $s = z(y)$ , see Figure 5.69 (a).

**Case 2.**  $\rho(u, y) = (2k - 4)$ ,  $\rho(u, s) = 2$ , and  $\mathcal{S}_b(u) = \{y, s\}$ , with two possibilities for  $\mathcal{Z}(u)$ ,

- $\diamond$  either  $\mathcal{Z}(u)$  consists of  $(k - 2)$  loops at  $y$  which do not intersect nor meet  $\Gamma$  away from  $y$ , and one loop at  $s$  which does not hit  $\Gamma$  away from  $s$ , and does not meet the loops at  $y$ ,
- $\diamond$  or  $\mathcal{Z}(u)$  consists of  $(k - 3)$  loops at  $y$  which do not intersect nor meet  $\Gamma$  away from  $y$ , and two simple arcs from  $y$  to  $s$  which do not meet except at  $y$  and  $s$ , and do not meet the loops except at  $y$ ; in this case we have a “generalized loop” which hits  $\Gamma$  at  $s$ ,

see Figures 5.69 (b) and 5.69 (d).

**Case 3.**  $\rho(u, y) = (2k - 4)$ ,  $\rho(u, s) = 1$ , and there exists another point  $s_1 \in \Gamma$ ,  $s_1 \neq s, y$  such that  $\mathcal{S}_b(u) = \{y, s, s_1\}$  and  $\rho(u, s_1) = 1$ . In this case there are two possibilities for  $\mathcal{Z}(u)$ ,

- $\diamond$  either  $\mathcal{Z}(u)$  consists of  $(k - 2)$  loops at  $y$  which do not intersect nor meet  $\Gamma$  away from  $y$ , and one arc from  $s$  to  $s_1$  which does not hit  $\Gamma$  away from  $s, s_1$ , and does not meet the loops at  $y$ ,

◇ or  $\mathcal{Z}(u)$  consists of  $(k - 3)$  loops at  $y$  which do not intersect nor meet  $\Gamma$  away from  $y$ , and two simple arcs, one from  $y$  to  $s$  and one from  $y$  to  $s_1$  which do not meet except at  $y$ , and do not meet the loops except at  $y$ ; in this case we have a “generalized loop” which contains a sub-arc of  $\Gamma$  from  $s$  to  $s_1$ ,

see Figures 5.69 (c) and 5.69 (e).

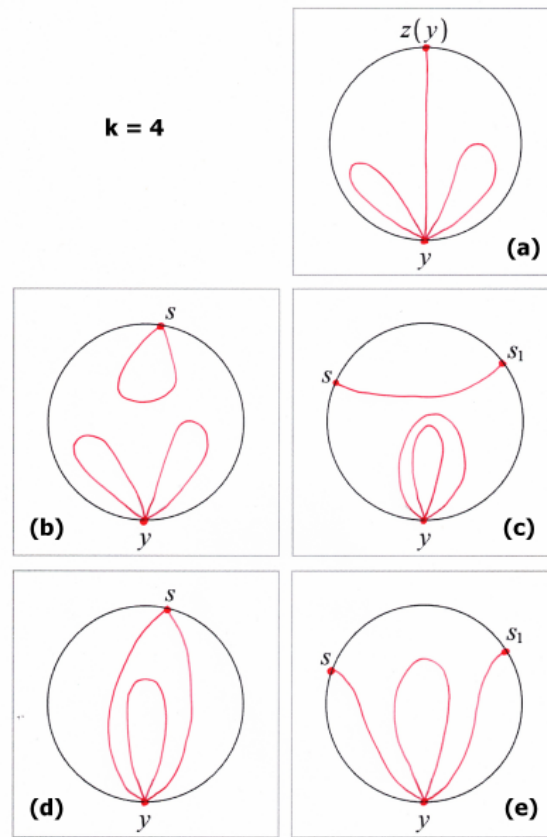


FIGURE 5.69. Nodal patterns for  $u \in V_{y,s}$  ( $k=4$ )

REMARKS 5.54.

- (i) The subcases in Cases 2 and 3 are distinguished by the fact that  $b_0(\mathcal{Z}(u)) = 1$  (as in Figures 5.69 (d) & (e)) or  $b_0(\mathcal{Z}(u)) = 2$ , as in Figures 5.69 (b) & (c), if  $s \neq z(y)$ . Since  $\dim V_{y,s} = 1$ , the subcases cannot occur simultaneously. Indeed, by Lemma 2.17 we would otherwise find a function  $u$  such that  $\rho(u, y) \geq (2k - 3)$  and  $\rho(y, s) \geq 1$ , with  $s \neq z(y)$ , contradicting Case 1.
- (ii) At this stage of the discussion, the location of  $z(y)$  with respect to  $y$ ,  $s$ , and  $s_1$  in Sub-figures 5.69 (b)–(e) is not clear. This will be explained in Lemma 5.57.

For a pair  $(y, s) \in \Gamma_{(2k-3)} \times \Gamma$  with  $y \neq s$ , since  $\dim V_{y,s} = 1$ , we can define the *combinatorial type* of a generator  $v_{y,s}$  at the point  $y$ , as we did for the generator  $u_y$  of  $U_y$  in Paragraph 5.2.3.2, taking the above cases into account.

When  $(y, s) = (y, z(y))$ , the combinatorial type is that of  $u_y$ , and we denote it by  $\tau_{u_y}$ . For example, the combinatorial type  $\tau_{u_y}$  of the function  $u_y$  whose nodal pattern

appears in Figure 5.69 (a) is given by

$$\tau_a^{5.69} = \begin{pmatrix} \downarrow & 1 & 2 & 3 & 4 & 5 \\ 3 & 2 & 1 & \downarrow & 5 & 4 \end{pmatrix},$$

When  $s \neq y$ , the combinatorial type  $\tau := \tau_{v_{y,s}}$  of a function  $v_{y,s}$  is described as follows. When the nodal set is connected, as in Figure 5.69 (d) and (e), we write  $\tau(j) = s$  (resp.  $s_1$ ) to indicate that the nodal semi-arc emanating from  $y$  tangentially to the ray labeled  $j$  ends up at  $s$  (resp.  $s_1$ ). When the nodal set has two components, as in Figure 5.69 (b) and (c), we write  $\tau(s) = s$  to indicate that there is a loop at  $s$ , and  $\tau(s) = s_1$  to indicate that there is a nodal interval from  $s$  to  $s_1$ . We describe the maps  $\tau$  by  $2 \times (2k - 2)$  matrices. The first row enumerates the rays at  $y$  and the rays at  $s$  and  $s_1$  (counter-clockwise). With this convention, the combinatorial type  $\tau_{v_{y,s}}$  of a function  $v_{y,s}$  whose nodal pattern appears in Figure 5.69 (b)–(e), is given by one of the following formulas.

$$\tau_{2,b}^{5.69} = \begin{pmatrix} 1 & 2 & 3 & 4 & s & s \\ 2 & 1 & 4 & 3 & s & s \end{pmatrix}, \quad \tau_{2,c}^{5.69} = \begin{pmatrix} 1 & 2 & 3 & 4 & s_1 & s \\ 2 & 1 & 4 & 3 & s & s_1 \end{pmatrix},$$

and

$$\tau_{1,d}^{5.69} = \begin{pmatrix} 1 & 2 & 3 & 4 & s & s \\ s & 3 & 2 & s & 1 & 4 \end{pmatrix}, \quad \tau_{1,e}^{5.69} = \begin{pmatrix} 1 & 2 & 3 & 4 & s_1 & s \\ s_1 & 3 & 2 & s & 1 & 4 \end{pmatrix}.$$

**5.6.4. Precise description of  $V_{y,s}$ .** In this subsection we analyze the behavior of a generator  $v_{y,s}$  of  $V_{y,s}$  when  $y$  and  $s$  vary. More precisely, Lemma 5.55 describes the behavior of  $v_{y,s}$  when  $y \in \Gamma_{(2k-3)}$  is fixed and  $s$  tends to  $y$  or to  $z(y)$ , and the behavior when  $s \in \Gamma_{(2k-3)}$  is fixed and  $y$  tends to  $s$ . Lemma 5.57 describes the global behavior of  $v_{y,s}$  for a given  $y \in \Gamma_{(2k-3)}$ .

LEMMA 5.55. *Assume that  $\Omega$  is simply connected. Let  $U := U(\lambda_k)$  with  $k \geq 3$ . Assume that  $\dim U = (2k - 2)$ . Given  $(y, s) \in \Gamma_{(2k-3)} \times \Gamma$ , with  $y \neq s$ , recall that*

$$V_{y,s} := \{u \in U \mid \rho(u, y) \geq 2k - 4 \text{ and } \rho(u, s) \geq 1\}.$$

Let  $v_{y,s}$  be a generator of  $V_{y,s}$ . The function  $v_{y,s}$  has the following properties.

- (i) When  $s = z(y)$ , the function  $\check{v}_{y,z(y)} = \check{u}_y$  vanishes on  $\Gamma$  precisely at the points  $y$  and  $z(y)$ , and changes sign at these points. When  $s \neq z(y)$  and  $\mathcal{S}_b(v_{y,s}) = \{y, s, s'\}$  with  $s \neq s'$ ,  $\rho(v_{y,s}, s) = \rho(v_{y,s}, s') = 1$ , the function  $\check{v}_{y,s}$  vanishes on  $\Gamma$  precisely at the points  $y, s$  and  $s'$ , does not change sign at  $y$ , and changes sign at  $s$  and  $s'$ . When  $s \neq z(y)$  and  $\mathcal{S}_b(v_{y,s}) = \{y, s\}$  with  $\rho(v_{y,s}, s) = 2$ , the function  $\check{v}_{y,s}$  vanishes on  $\Gamma$  precisely at the points  $y$  and  $s$ , and does not change sign.
- (ii) For fixed  $y \in \Gamma_{(2k-3)}$ , and  $s$  close enough to  $z(y)$ ,  $\mathcal{S}_b(v_{y,s}) = \{y, s, s'\}$ , with  $s' \neq s, y$ , and  $\rho(v_{y,s}, s) = 1$ ,  $\rho(v_{y,s}, s') = 1$ . Furthermore, when  $s$  tends to  $z(y)$ ,  $[v_{y,s}]$  tends to  $[u_y]$ , and  $s'$  tends to  $y$ .
- (iii) For fixed  $y \in \Gamma_{(2k-3)}$ , and  $s$  close enough to  $y$ ,  $\mathcal{S}_b(v_{y,s}) = \{y, s, s'\}$ , with  $s' \neq s, y$ , and  $\rho(v_{y,s}, s) = 1$ ,  $\rho(v_{y,s}, s') = 1$ . Furthermore, when  $s$  tends to  $y$ ,  $[v_{y,s}]$  tends to  $[u_y]$ , and  $s'$  tends to  $z(y)$ .
- (iv) For fixed  $s \in \Gamma_{(2k-3)}$ , and  $y \in \Gamma_{(2k-3)}$  close enough to  $s$ ,  $\mathcal{S}_b(v_{y,s}) = \{y, s, s'\}$ , with  $s' \neq y, s$ , and  $\rho(v_{y,s}, s) = 1$ ,  $\rho(v_{y,s}, s') = 1$ . Furthermore, when  $y$  tends to  $s$ ,  $[v_{y,s}]$  tends to  $[u_s]$ , and  $s'$  tends to  $z(s)$ .

*Proof.*

◇ *Proof of Assertion (i).* Use Lemma 2.19, and the description of the possible nodal patterns for  $V_{y,s}$  which follows from Lemma 5.52.

◇ *Proof of Assertion (ii).* Assume that the first statement is not true. Then, we can find a sequence  $\{s_n\}$  tending to  $z(y)$ , and a corresponding sequence  $\{u_n := v_{y,s_n}\} \subset \mathbb{S}(U)$  such that  $\rho(u_n, y) = (2k - 4)$ ,  $\rho(u_n, s_n) = 2$ , and  $u_n$  tends to some  $u \in \mathbb{S}(U)$ . Since the convergence is uniform in  $C^m$  for fixed  $m \geq 0$ , it follows that  $\rho(u, y) \geq (2k - 4)$  and  $\rho(u, z(y)) \geq 2$ , see Remark 2.11 (lower semi-continuity of  $\rho$ ), and hence  $u \in V_{y,z(y)}$ . By Lemma 5.52 (iii), we must have  $[u] = [u_y]$ , and we reach a contradiction since  $\rho(u_y, z(y)) = 1$ . This proves the first statement.

We now prove the second statement. Considering  $\{u_n\} \subset \mathbb{S}(U)$  such that  $\mathcal{S}_b(u_n) = \{y, s_n, s'_n\}$  with  $s_n \neq s'_n$  and  $s_n$  tends to  $z(y)$ , we may also assume that  $s'_n$  tends to some  $s'$ , and  $u_n$  tends to  $u$ . Then,  $\rho(u, y) \geq (2k - 4)$ , and  $\rho(u, z(y)) \geq 1$ ,  $\rho(u, s') \geq 1$ . Lemma 5.52 (iii) implies that  $[u] = [u_y]$ , and  $\check{u}(s') = 0$  so that  $s' \in \{y, z(y)\}$  (where  $\check{u}$  is defined by (2.12)). Assuming that  $s' = z(y)$ , we would have  $\rho(u, z(y)) = 2$ , leading to a contradiction. Indeed, in that case,  $s_n$  and  $s'_n$  would both tend to  $z(y)$ , and the derivative  $\partial_b \check{u}_n$  of the function  $\check{u}_n$  along the boundary would vanish at some  $t_n$  on the smallest arc between  $s_n$  and  $s'_n$ , with  $t_n$  tending to  $z(y)$ . Passing to the limit, we would have  $\partial_b \check{u}_y(z(y)) = 0$ , implying that  $\rho(u_y, z(y)) \geq 2$ . Assertion (ii) is proved.

◇ *Proof of Assertion (iii).* Assume that the first statement is false. Then, we can find a sequence  $\{s_n\}$  tending to  $y$ , and a corresponding sequence  $\{u_n := v_{y,s_n}\} \subset \mathbb{S}(U)$  such that  $\rho(u_n, y) = (2k - 4)$ ,  $\rho(u_n, s_n) = 2$ , and  $u_n$  tends to some  $u \in \mathbb{S}(U)$ . Then,  $\rho(u, y) \geq (2k - 4)$ . Applying the local structure theorem to  $u$ , and following the arguments in the proof of Lemma 5.16, Part (C), we may choose  $r_1 > 0$  such that the neighborhood  $D_+(r_1)$  of  $y$  satisfies Properties (B-a)–(B-d) in the proof of Lemma 5.16. We may also assume that the sequence  $\{s_n\}$  is contained in  $D_+(r_1)$ . The nodal set of  $u_n$  consists of either  $(k - 2)$  loops at  $y$  and a loop at  $s_n$ , or  $(k - 3)$  loops at  $y$  and two arcs from  $y$  to  $s_n$ , see Figure 5.69 (b-d). As in the proof of Lemma 5.16, Part (C), for  $r_0 < r_1$  small enough, each loop at  $y$  must cross  $C_+(r_0)$  at (at least) two distinct points; so does each loop at  $s_n$ , and each arc from  $y$  to  $s_n$ . We then conclude that  $\rho(u, y) \geq (2k - 2)$ . Euler's formula then implies that actually  $\rho(u, y) = (2k - 2)$ . This is not possible since  $y \in \Gamma_{(2k-3)}$ . This proves the first statement in Assertion (iii).

We now prove the second statement. If  $s_n$  tends to  $y$ , we have  $\mathcal{S}_b(u_n) = \{y, s_n, s'_n\}$ , with  $s_n \neq s'_n$ . The preceding argument also shows that no subsequence of  $s'_n$  can tend to  $y$ . We may then assume that  $s_n$  tends to  $y$  and  $s'_n$  tends to some  $s' \neq y$ , with  $u_n$  tending to some  $u$ . Then,  $\rho(u, y) \geq (2k - 4)$ , and the previous argument shows that  $\rho(u, y) \geq (2k - 3)$ , and  $\rho(u, s') \geq 1$ . Lemma 5.6 then shows that  $s' = z(y)$ , and that  $[u] = [u_y]$ . Assertion (iii) is proved.

◇ *Proof of Assertion (iv).* See Figure 5.70.

Assume that the first statement is false. Then, there exists a sequence  $\{y_n\} \subset \Gamma_{(2k-3)}$  which tends to  $s$ , with a corresponding sequence  $\{u_n := v_{y_n,s}\} \subset \mathbb{S}(U)$  tending to some  $u \in \mathbb{S}(U)$ , and such that  $\rho(v_{y_n,s}, s) = 2$ . The convergence of  $u_n$  to  $u$  being uniform in  $C^{2k}$ , we have  $\rho(u, s) \geq (2k - 4)$ . Lemma 2.20 and Lemma 5.52(ii) applied to  $u_n$  imply that  $\mathcal{Z}(u) \cup \Gamma$  is connected. Applying Euler's formula to  $u$ , we conclude

that  $(2k - 4) \leq \sum_{z \in \mathcal{S}_b(u)} \rho(u, z) \leq (2k - 2)$ . Since the functions  $\check{u}_n$  do not change sign on  $\Gamma$ ,  $\check{u}$  does not change sign either, so that  $\rho(u, s) \neq (2k - 3)$ . Applying the local structure theorem to  $u$  at  $s$ , and using the same proof as in Lemma 5.16, Part (C), (with the disc  $D_+(s, r_0)$  and circle  $C_+(s, r_0)$  centered at  $s$ ), we infer that  $\rho(u, s) = (2k - 2)$ . Indeed, the nodal sets  $\mathcal{Z}(u_n)$  consist either is  $(k - 2)$  loops at  $y_n$  (including a special loop touching  $s$ ), or  $(k - 3)$  loops at  $y_n$  and a loop at  $s$ . Since  $y_n$  tends to  $s$ , for  $r_0$  small enough, these loops must intersect  $C_+(s; r_0)$  at  $(2k - 2)$  distinct points, and we can conclude as in the proof of Lemma 5.16.

To prove the second statement, we can now choose a sequence  $\{y_n\}$  such that  $\rho(u_n, s) = 1$  for  $n$  large enough, so that  $\mathcal{S}_b(u_n) = \{y_n, s, s'_n\}$ , with  $s'_n \neq s$ . An argument similar to the previous one, shows that no subsequence of  $\{s'_n\}$  can tend to  $s$ . Since  $s \in \Gamma_{(2k-3)}$ , the only remaining possibility is that  $\rho(u, s) = (2k - 3)$ , and hence that  $u \in U_s$ . Assertion (iv) is proved.

The proof of Lemma 5.55 is complete.  $\square$

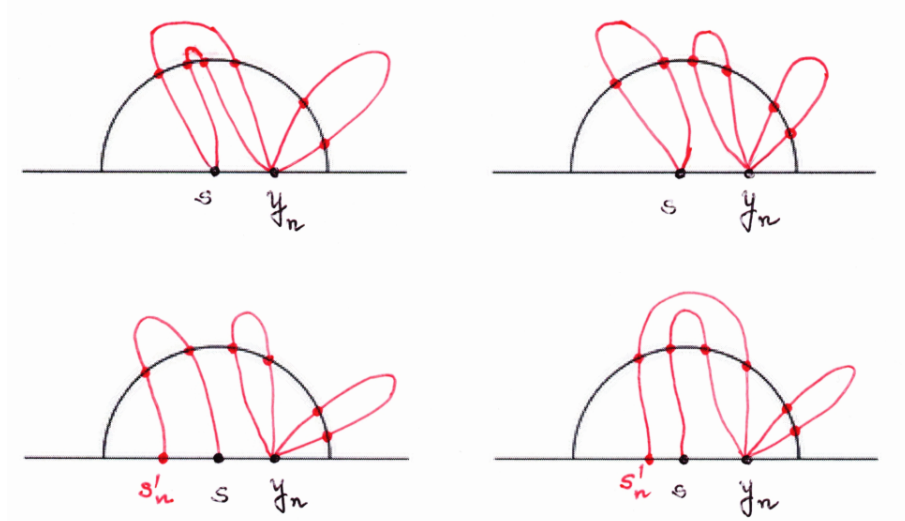


FIGURE 5.70. Proof of Lemma 5.55(iv)

We can enhanced the previous lemma by the following properties.

**PROPERTIES 5.56.** Assume that  $\Omega$  is simply connected, and that  $\dim U = (2k - 2)$ . Given  $(y, s) \in \Gamma_{(2k-3)} \times \Gamma$  with  $y \neq s$ , there exists  $\varepsilon_0$  such that

- (i) for all  $s \in \mathcal{A}(z(y); \varepsilon_0) \cup \mathcal{A}(y; \varepsilon_0) \setminus \{y, z(y)\}$ ,  $\rho(v_{y,s}, s) = 1$ ;
- (ii) for all  $\varepsilon < \varepsilon_0$ , there exists  $\eta > 0$  such that for all  $s \in \mathcal{A}(z(y); \eta) \setminus \{z(y)\}$ ,  $\mathcal{S}_b(v_{y,s}) = \{y, s, s'\}$  with  $s' \in \mathcal{A}(y; \varepsilon) \setminus \{y\}$ ;
- (iii) for all  $\varepsilon < \varepsilon_0$ , there exists  $\eta > 0$  such that for all  $s \in \mathcal{A}(y; \eta) \setminus \{y\}$ ,  $\mathcal{S}_b(v_{y,s}) = \{y, s, s'\}$  with  $s' \in \mathcal{A}(z(y); \varepsilon) \setminus \{z(y)\}$ .

Let  $s_1 \notin \{y, z(y)\}$ . Assume that the function  $v_{y,s_1}$  satisfies  $\rho(v_{y,s_1}, s_1) = 1$ , i.e.,  $\mathcal{S}_b(v_{y,s_1}) = \{y, s_1, s'_1\}$ , with  $s'_1 \neq s_1$ . Then,

- (a) there exists  $\varepsilon_1 > 0$ , such that for all  $s \in \mathcal{A}(s_1; \varepsilon)$ ,  $\rho(v_{y,s}, s) = 1$ ;
- (b) for all  $\varepsilon > 0$ , there exists  $\eta < \varepsilon_1$  such that for all  $s \in \mathcal{A}(s_1; \eta)$ ,  $s' \in \mathcal{A}(s'_1; \varepsilon)$ , i.e., the map  $s \mapsto s'$  is continuous.

LEMMA 5.57. Assume that  $\Omega$  is simply connected, and that  $\dim U = (2k - 2)$ . Let  $y \in \Gamma_{(2k-3)}$ . Then, the following properties hold.

- (i) For any  $s \in \mathcal{A}(y, z(y))$ , the function  $v_{y,s}$  satisfies  $\mathcal{S}_b(v_{y,s}) = \{y, s, s'\}$  with  $s' \in \mathcal{A}(y, z(y))$ , possibly with  $s = s'$ .
- (ii) There exists a unique  $s_1 \in \mathcal{A}(y, z(y))$  such that  $v_{y,s_1}$  satisfies  $\rho(v_{y,s_1}, s_1) = 2$ .
- (iii) For all  $s \in \mathcal{A}(s_1, z(y))$ ,  $\mathcal{S}_b(v_{y,s}) = \{y, s, s'\}$  with  $s' \in \mathcal{A}(y, s_1)$ . Furthermore when  $s$  moves counter-clockwise in  $\mathcal{A}(s_1, z(y))$ ,  $s'$  moves clockwise in  $\mathcal{A}(y, s_1)$ .
- (iv) For all  $s \in \mathcal{A}(y, s_1)$ ,  $\mathcal{S}_b(v_{y,s}) = \{y, s, s'\}$  with  $s' \in \mathcal{A}(s_1, z(y))$ . Furthermore when  $s$  moves counter-clockwise in  $\mathcal{A}(y, s_1)$ ,  $s'$  moves clockwise in  $\mathcal{A}(s_1, z(y))$ .

Similar statements hold for the arc  $\mathcal{A}(z(y), y)$ .

The statements in Lemma 5.57 are illustrated in Figure 5.71 (for the arc  $\mathcal{A}(y, z(y))$ ). The corresponding nodal patterns appear in Figure 5.76.

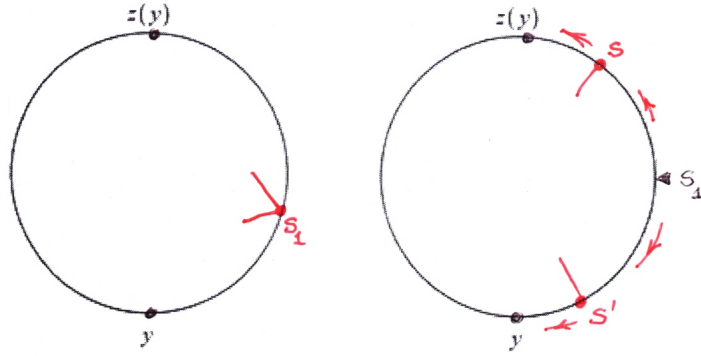


FIGURE 5.71. Lemma 5.57: Assertions (ii) and (iii)

*Proof of Lemma 5.57.* Choose a generator  $u_y$  of  $U_y$  such that  $\check{u}_y$  is positive in  $\mathcal{A}(y, z(y))$ , and negative in  $\mathcal{A}(z(y), y)$ .

*Assertion (i).* Assume that the assertion is false: there exists some  $s_0 \in \mathcal{A}(y, z(y))$  such that  $v_0 := v_{y,s_0}$  satisfies  $\mathcal{S}_b(v_0) = \{y, s_0, s'_0\}$ , with  $s'_0 \in \mathcal{A}(z(y), y)$ . Since  $s_0 \neq s'_0$ , Lemma 5.55 (i) implies that  $\check{v}_0$  vanishes on  $\Gamma$  only at the points  $y$ ,  $s_0$  and  $s'_0$ , does not change sign at  $y$ , and changes sign at  $s_0$  and  $s'_0$ . Choose  $v_0$  such that  $\check{v}_0 < 0$  in  $\mathcal{A}(s_0, s'_0)$ . For  $s \neq y, z(y)$ , introduce the function

$$\xi_s = a_0(s)u_y - b_0(s)v_0,$$

where

$$\begin{cases} a_0(s) = \check{v}_0(s) (\check{v}_0^2(s) + \check{u}_y^2(s))^{-\frac{1}{2}}, \\ b_0(s) = \check{u}_y(s) (\check{v}_0^2(s) + \check{u}_y^2(s))^{-\frac{1}{2}}. \end{cases}$$

Since  $b_0(s) \neq 0$ ,  $\rho(\xi_s, y) = 2k - 4$  and  $\rho(\xi_s, s) \geq 1$ , so that  $\xi_s \in V_{y,s}$ .

Choose  $s \in \mathcal{A}(s_0, z(y))$ . Since  $\check{v}_0$  only changes sign at  $s_0$  and  $s'_0$ ,  $\check{\xi}_s(s'_0) > 0$ . By Lemma 2.19, at  $y$  along  $\Gamma$ ,  $\check{u}_y$  vanishes at order  $(2k - 3)$ , while  $\check{v}_0$  vanishes at order  $(2k - 4)$ . In a pointed neighborhood  $\mathcal{J} \setminus \{y\}$  of  $y$  in  $\Gamma$ , we have that  $\check{\xi}_s \sim -b_0(s)\check{v}_0 < 0$ , and hence  $\check{\xi}_s$  vanishes at some  $s' \in \mathcal{A}(s'_0, y)$ . It follows that  $\xi_s \in V_{y,s}$  with  $\mathcal{S}_b(\xi_s) = \{y, s, s'\}$ ,  $\rho(\xi_s, s) = 1$ ,  $\rho(\xi_s, s') = 1$ .

Similarly, choosing  $t \in \mathcal{A}(y, s_0)$ , we have  $\check{\xi}_t(s'_0) < 0$  and  $\check{\xi}_t(z(y)) > 0$ , and  $\check{\xi}_t$  vanishes at some  $t' \in \mathcal{A}(z(y), s'_0)$ .

Finally, we conclude as above that  $\xi_t \in V_{y,t}$  with

$$\mathcal{S}_b(\xi_t) = \{y, t, t'\}, \rho(\xi_t, t) = 1, \rho(\xi_t, t') = 1.$$

These arguments can be visualized on Figure 5.72.

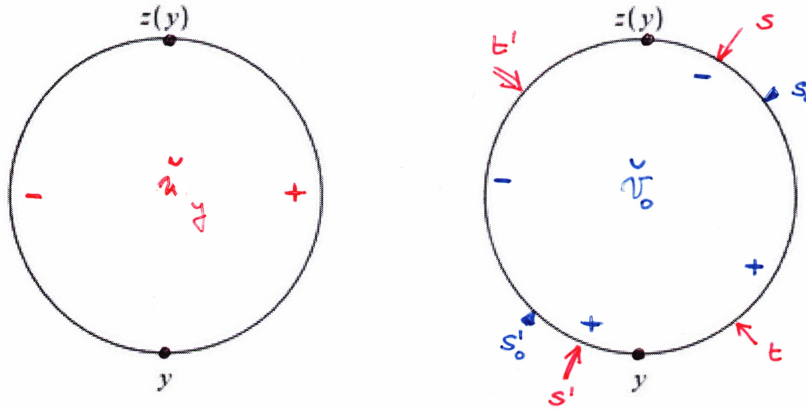


FIGURE 5.72. Proof of Lemma 5.57(i)

From the assumed existence of  $s_0$ , we conclude that, for all  $s \in \mathcal{A}(y, z(y))$ ,  $\xi_s \in V_{y,s}$  and  $\mathcal{S}_b(\xi_s) = \{y, s, s'\}$ , with  $s' \in \mathcal{A}(z(y), y)$ ,  $\rho(\xi_s, s) = 1$ ,  $\rho(\xi_s, s') = 1$ . Because  $s \in \mathcal{A}(s_0, z(y))$  implies that  $s' \in \mathcal{A}(s'_0, y)$ , with a parallel statement for  $t$ , the previous argument also shows that when the point  $s$  moves counter-clockwise in  $\mathcal{A}(y, z(y))$ , the point  $s'$  moves counter-clockwise in  $\mathcal{A}(z(y), y)$ . According to Lemma 5.55, Assertions (ii) and (iii),  $\xi_s$  tends to  $u_y$  when  $s$  tends to  $y$  or to  $z(y)$  in  $\mathcal{A}(y, z(y))$ . Looking at the behavior of the nodal sets, we reach a contradiction as Figure 5.73 shows. Assertion (i) is proved. ✓

REMARK 5.58. The previous arguments implicitly use the fact that the combinatorial type of  $v_{y,s}$  does not change when  $y$  is fixed and  $s$  varies in  $\Gamma \setminus \{y\}$  (the proof is similar to the proof of Lemma 5.24 (i)), see Subsection 5.6.3. Note also that the reasoning in Figure 5.73 is actually quite general, and only depends on the position of the arc from  $y$  to  $z(y)$  with respect to the loops.

*Proof of Assertion (ii).*

Let  $\gamma_1 : [0, \ell_1] \rightarrow \Gamma$  be an arc-length parametrization of  $\Gamma$ , such that  $\gamma_1(t)$  moves counter-clockwise, and  $\gamma_1(0) = \gamma_1(\ell_1) = y$ ,  $\gamma_1(\ell) = z(y)$ .

According to Lemma 5.55 (i), and to the above Assertion (i), taking  $s \in \mathcal{A}(y, z(y))$  close to  $y$ , we have  $\mathcal{S}_b(v_{y,s}) = \{y, s, s'\}$  with  $s' \in \mathcal{A}(y, z(y))$  close to  $z(y)$ . If  $s = \gamma_1(t)$  and  $s' = \gamma_1(t')$ , for  $t$  positive small enough, we have  $t < t'$ . Choose any such point  $s_0 = \gamma_1(t_0)$  such that  $v_0 = v_{y,s_0}$  satisfies  $\mathcal{S}_b(v_0) = \{y, s_0, s'_0\}$ , with  $s'_0 = \gamma_1(t'_0)$  and  $t_0 < t'_0$ . By Lemma 5.55 (i), the function  $\check{v}_0$  vanishes precisely at the points  $s_0$  and  $s'_0$  and changes sign at these points. We choose it so that it is positive on  $\mathcal{A}(s_0, s'_0)$ . Define  $\xi_s$  as in the proof of Assertion (i) (now with  $s'_0 \in \mathcal{A}(y, z(y))$ ). Take  $s \in \mathcal{A}(y, s_0)$ ,  $s = \gamma_1(t)$  with  $0 < t < t_0$ . With our previous choice of signs for  $\check{v}_y$ , we



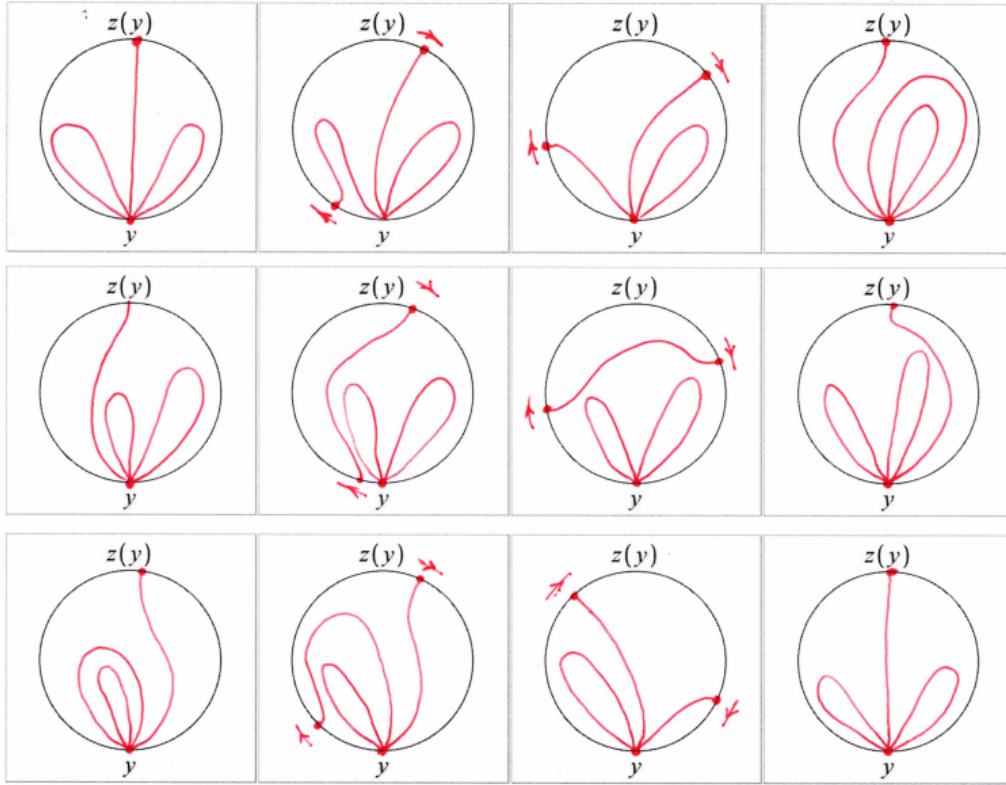


FIGURE 5.73. Proof of Lemma 5.57(i)

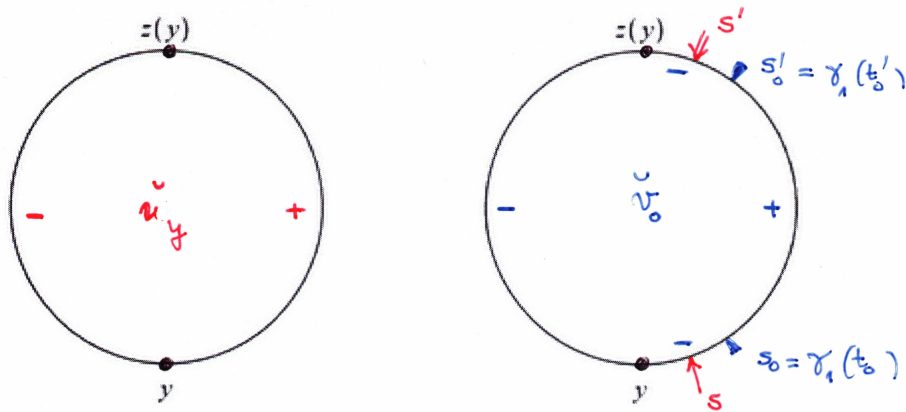


FIGURE 5.74. Proof of Lemma 5.57(ii)

find that  $\check{\xi}_s(z(y)) > 0$  and  $\check{\xi}_s(s'_0) < 0$ , so that  $\check{\xi}_s$  vanishes at some  $s'$  in  $\mathcal{A}(s'_0, z(y))$ . Since  $\xi_s \in V_{y,s}$ , we have  $\mathcal{S}_b(\xi_s) = \{y, s, s'\}$ , with  $s \in \mathcal{A}(y, s_0)$ ,  $s' \in \mathcal{A}(s'_0, z(y))$ ,  $\rho(\xi_s, s) = \rho(\xi_s, s') = 1$ . Then,  $s' = \gamma_1(t')$  with  $0 < t < t_0 < t' < \ell$ , so that the map  $(0, t_0) \ni t \mapsto t'$  is decreasing.

Introduce the set

$$J := \{t \in (0, \ell) \mid \mathcal{S}_b(v_{y, \gamma_1(t)}) = \{y, \gamma_1(t), \gamma_1(t')\} \text{ with } t < t'\}.$$

If  $t \in J$ ,  $\rho(v_{y,\gamma_1(t)}, \gamma_1(t)) = \rho(v_{y,\gamma_1(t')}, \gamma_1(t')) = 1$ . We have  $(0, t_0) \subset J$  so that  $J \neq \emptyset$ , and hence  $s_1 := \sup J$  exists. Since  $\rho(v_{y,s}, s) = 1$  is an open condition,  $s_1 \notin J$ . Take a subsequence  $\{t_n\} \subset J$  tending to  $s_1$ , and choose corresponding functions  $v_{y,t_n} \in \mathbb{S}(U) \cap V_{y,t_n}$ . A subsequence converges to some function  $v_1$  in  $\mathbb{S}(U)$  which satisfies  $\rho(v_1, y) \geq (2k - 4)$  and  $\rho(v_1, s_1) \geq 1$ . By Lemma 5.52, this implies that  $v_1 \in V_{y,s_1}$  (use Remark 2.11). Since  $s_1 \notin J$ , we must have  $\rho(v_1, s_1) = 2$ , so that  $v_1$  is a generator  $v_{y,s_1}$  of  $V_{y,s_1}$ .

*Proof of Assertions (iii) and (iv).* Take  $v_1 = v_{y,s_1}$  given by Assertion (ii). By Lemma 5.55 (i), we may choose this function such that  $\check{v}_1 \geq 0$  and vanishes only at  $y$  and  $s_1$ . For  $s \neq y, z(y)$ , introduce the functions,

$$\xi_s = a_1(s)u_y - b_1(s)v_1,$$

where

$$\begin{cases} a_1(s) = \check{v}_1(s) (\check{v}_1^2(s) + \check{u}_y^2(s))^{-\frac{1}{2}}, \\ b_1(s) = \check{u}_y(s) (\check{v}_1^2(s) + \check{u}_y^2(s))^{-\frac{1}{2}}. \end{cases}$$

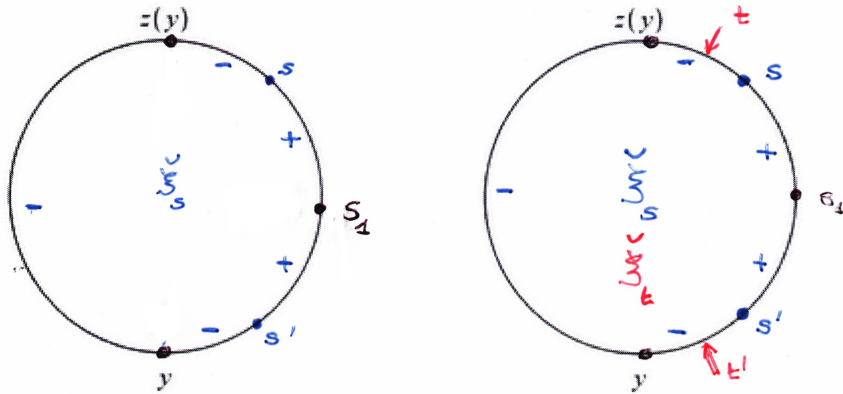


FIGURE 5.75. Proof of Lemma 5.57, Assertion (iii)

When  $s = s_1$ , we have  $\check{\xi}_{s_1} = -b_1(s_1)\check{v}_1 \leq 0$ , and  $\check{\xi}_{s_1}$  only vanishes at  $y$  and  $s_1$ ;  $\xi_{s_1} \in V_{y,s_1}$ . When  $s \in \mathcal{A}(y, z(y)) \setminus \{s_1\}$ , taking into account the properties of the functions involved, we find that

$$\begin{cases} \check{\xi}_s(z(y)) < 0, \\ \check{\xi}_s(s_1) > 0, \\ \check{\xi}_s < 0 \text{ in } J_y \setminus \{y\}, \end{cases}$$

where  $J_y$  is a small arc on  $\Gamma_1$  centered at  $y$ .

It follows that, for  $s \in \mathcal{A}(y, z(y)) \setminus \{s_1\}$ ,  $\xi_s \in V_{y,s}$ ,  $\mathcal{S}_b(\xi_s) = \{y, s, s'\}$ ,  $\rho(\xi_s, s) = \rho(\xi_s, s') = 1$ , with the point  $s$  on one side of  $s_1$  in  $\mathcal{A}(y, z(y))$ , and the point  $s'$  on the other side. For these points  $s, s'$ , we have  $V_{y,s} = V_{y,s'}$ , so that  $\xi_s$  and  $\xi_{s'}$  must be proportional (Lemma 5.52 (i)), and since the functions  $\check{\xi}_s$  and  $\check{\xi}_{s'}$  both take a positive value at  $s_1$ ,  $\xi_{s'} = a \xi_s$ , with  $a > 0$ .

We also have  $\check{\xi}_s(t)\check{\xi}_t(s) \leq 0$ , since

$$\check{\xi}_s(t)\check{\xi}_t(s) = - \left( \check{v}_1^2(s) + \check{w}_y^2(s) \right)^{-\frac{1}{2}} \left( \check{v}_1^2(t) + \check{w}_y^2(t) \right)^{-\frac{1}{2}} \left( \check{v}_1(s)\check{w}_y(t) - \check{w}_y(s)\check{v}_1(t) \right)^2 .$$

Choose  $s \in \mathcal{A}(s_1, z(y))$ , and  $t \in \mathcal{A}(s, z(y))$ . Then  $s', t' \in \mathcal{A}(y, s_1)$ . The functions  $\check{\xi}_s$  and  $\check{\xi}_t$  are positive at  $s_1$ , and hence positive respectively on the arcs  $\mathcal{A}(s', s)$  and  $\mathcal{A}(t', t)$ . We have  $\check{\xi}_s(t) < 0$ , and hence, using the above properties,  $\check{\xi}_{s'}(t) > 0$ , and  $\check{\xi}_t(s') < 0$ . This implies that  $t' \in \mathcal{A}(y, s')$ . We have proved that when  $s$  moves counter-clockwise in  $\mathcal{A}(s_1, z(y))$ ,  $s'$  move clockwise in  $\mathcal{A}(y, s_1)$ . This is coherent with Lemma 5.55(ii). The proof of Assertion (iv) is similar.  $\square$

REMARKS 5.59. (i) Lemma 5.57 corresponds to the first part of the proof of Lemma 3.5 in [HoMN1999] (from p.1181, line (-7), “We consider the function” to p.1182, line (+5), “the following nodal domain”).

(ii) Figure 5.76 displays the possible nodal patterns of  $u_y$ , and the corresponding nodal patterns for the function  $v_{y,s_1}$  with  $s_1 \in \mathcal{A}(y, z(y))$  (see Lemma 5.57 (ii)), and for the function  $v_{y,s}$  with  $s \in \mathcal{A}(s_1, z(y))$  (see Lemma 5.57 (iii)).

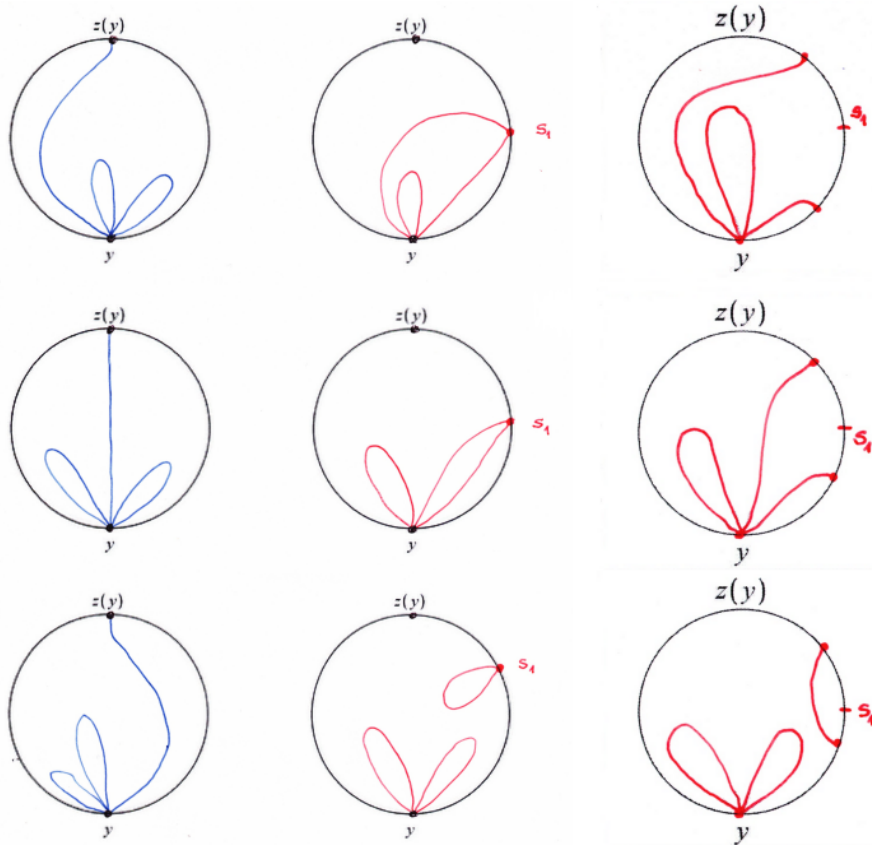


FIGURE 5.76. Lemma 5.57 (ii) and (iii): examples of nodal patterns for  $u_y$  and  $v_{y,s_1}$

### 5.7. Conclusion

The lemmas in Sections 5.2, 5.3, and 5.4 explain, expand or provide proofs for the lemmas and certain statements from [HoMN1999], Section 3. Although we

have mainly followed the ideas sketched in [HoMN1999], the way we organize the lemmas and some of our proofs are different. Correspondences are given in the table below.

In [HoMN1999, Lemma 3.5], the authors have implicitly assumed, without proof, that the set  $\Gamma_{(2k-2)}$  contains at least two elements. We take care of this issue in Lemmas 5.24 and 5.31. In their Lemma 3.6, they mention, without proof, that if  $y$  moves clockwise then  $z(y)$  moves counter-clockwise. We prove this assertion in Lemma 5.12.

In the final steps of their proof, [HoMN1999, p. 1185, line (-5)], the authors claim that the star at  $x$  rotates by some positive quantity when passing on  $\gamma_s$  over the point  $\eta \in \Gamma_{(2k-2)}$ . Our interpretation is rather that the star rotates when  $x$  moves on  $\gamma_s$ , from above a point  $\eta_1 \in \Gamma_{(2k-2)}$  to above the next point  $\eta_2 \in \Gamma_{(2k-2)}$  (see Subsection 5.4.2).

[HoMN1999], Section 3.9	This Chapter 5
Lemma p. 1178	Lemmas 5.6 and 5.10
Lemma 3.3	Lemmas 5.6, 5.10 and 5.24
Lemma 3.4	Lemma 5.8 and Section 5.6
Lemma 3.5	Lemmas 5.12 and 5.24
$\Gamma_{(2k-2)} \neq \emptyset$ (overlooked in Lemma 3.5)	Lemma 5.31
$\#(\Gamma_{(2k-2)}) \neq 1$ actually positive and even (overlooked in Lemma 3.5)	Lemma 5.24 Lemma 5.24
Lemma 3.6	Lemma 5.12 and 5.24
Lemma 3.7	Lemma 5.4
Lemma 3.8	Lemma 5.16
Section 3.9 p. 1184 ff	Subsections 5.3 and 5.4

TABLE 5.1. Correspondences between statements

### 5.8. Simpler proof of Lemma 5.16

In this section, we provide simpler statements and a simpler proof of Lemma 5.16.

Simpler statements:

- (i) If  $x \in \Omega$  tends to  $y \in \Gamma$ , then  $[w_x]$  tends to  $[u_y]$  in  $\mathbb{P}(U)$ .
- (ii)  $y \in \Gamma_{(2k-3)}$  if and only if there exists  $z \neq y$  in  $\Gamma$  such that for all  $\beta$  small enough, and all  $x$  close enough to  $y$ ,  $\mathcal{S}_b(w_x) \cap \mathcal{A}(y; \beta) = \{y(x)\}$  and  $\mathcal{S}_b(w_x) \cap \mathcal{A}(z; \beta) = \{z(x)\}$ .
- (iii)  $y \in \Gamma_{(2k-2)}$  if and only if for all  $\beta$  small enough, and all  $x$  close enough to  $y$ ,  $\mathcal{S}_b(w_x) \subset \mathcal{A}(y; \beta)$ .

*Proof.* Let  $\{x_n\} \subset \Omega$  be a sequence tending to  $y \in \Gamma$ . We work locally in a neighborhood of  $y$ , and actually in  $\mathbb{H}$  via a conformal map.

Let  $w_n := w_{x_n} = \sum_{j=1}^{2k-2} a_{n,j} \phi_j \in \mathbb{S}(U) \cap W_{x_n}$ . Without loss of generality, we may assume that this sequence converges to some  $w \in \mathbb{S}(U)$ ,  $C^m$ -uniformly for any given  $m \geq 1$ . Since  $\text{ord}(w_n, x_n) = (k-1)$  for all  $n$ ,  $\text{ord}(w, y) \geq (k-1) \geq 2$ , so that  $y$  is a singular point of  $w$ . Define  $q := \rho(w, y) \geq 1$ . Apply the local structure theorem

to  $w$  at the point  $y$ : for some  $r$  smaller than the energy radius (Lemma 5.17), the nodal set  $\mathcal{Z}(w)$  intersects the semi-circle  $C_+(y, r)$  at  $q$  points  $A_{y,j}^w(r)$ ,  $1 \leq j \leq q$ . The proof of the local structure theorem implies that for  $n$  large enough the function  $w_n$  vanishes precisely once in the “green arcs”  $\mathcal{G}_{y,j}^w(r) = \mathcal{A}(A_{y,j}^w(r), \alpha) \subset C_+(y, r)$ , and does not vanish elsewhere on  $C_+(y, r)$ . This implies that  $\#(\mathcal{Z}(w_n) \cap C_+(y, r)) = q$ .

According to Lemma 5.4, there are three possibilities

- (A)  $\mathcal{S}_b(w_n) = \emptyset$ .
- (B)  $\mathcal{S}_b(w_n) = \{z_{n,1}, z_{n,2}\}$  with  $z_{n,1} \neq z_{n,2}$  and  $\rho(w_n, z_{n,i}) = 1$ .
- (C)  $\mathcal{S}_b(w_n) = \{z_n\}$  with  $\rho(w_n, z_n) = 2$ .

In the three cases,  $\mathcal{Z}(w_n)$  contains at least  $(k-2)$  pairwise distinct loops at  $x$  which do not intersect away from  $x$ . When  $n$  is large enough, for energy reasons, each loop in  $\mathcal{Z}(w_n)$  intersects  $C_+(y, r)$  at at least two distinct points and hence  $q = \#(\mathcal{Z}(w_n) \cap C_+(y, r)) \geq (2k-4)$ .

If there exists an infinite sub-sequence  $\{w_{s(n)}\}$  satisfying (A), each  $\mathcal{Z}(w_{s(n)})$  contains  $(k-1)$  loops and hence  $q \geq (2k-2)$  and we must have  $w \in U_y$  and  $q = (2k-2)$ .

Otherwise, for  $n$  large enough,  $\mathcal{S}_b(w_n) \neq \emptyset$  and there are two nodal intervals in  $\mathcal{Z}(w_n)$  from  $x_n$  to the boundary. For energy reasons these intervals cannot both be contained in  $D_+(y, r)$  and at least one of them must exit  $D_+(y, r)$  so that  $q \geq (2k-4) + 1 = (2k-3)$ . This inequality implies that  $w \in U_y$  and that  $q \in \{2k-3, 2k-4\}$ .

In summary, at this point, we have proved that when  $x_n$  tends to  $y$ , any limit point  $w$  of the sequence  $\{w_n\}$  belong to  $U_y$  and since  $\dim U_y = 1$ , we conclude that  $[W_n]$  tends to  $[U_y]$ .

We can now make a more precise analysis, looking at whether  $y \in \Gamma_{(2k-3)}$  or  $y \in \Gamma_{(2k-2)}$ .

Assume that  $y \in \Gamma_{(2k-3)}$ . In that case, a limit point  $w$  of  $\{w_n\}$  belong to  $U_y$  and satisfies  $\mathcal{S}(w) = \{y, z\}$  for some  $z \neq y$ , with  $\rho(w, y) = (2k-3)$  and  $\rho(w, z) = 1$ . Since  $w_n$  tends to  $w$   $C^1$ -uniformly,  $\check{w}_n$  tends to  $\check{w}$ . Since  $\check{w}$  changes sign at  $y$  and  $z$ ,  $\check{w}_n$  must change sign near  $y$  and near  $z$ , so that  $\mathcal{S}_b(w_n)$  contains precisely two points and belongs to Case (B). Fixing some  $\beta > 0$  small enough we may choose  $z_{n,1} \in \mathcal{A}(y; \varepsilon)$  and  $z_{n,2} \in \mathcal{A}(z, \beta)$ .

Assume that  $y \in \Gamma_{(2k-2)}$ . In that case,  $\mathcal{S}_b(w) = \{y\}$ . Assume that there exists an infinite sequence such that  $\mathcal{S}_b(w_n) = \{z_{n,1}, z_{n,2}\}$ , possibly with  $z_{n,1} = z_{n,2}$ . We may assume that  $z_{n,1}$  tends to  $z_1$  and  $z_{n,2}$  tends to  $z_2$ . Since  $\check{w}_n$  tends uniformly to  $\check{w}$ , we have  $\check{w}(z_1) = \check{w}(z_2) = 0$  and since  $\check{w}$  only vanishes at  $y$ , we conclude that  $z_1 = z_2$ .

In summary, if  $x_n$  tends to  $y \in \Gamma_{(2k-2)}$ , and if  $w$  is a limit point of  $\{w_n\}$  then for all  $\beta$ , there exists  $N_\beta$  such that  $\mathcal{S}_n(w_n) \subset \mathcal{A}(y; \beta)$ , including the case  $\mathcal{S}_b(w_n) = \emptyset$ .



## CHAPTER 6

### Further Results

#### 6.1. Upper Bounds on the Multiplicities and the Nodal Line Conjecture

When  $k = 2$ , Proposition 4.3 gives  $\text{mult}(\lambda_2) \leq 3$ . A natural question, in view of Table 1.1 in Section 1.2, is whether this bound is sharp (depending on the boundary condition). As we shall see, this question is related to the so-called “nodal line conjecture”.

**6.1.1. Nodal sets of second eigenfunctions.** We use the notation of Subsection 4.1.2, and write the boundary of the domain  $\Omega$  as  $\Gamma = \bigcup_{j=1}^q \Gamma_j$ , with  $q \geq 1$ . Let  $u \in U(\lambda_2)$  be any second eigenfunction. By Courant’s Theorem 2.4,  $u$  has exactly two nodal domains. Euler’s formula (4.8) yields

$$(6.1) \quad \begin{cases} 0 = \kappa(u) - 2 = [b_0(\mathcal{Z}(u) \cup \Gamma(u)) - 1] + \frac{1}{2} \sum_{z \in \mathcal{S}_i(u)} (\nu(u, z) - 2) \\ \quad \quad \quad + \sum_{j \in J(u)} \frac{1}{2} \left( \sum_{z \in \mathcal{S}_b(u) \cap \Gamma_j} \rho(u, z) - 2 \right). \end{cases}$$

Since all the terms on the right hand side are nonnegative (use Corollary 2.13 and the definition of  $J(u)$ ), we immediately deduce that

$$(6.2) \quad \begin{cases} \mathcal{Z}(u) \cup \Gamma(u) \text{ is connected,} \\ \sum_{z \in \mathcal{S}_i(u)} (\nu(u, z) - 2) = 0 \text{ i.e., } \mathcal{S}_i(u) = \emptyset, \\ \sum_{z \in \mathcal{S}_b(u) \cap \Gamma_j} \rho(u, z) = 2 \quad \forall j \in J(u). \end{cases}$$

The structure of  $\mathcal{Z}(u)$  depends on whether  $J(u) = \emptyset$  or  $J(u) \neq \emptyset$ . We now consider the two simplest situations. The proofs of the following properties are clear.

**PROPERTY 6.1.** *Assume that  $\Omega$  is simply connected. Let  $u$  be a second eigenfunction. Then, either  $\mathcal{Z}(u)$  does not hit  $\Gamma$  and  $\mathcal{S}(u) = \emptyset$ , or  $\mathcal{Z}(u)$  hits  $\Gamma$ ,  $\mathcal{S}_i(u) = \emptyset$ , and  $\sum_{z \in \mathcal{S}_b(u)} \rho(u, z) = 2$ . More precisely, there are three distinct possibilities.*

- (a) *If  $J(u) = \emptyset$ , then  $\mathcal{Z}(u)$  is a nodal circle, i.e., a simple closed regular connected curve contained in  $\Omega$ , not touching  $\Gamma$ . This case is characterized by the fact that the function  $\check{u}$  defined in (2.12) does not vanish on  $\Gamma$ .*
- (b) *If  $J(u) = \{1\}$  and  $\mathcal{S}_b(u) = \{y\}$  for some  $y \in \Gamma$  with  $\rho(u, y) = 2$ , then  $\mathcal{Z}(u)$  is a nodal loop at  $y$ , i.e.,  $\mathcal{Z}(u) \setminus \{y\}$  a simple regular connected curve contained in  $\Omega$ . This case is characterized by the fact that the function  $\check{u}$  vanishes only at  $y_1$  on  $\Gamma$ , and does not change sign.*
- (c) *If  $J(u) = \{1\}$  and  $\mathcal{S}_b(u) = \{y_1, y_2\}$  for some  $y_1 \neq y_2 \in \Gamma$  with  $\rho(u, y_1) = 1$ ,  $\rho(u, y_2) = 1$ , then  $\mathcal{Z}(u)$  is a nodal arc from  $y_1$  to  $y_2$ , i.e.,  $\mathcal{Z}(u) \setminus \{y_1, y_2\}$  is a simple regular connected arc contained in  $\Omega$ . This case is characterized by the fact that the function  $\check{u}$  vanishes precisely at  $y_1$  and  $y_2$  on  $\Gamma$ , and changes sign at these points.*

**PROPERTY 6.2.** *Assume that  $\Omega$  has one hole, and write  $\Gamma = \Gamma_1 \cup \Gamma_2$ . Let  $u$  be a second eigenfunction. Then, either  $\mathcal{Z}(u)$  does not hit  $\Gamma$  and  $\mathcal{S}(u) = \emptyset$ , or  $\mathcal{Z}(u)$  hits*

$\Gamma$ ,  $\mathcal{S}_i(u) = \emptyset$ , and  $\sum_{z \in \mathcal{S}_b(u) \cap \Gamma_j} \rho(u, z) = 2$  for all  $j \in J(u)$ . More precisely, there are three distinct cases (up to relabeling the two components of  $\Gamma$ ).

- (1) If  $J(u) = \emptyset$ , then  $\mathcal{Z}(u)$  is a nodal circle contained in  $\Omega$ , not touching  $\Gamma$ . This case is characterized by the fact that the function  $\check{u}$  defined in (2.12) does not vanish on  $\Gamma$ .
- (2) If  $J(u) = \{1\}$ , then either  $\mathcal{S}_b(u) = \{y\}$  for some  $y \in \Gamma_1$  with  $\rho(u, y_1) = 2$ , or  $\mathcal{S}_b(u) = \{y_1, y_2\}$  for some  $y_1 \neq y_2 \in \Gamma_1$  with  $\rho(u, y_1) = \rho(u, y_2) = 1$ . We have either a nodal loop at  $y$ , or a nodal arc from  $y_1$  to  $y_2$ . This case is characterized by the fact that the function  $\check{u}$  vanishes only at  $y$  (without changing sign along  $\Gamma_1$ ), or vanishes at  $y_1$  and  $y_2$  (and changes sign along  $\Gamma_1$ ). In both subcases,  $\check{u}$  does not vanish on  $\Gamma_2$ .
- (3) If  $J(u) = \{1, 2\}$ , then  $\mathcal{Z}(u)$  hits both component  $\Gamma_1$  and  $\Gamma_2$  at one point with index 2, or at two distinct points of index 1. Furthermore, the components  $\Gamma_1$  and  $\Gamma_2$  are linked by two nodal arcs (possibly with one or two common boundary points).

REMARK 6.3. It is not clear a priori whether the possible nodal patterns described in Property 6.1 or 6.2 are actually realized for some choice of domain  $\Omega$  and potential  $V$  (when  $\Omega$  is convex and  $V \equiv 0$ , see [Ales1994]). Applying Lemmas 2.15 or 2.16, one can at least prescribe one or two boundary singular points.

- (i) Assume that  $\dim U(\lambda_2(-\Delta + V)) \geq 3$ . If  $\Omega$  is simply connected, then there exists an eigenfunction whose nodal set satisfies (b), resp. (c), in Properties 6.1. If  $\Omega$  has one hole, then there exists an eigenfunction whose nodal set hits both  $\Gamma_1$  and  $\Gamma_2$ .
- (ii) Assume that  $\dim U(\lambda_2(-\Delta + V)) = 2$ . Then, there exists an eigenfunction whose nodal domain hits  $\Gamma$ .

Nodal sets and  $\text{mult}(\lambda_2)$  are known precisely in few circumstances only, either in very specific cases, or under additional assumptions on the domain (some convexity or symmetry conditions, see [Shen1988], [Putt1990], [Putt1991] in the simply connected case, and [Kiwa2018] for a convex domain with a convex sub-domain removed).

The following figures display some particular cases. The second (Dirichlet or Neumann) eigenvalue of an equilateral triangle with rounded corners has multiplicity two, with one symmetric and one antisymmetric eigenfunction.

The nodal domains of the symmetric eigenfunction appear in Figure 6.1 (left), see [BeHe2021t]. The second (Dirichlet or Neumann) eigenvalue of an ellipse is simple with nodal domains as in Figure 6.1 (center); this is a particular case of the domains described in [Shen1988], [Putt1990] and [Putt1991]. The nodal set of a second Dirichlet eigenvalue of  $D \setminus B$ , where  $D, B$  are convex symmetric domains, has been studied in [Kiwa2018], see Figure 6.1 (right).

Numerical computations, playing with the position of the holes, give rise to some other patterns, see Figure 6.2.

In view of the above remarks, the following questions are natural.

**Question 1:** Does there exist a second eigenfunction of  $-\Delta + V$  whose nodal set is a nodal circle ?

**Question 2:** Does there exist a second eigenfunction of  $-\Delta + V$  whose nodal set is a nodal loop at some  $y \in \Gamma$  ?



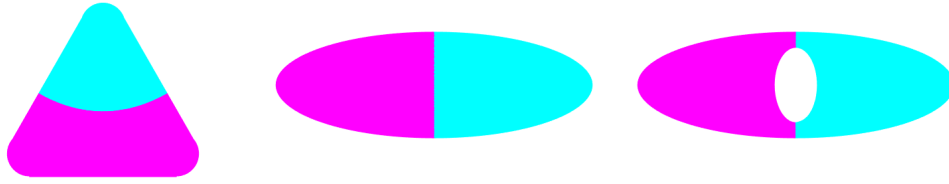


FIGURE 6.1. Nodal patterns of second eigenfunctions

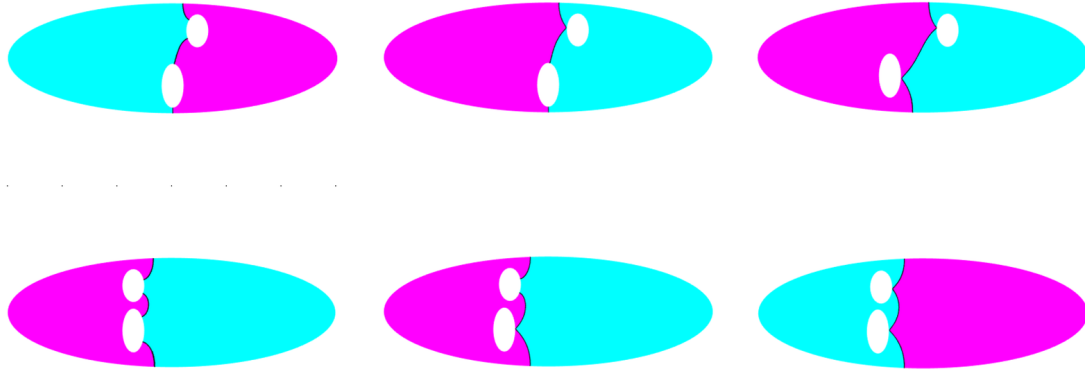


FIGURE 6.2. Nodal patterns of second eigenfunctions

**6.1.2. The nodal line conjecture.** For a simply connected domain  $\Omega$ , Pleijel [Plej1956, p. 546] observed that a second Neumann eigenfunction of  $-\Delta$  cannot have a closed nodal line. The idea is to use the inequality

$$\lambda_2(D, -\Delta, \mathbf{n}) \leq \lambda_1(D, -\Delta, \mathfrak{d})$$

between the second Neumann eigenvalue and the first Dirichlet eigenvalue of  $-\Delta$  in a domain  $D \subset \mathbb{R}^2$ , and the monotonicity property of the first Dirichlet eigenvalue. Indeed, if there exists a second Neumann eigenfunction  $u_2$  one of whose two nodal domains (say  $D_1$ ) has the property that  $\partial D_1 \cap \Gamma$  consists of isolated points (which occurs in particular when  $\partial D_1 \subset \Omega$ ), then the restriction of  $u_2$  to  $D_1$  is the ground state of the Dirichlet problem in  $D_1$ ,  $\lambda_1(D_1, \mathfrak{d}) = \lambda_2(\Omega, \mathbf{n})$ . By the strict domain monotonicity of the Dirichlet eigenvalues, we get

$$\lambda_1(\Omega, \mathfrak{d}) < \lambda_1(D_1, \mathfrak{d}) = \lambda_2(\Omega, \mathbf{n}),$$

hence a contradiction. This argument may fail when  $\Omega$  has a hole because both nodal domains of  $u$  may touch the boundary.

The inequality  $\lambda_2(D, -\Delta, \mathbf{n}) \leq \lambda_1(D, -\Delta, \mathfrak{d})$  is due to Szegö (1954) when  $\Omega \subset \mathbb{R}^2$  is simply connected and smooth. The strict inequality is proved in an earlier paper of Pólya (1952) which does apparently not use the assumption that the domain is simply connected. It was later generalized to higher dimensions, and smooth enough domains (not necessarily simply connected) by Weinberger (1956), see [Payn1967], Theorem 3, p. 463. It has been extended to domains with  $C^1$  boundary, see [Maz1991] in which Mazzeo revisits the earlier paper of L. Friedlander [Frie1991].

When  $\partial D_1$  meets  $\Gamma$  we actually need the inequality to hold for domains with piecewise  $C^1$  boundary (see [ArMa2007, ArMa2012] for the Lipschitz case).

In view of Pleijel's observation, Payne conjectured that a second Dirichlet eigenfunction of  $-\Delta$  cannot have a closed nodal line, see [Payn1967], Conjecture 5, p. 467. One can make a similar conjecture for second Robin eigenfunctions, and also consider domains in  $\mathbb{R}^n$ ,  $n \geq 3$ , see for example [Dama2000], [Four2001], [FrKr2008], [Jeri1991], [Ken2013] and their bibliographies.

REMARK 6.4. As observed in [Liq1995] (end of Section 2, p. 277), if a simply connected domain satisfies the *nodal line conjecture*, then  $\dim U(\lambda_2) \leq 2$ . This is an immediate consequence of Remark 6.3(ii).

In the next subsections, we consider the three boundary conditions, Dirichlet, Neumann and Robin separately.

**6.1.3. Dirichlet boundary condition.** The following results are due to Lin and Ni.

◇ [LiNi1988, Theorem 3.6]: For all  $n \geq 2$ , there exists a radius  $R_n$  and a nonzero smooth radial potential  $V_n$ , such that

$$\text{mult}(\lambda_2; B(R_n), -\Delta + V_n, \mathfrak{d}) = 1,$$

and the corresponding eigenfunction is radial, with nodal set a sphere in  $B(R_n)$ . Here,  $B(R_n)$  is the ball of radius  $R_n$  in  $\mathbb{R}^n$ .

◇ [LiNi1988, Theorem 3.8]: For all  $n \geq 2$ , there exists a radius  $R_n$  and a nonzero smooth radial potential  $V_n$ , such that

$$\text{mult}(\lambda_2; B(R_n), -\Delta + V_n, \mathfrak{d}) = (n + 1),$$

and there exists a radial second eigenfunction.

In dimension 2, the second assertion implies that the bound of the multiplicity  $\text{mult}(\lambda_2; \Omega, -\Delta + V, \mathfrak{d}) \leq 3$  is sharp.

The following results are due to M. and T. Hoffmann-Ostenhof and Nadirashvili [HoHN1997, HoHN1998] (see for the second statement [HeHJ2020] for corrections and complements).

◇ [HoHN1998, Theorem 2.1]: There exists  $N_0$  and domains  $D_{N,\varepsilon} \subset \mathbb{R}^2$  such that for all  $N \geq N_0$ , and  $\varepsilon$  small enough,  $\lambda_2(D_{N,\varepsilon}; -\Delta, \mathfrak{d})$  is simple, with a closed nodal set contained in  $D_{N,\varepsilon}$ . The domain  $D_{N,\varepsilon}$  is homeomorphic to a disk minus  $N$  points.

◇ [HoHN1998, Theorem 2.2]: For all  $N \geq 3$ , and  $\varepsilon$  small enough, the domains  $D_{N,\varepsilon} \subset \mathbb{R}^2$  satisfy

$$\text{mult}(\lambda_2; D_{N,\varepsilon}, -\Delta, \mathfrak{d}) = 3.$$

The second assertion implies that the upper bound 3 for the second Dirichlet eigenvalue of  $-\Delta$  is sharp for non simply connected domains.

We refer to [DaGH2021] for a counter-example to the nodal line conjecture for the Laplacian in a domain with six holes. However, counter-examples are still missing for domains with less holes.

The nodal line conjecture for  $(\Omega, -\Delta)$  is known to be true when  $\Omega$  is a bounded *convex domain* in  $\mathbb{R}^2$ : [Payn1973] and [Lin1987] (under additional symmetry assumptions), [Mela1992] (smooth convex domains) and [Ales1994] (general convex domains). This is also the case for domains which are convex in one direction only<sup>1</sup>

As a by-product of these results, we have the upper bound

$$\text{mult}(\lambda_2; \Omega, -\Delta, \mathfrak{d}) \leq 2 \text{ for any convex bounded domain } \Omega.$$

This bound holds for domains which are convex in one direction and for domains which satisfy the nodal line conjecture (see Remark 6.4). This result supports the following conjecture.

CONJECTURE 6.5.

$$\text{mult}(\lambda_2; \Omega, -\Delta, \mathfrak{d}) \leq 2 \text{ for any simply connected bounded domain } \Omega.$$

**6.1.4. Neumann boundary condition.** The discussion in Paragraph 6.1.2 shows that the nodal line conjecture holds for the Neumann Laplacian in any simply connected bounded regular domain in  $\mathbb{R}^2$ . Nadirashvili proved that the multiplicity of the second eigenvalue of a simply connected domain with nonpositive curvature is at most 2 and that this estimate is sharp, see [Nadi1987], Theorem 2 and Corollary 1. As a matter of fact, his proof also shows that the nodal line conjecture is true in such domains (for the Neumann condition).

**6.1.5. Robin boundary condition.** As observed by James B. Kennedy<sup>2</sup> in [Ken2011], the proof of the nodal line conjecture for the  $h$ -Robin boundary condition works in the same way as in the case of Neumann condition provided that the following inequality holds,

$$\lambda_2(h, \Omega) \leq \lambda_1^D(\Omega).$$

Observing the monotonicity of the Robin problem with respect to  $h$ , we obtain the existence of some  $h_\Omega > 0$  such that this inequality holds for  $h \leq h_\Omega$ .

J.B. Kennedy also shows that, as in the Dirichlet case (which corresponds to  $h = +\infty$ ), one can find examples of multiply connected domains for which counter examples to the nodal line conjecture can be constructed. One can also expect to construct examples for which the multiplicity is 3 (as in [HoHN1998] and [HeHJ2020]) but this is still open at the moment.

On the positive side, it is natural to ask if convexity is enough to ensure multiplicity at most 2 for every Robin parameter  $h > 0$ , following Lin's approach in [Lin1987]. This is still open at the moment. What we do know is that a sufficient condition on  $\Omega$  is that nodal line conjecture holds (Remark 6.4).

## 6.2. Upper Bounds for Multiplicities vs Courant-sharp Eigenvalues

For simplicity, let us only consider Dirichlet eigenvalues in a  $C^\infty$  bounded domain  $\Omega \subset \mathbb{R}^2$ . The upper bounds on the eigenvalue multiplicities strongly rely on Courant's nodal domain theorem. As observed in [HoMN1999], they are actually a consequence of the following 3-step result,  $n \in \{1, 2, 3\}$ , provided that the third step ( $n = 3$ ) is correct.

<sup>1</sup>See [Liq1995, Corollary 2.7]. Note however that the other results on the multiplicity presented in this paper are true under strong additional conditions only. We thank the author for clarifying this point.

<sup>2</sup>We thank J.B. Kennedy for useful discussions around this problem.

PROPOSITION 6.6. Let  $U(\lambda)$  be a Dirichlet eigenspace of  $-\Delta + V$ . Assume that

$$\sup \{ \kappa(u) \mid u \in U(\lambda) \} = \ell$$

for some  $\ell \geq 3$ . Then  $\dim(U(\lambda)) \leq (2\ell - n)$ .

Indeed, since  $u \in U(\lambda_k)$  implies that  $\kappa(u) \leq k$  (Courant's theorem):

- (1) The first step,  $n = 1$ , yields the upper bound  $\text{mult}(\lambda_k) \leq (2k - 1)$ , see Theorem 1 in [Nadi1987].
- (2) The second step,  $n = 2$ , yields the upper bound  $\text{mult}(\lambda_k) \leq (2k - 2)$ , see Lemma 2.13 in [HoMN1999] or Theorem 4.1.
- (3) The third step,  $n = 3$ , yields the upper bound  $\text{mult}(\lambda_k) \leq (2k - 3)$ , see Theorem B in [HoMN1999] or Theorem 5.1.

According to Pleijel [Plej1956], the equality in Courant's Theorem 2.4 can only occur for finitely many eigenvalues, the so-called *Courant-sharp* eigenvalues. The eigenvalue  $\lambda_k$  is called *Courant-sharp* whenever the associated eigenspace  $U(\lambda_k)$  contains an eigenfunction with  $k$  nodal domains, the maximum number allowed by Courant's nodal domain theorem. If  $\lambda_k$  is not a Courant-sharp eigenvalue, in particular if  $k$  is large enough (depending on the geometry of the domain, see Remark 6.7 below),  $u \in U(\lambda_k)$  implies that  $\kappa(u) \leq (k - 1)$ , and the above proposition implies that  $\text{mult}(\lambda_k) \leq (2k - 2 - n)$ . When  $\lambda_k$  is not Courant-sharp, the upper bound for the multiplicity can be improved by 2.

Proposition 6.6 can be restated as

$$(6.3) \quad \text{mult}(\lambda_k) \leq 2 \sup_{u \in U(\lambda_k)} \kappa(u) - 1.$$

Since  $\sup_{u \in U(\lambda_k)} \kappa(u) \leq k$ , we obtain

$$\limsup_{k \rightarrow +\infty} \frac{\text{mult}(\lambda_k)}{k} \leq 2.$$

We can continue the discussion a little further by recalling Pleijel's proof.

*Sketch of Pleijel's proof.* Let  $\Omega \subset \mathbb{R}^n$  be an open set of finite measure. For  $k \in \mathbb{N}$ , let  $\bar{\kappa}(\lambda_k)$  be the maximal number of nodal domains of an eigenfunction corresponding to the Dirichlet eigenvalue  $\lambda_k(\Omega)$ . Choose some Dirichlet eigenfunction  $u$  associated with  $\lambda_k$  and such that  $\kappa(u) = \bar{\kappa}(\lambda_k)$ . Let  $\{\omega_\alpha\}_\alpha$  be the nodal domains of  $u$ . The first Dirichlet eigenvalue  $\lambda_1(\omega_\alpha)$  is equal to  $\lambda_k(\Omega)$  and satisfies the Faber-Krahn inequality (see [BeMe1982]),

$$\lambda_1(\omega_\alpha) |\omega_\alpha|^{\frac{2}{n}} \geq \lambda_1(\mathbb{B}_1) |\mathbb{B}_1|^{\frac{2}{n}} =: F_n,$$

where  $\mathbb{B}_1$  denotes the unit ball in  $\mathbb{R}^n$ ,  $|\Omega|$  the volume of  $\Omega$ , and where  $F_n$  is some universal constant (see [BeMe1982]). Then,

$$\frac{\bar{\kappa}(\lambda_k)}{k} = \frac{\lambda_k(\Omega)^{\frac{n}{2}}}{k} \sum_\alpha \lambda_1(\omega_\alpha)^{-\frac{n}{2}} \leq F_n^{-\frac{n}{2}} \frac{\lambda_k(\Omega)^{\frac{n}{2}}}{k} \sum_\alpha |\omega_\alpha| = F_n^{-\frac{n}{2}} \frac{\lambda_k(\Omega)^{\frac{n}{2}}}{k} |\Omega|.$$

On the other hand, Weyl's asymptotic formula [Horm2007c, Corollary 17.5.8]

$$N(\lambda) := \# \{j \mid \lambda_j < \lambda\} \sim C_{W,n} |\Omega| \lambda^{\frac{n}{2}},$$

where  $C_{W,n}$  is a universal constant (Weyl's constant), implies that

$$\lambda_k(\Omega)^{\frac{2}{n}} \sim C_{W,n}^{-1} \frac{k}{|\Omega|}.$$

It follows that

$$(6.4) \quad \limsup_{k \rightarrow \infty} \frac{\bar{\kappa}(\lambda_k)}{k} \leq F_n^{-\frac{n}{2}} C_{W,n}^{-1} =: \gamma_n,$$

and it turns out that the constant  $\gamma_n$  is (strictly) less than 1.

In dimension 2,  $\gamma_2 = \frac{4}{j_{0,1}^2}$  where  $j_{0,1}$  is the first positive zero of the Bessel function  $J_0$ , and hence we obtain Pleijel's estimate [Plej1956]

$$(6.5) \quad \limsup_{k \rightarrow \infty} \frac{\bar{\kappa}(\lambda_k)}{k} \leq \frac{4}{j_{0,1}^2} < 1.$$

As a consequence of Weyl's asymptotic formula, Pleijel's method for Dirichlet eigenvalues, and Equation (6.3), we obtain the improved estimate

$$(6.6) \quad \limsup_{k \rightarrow +\infty} \frac{\text{mult}(\lambda_k)}{k} \leq 2\gamma < 2.$$

For a *regular* bounded domain  $\Omega$  in  $\mathbb{R}^2$ , Weyl's asymptotic formula reads

$$(6.7) \quad N(\lambda) = \frac{|\Omega|}{4\pi} \lambda + O(\sqrt{\lambda}).$$

For Weyl's formula with a remainder term, we refer to Theorem 29.3.3 in Hörmander's book [Horm2009d] and to Ivrii's papers [Ivri1980r, Ivri1980]. These references actually give a much more precise formula which yields a two-term asymptotic formula under an assumption on the set of periodic billiard trajectories [Horm2009d, Corollary 29.3.4].

For any  $\delta$  small enough,

$$(6.8) \quad \text{mult}(\lambda_k) = N(\lambda_k + \delta) - N(\lambda_k - \delta).$$

According to (6.7), we should expect that

$$\text{mult}(\lambda_k) = O(\sqrt{\lambda_k}),$$

and hence

$$\limsup_{k \rightarrow +\infty} \frac{\text{mult}(\lambda_k)}{k} = 0,$$

which shows that the inequality (6.6) is not really pertinent when the domain is regular.

For extensions and improvements of Pleijel's theorem, we refer to [Peet1957], [BeMe1982], [Bour2015] and [Stein2014]. Pleijel's method does not readily apply to Neumann eigenvalues. This is because there exist nodal domains whose boundary contain a portion of the boundary of  $\Omega$ . For the extension of Pleijel's theorem to the Neumann or Robin boundary condition, we refer to [Polt2009], [Lena2019], [HaSh2023] and [BeCM2023].

REMARK 6.7. For a bounded domain  $\Omega \subset \mathbb{R}^n$  with  $C^2$  boundary, and Dirichlet boundary condition, one can show that there exists a constant  $C(\Omega)$ , depending on  $\Omega$  and invariant under dilations, such that for  $k > C(\Omega)$ , the  $k$ th Dirichlet eigenvalue  $\lambda_k$  is not Courant-sharp. In dimension 2, the constant  $C(\Omega)$  can be estimated in terms of the area  $|\Omega|$ , the length  $|\Gamma|$  of the boundary, the curvature and the cut-distance of  $\Gamma$ . We refer to [BeHe2016, Theorem 1.3] for more details, and to [BeGi2016, Theorem 1] for an extension to less regular domains. The proof of this result makes use of a lower bound on the remainder term  $R(\lambda) := N(\lambda) - \frac{|\Omega|}{4\pi} \lambda$  in

Weyl's asymptotic estimate, as given for example in [BeLi2001].

For the case of domains with Neumann or Robin boundary condition, we refer to [GiLe2020].

REMARK 6.8. In order to estimate  $\text{mult}(\lambda_k)$  asymptotically, we could use the relation (6.8) together with a geometrical control of  $N(\lambda)$  as in Safarov [Safa2001] or Van den Berg–Lianantonakis [BeLi2001] who give estimates of the form

$$|N(\lambda) - C_n |\Omega| \lambda^{n/2}| \leq C_{geom}(\Omega) \lambda^{(n-1)/2} \ln \lambda,$$

where  $C_n$  is Weyl's constant.

## Bibliography

- [Ales1994] Giovanni Alessandrini. Nodal lines of eigenfunctions of the fixed membrane problem in general convex domains. *Comment. Math. Helv.*, 69(1):142–154, 1994. [168](#), [171](#)
- [Ales1998] Giovanni Alessandrini. On Courant’s nodal domain theorem. *Forum Math.*, 10(5):521–532, 1998. [12](#)
- [ArMa2007] Wolfgang Arendt and Rafe Mazzeo. Spectral properties of the Dirichlet-to-Neumann operator on Lipschitz domains. *Ulmer Seminare*, 12:28–38, 2007. [170](#)
- [ArMa2012] Wolfgang Arendt and Rafe Mazzeo. Friedlander’s eigenvalue inequalities and the Dirichlet-to-Neumann semigroup. *Commun. Pure Appl. Anal.*, 11(6):2201–2212, 2012. [170](#)
- [Aron1957] Nachman Aronszajn. A unique continuation theorem for solutions of elliptic partial differential equations or inequalities of second order. *J. Math. Pures Appl. (9)*, 36:235–249, 1957. [13](#), [25](#), [31](#)
- [BaPP2024] Luca Battaglia, Angela Pistoia, and Luigi Provenzano. On the critical points of Steklov eigenfunctions. 2024. [116](#)
- [BeBo1982] Lionel Bérard-Bergery and Jean-Pierre Bourguignon. Laplacians and Riemannian submersions with totally geodesic fibres. *Illinois J. Math.*, 26(2):181–200, 1982. [12](#)
- [BeCM2023] Thomas Beck, Yaiza Canzani, and Jeremy L. Marzuola. Uniform upper bounds on Courant sharp Neumann eigenvalues of chain domains. [173](#)
- [BeGM1971] Marcel Berger, Paul Gauduchon, and Edmond Mazet. *Le spectre d’une variété riemannienne*. Lecture Notes in Mathematics, Vol. 194. Springer-Verlag, Berlin-New York, 1971. [24](#)
- [BeGi2016] Michiel van den Berg and Katie Gittins. On the number of Courant-sharp Dirichlet eigenvalues. *J. Spectr. Theory*, 6(4):735–745, 2016. [173](#)
- [BeHe2015r] Pierre Bérard and Bernard Helffer. Nodal sets of eigenfunctions, Antonie Stern’s results revisited. In *Actes de Séminaire de Théorie Spectrale et Géométrie. Année 2014–2015*, pages 1–37. St. Martin d’Hères: Université de Grenoble I, Institut Fourier, 2015. [12](#)
- [BeHe2015s] Pierre Bérard and Bernard Helffer. Edited extracts from Antonie Stern’s thesis. In *Actes de Séminaire de Théorie Spectrale et Géométrie. Année 2014–2015*, pages 39–72. St. Martin d’Hères: Université de Grenoble I, Institut Fourier, 2015. [12](#)
- [BeHe2016] Pierre Bérard and Bernard Helffer. The weak Pleijel theorem with geometric control. *J. Spectr. Theory*, 6(4):717–733, 2016. [173](#)
- [BeHe2021t] Pierre Bérard and Bernard Helffer. Level sets of certain Neumann eigenfunctions under deformation of Lipschitz domains application to the extended Courant property. *Ann. Fac. Sci. Toulouse Math. (6)*, 30(3):429–462, 2021. [168](#)
- [BeKr1987] Steven R. Bell and Steven G. Krantz. Smoothness to the boundary of conformal maps. *Rocky Mountain J. Math.*, 17(1):23–40, 1987. [28](#), [42](#)
- [BeLi2001] Michiel van den Berg and Maria Lianantonakis. Asymptotics for the spectrum of the Dirichlet Laplacian on horn-shaped regions. *Indiana Univ. Math. J.*, 50(1):299–333, 2001. [174](#)
- [BeMe1982] Pierre Bérard and Daniel Meyer. Inégalités isopérimétriques et applications. *Ann. Sci. École Norm. Sup. (4)*, 15(3):513–541, 1982. [12](#), [172](#), [173](#)
- [BeNP2016] Aleksandr Berdnikov, Nikolai Nadirashvili, and Alexei Penskoï. Bounds on multiplicities of Laplace-Beltrami operator eigenvalues on the real projective plane. arXiv:1612.04805, 2016. [7](#), [104](#)

- [Berd2018] Aleksandr Berdnikov. Bounds on multiplicities of Laplace operator eigenvalues on surfaces. *J. Spectr. Theory*, 8(2):541–554, 2018. [6](#), [8](#), [48](#)
- [Bers1955] Lipman Bers. Local behavior of solutions of general linear elliptic equations. *Comm. Pure Appl. Math.*, 8:473–496, 1955. [13](#)
- [Bess1980] Gérard Besson. Sur la multiplicité de la première valeur propre des surfaces riemanniennes. *Ann. Inst. Fourier (Grenoble)*, 30(1):x, 109–128, 1980. [7](#), [8](#), [15](#), [24](#), [48](#)
- [BoHe2017] Virginie Bonnaillie-Noël and Bernard Helffer. Nodal and spectral minimal partitions—the state of the art in 2016. In *Shape optimization and spectral theory*, pages 353–397. De Gruyter Open, Warsaw, 2017. [8](#), [75](#)
- [Bona2009] Francis Bonahon. *Low-dimensional geometry*, volume 49 of *Student Mathematical Library*. American Mathematical Society, Providence, RI; Institute for Advanced Study (IAS), Princeton, NJ, 2009. From Euclidean surfaces to hyperbolic knots, IAS/Park City Mathematical Subseries. [70](#)
- [Bour2015] Jean Bourgain. On Pleijel’s nodal domain theorem. *Int. Math. Res. Not. IMRN*, (6):1601–1612, 2015. [173](#)
- [BuCo1985] Marc Burger and Bruno Colbois. À propos de la multiplicité de la première valeur propre du Laplacien d’une surface de Riemann. *C. R. Acad. Sci. Paris Sér. I Math.*, 300(8):247–249, 1985. [9](#)
- [Chen1976] Shiu Yuen Cheng. Eigenfunctions and nodal sets. *Comment. Math. Helv.*, 51(1):43–55, 1976. [7](#), [8](#), [15](#), [24](#), [43](#)
- [CiJLS2022] Donato Cianci, Chris Judge, Samuel Lin, and Craig Sutton. Spectral multiplicity and nodal sets for generic torus-invariant metrics. arXiv:2207.14405 (Version 1), 2022, 2022. [12](#)
- [CoCo1988] Bruno Colbois and Yves Colin de Verdière. Sur la multiplicité de la première valeur propre d’une surface de Riemann à courbure constante. *Comment. Math. Helv.*, 63(2):194–208, 1988. [9](#)
- [CoGGS2024] Bruno Colbois, Alexandre Girouard, Carolyn Gordon, and David Sher. Some recent developments on the Steklov eigenvalue problem. *Rev. Mat. Complut.*, 37(1):1–161, 2024. [5](#)
- [ColV1986] Yves Colin de Verdière. Sur la multiplicité de la première valeur propre non nulle du Laplacien. *Comment. Math. Helv.*, 61(2):254–270, 1986. [9](#)
- [ColV1987] Yves Colin de Verdière. Construction de laplaciens dont une partie finie du spectre est donnée. *Ann. Sci. École Norm. Sup. (4)*, 20(4):599–615, 1987. [7](#), [9](#)
- [Colb1985] Bruno Colbois. Petites valeurs propres du Laplacien sur une surface de Riemann compacte et graphes. *C. R. Acad. Sci. Paris Sér. I Math.*, 301(20):927–930, 1985. [9](#)
- [Cour1923] R. Courant. Ein allgemeiner Satz zur Theorie der Eigenfunktionen selbstadjungierter Differentialausdrücke. *Nachr. Ges. Wiss. Göttingen, Math.-Phys. Kl.*, 1923:81–84, 1923. [12](#)
- [DaGH2021] Joel Dahne, Javier Gómez-Serrano, and Kimberly Hou. A counterexample to Payne’s nodal line conjecture with few holes. *Commun. Nonlinear Sci. Numer. Simul.*, 103:Paper No. 105957, 13, 2021. [170](#)
- [Dama2000] Lucio Damascelli. On the nodal set of the second eigenfunction of the Laplacian in symmetric domains in  $\mathbb{R}^N$ . *Atti Accad. Naz. Lincei Cl. Sci. Fis. Mat. Natur. Rend. Lincei (9) Mat. Appl.*, 11(3):175–181, 2000. [170](#)
- [Dies2017] Reinhard Diestel. *Graph theory*, volume 173 of *Graduate Texts in Mathematics*. Springer, Berlin, fifth edition, 2017. [20](#), [21](#)
- [DoFe1990a] Harold Donnelly and Charles Fefferman. Nodal sets of eigenfunctions: Riemannian manifolds with boundary. In *Analysis, et cetera*, pages 251–262. Academic Press, Boston, MA, 1990. [13](#), [25](#)
- [FoBP2024] Maxime Fortier Bourque and Bram Petri. The Klein quartic maximizes the multiplicity of the first positive eigenvalue of the Laplacian. *J. Differential Geom.*, 128(2):521–556, 2024. [7](#)



- [FoGPP2023] Maxime Fortier Bourque, Émile Gruda-Mediavilla, Bram Petri, and Mathieu Pineault. Two counterexamples to a conjecture of Colin de Verdière on multiplicity. 2023. [7](#)
- [Four2001] Søren Fournais. The nodal surface of the second eigenfunction of the Laplacian in  $\mathbf{R}^D$  can be closed. *J. Differential Equations*, 173(1):145–159, 2001. [170](#)
- [FrKr2008] P. Freitas and D. Krejřičík. Location of the nodal set for thin curved tubes. *Indiana Univ. Math. J.*, 57(1):343–375, 2008. [170](#)
- [FrSc2016] Ailana Fraser and Richard Schoen. Sharp eigenvalue bounds and minimal surfaces in the ball. *Invent. Math.*, 203(3):823–890, 2016. [5](#)
- [Frie1991] Leonid Friedlander. Some inequalities between Dirichlet and Neumann eigenvalues. *Arch. Rational Mech. Anal.*, 116(2):153–160, 1991. [169](#)
- [GaHuLa2004] Sylvestre Gallot, Dominique Hulin, and Jacques Lafontaine. *Riemannian geometry*. Universitext. Springer-Verlag, Berlin, third edition, 2004. [24](#)
- [GiHe2019] Katie Gittins and Bernard Helffer. Courant-sharp Robin eigenvalues for the square and other planar domains. *Port. Math.*, 76(1):57–100, 2019. [13](#), [14](#)
- [GiLe2020] Katie Gittins and Corentin Léna. Upper bounds for Courant-sharp Neumann and Robin eigenvalues. *Bull. Soc. Math. France*, 148(1):99–132, 2020. [174](#)
- [GiTr1977] David Gilbarg and Neil S. Trudinger. *Elliptic partial differential equations of second order*. Springer-Verlag, Berlin-New York, 1977. Grundlehren der Mathematischen Wissenschaften, Vol. 224. [29](#)
- [Gibl2010] Peter Giblin. *Graphs, surfaces and homology*. Cambridge University Press, Cambridge, third edition, 2010. [20](#), [21](#), [23](#)
- [GoSa1995] Daniel H. Gottlieb and Geetha Samaranyake. The index of discontinuous vector fields. *New York J. Math.*, 1:130–148, electronic, 1994/95. [116](#)
- [Gott1990] Daniel Henry Gottlieb. Vector fields and classical theorems of topology. *Rend. Sem. Mat. Fis. Milano*, 60:193–203, 1990. [116](#)
- [HaSh2023] Asma Hassannezhad and David Sher. On Pleijel’s nodal domain theorem for the Robin problem. arXiv:2303.08094, 2023. [173](#)
- [HaWi1953] Philip Hartman and Aurel Wintner. On the local behavior of solutions of non-parabolic partial differential equations. *Amer. J. Math.*, 75:449–476, 1953. [13](#)
- [HeHJ2020] Bernard Helffer, Thomas Hoffmann-Ostenhof, François Jauberteau, and Corentin Léna. On the multiplicity of the second eigenvalue of the Laplacian in non simply connected domains – with some numerics –. *Asymptotic Analysis*, 121(1):35–57, 2021. [170](#), [171](#)
- [HeHN2002] Bernard Helffer, Maria Hoffmann-Ostenhof, Thomas Hoffmann-Ostenhof, and Nikolai Nadirashvili. Spectral theory for the dihedral group. *Geom. Funct. Anal.*, 12(5):989–1017, 2002. [8](#)
- [HeHO1999] Bernard Helffer, Maria Hoffmann-Ostenhof, Thomas Hoffmann-Ostenhof, and Mark P. Owen. Nodal sets for groundstates of Schrödinger operators with zero magnetic field in non-simply connected domains. *Comm. Math. Phys.*, 202(3):629–649, 1999. [8](#)
- [HeHT2009] Bernard Helffer, Thomas Hoffmann-Ostenhof, and Susanna Terracini. Nodal domains and spectral minimal partitions. *Ann. Inst. H. Poincaré Anal. Non Linéaire*, 26(1):101–138, 2009. [8](#)
- [HoHN1997] Maria Hoffmann-Ostenhof, Thomas Hoffmann-Ostenhof, and Nikolai Nadirashvili. The nodal line of the second eigenfunction of the Laplacian in  $\mathbf{R}^2$  can be closed. *Duke Math. J.*, 90(3):631–640, 1997. [170](#)
- [HoHN1998] Maria Hoffmann-Ostenhof, Thomas Hoffmann-Ostenhof, and Nikolai Nadirashvili. On the nodal line conjecture. In *Advances in differential equations and mathematical physics (Atlanta, GA, 1997)*, volume 217 of *Contemp. Math.*, pages 33–48. Amer. Math. Soc., Providence, RI, 1998. [170](#), [171](#)
- [HoHN1999] Maria Hoffmann-Ostenhof, Thomas Hoffmann-Ostenhof, and Nikolai Nadirashvili. On the multiplicity of eigenvalues of the Laplacian on surfaces. *Ann. Global Anal. Geom.*, 17(1):43–48, 1999. [5](#), [6](#), [7](#), [15](#), [43](#), [48](#)

- [HoMN1999] Thomas Hoffmann-Ostenhof, Peter W. Michor, and Nikolai Nadirashvili. Bounds on the multiplicity of eigenvalues for fixed membranes. *Geom. Funct. Anal.*, 9(6):1169–1188, 1999. [5](#), [6](#), [7](#), [8](#), [15](#), [48](#), [57](#), [59](#), [81](#), [82](#), [88](#), [146](#), [163](#), [164](#), [171](#), [172](#)
- [Horm2007c] Lars Hörmander. *The analysis of linear partial differential operators. III*. Classics in Mathematics. Springer, Berlin, 2007. Pseudo-differential operators, Reprint of the 1994 edition. [172](#)
- [Horm2009d] Lars Hörmander. *The analysis of linear partial differential operators. IV*. Classics in Mathematics. Springer-Verlag, Berlin, 2009. Fourier integral operators, Reprint of the 1994 edition. [173](#)
- [Ivri1980] Victor Ja. Ivriĭ. Second term of the spectral asymptotic expansion of the Laplace-Beltrami operator on manifolds with boundary. *Funct Anal Its Appl.*, 14(2):98–106, 1980. [173](#)
- [Ivri1980r] Victor Ja. Ivriĭ. The second term of the spectral asymptotics for a Laplace-Beltrami operator on manifolds with boundary. *Funktsional. Anal. i Prilozhen.*, 14(2):25–34, 1980. [173](#)
- [Jam2016] Pierre Jammes. Multiplicité du spectre de Steklov sur les surfaces et nombre chromatique. *Pacific J. Math.*, 282(1):145–171, 2016. [5](#)
- [Jeri1991] David Jerison. The first nodal line of a convex planar domain. *Internat. Math. Res. Notices*, (1):1–5, 1991. [170](#)
- [JuZe2022] Junhyuk Jung and Steve Zelditch. 2-nodal domain theorems for higher dimensional circle bundles. arXiv: 2207.13498 (Version 1), 2022, 2022. [12](#)
- [KaKP2014] Mikhail Karpukhin, Gerasim Kokarev, and Iosif Polterovich. Multiplicity bounds for Steklov eigenvalues on Riemannian surfaces. *Ann. Inst. Fourier (Grenoble)*, 64(6):2481–2502, 2014. [5](#)
- [Ken2011] James B. Kennedy. The nodal line of the second eigenfunction of the Robin Laplacian in  $\mathbb{R}^2$  can be closed. *J. Differential Equations*, 251(12):3606–3624, 2011. [171](#)
- [Ken2013] James B. Kennedy. Closed nodal surfaces for simply connected domains in higher dimensions. *Indiana Univ. Math. J.*, 62(3):785–798, 2013. [170](#)
- [Kiwa2018] Rola Kiwan. On the nodal set of a second Dirichlet eigenfunction in a doubly connected domain. *Ann. Fac. Sci. Toulouse Math. (6)*, 27(4):863–873, 2018. [168](#)
- [LeMa2024] Cyril Letrouit and Simon Machado. Maximal multiplicity of Laplacian eigenvalues in negatively curves surfaces. 2024. [9](#)
- [Lena2019] Corentin Léna. Pleijel’s nodal domain theorem for Neumann and Robin eigenfunctions. *Ann. Inst. Fourier (Grenoble)*, 69(1):283–301, 2019. [173](#)
- [Lewy1977] Hans Lewy. On the minimum number of domains in which the nodal lines of spherical harmonics divide the sphere. *Comm. Partial Differential Equations*, 2(12):1233–1244, 1977. [12](#)
- [LiNi1988] Chang Shou Lin and Wei-Ming Ni. A counterexample to the nodal domain conjecture and a related semilinear equation. *Proc. Amer. Math. Soc.*, 102(2):271–277, 1988. [170](#)
- [Lin1987] Chang Shou Lin. On the second eigenfunctions of the Laplacian in  $\mathbf{R}^2$ . *Comm. Math. Phys.*, 111(2):161–166, 1987. [171](#)
- [Liq1995] Zhang Liquan. On the multiplicity of the second eigenvalue of Laplacian in  $\mathbf{R}^2$ . *Comm. Anal. Geom.*, 3(1-2):273–296, 1995. [170](#), [171](#)
- [Maz1991] Rafe Mazzeo. Remarks on a paper of L. Friedlander concerning inequalities between Neumann and Dirichlet eigenvalues. *Internat. Math. Res. Notices*, 1991(4):41–48, 1991. eigenvalues” [Arch. Rational Mech. Anal. **116** (1991), no. 2, 153–160; MR1143438 (93h:35146)]. [169](#)
- [Mela1992] Antonios D. Melas. On the nodal line of the second eigenfunction of the Laplacian in  $\mathbf{R}^2$ . *J. Differential Geom.*, 35(1):255–263, 1992. [29](#), [171](#)
- [Mikh1978] V. P. Mikhaĭlov. *Partial differential equations*. “Mir”, Moscow; distributed by Imported Publications, Chicago, Ill., 1978. Translated from the Russian by P. C. Sinha. [29](#)
- [Miln1997] John W. Milnor. *Topology from the differentiable viewpoint*. Princeton University Press, Princeton, NJ, 1997. Revised reprint of the 1965 original. [44](#), [49](#), [116](#)

- [Nadi1987] Nikolai S. Nadirashvili. Multiple eigenvalues of the Laplace operator (Russian). *Mat. Sb. (N.S.)*, 133(175)(2):223–237, 272, 1987. Translation, Math USSR-Sb. 61 225–238 1988. [7](#), [8](#), [15](#), [43](#), [48](#), [59](#), [171](#), [172](#)
- [Paga1990] Kurt F. Pagani. *Geometrische Eigenschaften der Lösungen von quasilinearen, elliptischen Differentialgleichungen zweiter Ordnung in der Ebene*. Zürich: ETH Zürich, 1990. [24](#)
- [Payn1967] Lawrence E. Payne. Isoperimetric inequalities and their applications. *SIAM Rev.*, 9:453–488, 1967. [169](#), [170](#)
- [Payn1973] Lawrence E. Payne. On two conjectures in the fixed membrane eigenvalue problem. *Z. Angew. Math. Phys.*, 24:721–729, 1973. [171](#)
- [Peet1957] Jaak Peetre. A generalization of Courant’s nodal domain theorem. *Math. Scand.*, 5:15–20, 1957. [173](#)
- [PiVe2020] Stefano Pigola and Giona Veronelli. The smooth Riemannian extension problem. *Ann. Sc. Norm. Super. Pisa Cl. Sci. (5)*, 20(4):1507–1551, 2020. [33](#)
- [Plej1956] Åke Pleijel. Remarks on Courant’s nodal line theorem. *Comm. Pure Appl. Math.*, 9:543–550, 1956. [12](#), [59](#), [169](#), [172](#), [173](#)
- [Polt2009] Iosif Polterovich. Pleijel’s nodal domain theorem for free membranes. *Proc. Amer. Math. Soc.*, 137(3):1021–1024, 2009. [173](#)
- [Putt1990] Rolf Pütter. On the nodal lines of second eigenfunctions of the fixed membrane problem. *Comment. Math. Helv.*, 65(1):96–103, 1990. [168](#)
- [Putt1991] Rolf Pütter. On the nodal lines of second eigenfunctions of the free membrane problem. *Appl. Anal.*, 42(3–4):199–207, 1991. [168](#)
- [Safa2001] Yuri Safarov. Fourier Tauberian theorems and applications. *J. Funct. Anal.*, 185(1):111–128, 2001. [174](#)
- [Salo2014] Mikko Salo. Unique continuation for elliptic equations. Notes edited by Mikko Salo. Department of Mathematics and Statistics. University of Jyväskylä. Finland., 2014. [31](#)
- [Seve2002] Bruno Sévenec. Multiplicity of the second Schrödinger eigenvalue on closed surfaces. *Math. Ann.*, 324(1):195–211, 2002. [7](#)
- [Shen1988] Chao Liang Shen. On the nodal sets of the eigenfunctions of the string equation. *SIAM J. Math. Anal.*, 19(6):1419–1424, 1988. [168](#)
- [SoZe2011] Christopher D. Sogge and Steve Zelditch. Lower bounds on the Hausdorff measure of nodal sets. *Math. Res. Lett.*, 18(1):25–37, 2011. [12](#)
- [Stei2014] Stefan Steinerberger. A geometric uncertainty principle with an application to Pleijel’s estimate. *Ann. Henri Poincaré*, 15(12):2299–2319, 2014. [173](#)
- [Ster1925] Antonie Stern. *Bemerkungen über asymptotisches Verhalten von Eigenwerten und Eigenfunktionen*. Math-Naturwiss. Diss., Universität Göttingen, 1925. [12](#)
- [Vali1966] Georges Valiron. *Théorie des Fonctions (3ème édition)*. Masson et Cie, Paris, 1966. [24](#)
- [YaZh2021] Yunyan Yang and Jie Zhou. Blow-up analysis involving isothermal coordinates on the boundary of compact Riemann surface. *J. Math. Anal. Appl.*, 504(2):Paper No. 125440, 39, 2021. [18](#), [33](#)



## Alphabetical Index

- $G_0(u, M)$ , 21  
 $\Gamma$   
 $\Gamma = \partial\Omega$ , 27  
 $\Gamma(u)$ , 23, 58  
 $\Gamma_{(2k-3)}, \Gamma_{(2k-2)}$ , 81, 86  
 $\Gamma_{0,(2k-2)}, \Gamma_{0,(2k-3)}$ , 88  
 $\alpha_0(G)$ , 20  
 $\alpha_1(G)$ , 20  
 $\beta(u)$ , 22  
 $\chi(M)$ , 7  
 $\gamma$   
 $\gamma(M)$ , 7  
 $\gamma_{j,\tau(j)}$ , 46  
 $\kappa(u)$ , 12, 22  
 $\nu(u, x)$ , 14  
 $\rho(u, x)$ , 14  
 $\sigma(u)$ , 22  
 $\sigma_i(u), \sigma_b(u)$ , 22  
 $\tau$   
 $\tau_x^U$ , 86  
 $\tau_{x,u}$ , 45  
 $\tau_{y,z}$ , 61  
 $\mathcal{A}(y_1, y_2)$ , 82  
 $C_n$ , 39  
 $G(u, M)$ , 21  
 $\mathcal{G}_u$ , 20  
 $J(u)$ , 58  
 $P_p$ , 90  
 $\mathbb{P}(U)$ , 49  
 $Q_p$ , 90  
 $R$   
 $R_\beta$ , 39  
 $R_{p+1}$ , 25  
 $S_n$ , 39  
 $\mathbb{S}(U)$ , 49  
 $\mathcal{S}(u)$ , 14  
 $\mathcal{S}_i(u), \mathcal{S}_b(u)$ , 14  
 $U_y$ , 81, 85  
 $U_y^1, U_y^1$ , 62  
 $V_{y,z}$ , 60  
 $W_x$ , 44, 81, 83  
 $\mathcal{Z}(u)$ , 12  
 $\mathcal{Z}_x(u)$ , 83  
 $b_0$ , 8  
 $c(G)$ , 20  
 $\text{mult}(\lambda_k)$ , 5  
 $\text{ord}(u, x)$ , 13  
 $r(G, M)$ , 20  
 $\check{u}$ , 18  
 $v_t$   
 $\check{v}(t, \xi_1)$ , 93  
 $v(t, \xi_1, \xi_2)$ , 93  
 $v_t$ , 88  
 $v_t(\xi_1, \xi_2)$ , 88  
 $w_t$   
 $\check{w}(t, \xi_1)$ , 93  
 $w(t, \xi_1, \xi_2)$ , 93  
 $w_t$ , 90  
 $z(y)$ , 81  
 $[u]$ , 58  
Aronszajn Theorem, 31, 32  
Bouquet of loops, 45  
 $p$ -bouquet, 45  
Chromatic number, 7  
Combinatorial type, 45, 61  
Component (connected), 12  
Courant nodal Theorem, 8, 12, 59, 171  
Courant-sharp, 51, 59  
Critical zero, 13, 26  
boundary, 13  
interior, 13  
Degree (vertex), 21  
Dirichlet condition, 11

- Eigenspace, 12
- Eigenvalue labeling, 12
- Eigenvalue problem, 11
  - $h$ -Robin, 11
  - closed, 11
  - with boundary, 11
- Energy argument, 96
- Euler characteristic, 7, 49
- Euler formula, 8, 23
- Euler formula for nodal sets, 23
- Exterior of a loop, 136
- Faber-Krahn inequality, 172
- Genus, 7
- Graph, 20
- Harmonic function, 25
- Hausdorff distance, 19
- Index  $\nu(u, x)$ , 14, 16
- Index  $\rho(u, x)$ , 14
- Interior of a loop, 136
- Labeling (eigenvalue), 5
- Labeling (nodal domains), 51, 134
- Laplace-Beltrami operator, 5, 11, 24
- Local structure Theorem, 13
- Multigraph, 21
- Multiplicity, 12, 170
- Neumann condition, 11
- Nodal circle, 14
- Nodal domain, 12
- Nodal interval, 14
- Nodal line, 12
- Nodal line conjecture, 169
- Nodal loop, 14
- Nodal pattern, 60
- Nodal set, 12
- Nodal word, 50
- Nodal word (standard), 52
- Payne conjecture, 170
- Pleijel Theorem, 12, 59, 172
- Poincaré-Hopf theorem, 44, 49, 116
- Riemannian measure, 11
- Riemannian sphere, 5
- Robin condition, 11
- Rotating function argument, 44, 46, 48, 68, 84, 86
- Schrödinger operator, 5, 11
- Signature, 135
- Signature (nodal patterns), 134
- Signature of a word, 106
- Singular point, 14
  - boundary, 14
  - interior, 14
- Standard labeling, 52
- Strong unique continuation property, 31
- Unique continuation property (boundary), 29
- Unique continuation Theorem, 25
- Vanishing order, 13, 17, 18
- Vertex-edge addition, 21
- Weyl asymptotic formula, 172